Maria Videgain Marco

Producción y caracterización de biochar. Evaluación de sus efectos sobre el sistema suelo-planta-microorganismos.

Director/es
Dr. D. Francisco Javier García Ramos
Dr. D. Joan Josep Manyà Cervelló
Dra. Dª. María Del Carmen Jaizme Vega

http://zaguan.unizar.es/collection/Tesis

Tesis Doctoral

PRODUCCIÓN Y CARACTERIZACIÓN DE BIOCHAR. EVALUACIÓN DE SUS EFECTOS SOBRE EL SISTEMA SUELO-PLANTA-MICROORGANISMOS.

Autor

Maria Videgain Marco

Director/es

Dr. D. Francisco Javier García Ramos
Dr. D. Joan Josep Manyà Cervelló
Dra. Dª. María Del Carmen Jaizme Vega

UNIVERSIDAD DE ZARAGOZA
Escuela de Doctorado

2021

TESIS DOCTORAL

Producción y caracterización de biochar. Evaluación de sus efectos sobre el sistema suelo-planta-microorganismos

María Videgain Marco

ESCUELA POLITÉCNICA SUPERIOR – UNIVERSIDAD DE ZARAGOZA

CIENCIAS AGRARIAS Y DEL MEDIO NATURAL

2021

Universidad Zaragoza

PRODUCCIÓN Y CARACTERIZACIÓN DE BIOCHAR. EVALUACIÓN DE SUS EFECTOS SOBRE EL SISTEMA SUELO-PLANTA-MICROORGANISMOS

Memoria presentada por

María Videgain Marco

para optar al Grado de Doctora por la Universidad de Zaragoza

Directores:

Dr. Francisco Javier García Ramos

Dr. Joan Josep Manyà Cervelló

Dra. María del Carmen Jaizme Vega

ESCUELA POLITÉCNICA SUPERIOR DE HUESCA – UNIVERSIDAD DE ZARAGOZA

DEPARTAMENTO DE CIENCIAS AGRARIAS Y DEL MEDIO NATURAL

Huesca, 25 de octubre de 2021

Universidad
Zaragoza
1542

D. Francisco Javier García Ramos, Catedrático de Universidad en el Departamento de Ciencias Agrarias y del Medio Natural de la Universidad de Zaragoza, D. Joan Josep Manyà Cervelló, Profesor Titular de Universidad en el Departamento de Ingeniería Química y Tecnologías del Medio Ambiente, y Dña. María del Carmen Jaizme Vega, Investigadora del Instituto Canario de Investigaciones Agrarias,

CERTIFICAN

Que la presente memoria titulada:

PRODUCCIÓN Y CARACTERIZACIÓN DE BIOCHAR. EVALUACIÓN DE SUS EFECTOS SOBRE EL SISTEMA SUELO-PLANTA-MICROORGANISMOS

Ha sido realizada por **Dña. María Videgain Marco** en la Escuela Politécnica Superior de la Universidad de Zaragoza, y autorizan su presentación como compendio de publicaciones para optar al grado de Doctora por la Universidad de Zaragoza.

Y para que así conste, firman el presente certificado en Huesca, a 25 de octubre de 2021.

Fdo. Dr. F. Javier García Ramos   Fdo. Dr. Joan J. Manyà Cervelló   Fdo. Dra. M. Carmen Jaizme Vega

Informe sobre las publicaciones derivadas de la tesis doctoral

Esta Tesis doctoral se presenta bajo la modalidad de compendio de publicaciones, habiendo sido autorizada por sus directores y por la Comisión del Programa de Doctorado de Ciencias Agrarias y del Medio Natural de la Universidad de Zaragoza.

Se adjuntan cuatro publicaciones con unidad temática, todas pertenecientes a revistas indexadas en el *Journal Citation Reports* (JCR) de *Web of Sciences*. María Videgain ha sido primera firmante en tres de ellas y tercera firmante en una de ellas. Las publicaciones son:

1. Manyà, J. J.; Alvira, D.; Videgain, M.; Duman, G.; Yanik, J. Assesing the importance of pyrolysis process conditions and feedstock type on the combustion performance of agricultural-residue-derived chars. *Energy & Fuels* 2021, 35, 3174-3185. DOI: 10.1021/acs.energyfuels.0c04180.

Factor de impacto (JCR 2020): 3,605 (Q2 - Engineering, Chemical).

2. Videgain, M.; Manyà, J. J.; Vidal, M.; Correa, E. C.; Diezma, B.; García-Ramos, F. J. Influence of feedstock and final pyrolysis temperature on breaking strength and dust production of wood-derived biochars. *Sustainability* 2021, 13, *en prensa*.

Factor de impacto (JCR 2020): 3,251 (Q2 - Environmental Sciences).

3. Videgain, M.; Marco, P.; Martí, C.; Jaizme-Vega, M. C.; Manyà, J. J.; García-Ramos, F. J. Effects of biochar application in a sorghum crop under greenhouse conditions: growth parameters and physicochemical fertility. *Agronomy* 2020, 10, 104. DOI: 10.3390/agronomy10010104.

Factor de impacto (JCR 2020): 3,417 (Q1 - Agronomy).

4. Videgain, M.; Marco, P.; Martí, C.; Jaizme-Vega, M. C.; Manyà, J. J.; García-Ramos, F. J. The effects of biochar on indigenous arbuscular mycorrhizae fungi from agroenvironments. *Plants* 2021, 10, 950. DOI: 10.3390/plants10050950.

Factor de impacto (JCR 2020): 3,935 (Q1 - Plant Sciences).

CITESCORE 3.9 SCOPUS

IMPACT FACTOR 3.251

CERTIFICATE OF ACCEPTANCE

Certificate of acceptance for the manuscript (**sustainability-1378786**) titled:

Physical and Mechanical Characterization of Wood-derived Biochars for Field Applications: Influence of Feedstock and Final Pyrolysis Temperature on Breaking Strength and Dust Production

Authored by:

María Videgain; Joan J. Manyà; Mariano Vidal; Eva Cristina Correa; Belén Diezma; F. Javier García-Ramos

has been accepted in *Sustainability* (ISSN 2071-1050) on 23 October 2021

Agradecimientos

Es muy difícil sintetizar en estas páginas todas las palabras de gratitud que tengo hacia las personas que me han ayudado a sacar adelante este trabajo.

Las GRACIAS con mayúsculas se dirigen a mis directores de tesis en la cercanía, F. Javier García Ramos y Joan Manyà Cervelló ya que, sin su ayuda, no estaría escribiendo esta página. Joan, por abrirme los ojos al biochar, por llevarme al otro lado del mundo, por aguantar mis estreses de última hora y porque es una pasada lo que se aprende contigo siempre, gracias. Javier, por animarme incondicionalmente, de principio a fin, y no dejarme caer en ningún momento, por el montón de cosas diferentes que se aprenden trabajando contigo, por dejarme trabajar en libertad total, por tener siempre palabras de motivación para el trabajo, y para el resto de cosas de la vida, por los bocadillos de panceta, gracias. A los dos, gracias por ser mis amigos.

Gracias a Mery Jaizme Vega, mi directora de tesis que, aunque en la lejanía, ha estado siempre muy cerca. Por la tremenda motivación que me despertaste hacia las micorrizas y la agroecología, por tu forma de ser y la forma en que razonas las cosas, por acogerme en el sur del sur y así guardarme una experiencia única, gracias. Me has hecho mirar el mundo desde otro punto de vista ("que no es otra cosa que la vista que se tiene desde cierto punto").

Agradezco a Christian Di Stasi y a Gianluca Greco, mis amigos y compañeros italianos, toda su ayuda para el desarrollo de experimentos y trabajos de laboratorio. Sin vosotros esta tesis y estos años de trabajo no hubieran sido lo mismo.

Agradezco a todos los miembros de la Escuela Politécnica Superior de Huesca (PDI y PAS) por ayudarme en determinados momentos con algún punto del trabajo o por los ánimos que me han dado siempre para continuar, y en especial a Manuel Azuara, Mariano Vidal, Clara Martí, Gemma Sausán y Darío Alvira, quienes han estado involucrados directamente en este trabajo. Un agradecimiento a parte es para José Casanova y Pablo Martín, que además de ayudarme en todo siempre, aguantan mis penurias por los pasillos.

Agradezco al equipo de investigación en truficultura del CITA el respaldo que me han dado siempre en todo. Gracias a Pedro Marco (como investigador y como "amigo-primo-hermano"), a Sergio Sánchez y a Sergi García por toda la ayuda y cariño que me brindáis siempre.

Agradezco a Javier Nocito, compañero de siembras y cosechas, la ayuda en esta última etapa para poder sobrellevar el trabajo.

Agradezco a Belén Diezma y a Eva Cristina Correa la ayuda que me han dado desde la Universidad Politécnica de Madrid, y por abrirme las puertas de su laboratorio para trabajar allí.

Fuera del ámbito laboral, agradezco a todos mis amigos los ánimos que he recibido para no desistir. Especialmente a Elena y Lorena, con quienes estos años he podido despejar la mente (o nublarla) de verdad. Y a las "rangers" Carolina, Clara y Julia, gracias por estar ahí siempre. Gracias a Lidia por ayudarme en la parte artística de esta tesis, te he sentido muy cerca a pesar de la gran lejanía estos años. Y gracias a Diana, por ayudarme a sobrellevar todo, el trabajo y el no trabajo, por los necesarios raticos de las tardes que me has dedicado estos años.

Gracias a mis amigos Sanagustín de Albero, por ser como una familia cuando no he podido escaparme a estar con la mía.

Gracias a Blues por sacarme de paseo un rato cada día. Y a Silvestre y la pandi por la compañía.

Todo el tiempo dedicado a este trabajo lo he restado al de pasar con mi gente, y de ese tiempo el que más pesa, es el que no he pasado con mi familia (la de Zaragoza, la de San Martín y la de Huesca), ni con mi abuela a los 103 años. Gracias por entenderlo a todos. A mi madre y a mi hermano, porque gracias a ellos, todo. Gracias al optimismo que transmite mi madre, siempre, y en especial en las curvas.

Gracias a Diego, por la paciencia y los ánimos, por ayudarme, por creer en mí, y por poner banda sonora a mi vida.

"I learned you get what you can get

So, if you are rough enough… you can get!"

Adaptado de Bruce Springsteen

A mi padre,

con quien me hubiera encantado
hablar de esto

Resumen

El manejo convencional del suelo derivado de la agricultura intensiva está incrementando el riesgo de desertificación, además de otras consecuencias relacionadas con la emisión de gases de efecto invernadero, contaminación de aguas y pérdida de biodiversidad. El bajo nivel de materia orgánica en los suelos agrícolas es uno de los principales factores que condicionan su degradación.

Dentro del contexto de desarrollo de modelos de gestión agraria sostenible se encuentra la revalorización de residuos vegetales a través de la producción de biochar. El biochar es un material carbonoso sólido que se obtiene de la descomposición térmica de residuos orgánicos a temperaturas relativamente bajas (< 700 °C) y baja o nula concentración de oxígeno en un proceso denominado pirólisis. Este proceso estabiliza el carbono existente en la biomasa en una forma muy resistente a la degradación fisicoquímica o microbiológica. Su aplicación al suelo como enmienda orgánica ha sido muy estudiada en los últimos años por su capacidad para mejorar las propiedades de algunos suelos, así como mejorar el rendimiento de los cultivos y contribuir al secuestro de carbono en el suelo.

Los beneficios de la aplicación de biochar sobre los servicios ecosistémicos están ligados a su localización específica y son muy dependientes del tipo de biomasa utilizada en el proceso de pirólisis, así como de las condiciones de operación del proceso. El grado de conocimiento sobre el efecto del biochar en el sistema suelo-planta-microorganismos es muy reciente y los resultados disponibles son muy variables y dependientes del tipo de experimento llevado a cabo.

El presente trabajo de investigación ha tenido como objetivo ampliar el conocimiento científico actual relativo a la revalorización de residuos agrícolas y forestales como enmiendas orgánicas a través de la producción de biochar.

En primer lugar, se ha evaluado la idoneidad de diferentes residuos lignocelulósicos de origen agrícola (sarmiento de viña, paja de trigo peletizada y rastrojo de maíz) como precursores de biochar, producido este último mediante pirólisis lenta y bajo distintas condiciones de proceso. Se ha estudiado el efecto de los tres principales factores que regulan el proceso de pirólisis (temperatura final, presión absoluta y tiempo de residencia de la fase vapor en el interior del reactor) sobre una selección de variables respuesta que han sido analizadas en todas las muestras de biochar.

Se han analizado las propiedades mecánicas de dos tipos de biochar, procedentes de viña y de encina, con el objetivo de facilitar las aplicaciones a gran escala en el suelo. Se ha analizado, para cada muestra de biochar, su resistencia al impacto, a esfuerzo cortante y a compresión. Además, se ha simulado el proceso de aplicación en campo a través de un agitador automático y se han determinado las variaciones en la distribución del tamaño de partícula de las muestras de biochar bajo diferentes grados de humectación.

Los efectos de la aplicación de biochar sobre el sistema suelo-planta-microorganismos han sido evaluados a través del desarrollo de un ensayo de larga duración con un cultivo de sorgo (*Sorghum bicolor*), bajo condiciones de invernadero, en el que se ha analizado el efecto de la temperatura final de pirólisis y la dosis de biochar sobre la generación de biomasa y algunas propiedades físicas, químicas y biológicas de dos sustratos de diferentes texturas. Por último, se ha evaluado la aptitud del biochar como componente del sustrato de cultivo en el proceso de reproducción del banco nativo de micorrizas arbusculares de un suelo.

Los resultados indican que las biomasas agrícolas estudiadas son adecuadas para la producción de biochar, cuyas propiedades se han visto principalmente afectadas, en primer lugar, por el tipo de biomasa y, en segundo lugar, por las condiciones de pirólisis. Dentro de éstas, la temperatura final de pirólisis ha sido el factor que más ha influenciado las características de los biochars obtenidos.

Respecto al comportamiento mecánico de residuos de poda, los biochars producidos a partir de restos de poda de encina han resultado significativamente más resistentes que los de sarmiento de viña, independientemente de la temperatura final de pirólisis adoptada. El tipo de biomasa, la temperatura final de pirólisis y el tipo de procesado mecánico han tenido efectos significativos sobre la distribución del tamaño de partícula, siendo el biochar de encina el que ha generado una mayor cantidad de partículas finas. La aportación de humedad al biochar se ha mostrado eficaz para aquellas muestras de biochar que presentan una estructura estable y valores relativamente altos de capacidad de retención de agua.

La aplicación de biochar procedente de sarmiento de viña a 400 °C ha tenido efectos significativos sobre la producción de biomasa radicular en el cultivo de sorgo. Además, se ha constatado un mayor número de plantas que han producido grano bajo la aplicación de este tipo de biochar. Este biochar también ha tenido un efecto positivo sobre el grado de micorrización de las plantas, el contenido de esporas de micorrizas arbusculares en el suelo, y el incremento de las poblaciones de *Pseudomonas* genus. Este buen resultado ha motivado el empleo de este biochar concreto como componente del sustrato de cultivo en el proceso de multiplicación del inóculo nativo de micorrizas arbusculares de un suelo. El resultado de dicho estudio ha sido positivo.

La aplicación de biochar ha tenido un efecto positivo con la mejora de la capacidad de retención de agua de los sustratos de cultivo utilizados. Esta mejora aumentó con la temperatura final de pirólisis del biochar. Por último, se han detectado incrementos significativos de la adición de biochar en el contenido de K, Ca y Mg de los sustratos de cultivo.

Abstract

Conventional soil management derived from intensive agriculture is increasing the risk of desertification; in addition, the emission of greenhouse gas emissions, water pollution and loss of biodiversity are also potential risks. The low level of organic matter in agricultural soils is one of the main factors conditioning their potential to suffer degradation.

In the context of the development of sustainable agricultural management models, management of plant waste via the production of biochar appears as an interesting alternative. Biochar is a solid carbonaceous material obtained from the thermal decomposition of organic waste at relatively low temperatures (< 700 ° C) and with low or no oxygen concentration in a process known as pyrolysis. This process stabilizes the biomass carbon making it resistance to physicochemical or microbiological degradation. Soil application as an organic amendment has been widely studied in recent years due to its ability to improve the properties of some soils, as well as to improve crop yields and contribute to soil carbon sequestration.

The benefits of applying biochar on ecosystem services are site-specific and highly depend on the type of biomass used in the process, and the pyrolysis operating conditions. The degree of knowledge on the effect of biochar on the soil-plant-microorganism system is very recent and the results available so far are extremely variable and depend on the type of experiment carried out.

The present work has been developed with the aim at providing scientific knowledge on the application of agricultural and forestry residues-derived biochar as organic amendment.

First, the potential of different agricultural lignocellulosic residues (vine shoot, pelletized wheat straw and corn stover) to be used as biochar precursors was evaluated. Biochar was produced via slow pyrolysis under different operating conditions. The effect of the three main factors regulating the pyrolysis process (final temperature, absolute pressure and residence time of the vapor phase inside the reactor) on a several response variables was assessed.

Mechanical properties of two types of biochar (i.e., from vine shoots and holm oak pruning) were also measured with the aim at providing useful knowledge and experience for biochar application at large scale. These biochars were characterized in terms of resistance to impact, shear stress and compression. Furthermore, a field application process was simulated using an automatic agitation system and the changes in the particle size distribution of biochar samples were determined under different moisture contents.

The effects of biochar application on the soil-plant-microorganism system was evaluated by developing a long-term trial using a sorghum (*Sorghum bicolor*) crop, under greenhouse conditions. The effect of the final pyrolysis temperature and biochar dosage on the generation of biomass and some physical, chemical and biological properties, was

evaluated for two substrates with different textures. Finally, the suitability of biochar as growing media component in the reproduction process of indigenous bank of arbuscular mycorrhizae in a soil was assessed.

The results obtained confirmed the suitability of the selected biomasses as biochar precursors. The observed differences in the properties of resulting biochars were explained by the type of biomass and, to a lesser extent, the pyrolysis operating conditions. Among the latter, the final pyrolysis temperature was the most influencing factor.
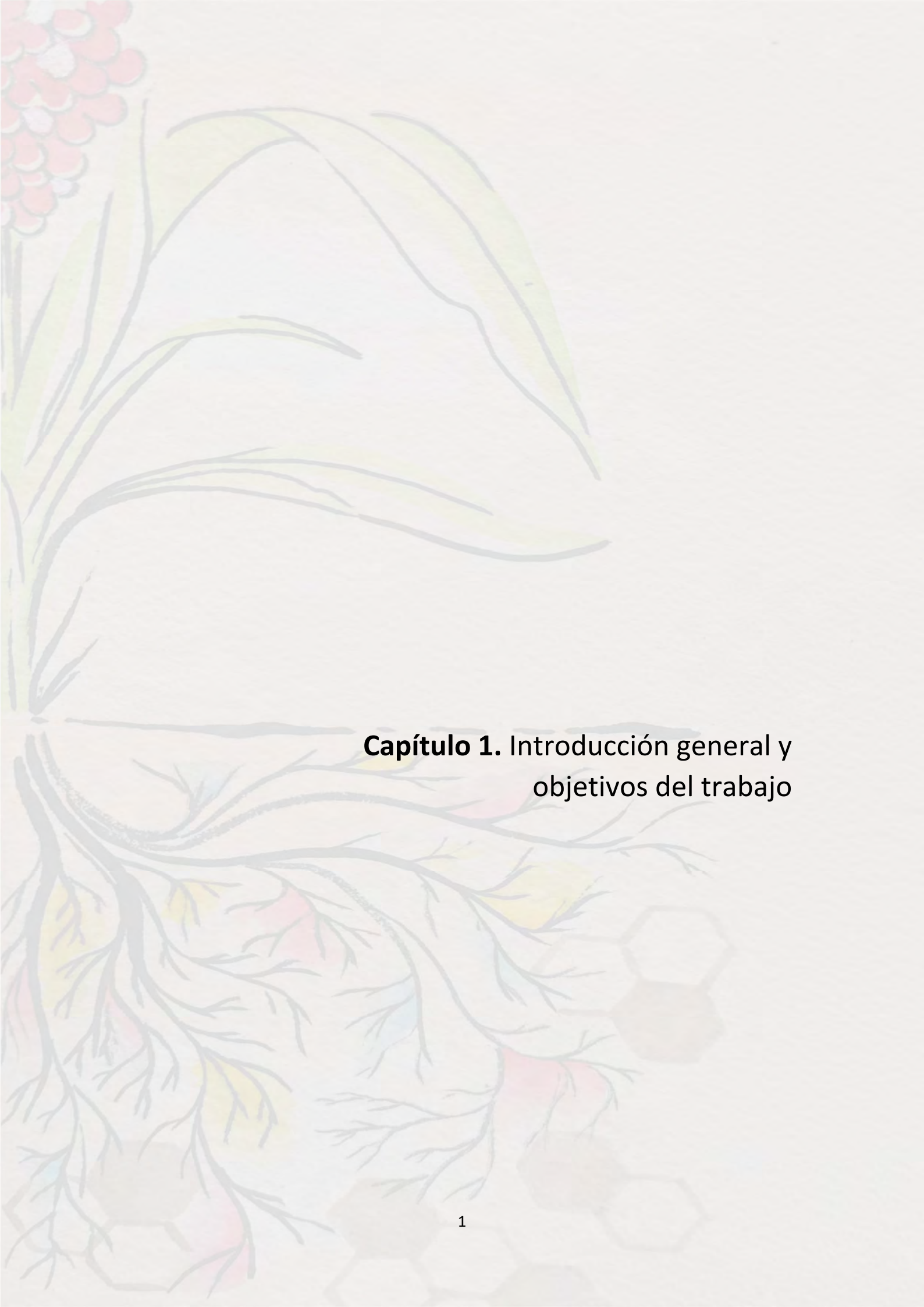
Regarding the mechanical behavior of pruning residues, biochar produced from holm oak pruning remains has been significantly more resistant than those from vine shoots, regardless of the final pyrolysis temperature. The type of biomass, the final pyrolysis temperature and the mechanical processing significantly affected the particle size distribution of biochars. Oak-derived biochar generated a higher number of fine particles. Biochar moistening appeared as a recommended practice when biochar samples has a stable structure and relatively high-water retention capacity.

The application of vine shoots-derived biochar, produced at 400 °C, significantly affected the production of root biomass in sorghum crop. In addition, a larger number of plants have been found to produce grain under the application of this type of biochar. This biochar also had a positive effect on the mycorrhization degree of the plants, the content of arbuscular mycorrhizae spores in the soil, and the increase in *Pseudomonas* genus populations. These encouraging results motivated the study of this specific biochar as a component of the culture substrate in the multiplication process of indigenous arbuscular mycorrhizae from a soil. The suitability of the tested biochar for this purpose was successfully demonstrated.

The application of biochar had a positive effect on the improvement of the water retention capacity of growing substrates. This improvement increased further for biochars produced at the highest temperature. Finally, significant increases of the addition of biochar on the K, Ca and Mg contents into the growing media have been detected.

Tabla de contenido

Capítulo 1. Introducción general y
objetivos del trabajo

1.1. El suelo: recurso no renovable

El suelo constituye el soporte básico para la existencia de los ecosistemas terrestres. Se trata de un recurso no renovable, por lo que cualquier proceso de degradación que sufra tiene consecuencias irreversibles en la mayoría de los casos (Meco et al., 2011). Desde un punto de vista medioambiental, el manejo convencional del suelo derivado de la agricultura intensiva incrementa la erosión, la compactación y la pérdida de fertilidad, situándolo en riesgo de desertificación. Además, este manejo tiene otras consecuencias relacionadas con la emisión de gases de efecto invernadero, la contaminación de las aguas superficiales y subterráneas, y la pérdida de biodiversidad (Schiefer et al., 2016; Turpin et al., 2017; Shahzad et al., 2018; Farooq et al., 2019).

En este contexto, el desarrollo de modelos de gestión agraria sostenible se hace prioritario. El esfuerzo de muchos investigadores y técnicos se centra en la actualidad en evaluar e impulsar técnicas de manejo sostenible que conserven y favorezcan los principales servicios ecosistémicos (mantener la productividad, favorecer la biodiversidad, conservar el suelo y mitigar el cambio climático).

El bajo nivel de materia orgánica en los suelos agrícolas es uno de los principales factores que condicionan su tendencia a la degradación. La incorporación de los restos de cosecha al suelo es una de las prácticas que contribuyen a mejorar la fertilidad del mismo, incrementando además la eficiencia del agroecosistema, puesto que disminuye la cantidad de biomasa exportada del mismo. En ambientes semiáridos –como podrían ser los sistemas agrarios de secano españoles– los restos de cosecha aumentan la materia orgánica y el contenido de nutrientes en el suelo. Sin embargo, los suelos de zonas degradadas presentan escasos niveles de vegetación, debido principalmente a su baja productividad. Es por ello que el contenido de materia orgánica disminuye con el tiempo, tanto por los mínimos aportes como por el proceso de mineralización de los contenidos existentes (García et al., 2014). Por otra parte, esta práctica no resulta recomendable en algunas situaciones; por ejemplo: cuando existe una posible presencia en los restos vegetales de inóculo de determinados hongos que pueden afectar al cultivo (sirva como ejemplo el caso de la viticultura, en la que los manuales de agricultura integrada recomiendan la quema de los restos de poda), o cuando se produce emisión de sustancias fitotóxicas procedente de la descomposición de los restos de cultivo en ambientes húmedos.

Una forma de mejorar la calidad y productividad de los suelos degradados es agregar materia orgánica exógena a los mismos (Tejada et al., 2010). Esta aplicación supone una mejora de la fertilidad de los suelos en sus tres componentes: la parte física (contribuyendo a mejorar la estructura y porosidad, y como consecuencia la capacidad de retención de agua), la química (mejorando el contenido de macro y microelementos), y la biológica (estimulando la actividad de los microorganismos).

Durante años, la reposición de materia orgánica en los suelos se ha realizado a través de la aplicación de estiércoles o compost. En la actualidad, el balance entre necesidades y disponibilidad de nutrientes procedentes de subproductos ganaderos no guarda un

equilibrio, por lo que se hace imprescindible buscar nuevas fuentes de materia orgánica; por ejemplo, aquellas basadas en residuos orgánicos. En este sentido, la correcta caracterización de los residuos, la evaluación de su efecto a largo plazo en el suelo y la aplicación de procesos de estabilización son aspectos prioritarios, puesto que además de ser fuente de materia orgánica y nutrientes esenciales para las plantas, los residuos orgánicos también pueden contener elementos potencialmente tóxicos que suponen un riesgo para el ecosistema (García et al., 2014).

1.2. El biochar como estrategia de enmienda de suelos

1.2.1. El concepto de biochar

El término biochar se define como un material carbonoso sólido obtenido a partir de biomasa mediante descomposición térmica a temperaturas relativamente bajas (< 700°C) y baja o nula concentración de oxígeno, en un proceso conocido como pirólisis (International Biochar Initiative, 2015). La definición más extendida del biochar se complementa con el consenso científico que establece como objetivo de su producción la aplicación al suelo como enmienda (ya sea para mejorar las propiedades del mismo, almacenar carbono y/o retener agua), así como la obligación de que el proceso de obtención sea sostenible a todos los niveles; de esta forma se diferencia del *char* o *carbón* que se produce con finalidad energética, procesos de filtrado, reductores en la industria metalúrgica, etc. (Guo et al., 2016).

La estructura del biochar es relativamente porosa, rica en carbono estable y otros nutrientes para las plantas como nitrógeno, fósforo o azufre, junto con cenizas, hidrógeno y oxígeno. La superficie porosa del biochar contiene además numerosos grupos funcionales y elementos húmicos y fúlvicos extractables. Debido a la presencia de carbono aromático, la estructura molecular del biochar posee un alto grado de estabilidad frente a la degradación, tanto química como microbiológica (Godoi et al., 2009). Por lo tanto, el tiempo de residencia del biochar en el suelo se sitúa en el intervalo de cientos hasta miles de años, es decir, aproximadamente entre 10 y 1000 veces superior que los tiempos de residencia de otros tipos de biomasa en el suelo (Rosas, 2015). El uso de biochar está adquiriendo gran repercusión en los últimos años, ya que puede ser una vía de actuación simultánea para mejorar la productividad de suelos agrícolas, valorizar residuos y reducir las emisiones de CO_2 (García et al., 2014). Hasta la actualidad se ha publicado un gran número de estudios describiendo diversos aspectos del biochar relacionados con su producción, caracterización y aplicación (entre ellos Guo et al., 2016; Camps Arbestain et al., 2014; Albuquerque et al., 2016; Manyà y Gascó, 2021). Sin embargo, el espectro de resultados es muy amplio cuando se analiza la influencia del biochar sobre la fertilidad del suelo. Se puede afirmar que sus beneficios son sitio-específicos (Blanco-Canqui, 2021), muy dependientes del tipo de biomasa utilizada para su producción y de las condiciones experimentales de la pirólisis (Manyà et al., 2014; Manyà et al., 2018), como se explica en los siguientes apartados.

1.2.2. Contexto histórico del biochar

La investigación y el estudio del biochar como enmienda de suelos son relativamente recientes. No obstante, el uso del carbón vegetal se remonta a miles de años. Como residuo no intencional del fuego, era uno de los materiales utilizados en las pinturas rupestres del Paleolítico superior (Antal y Grønli, 2003). En países como Inglaterra o Japón, el uso del carbón vegetal fue tema de investigaciones relacionadas con la agricultura a finales del S. XIX y a lo largo del S. XX. En Japón, es común el uso del biochar en suelos, así se ha encontrado detallado su uso en viejos textos de agricultura del año 1697, y fue durante la década de los años ochenta cuando se intensificó su investigación (Lehmann, 2009). En España, el oficio de carbonero tuvo una gran relevancia, desde el uso de carbón como fuente de calor para cocinar, para los braseros, la herrería o los vehículos a gasógeno (Monesma, 1993).

El interés en los últimos años por la aplicación en suelos de este material se debe principalmente al descubrimiento de partículas similares al carbón en suelos muy fértiles y de alto contenido en carbono del Amazonas en Brasil, denominados localmente como *Terra preta do Indio*; estos suelos son ricos en carbono orgánico y poseen un nivel de fertilidad mayor al de los suelos adyacentes. La recalcitrancia de este material (término utilizado para indicar materia orgánica muy persistente por su estabilidad o resistencia a los procesos de degradación microbianos o fisicoquímicos del suelo) frente a otras enmiendas orgánicas y su contribución al incremento de la disponibilidad de nutrientes en el suelo también han contribuido a su desarrollo.

1.2.3. Producción de biochar mediante pirólisis

La pirólisis es un proceso termoquímico mediante el cual el material orgánico se descompone por la acción del calor en una atmósfera libre o deficiente de oxígeno. A través de este proceso, la biomasa se descompone en fracciones de producto: (a) una mezcla de gases no condensables, (b) vapores que después de su condensación dan lugar a líquidos de pirólisis (también conocidos como aceite de pirólisis o *biooil*) y (c) un residuo sólido, conocido como biochar (Ronsse et al., 2021). Los gases no condensables abandonan el sistema y, a través de su combustión, pueden ser reutilizados para aportar calor al proceso. Las transformaciones físicas y químicas que tienen lugar durante el proceso de pirólisis son complejas y dependientes del tipo de biomasa y de las condiciones experimentales, lo que también condiciona el rendimiento a producto de cada una de las fracciones (Dhyani, 2018).

La pirólisis es una reacción endotérmica. De acuerdo a Van de Velden et al. (2010), los requerimientos de calor necesarios para el proceso de pirólisis de un amplio rango de biomasas agrícolas y forestales están en el rango comprendido entre 207 y 434 kJ kg^{-1}. Sin embargo, existen reacciones secundarias de índole exotérmica, donde los vapores de pirólisis liberados durante la descomposición térmica inicial sufren procesos de craqueo o polimerización (Anca-Couce, 2017). En función de la intensidad de dichas

reacciones exotérmicas, la demanda global de energía para mantener el proceso de pirólisis puede ser realmente bajo.

Como resultado de la amplia investigación del proceso (sirvan como ejemplo los estudios de Di Blasi et al., 1999; Stenseng et al., 2001; Manyà et al., 2003; González et at al., 2005; Hu et al., 2007; Giuntoli et al., 2009), las principales variables que afectan al proceso de producción de carbón vegetal y a las características físicas, químicas y biológicas de éste, cada vez están más estudiadas; estas variables son: temperatura final de pirólisis, presión absoluta, tiempos de residencia de la fase vapor en el interior del reactor, velocidad de calentamiento, tamaño de partícula y atmósfera de pirólisis (Manyà, 2012). En función del producto deseado, estas condiciones experimentales pueden ajustarse. Por lo general, altas velocidades de calentamiento y tiempos de residencia bajos favorecen la formación de productos condensables, mientras que velocidades de calentamiento más bajas y tiempos de residencia elevados favorecen la formación de productos gaseosos no condensables, debido a la mayor intensidad de reacciones secundarias de craqueo y/o reformado. El rendimiento del producto sólido se ve favorecido a velocidades de calentamiento muy bajas (menos de 20 °C min^{-1}) y temperaturas relativamente bajas.

Como se puede deducir del párrafo anterior, la variable más importante que permite diferenciar los procesos de pirólisis es la velocidad de calentamiento. La pirólisis puede clasificarse en dos principales tipologías: pirólisis lenta (a bajas velocidades de calentamiento, menores de 80 °C min^{-1}, y tiempos de residencia —tanto del sólido como de los vapores de pirólisis— elevados) y pirólisis rápida (a elevadas velocidades de calentamiento, mayores de 1000 °C min^{-1}, y tiempo de residencia muy reducido) (Ronsse et al., 2021).

El proceso de pirólisis se puede llevar a cabo en distintas tipologías de reactor. Existe un amplio rango de tecnologías a través de las cuales, el biochar se obtiene como producto principal o como co-producto. Los principales tipos de reactores se clasifican en (Ronsse et al., 2021): reactores de pirólisis rápida (un ejemplo son los reactores de lecho fluidizado o los de cono rotativo) y reactores de pirólisis lenta e intermedia (reactores de tornillo sin fin, hornos rotatorios o unidades discontinuas).

La producción de biochar mediante pirólisis se presenta como una posible alternativa tecnológica para obtener un balance de carbono negativo. El biochar producido a partir de residuos biomásicos se incorpora al suelo proporcionando un sistema de almacenamiento de carbono estable durante mucho tiempo. De este modo, podría eliminarse CO_2 de la atmósfera, ya que, en primer lugar, el CO_2 se asimila durante el crecimiento de las plantas y, posteriormente, el carbono estable del biochar permanecería almacenado en el suelo, evitando su retorno a la atmósfera debido a la descomposición. Además, los co-productos del proceso de pirólisis (gas y biooil) se consideran combustibles renovables que podrían sustituir a los combustibles fósiles en la producción de electricidad u otros usos.

Los resultados preliminares indican que la co-producción de biochar y bioenergía no sólo conduce a una retención neta de CO_2, sino que la presencia del biochar en el suelo puede disminuir las emisiones de otros gases de efecto invernadero, como el óxido nitroso (N_2O) y metano (CH_4) (García et al., 2014).

El presente trabajo se centra en la producción de biochar a partir de residuos lignocelulósicos, que están compuestos por tres componentes principales: celulosa, hemicelulosa y lignina. En función del tipo de biomasa seleccionada, se establecen diferencias en la proporción de cada componente. Comparativamente, la estructura rígida de los árboles posee una proporción alta de lignina, mientras que las especies herbáceas son más celulósicas (Askeland et al., 2019). La hemicelulosa es el componente que se degrada con mayor facilidad, alcanzando su degradación completa a temperaturas cercanas a 330 °C (Yeo et al., 2017; Buss et al., 2015). La mayor parte de la degradación de la celulosa ocurre a temperaturas de aproximadamente 427 °C, aunque puede comenzar a menores temperaturas, generando materia volátil (Buss et al., 2015). La lignina es el componente más recalcitrante, cuya degradación completa se produce a temperaturas superiores a los 607 °C (Yeo, et al., 2017).

1.2.4. Composición y propiedades del biochar

Entre los componentes principales del biochar se encuentran los siguientes: carbono fijo, materia volátil, materia inorgánica (cenizas) y humedad (Antal y Grønli, 2003). A medida que aumenta la temperatura de pirólisis, se incrementa la proporción de carbono aromático presente, debido al aumento relativo en la pérdida de material volátil (inicialmente agua, seguido por hidrocarburos, vapores alquitranados, H_2, CO y CO_2), y la conversión de alquilos (Baldock y Smernik, 2002; Dermibas, 2004).

Como ya se ha comentado anteriormente, el biochar es un material relativamente poroso y, en consecuencia, posee cierta área superficial específica (Lehmann y Joseph, 2015). Esta propiedad determina la reactividad y la capacidad del biochar para retener iones en superficie; además, la porosidad también es responsable de la capacidad de retención de agua (Steiner, 2016). Desde un punto de vista agronómico, el área específica junto a la densidad (que suele ser bastante baja en el biochar) son características interesantes a la hora de establecer un uso adecuado del biochar.

Las condiciones de pirólisis regulan las características del biochar relacionadas con el contenido de materia orgánica volátil y la estabilidad del biochar en el tiempo, mientras que otras propiedades, como el contenido de elementos nutrientes para las plantas, dependen en mayor medida del tipo de biomasa seleccionada para el proceso (Steiner, 2016).

El contenido de carbono total en el biochar oscila entre 172 y 905 g Kg^{-1}; sin embargo, la media para una amplia variedad de materiales se encuentra por debajo de 550 g Kg^{-1}. El contenido de N total varía entre 1,7 y 78,2 g Kg^{-1}, dependiendo de la materia prima (Chan y Xu, 2009). A pesar de parecer alto, el contenido de N total presente en el

biochar puede ser no necesariamente beneficioso para los cultivos, ya que el N se encuentra principalmente en una forma no disponible.

El contenido de P total y K total presentes en el biochar oscilan en un rango amplio en función de la materia prima utilizada (Chan y Xu, 2009). En general, la variabilidad en los contenidos de N, P y K totales en el biochar son más amplios que los que aparecen recogidos en la literatura para los fertilizantes orgánicos típicos (García et al., 2014).

La microscopía electrónica de barrido (SEM) es una técnica útil para analizar la morfología del biochar. La estructura macroporosa (poros de más de 50 nm de diámetro) del carbón vegetal producido a partir de biomasa lignocelulósica hereda la arquitectura de la materia prima, y es potencialmente importante para la retención de agua y la capacidad de adsorción del suelo (Day et al., 2005). La superficie específica medida por adsorción de gas, sin embargo, es mayormente microporosa (poros inferiores a 2 nm). Los microporos no son relevantes para las raíces de plantas, microorganismos, ni para la solución del suelo. La temperatura de pirólisis es el principal factor que gobierna las propiedades texturales, lo que lleva a sugerir que el biochar producido a temperaturas relativamente bajas (con escaso desarrollo poroso) puede ser adecuado para controlar la liberación de nutrientes de los fertilizantes (Day et al., 2005), mientras que aquellos obtenidos a altas temperaturas darían lugar a materiales análogos al carbón activado (Owaga et al., 2006).

Diferentes organizaciones (International Biochar Initiative, European Biochar Fundation, British Biochar Fundation, etc.) han propuesto un conjunto de características a analizar con el objetivo de definir la calidad del biochar para su uso en agricultura. Estos parámetros son:

- Distribución del tamaño de partícula.
- pH.
- Área superficial específica.
- Contenido de carbono y nutrientes.
- Contenido de compuestos volátiles.
- Contenido de ceniza.
- Capacidad de retención hídrica.
- Densidad aparente.
- Volumen de poro.
- Contenido de contaminantes (metales pesados, hidrocarburos aromáticos policíclicos, etc.).

Las guías publicadas por estas organizaciones describen los métodos analíticos recomendados para el análisis de las propiedades físicas y químicas, instrucciones para el correcto almacenamiento y condiciones de aplicación que aseguren la calidad de los potenciales biochars comerciales. Junto con otros trabajos de investigación (Major, 2010; Liu, 2013; Das et al., 2020), estas guías enfatizan sobre la necesidad de pre-acondicionar y caracterizar correctamente los lotes de biochar después de estos

tratamientos para su correcta aplicación (por ejemplo, después del triturado, humectación, etc.). Todavía hay barreras técnicas y prácticas, tanto para el manejo seguro, como para la correcta aplicación a gran escala del biochar (Sadasivam y Reddy, 2015).

La caracterización de la distribución del tamaño de partícula de cada biochar también es un parámetro de interés. Los disturbios naturales o mecánicos en el proceso de aplicación del biochar pueden dar lugar a la emisión de partículas finas a la atmósfera inferiores a 10 μm (PM_{10}), las cuales pueden permanecer en el ambiente y penetrar en el tracto respiratorio de los humanos (Geraldi et al., 2019; Li et al., 2018). Además, los aerosoles de carbón antropogénico tienen un gran potencial de radiación, contribuyendo al efecto del cambio climático (Maienza et al., 2017). Las partículas finas de biochar pueden facilitar el transporte de contaminantes adsorbidos al ambiente, a través de procesos de percolación y lixiviación (Wang et al., 2013). Por último, el polvo generado por el biochar es susceptible a la ignición, cuando se encuentra almacenado en espacios cerrados (Das et al., 2020). En este sentido, la humectación del biochar es una práctica recomendada para su aplicación, aunque no están publicadas dosis de humedad específicas. Por todo ello, la susceptibilidad del biochar a la fragmentación y generación de partículas finas es un tema de interés que no ha sido investigado en profundidad.

1.3. Efectos del biochar sobre el sistema suelo-planta-microorganismos

El grado de conocimiento sobre el efecto del biochar en el sistema suelo-planta es muy reciente y los resultados consultados son muy variables y dependientes del tipo de experimento llevado a cabo.

Una de las ventajas del uso del biochar como enmienda del suelo es que el C puede ser almacenado durante cientos de años, dada la estabilidad del biochar, mejorando el crecimiento de las plantas y el secuestro de carbono en el suelo (Lehmann et al., 2006). No obstante, se ha encontrado que existe otra fracción del biochar que no sería estable a largo plazo (Sohi et al., 2009); de este modo se ha sugerido que el biochar estaría formado por componentes estables y otros que, en cambio, serían degradables. Se necesita un mayor número de estudios que investiguen acerca de la estabilidad del biochar a corto y largo plazo bajo suelos y climas diferentes. Las condiciones de pirólisis, así como las características de la materia prima utilizada en la producción de biochar, serían los aspectos que determinarían la proporción de componentes relativamente lábiles en el biochar.

La aplicación del biochar como enmienda está motivada por su capacidad para mejorar el rendimiento de los cultivos y alterar las propiedades físicas y químicas del suelo, como la capacidad de retención de agua, pH, capacidad de intercambio catiónico y retención de nutrientes (Al-Wabel et al., 2018; Igalavithana et al., 2016; Bohara et al., 2019), así como algunos estudios también reportan la capacidad de este material para reducir la lixiviación y escorrentía superficial, así como la absorción de pesticidas y

metales pesados (Major, 2010). Sin embargo, como ya se ha comentado, esta influencia está fuertemente ligada a la temperatura final de pirólisis del biochar, tamaño de partícula, textura del suelo y mineralogía (Butnan et al., 2015; Guo, 2016).

Por lo general, el biochar aumenta la productividad y calidad del suelo, sobre todo en suelos ácidos y pobres en nutrientes, como por ejemplo los oxisoles. En la revisión de Sohi et al. (2009) se analizaron 13 estudios de diferentes autores en los que se obtuvieron incrementos de productividad en los diferentes cultivos realizados. Se propusieron tres mecanismos para tratar de explicar cómo el biochar permitió aumentar la producción en cosechas: (i) por la modificación directa de la química del suelo debido a la composición del biochar, (ii) el biochar está formado por superficies químicamente activas que permiten modificar la dinámica de los nutrientes en el suelo o bien catalizan reacciones útiles para la obtención de un suelo fértil, y (iii) el biochar modifica físicamente el suelo de manera que beneficia el crecimiento de las raíces y aumenta la retención de agua y nutrientes.

Por otra parte, la interacción del biochar con los fertilizantes, así como los efectos sobre la biota del suelo y sus implicaciones sobre la ecología del mismo son factores todavía poco conocidos en este sentido (Lehmann et al., 2011). Las investigaciones al respecto están orientadas al estudio de la estructura física del biochar y las interacciones con microorganismos, como las micorrizas, si bien se ha encontrado variabilidad en los resultados. Algunos estudios han encontrado incrementos de la actividad microbiana en suelos enriquecidos con biochar (Steiner et al., 2008). Dichos estudios hacen referencia a la capacidad del biochar, debido a su estructura en microporos, para permitir el establecimiento de colonias microbianas.

Los microorganismos benéficos habitantes de la zona rizosférica son fundamentales para mantener las producciones agrícolas. Actualmente, estos factores biológicos del suelo se han convertido en criterios de importancia para valorar la fertilidad del suelo.

Un indicador de calidad es una propiedad del suelo relacionada con alguna o varias funciones del mismo. Para que una propiedad pueda ser un indicador de calidad debe, ante todo, ser sensible ante cambios en el uso del suelo, a diferentes manejos del mismo y a cambios climáticos y antropogénicos (Shukla et al., 2006). Para evaluar la calidad del suelo es necesario tener un conjunto mínimo de datos formado por un número de indicadores, diferentes en función de los aspectos del suelo que se quieran evaluar. Para utilizar estos indicadores de un modo razonable deben ser fáciles de medir, reproducibles, fáciles de entender y deben albergar aspectos físicos, químicos y biológicos (Imaz y Virto, 2010).

 Hoy en día, el concepto de "calidad del suelo" se relaciona directamente con la productividad, la salud y la sostenibilidad de los sistemas agrícolas (Barea, 2009). Desde el punto de vista agronómico la "calidad del suelo" es expresada como "fertilidad" y define la capacidad de un suelo para soportar plantas sanas y productivas (Jaizme-Vega, 2011). La Figura 1 resume la interacción de los diferentes factores que influyen en la calidad del suelo.

Figura 1.- Interacción de los diferentes factores que influyen en la calidad del suelo (adaptado de Barea, 2017).

Las interacciones entre las propiedades físicas, químicas, biológicas y climáticas del sistema son las que identifican la fertilidad de los suelos, y en este contexto, los hongos micorrícicos se consideran como componentes clave de dicha fertilidad, bien sea a través de la propia simbiosis o por su interacción con otros microorganismos de la rizosfera (Jaizme Vega, 2019). El efecto del biochar sobre este tipo de hongos y otros microorganismos ha sido estudiado por diferentes autores (Lehmann et al., 2011; LeCroy et al., 2013; Hammer et al., 2014; Elzobair et al., 2016; Warnock et al., 2010) habiéndose obtenido resultados alentadoramente positivos, lo que invita a profundizar en este tipo de investigaciones y a abrir posibilidades en este marco de fertilización biológica de los suelos.

1.4. Objetivos y justificación de la tesis doctoral

Como se desprende de los apartados anteriores, el interés de cada tipo de biochar como enmienda orgánica es sitio-específico y dependiente del tipo de biomasa utilizada como precursor, así como de las condiciones de pirólisis. Este trabajo de investigación se ha desarrollado para contribuir al conocimiento científico actual relativo a la revalorización de residuos agrícolas y forestales específicos como enmiendas orgánicas a través de la producción de biochar.

Los objetivos principales de este trabajo de investigación han sido:

1. Evaluar la viabilidad de diferentes residuos lignocelulósicos de origen agroforestal como precursores de biochar, producido mediante pirólisis lenta bajo distintas condiciones de operación.

2. Estudiar el efecto de las condiciones de operación y el tipo de biomasa sobre las propiedades fisicoquímicas del biochar producido.
3. Analizar el comportamiento mecánico del biochar producido a partir de residuos de poda.
4. Evaluar los efectos de la aplicación de biochar producido bajo diferentes condiciones de pirólisis sobre el desarrollo de un cultivo modelo en condiciones de invernadero y sobre ciertos parámetros fisicoquímicos del suelo.
5. Estudiar cómo la adición de biochar influye en los indicadores de la actividad biológica del suelo.

Como resultado de planificar las actividades de investigación necesarias para la consecución de los objetivos anteriores, se han identificado una serie de objetivos específicos que suponen aspectos novedosos dentro del contexto de este estudio:

- Analizar la distribución del tamaño de partícula y la emisión de partículas de polvo de biochars procedentes de residuos de poda producidos bajo diferentes temperaturas finales de pirólisis, a través de la simulación del movimiento de una abonadora comercial para su aplicación en el suelo.
- Implementar el uso de técnicas reológicas (texturómetro) para evaluar la resistencia a rotura del biochar procedente de residuos de poda.
- Evaluar la aptitud del biochar producido como componente del sustrato de cultivo en producción de planta en contenedor y su idoneidad como sustrato en el proceso de reproducción de inóculo nativo de hongos formadores de micorrizas.

Sin ser un objetivo específico, cabe mencionar que todas las muestras de biochar presentadas y analizadas en los trabajos que conforman la presente tesis doctoral han sido producidas por la autora de la tesis. Para este fin, se ha utilizado la planta de pirólisis a escala de laboratorio del Grupo de Investigación en Procesos Termoquímicos (GPT) de la Escuela Politécnica Superior de Huesca. A lo largo de la tesis se han desarrollado un total de 37 experimentos que han permitido obtener las cantidades necesarias de biochar para realizar los trabajos presentados en esta memoria.

1.5. Justificación de la unidad temática de los artículos

El documento de tesis se estructura en siete capítulos, cuatro de ellos correspondientes a publicaciones científicas relacionadas con los objetivos anteriores:
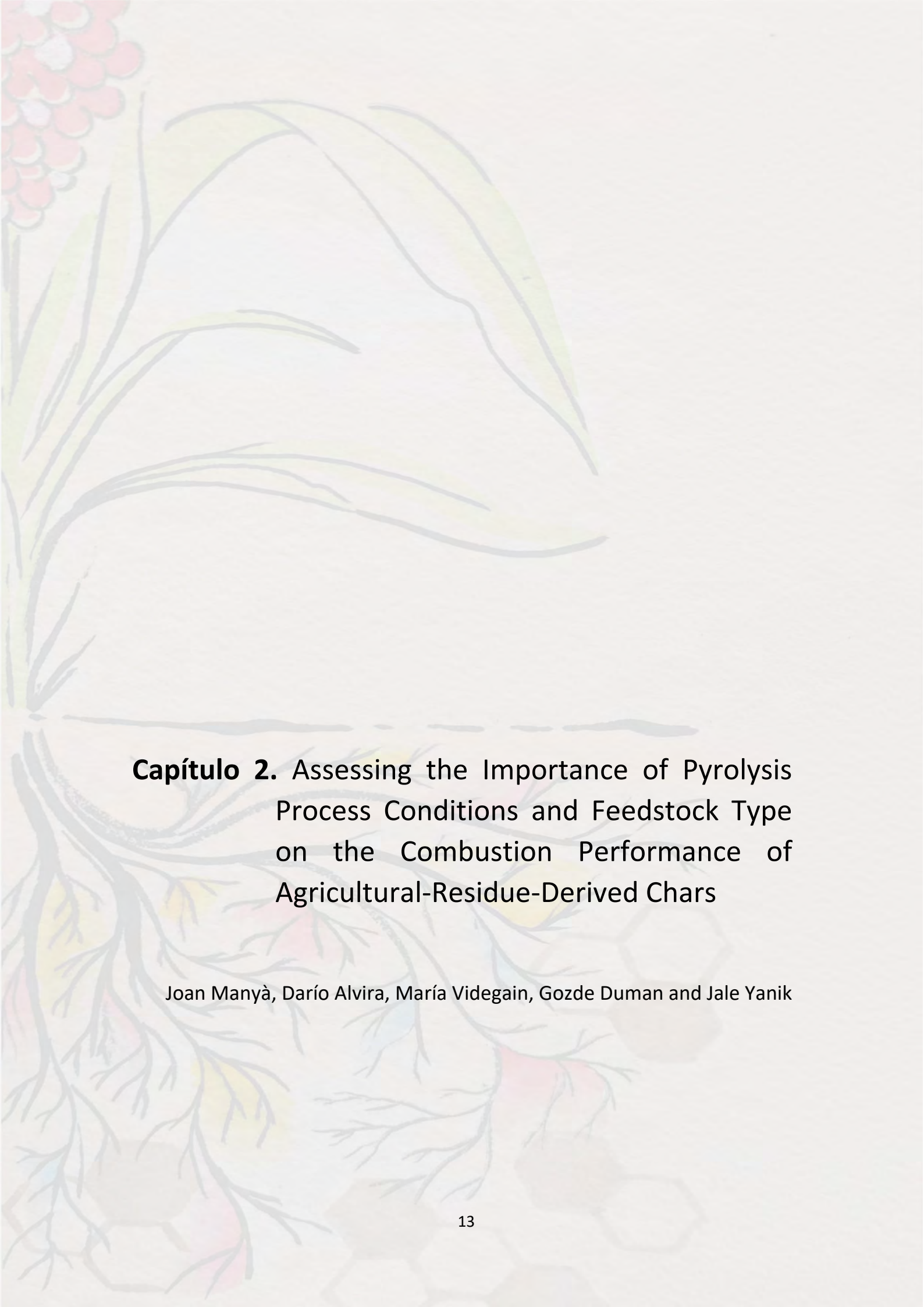
Capítulo 2 (relacionado con los objetivos 1 y 2 de la tesis): *Assessing the importance of pyrolysis process conditions and feedstock type on the combustion performance of agricultural-residue-derived chars.* En este trabajo se evaluó la aptitud de tres tipos de biomasa lignocelulósica como precursores de biochar y se evaluó el efecto de las condiciones de operación del proceso de pirólisis sobre las características químicas del producto obtenido. La contribución de la autora a este trabajo fue la realización de todos los experimentos de pirólisis, así como la caracterización química de las muestras

obtenidas y el análisis de resultados. La parte del trabajo relacionada con el rendimiento de combustión de los productos obtenidos escapa de los objetivos de esta tesis doctoral. A partir de los resultados obtenidos, se seleccionó el tipo de biomasa lignocelulósica más apropiada para el resto de experimentos de la tesis.

Capítulo 3 (relacionado con el objetivo 3 de la tesis): *Influence of feedstock and final pyrolysis temperature on breaking strength and dust production of wood-derived biochars.* A partir de residuos de poda de dos especies lignocelulósicas se realizaron experimentos de producción de biochar a diferentes temperaturas. Los biochars obtenidos fueron caracterizados morfológicamente y se sometieron a pruebas de resistencia a rotura para caracterizar su comportamiento mecánico. Se estudiaron los cambios en la distribución del tamaño de partícula de los biochars simulando el proceso de aplicación en el suelo.

Capítulo 4 (relacionado con el objetivo 4 de la tesis): *Effects of biochar application in a sorghum crop under greenhouse conditions: growth parameters and physicochemical fertility.* En este trabajo se evaluó el efecto del biochar producido a partir de sarmientos de viña sobre el desarrollo de un cultivo de sorgo en invernadero, así como algunas propiedades fisicoquímicas de los suelos utilizados para su cultivo.

Capítulo 5 (relacionado con el objetivo 5 de la tesis): *The effects of biochar on indigenous arbuscular mycorrhizae fungi from agroenvironments.* La primera parte de este trabajo complementa el artículo del capítulo anterior, evaluando los efectos sobre algunos indicadores de la actividad biológica del suelo en el ensayo realizado sobre sorgo en condiciones de invernadero. En el segundo experimento, se evaluó la aptitud del biochar como componente del sustrato de cultivo en la reproducción de inóculo nativo de uno de los suelos de estudio. El inóculo obtenido fue testado en un tercer experimento con plantas de lechuga bajo diferentes condiciones de irrigación.

Capítulo 2. Assessing the Importance of Pyrolysis Process Conditions and Feedstock Type on the Combustion Performance of Agricultural-Residue-Derived Chars

Joan Manyà, Darío Alvira, María Videgain, Gozde Duman and Jale Yanik

Assessing the Importance of Pyrolysis Process Conditions and Feedstock Type on the Combustion Performance of Agricultural-Residue-Derived Chars

Joan J. Manyà,* Darío Alvira, María Videgain, Gozde Duman, and Jale Yanik
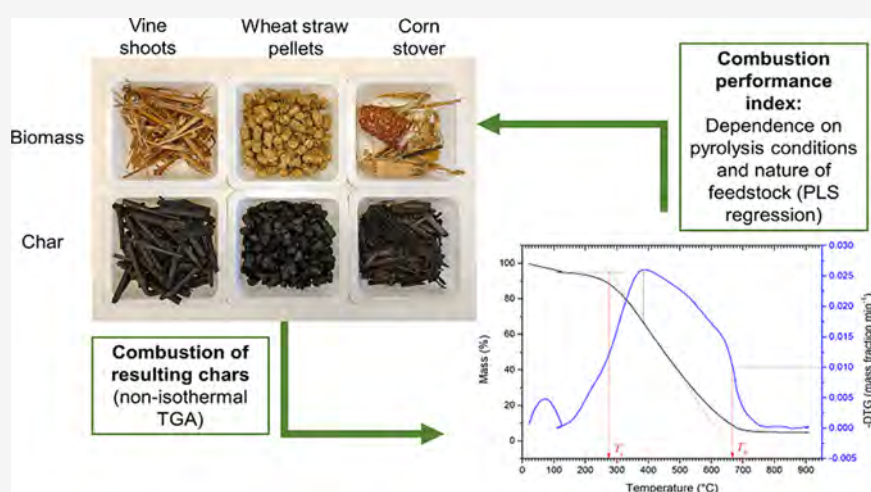
ACCESS | 　📊 Metrics & More | 　📰 Article Recommendations | 　ⓢ Supporting Information

ABSTRACT: The combustion performance of chars derived from vine shoots, wheat straw, and corn stover was investigated to assess the influence of both the biomass precursor and pyrolysis operating conditions. Chars were produced through slow pyrolysis at different peak temperatures (350 and 500 °C), pressures (0.1 and 0.5 MPa), and residence times of the vapor phase (50 and 150 s). From the thermogravimetric curves obtained under air, the combustion performance index (S) was calculated for each char. Apparent kinetics were also estimated using the Coats−Redfern method and assuming an F3/2 reaction model. Results show that the combustion patterns of chars were more influenced by the type of feedstock than by the pyrolysis conditions. Corn stover appeared to be the most interesting feedstock in order to produce chars with tuned reactivity. Results from partial least-squares (PLS) regression revealed that the most important factors affecting S were the contents of potassium (negative effect) and cellulose (positive effect) in the original biomass.

1. INTRODUCTION

Biomass is the only renewable resource of carbonaceous fuels, and therefore, it has attracted considerable attention as a replacement for coal in both power plants and domestic heating. Nevertheless, if directly used as fuel, biomass features some drawbacks, such as a low energy density, low calorific value, and high energy requirement for grinding. Thermochemical conversion technologies (such as slow pyrolysis, torrefaction, and hydrothermal carbonization) are valuable pathways for converting lignocellulose biomass into a char product with improved fuel quality.[1]

Slow pyrolysis is a well-known process, in which biomass is slowly heated under an inert gas environment up to typically 350−650 °C. A lot of research has been done on the effects of pyrolysis operating conditions and biomass feedstock on the yield and physicochemical properties of produced chars.[2−6]

However, more efforts are required to better clarify the above-mentioned effects on the performance of biomass char as an energy carrier.

To assess the fuel properties of biomass char, both the ignition and burnout temperatures are commonly used to describe the combustion behavior.[7] The ignition temperature is defined as the minimum temperature at which a given fuel ignites spontaneously in an environment without any external source of ignition.[8] For its part, the burnout temperature refers to the

temperature at which the fuel is almost completely consumed.[7] From thermogravimetric analysis (TGA) data, it is possible to estimate both ignition and burnout temperatures and also calculate the so-called combustion performance index (S), as has recently been reported by Mundike et al.[9] and Wang et al.[10] This index is a measure of the burning ability of a fuel, and a higher value reflects a more satisfactory combustion performance.[11] Knowledge of the combustion performance and kinetics of biomass chars is of great importance to properly design industrial-scale combustors, where the residence time of fuel particles is very short.[12]

Previous research has compared the combustion (or cocombustion) performance of a number of biomass-derived chars produced from different feedstocks and under different operating conditions.[13−16] These preliminary studies pointed out that char reactivity is affected by pyrolysis operating conditions under which char is obtained. The most assessed parameter was the pyrolysis peak temperature, for which an inversely proportional relationship with char reactivity has been reported.[13,14,16] Regarding the effect of pyrolysis pressure, Recari et al.[16] reported a gradual decrease in the reactivity of spruce-derived chars when pyrolysis was conducted at 1.0 and 2.0 MPa. The authors attributed this finding to the promotion of secondary charring reactions during pressurized pyrolysis. Furthermore, char combustion reactivity is strongly affected by the nature of the biomass feedstock. In this sense, the availability of alkaline and alkaline-Earth species in the ash can catalyze the reaction of combustion.[14] Recently, Pang et al.[15] reported that lignocellulosic composition of raw biomass plays a key role in determining the morphology and reactivity of the resulting chars. The authors stated that biomass with relatively high contents of lignin and cellulose could lead to increased amounts of low reactive thick-walled chars. In a more recent study, Yan et al.[17] confirmed the negative effect of the lignin content on the reactivity of biomass-derived chars.

Agricultural residues from crops have a great potential as renewable energy source, given their truly sustainable availability, which was estimated at 85 millions of tons per year in the EU.[18] A significant fraction of them comes from maize, wheat, and vine crops in the form of corn stover, wheat straw, and vine shoots (from pruning), respectively. Hence, in-depth studies on the combustion characteristics of chars produced from these precursors through slow pyrolysis at different operating conditions are highly encouraged.

For all the reasons mentioned above, the present study aims to investigate the effects of both the biomass precursor and pyrolysis operating conditions on the combustion performance and relative reactivity of the resulting chars. As operating pyrolysis process parameters, the following was considered in our study: peak temperature (350 and 500 °C), absolute pressure (0.1 and 0.5 MPa), and residence time of the gas phase within the pyrolysis reactor (50 and 150 s). The combustion behavior of all produced chars was investigated using thermogravimetric analysis (TGA) under dynamic (i.e., non-isothermal) heating conditions.

2. EXPERIMENTAL SECTION

2.1. Materials. Three biomass precursors were selected in this study: vine shoots (VS), wheat straw (WS), and corn stover (CS). Vine shoots (*Vitis vinifera L.*) of the grape variety Cabernet Sauvignon were collected during winter pruning in a vineyard located in the wine region of Somontano (Huesca province, Spain). They were selected by diameter (between 8.5 and 15 mm) and cut into smaller pieces of 4−7

cm in length. Wheat straw (*Triticum spp.*) pellets (7 mm OD and approximately 12 mm long) were supplied by a Belgian company, and no binder was used in making them. Corn stover (*Zea mays*), which was collected after cob harvesting in an irrigated field located in the province of Huesca (Spain), consisted of a mixture of corncob (15.4 wt %), leaf (80.1 wt %), and stalk (4.5 wt %). Leaves were cut into pieces of 14−16 cm in length and 1.0−2.0 mm in thickness. Relatively large particle sizes were used for two reasons: (1) to improve the carbonization efficiency (i.e., fixed-carbon yield) during pyrolysis, since using larger particles promotes the secondary charring reactions at an intraparticle level;[19] and (2) to avoid high-energy-intense biomass pretreatments for size reduction.

For all the biomass sources, proximate analyses were performed according to the procedure described below. Briefly, 1 g of powdered sample was weighed on a predried ceramic crucible and placed in a convection oven at 105 ± 5 °C for at least 4 h. After weighing, the sample was placed back into the oven at the same temperature until a constant dry weight was reached. To estimate the volatile matter content, the crucible containing the resulting oven-dried sample (with the lid placed on) was put in a muffle furnace at 925 ± 10 °C for 7 min. Finally, the ash content was determined by putting the open crucible containing the resulting volatile-free sample in the muffle furnace at 730 ± 10 °C for at least 2 h.

A CHN628 elemental analyzer from LECO (USA) was used to conduct the ultimate analyses in accordance with the ASTM Standard D5373-16. In addition, X-ray fluorescence (XRF) spectroscopy analysis (using an ADVANT'XP+XRF spectrometer from Thermo ARL, Switzerland) was performed in order to determine the inorganic constituents of the biomass ash according to ASTM Standard D4326-04.

Neutral detergent fiber (NDF), acid detergent fiber (ADF), and acid detergent lignin (ADL) were determined for all the biomass sources using a fiber analyzer (ANKOM 200, USA) and according to the method proposed by Van Soest et al.[20] Thus, it was possible to estimate the lignocellulosic constituents from the above-mentioned parameters as follows:[21] lignin (ADL), cellulose (ADF − ADL), and hemicelluloses (NDF − ADF). Organic extractives were previously extracted in a dried cotton cellulose thimble, which was inserted in a Soxhlet extractor, using a mixture of ethanol and toluene (1:2 v/v) as solvent.

2.2. Production and Characterization of Chars. Chars from the three biomass sources (at the particle size ranges detailed above) were produced through slow pyrolysis at the above-mentioned different operating conditions. Biomass feedstock was heated at an average heating rate of 5 °C min^{-1} to the desired peak temperature and then held for a soaking time of 60 min (at that temperature) to ensure the thermal equilibrium. The initial sample mass of biomass was approximately 300 g for WS and VS and 130 g for CS, due to its lower apparent density.

The bench-scale pyrolysis device consisted of a cylindrical and vertical reactor (140 mm ID and 465 mm long) made of EN 1.4835 austenitic chromium−nickel steel. The corresponding schematic diagram is shown in Figure S1 (Supporting Information). More details regarding the configuration of the system are available in previous publications.[22,23] A back-pressure regulator was used to maintain the pressure of the pyrolysis reactor at a desired value. The volumetric flow rate at standard temperature and pressure (STP) conditions of the carrier gas (N$_2$) was adjusted to keep a constant real flow rate of N$_2$ within the reactor (at the corresponding pressure and peak temperature) of 6.48 or 2.09 L min^{-1} to get carrier gas residence times of 50 and 150 s, respectively.

Produced chars were characterized by both proximate and ultimate analyses following the same procedures as described in Section 2.1. Results from these analyses were used to determine the fixed-carbon content (x_{FC}) and atomic H:C and O:C ratios. The high heating value (HHV) of solid fuels (for both biomass sources and derived chars) was measured using a calorimeter (model C-200) from IKA (Germany).

Due to the highly microporous structure of biomass-derived pyrolysis chars,[24] specific surface areas (S_{BET}) were determined from the CO$_2$ adsorption isotherms at 0 °C (using an ASAP 2020 gas sorption analyzer from Micromeritics, USA). Samples (120−175 mg)

were previously degassed under dynamic vacuum conditions to constant weight at 150 °C. Pore size distribution and ultramicropore volume (V_{ultra}) were estimated using a density functional theory (DFT) model for slit-pore geometry.

2.3. Combustion Behavior of Chars. Thermogravimetric curves under air atmosphere were obtained for all the chars using a TGA device (model STA 449 F3 Jupiter system) from Netzsch (Germany). Approximately 100 mg of char, which was previously crushed and sieved to a fraction of 150−500 μm, was first heated under N_2 (100 mL min^{-1} STP) from room temperature to 110 °C (with a soaking time of 30 min) to ensure complete drying. Then, the atmosphere was switched to air (100 mL min^{-1} STP), and dried samples were heated at 10 °C min^{-1} up to 900 °C. Raw TGA curves were corrected by the corresponding blank test.

From experimental TG and DTG curves, the following parameters were determined: ignition temperature (T_i), burnout temperature (T_b), temperature at which the highest mass-loss rate took place (T_{max}), and combustion performance index (S). T_i was estimated according to the intersection method (IM),[7] whereas T_b was identified at the temperature where the combustion rate diminished to less than 1 wt % min^{-1}.[9] S was calculated according to eq 1, where DTG_{max} and DTG_{mean} correspond to the maximum (at T_{max}) and mean values (between T_i and T_b) of the DTG curve, respectively.[9,11]

$$S = \frac{DTG_{max}DTG_{mean}}{(T_i)^2 T_b} \tag{1}$$

2.4. Apparent Kinetics. The Coats−Redfern (CR) procedure, which is one of several integral methods used to estimate apparent reactivity parameters from nonisothermal reaction data,[25,26] was adopted in the present study. The apparent reaction rate of a solid−gas reaction can be expressed as follows

$$\frac{d\alpha}{dt} = k(T)f(\alpha) \tag{2}$$

where α corresponds to the extent of conversion (the mass loss at a given time divided by the total mass loss), $k(T)$ is the temperature-dependent reaction rate constant, and $f(\alpha)$ is the model describing the mechanism. The Arrhenius equation, given in eq 3, is often used to describe $k(T)$.

$$k(T) = A\exp\left(\frac{-E_a}{RT}\right) \tag{3}$$

In eq 3, A is the apparent pre-exponential factor, and E_a is the apparent activation energy. The expression for $g(\alpha)$, which corresponds to the integrated form of $f(\alpha)$, is obtained by rearranging eqs 2 and 3, and then integrating, leading to the following general expression

$$g(\alpha) = A\int_0^t \exp\left(\frac{-E_a}{RT}\right)dt \tag{4}$$

For a constant heating rate ($\beta = dT/dt$), eq 4 can be rewritten as

$$g(\alpha) = \frac{A}{\beta}\int_0^T \exp\left(\frac{-E_a}{RT}\right)dT \tag{5}$$

Despite the assumption that both A and E_a are constant across the temperature range, the so-called temperature integral shown in eq 5 cannot be solved analytically. The CR procedure is based on a numerical approximation to the solution of the temperature integral, which results in the following linear expression[27]

$$\ln\left(\frac{g(\alpha)}{T^2}\right) = -\left(\frac{E_a}{R}\right)\left(\frac{1}{T}\right) + \ln\left(\frac{AR}{E_a\beta}\right)\left(1 - \frac{2RT_{avg}}{E_a}\right) \tag{6}$$

where T_{avg} is the average temperature for the selected conversion range (typically 0.1−0.9). Plots of $\ln[g(\alpha)/T^2]$ versus $1/T$ (i.e., CR plots) will then result in straight lines, for which the slope and intercept allow an estimation of E_a and A, respectively.

3. RESULTS AND DISCUSSION

3.1. Composition of Biomass Precursors. Table 1 reports the results obtained for the three feedstocks from proximate,

Table 1. Results from Proximate, Ultimate, Ash Composition, and Biomass Constituents Analyses of Biomass Feedstocks (VS, WS, and CS)

proximate (wt % from triplicate)	VS	WS	CS
moisture	7.97 ± 0.68	6.60 ± 0.20	7.27 ± 0.31
ash (dry basis)	1.08 ± 0.05	3.93 ± 0.28	2.70 ± 0.20
volatile matter (dry basis)	74.0 ± 1.19	83.2 ± 0.55	86.6 ± 0.11
fixed carbon (dry basis)	24.9 ± 1.91	12.8 ± 0.45	10.7 ± 0.49
ultimate (wt % in daf[a] basis from triplicate)			
C	47.1 ± 0.14	49.0 ± 0.52	44.4 ± 0.31
H	5.29 ± 0.09	7.01 ± 0.04	5.60 ± 0.04
N	0.66 ± 0.05	0.70 ± 0.01	0.43 ± 0.01
O[b]	47.0	43.3	49.6
O:C (atomic ratio)	0.748	0.663	0.837
H:C (atomic ratio)	1.348	1.717	1.514
fuel rate[c]	0.213	0.161	0.103
HHV (MJ kg^{-1} dry basis)	18.0	17.9	18.2
lignocellulosic constituents and extractives (wt % in dry basis from duplicate)			
hemicelluloses	9.26 ± 0.97	26.9 ± 2.2	21.4 ± 0.5
cellulose	29.3 ± 1.9	37.1 ± 3.4	40.5 ± 0.9
lignin	19.2 ± 1.4	10.9 ± 1.8	9.68 ± 0.50
extractives	4.54 ± 0.37	6.57 ± 0.52	8.94 ± 0.77
inorganic matter as equivalent oxides (wt % of ash from triplicate)			
CaO	58.3 ± 0.25	25.01 ± 0.42	30.7 ± 0.23
K_2O	18.4 ± 0.12	38.2 ± 0.45	9.85 ± 0.15
MgO	6.66 ± 0.14	2.09 ± 0.05	3.45 ± 0.17
SiO_2	5.73 ± 0.08	24.3 ± 0.48	31.4 ± 0.23
Fe_2O_3	3.51 ± 0.11	0.82 ± 0.04	6.49 ± 0.12
P_2O_5	1.24 ± 0.06	3.20 ± 0.08	4.13 ± 0.10
Al_2O_3	2.57 ± 0.07	1.19 ± 0.04	4.85 ± 0.12
PbO	1.24 ± 0.04	0.32 ± 0.02	4.13 ± 0.10
S (inorganic)	0.26 ± 0.02	1.88 ± 0.05	2.50 ± 0.08
Cl (inorganic)	0.48 ± 0.02	2.19 ± 0.06	0.59 ± 0.03
MnO	0.53 ± 0.03	0.23 ± 0.01	0.53 ± 0.03
ZnO	0.32 ± 0.02	ND[d]	0.24 ± 0.02
SnO_2	0.26 ± 0.02	0.24 ± 0.01	0.45 ± 0.03
TiO_2	0.34 ± 0.02	ND	0.59 ± 0.03

[a]Dry-ash-free. [b]Oxygen is calculated by difference. [c]Determined by dividing the fixed-carbon content by the volatile matter content. [d]Not detected.

ultimate, ash composition (as weight percentages of major oxides), and biomass constituent analyses. As the table shows, VS had a considerably higher fixed-carbon content than that of CS and WS. This fact is consistent with the higher lignin content also reported in Table 1 for VS, since lignin is the biomass constituent that gives the highest char yield.[28,29]

As also shown in Table 1, the ashes from all the biomass sources contained considerably amounts of alkaline and alkaline-Earth metallic (AAEM) species (Ca, K, and Mg). It is well-known that these inorganic elements can significantly affect both the char yield and its reactivity. During the course of biomass pyrolysis, alkali elements (especially K) simultaneously catalyze the primary devolatilization reactions (for both hemicelluloses and cellulose) and the cracking and polymerization reactions of tar vapors.[30,31] Furthermore, the presence of Ca and Mg could partly inhibit the thermal degradation of hemicelluloses.[32]

Table 2. Properties Determined for the Produced Chars[a]

char	y_{char}[b]	x_{FC}[c]	x_{ash}[d]	O:C (atomic ratio)	H:C (atomic ratio)	fuel ratio[e]	HHV (MJ kg^{-1})[f]	S_{BET} (m^2 g^{-1})	V_{ultra} (cm^3 g^{-1})
VS_350_0.1_50	0.446	0.479	0.054	0.126	0.910	0.974	25.3	135	0.032
VS_350_0.1_150	0.427	0.450	0.078	0.082	0.840	0.889	25.6	134	0.035
VS_350_0.5_50	0.400	0.423	0.064	0.120	0.944	0.783	25.5	116	0.022
VS_350_0.5_150	0.401	0.420	0.060	0.103	0.907	0.772	24.9	127	0.029
VS_425_0.3_100[g]	0.327	0.553	0.091	0.052	0.680	1.362	26.1	164	0.046
VS_500_0.1_50	0.309	0.621	0.067	0.027	0.555	1.756	27.1	209	0.066
VS_500_0.1_150	0.342	0.624	0.064	0.038	0.572	1.776	27.5	208	0.064
VS_500_0.5_50	0.296	0.612	0.068	0.030	0.504	1.905	27.6	219	0.075
VS_500_0.5_150	0.332	0.602	0.067	0.027	0.526	1.625	27.4	217	0.069
WS_350_0.1_150	0.337	0.622	0.105	0.162	0.755	1.837	26.7	112	0.023
WS_350_0.5_150	0.337	0.654	0.106	0.226	0.766	2.116	27.1	95.1	0.015
WS_425_0.3_150[g]	0.282	0.743	0.138	0.154	0.594	3.353	26.8	132	0.031
WS_500_0.1_150	0.264	0.781	0.146	0.099	0.474	4.187	28.0	140	0.033
WS_500_0.5_150	0.262	0.815	0.142	0.108	0.473	5.144	27.8	160	0.043
CS_350_0.1_150	0.397	0.551	0.055	0.223	0.837	1.298	25.6	123	0.027
CS_350_0.5_150	0.374	0.559	0.045	0.210	0.766	1.328	27.6	143	0.032
CS_425_0.3_150[g]	0.334	0.665	0.093	0.132	0.655	2.188	27.3	158	0.044
CS_500_0.1_150	0.271	0.759	0.089	0.081	0.474	3.461	27.8	215	0.067
CS_500_0.5_150	0.301	0.734	0.082	0.141	0.527	3.013	27.7	211	0.062

[a]Denoted as XX_T_P_τ (XX: feedstock type; T: peak temperature in °C; P: absolute pressure in MPa; τ: residence time in s). [b]Char yield (mass fraction in daf basis). [c]Fixed-carbon content (mass fraction in daf basis). [d]Ash content (mass fraction in dry basis). [e]Determined by dividing the fixed-carbon content by the volatile matter content. [f]Dry basis. [g]Center point (reported values correspond to the averages of three replicates).

Concerning the catalytic effects of AAEM species on char combustion, potassium seems to be the most active element.[33,34]

3.2. Yields and Properties of Chars. Table 2 reports the yields (y_{char}) properties determined for all the chars produced in this study, which were denoted as XX_T_P_τ (XX: feedstock type; T: peak temperature in °C; P: absolute pressure in MPa; τ: residence time of the vapor phase in s). To objectively assess the effects of pyrolysis conditions on the response variables given in Table 2, a two-level factorial design of experiments (with three replicates at the center point) was adopted for each biomass precursor. For this purpose, Minitab 17 software was used.

For VS-derived chars, results from the statistical analyses are summarized in Table S1, where it can be observed that the pyrolysis peak temperature significantly affected all the char properties assessed. As expected, an increase in the highest treatment temperature resulted in a decrease in y_{char} and an increase in the fixed-carbon content and heating value of the resulting chars, due to the higher extent of deoxygenation achieved. The rest of operating factors showed marginal or negligible effects on the response variables. Within the range of pressures analyzed here (0.1–0.5 MPa), none of the char properties assessed were significantly affected by this factor, suggesting that the previously reported increase in the fixed-carbon content with pressure[3,35] should be restricted to more severe pressurization conditions (i.e., in the range of 0.5–1.1 MPa). With regard to the residence time of the gas phase, a marginal effect was observed for only the atomic H:C ratio (for the interaction effect T·τ).

For both WS- and CS-derived chars, for which the residence time was not included in the statistical study due to practical reasons (the high carrier gas flow rates that were required for experiments at the lowest gas residence time caused blockages in the outlet tubing and subsequent overpressure generation), results from the corresponding statistical analyses are presented in Tables S2 and S3, respectively. As observed in the case of VS, the highest treatment temperature was the most important factor affecting the yields and properties of produced chars for

both WS and CS. However, the effect of the absolute pressure (either the main effect P or the interaction effect T·P) on the properties of produced chars was more relevant when CS was used as precursor. As can be deduced from Table S3, at the highest level of temperature (i.e., 500 °C), an increased pressure led to an increase in the atomic O:C ratio and related decreases in both the heating value and fuel ratio. This finding could be explained by a slightly increased trapping of volatiles when pyrolysis was conducted at 0.5 MPa. In fact, the mass yield obtained for the CS_500_0.5_150 char was 11.1% higher than that of CS_500_0.1_150. The observed higher oxygen content in the resulting CS-derived char (when pyrolysis pressure was set to 0.5 MPa) agrees well with earlier studies. Wafiq et al.[36] reported an increase in the oxygen content in Miscanthus-derived chars when the pyrolysis pressure raised from 0.1 to 1.0–1.5 MPa, whereas Qin et al.[37] recently reported a marked increase in the content of oxygenated functional groups on the surface of pine-nut-shell-derived chars when the pressure raised from 0.1 to 1.0–2.0 MPa.

The reason behind the observed more significant effect of the absolute pressure on volatile trapping for CS-derived chars, with respect to the other biomass types studied here, could possibly be attributed to the different role played by the inherent inorganic constituents. In this context, it could be assumed that the above-mentioned catalytic effect of potassium during the thermal degradation of CS was weaker than in the other two cases (VS and WS). In addition to the relatively low content of K in the CS ashes (9.85 wt % as K_2O, as shown in Table 1), the availability of active K-containing species during the course of pyrolysis could also be limited.

3.3. Combustion Behavior of Chars. Figures 1–3 show the DTG combustion profiles for VS-, WS-, and CS-derived chars. An example of how the ignition and burnout temperatures were estimated from the TG/DTG combustion profile is given in Figure S2. Combustion of biomass-derived chars usually takes place according to a multistep process, during which at least two distinct DTG peaks (those corresponding to solid devolatiliza-
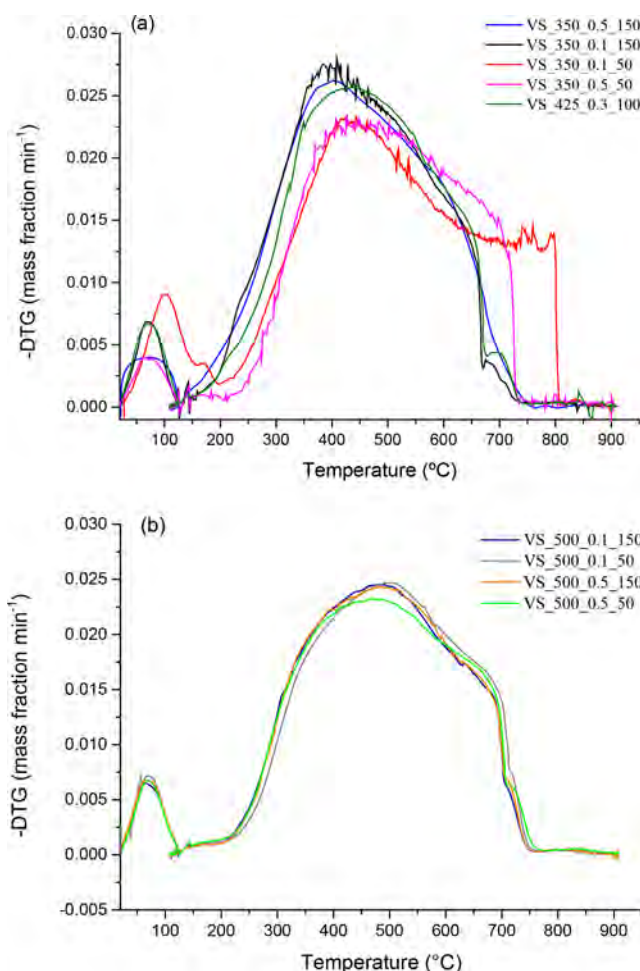
Figure 1. Differential thermogravimetric (DTG) combustion profiles of VS-derived chars: (a) chars produced at 350 and 425 °C; (b) chars produced at 500 °C.
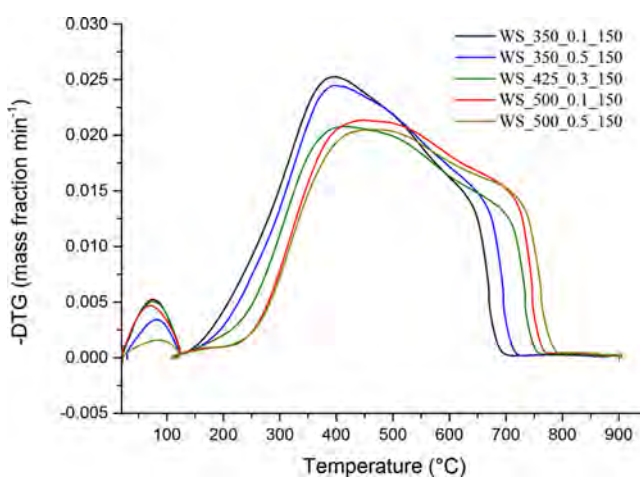

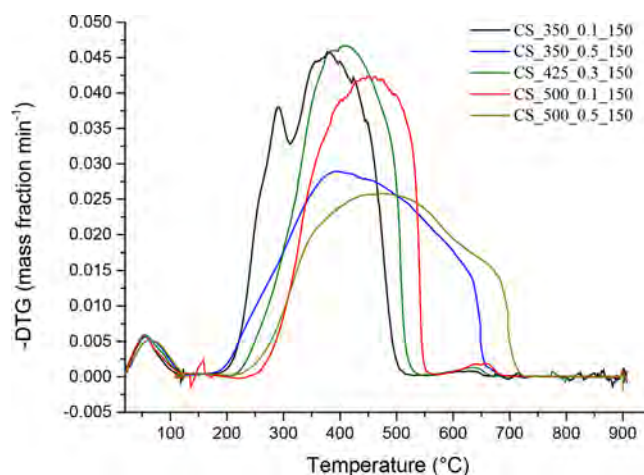**Figure 2.** DTG combustion profiles of WS-derived chars.

Figure 3. DTG combustion profiles of CS-derived chars.

fractions of hemicelluloses and cellulose, especially for chars pyrolyzed at 350 °C), while at temperatures above T_{max}, it could be ascribed to the reaction of more condensed structures.[11] The relative abundance of more stable forms of carbons may be related to the configuration of the pyrolysis reactor (in which the carrier gas did not pass through the bed), which might result in a higher carbonization efficiency due to the extended contact time between the primary volatiles and the solid matrix.

Table 3 lists the characteristic temperatures and combustion performance indices, which were calculated according to the

Table 3. Combustion Patterns Determined for the Produced Chars[a]

char	T_i (°C)	T_b (°C)	T_{max} (°C)	$S \cdot 10^7$ (wt %^{2} min^{-2} °C^{3-})
VS_350_0.1_50	297	788	424	0.555
VS_350_0.1_150	278	661	386	1.137
VS_350_0.5_50	310	720	431	0.621
VS_350_0.5_150	274	671	382	1.036
VS_425_0.3_100[b]	296	678	430	0.910
VS_500_0.1_50	320	710	497	0.692
VS_500_0.1_150	306	699	485	0.758
VS_500_0.5_50	300	702	467	0.626
VS_500_0.5_150	306	700	486	0.644
WS_350_0.1_150	275	660	397	0.895
WS_350_0.5_150	284	684	399	0.860
WS_425_0.3_150[b]	299	712	416	0.640
WS_500_0.1_150	316	738	446	0.525
WS_500_0.5_150	317	750	447	0.472
CS_350_0.1_150	278	485	381	4.566
CS_350_0.5_150	281	643	392	1.321
CS_425_0.3_150[b]	310	515	416	3.179
CS_500_0.1_150	333	542	449	2.560
CS_500_0.5_150	315	694	475	0.798

[a]Denoted as XX_T_P_τ (XX: feedstock type; T: peak temperature in °C; P: absolute pressure in MPa; τ: residence time in s). [b]Center point (reported values were calculated from the average data of the three replicates).

tion and char oxidation) can easily be distinguished.[38] Nevertheless, these two DTG peaks were clearly observed for only one char (CS_350_0.1_150, as shown in Figure 3). For the rest of chars produced in the present study, the DTG curves only exhibited a main mass-loss peak. At temperatures below T_{max}, this peak could mainly be due to the decomposition of volatiles that remained in the carbonized solid (as well as remaining

methodology described in Section 2.3. For VS-derived chars, results from the statistical analyses of the data given in Table 3 revealed a significant effect of the gas residence time, pyrolysis peak temperature, and interaction between them on the combustion performance index (see the normal plot of
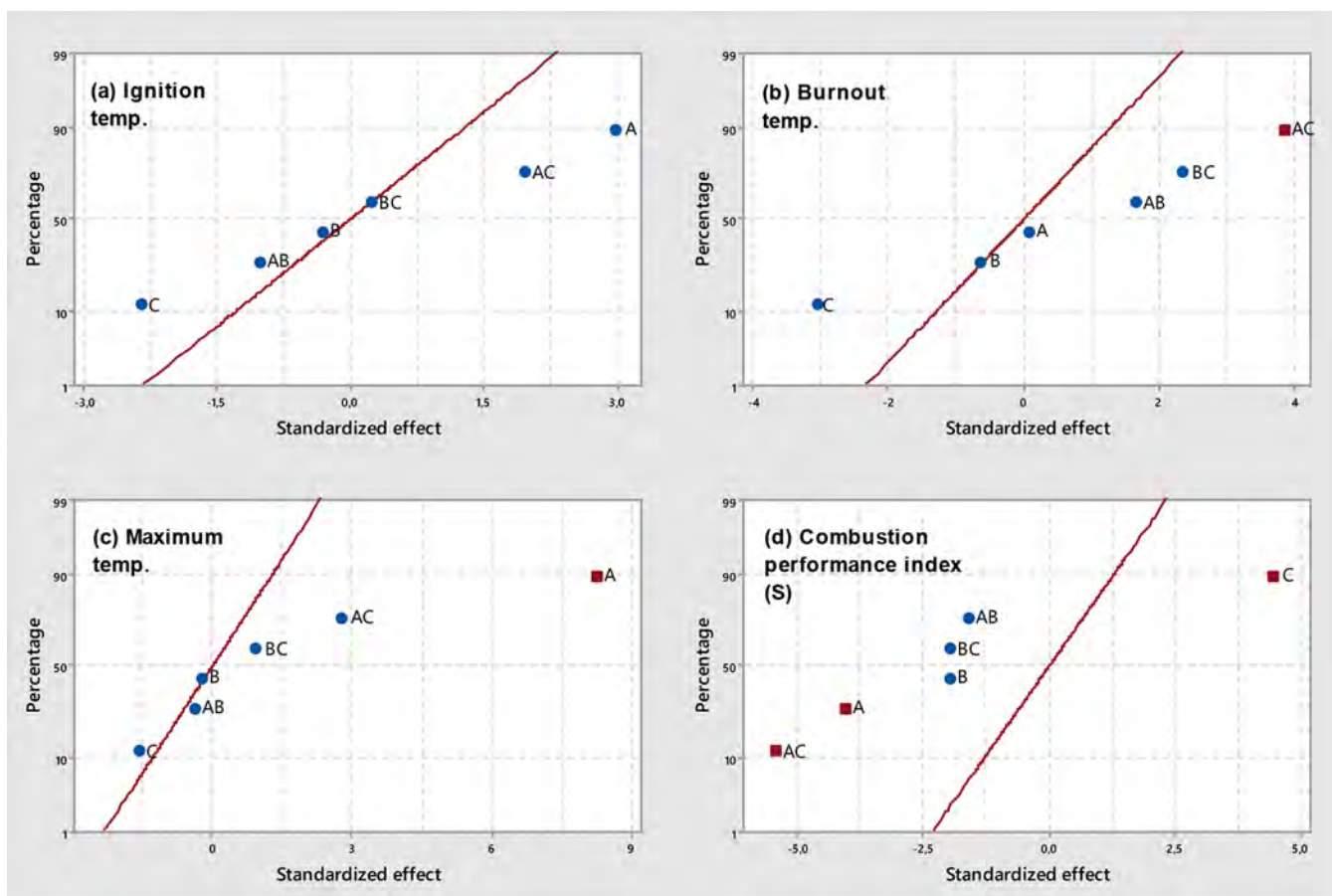
Figure 4. Normal plots of standardized effects ($\alpha = 0.05$) for VS-derived chars: (a) T_i, (b) T_b, (c) T_{max}, and (d) S (square, significant effect; circle, not significant effect; A, temperature; B, pressure; C, residence time).

standardized effects in Figure 4d and the summary statistics in Table S4). At low pyrolysis peak temperatures, an increase in the gas residence time led to higher values of S, whereas a marked decrease in the combustion performance index was ascribed to higher values of both T and τ factors. These relatively low values of S could mainly be explained by the related increase in the burnout temperature when both the pyrolysis peak temperature and gas residence time were set at their highest levels (see Figure 4b). The important role that the gas residence time seems to play in the combustion performance was somewhat unexpected in view of the almost negligible effects of τ on the measured properties of VS-derived chars. It would be expected that an increase in the residence time of the gas phase should result in a higher carbonization efficiency, since the primary volatiles have more time to undergo secondary charring reactions, thus increasing the fixed-carbon content, which is often related to higher values of T_b. Nevertheless, the fixed-carbon content of VS-derived chars was only significantly affected by the peak pyrolysis temperature (see Table S1), suggesting that the residence time of the gas phase could influence other features of the resulting chars related to, for instance, their chemical and/or morphological structure. Further studies would be needed to clarify the role of the gas residence time in the enhancement (or decrement) of char reactivity.

The influence of pyrolysis pressure and peak temperature on the combustion performance of both WS- and CS-derived chars is summarized graphically in Figures 5 and 6, respectively (the results from statistical analyses are given in Tables S5 and S6, respectively). For chars produced from wheat straw, it can be

seen that the pyrolysis peak temperature was the only factor that negatively affected the combustion performance, leading to a marked increase in both T_i and T_{max} values and a related significant decrease in the value of S when chars were produced at the highest peak temperature. Contrary to what was observed for chars produced from VS and WS, the combustion performance of CS-derived chars was strongly affected by pyrolysis pressure. As shown in Figure 6d (and reported in Table A.6), the pressure applied during pyrolysis exerted a more pronounced effect than peak temperature on the combustion performance index values of resulting chars. The poorer combustion performance observed for CS-derived chars produced at the highest level of pressure, despite their relatively higher oxygen content, agrees with the previous results reported by Recari et al.[16] for wood spruce chars and could be related to differences in the oxygen diffusion rate at relatively high temperatures, where the combustion is under both kinetic and internal diffusion control.[39,40] Unfortunately, the textural properties reported in Table 2 (S_{BET} and V_{ultra}) did not show any significant influence of pressure. This finding suggests that more advanced textural characterization techniques—rather than traditional N_2 and CO_2 adsorption isotherms—are required to better explore the wide microporosity and mesopororisity domains in order to find relevant differences that could affect the oxygen diffusion rate.

The large variability in the combustion-related variables among the chars produced from different biomass precursors could suggest that the effect of the feedstock on the combustion behavior was much stronger than those of the pyrolysis
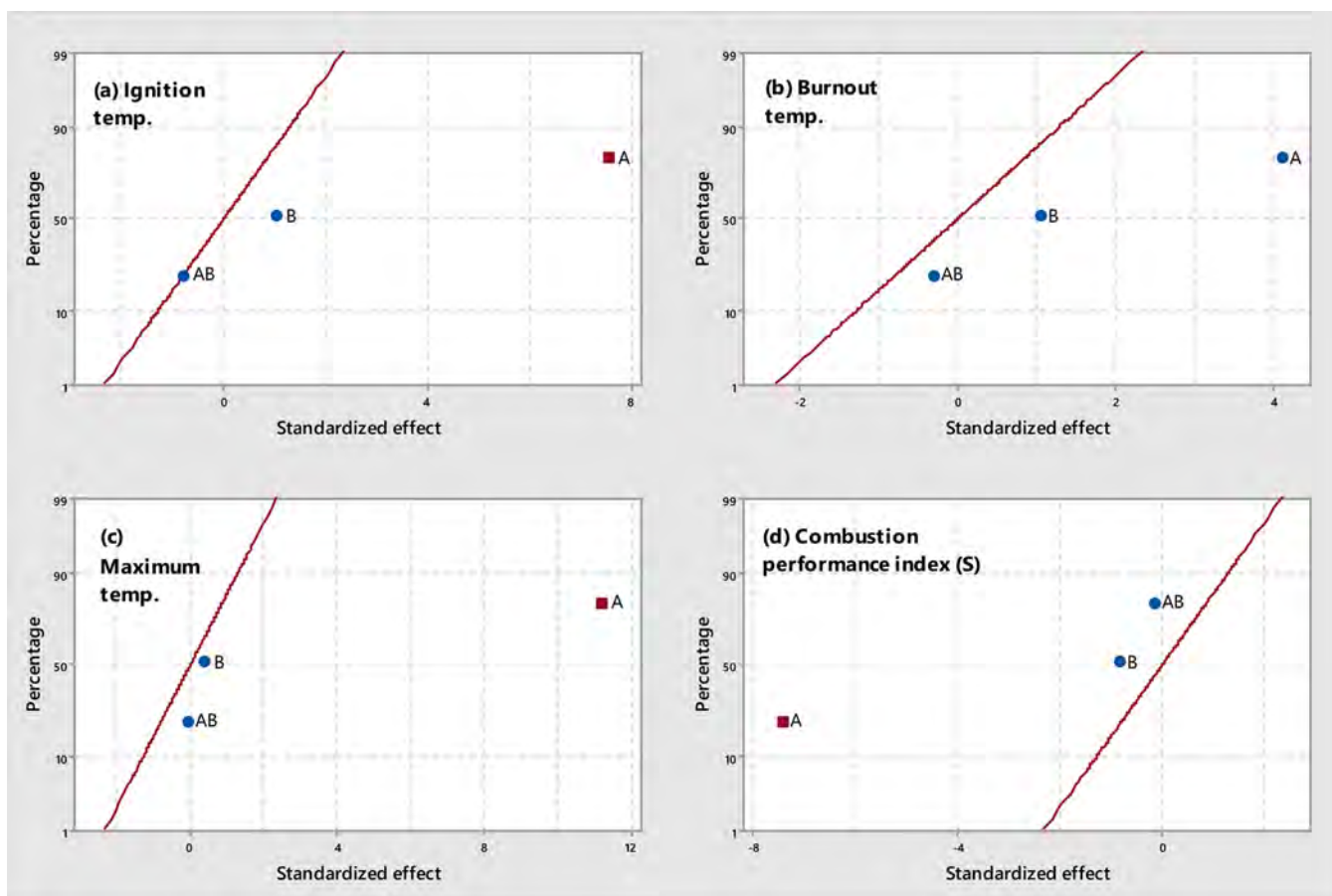
Figure 5. Normal plots of standardized effects ($\alpha = 0.05$) for WS-derived chars: (a) T_i, (b) T_b, (c) T_{max}, and (d) S (square, significant effect; circle, not significant effect; A, temperature; B, pressure).

conditions. The highest value of S was measured for the CS_350_0.1_150 char (4.566×10^{-7} wt $\%^2$ min^{-2} °C^{3-}), which was much higher than the highest S values measured for both VS- and WS-based chars (1.137×10^{-7} and 0.895×10^{-7} wt $\%^2$ min^{-2} °C^{3-}, respectively).

3.4. Apparent Kinetic Parameters and Char Reactivity. The estimation of the apparent kinetic parameters (E_a and A) was performed according to the CR procedure (see Section 2.4) for a conversion range of $0.1 \leq \alpha \leq 0.9$. As a preliminary step, the resulting CR plots obtained for a number of expressions of $g(\alpha)$ (those corresponding to different reaction mechanisms, as shown in Table S7) were compared for a given char (VS_500_0.5_150). The best linear fit to the CR plot was observed for the F3/2 chemical reaction mechanism (see Figure S3). Since the aim of this study was to compare the relative reactivity of biomass-derived chars, E_a and A were estimated for all of them by assuming the same kinetic expression (F3/2).

The calculated kinetic parameters are summarized in Table 4, which also lists the average values of the temperatures range (T_{avg}) and the coefficients of determination (R^2) obtained for the linear fit to the CR plots. To take into account the well-known kinetic compensation effect, the relative reactivity (R) with respect to a reference case was calculated according to the following equation[25]

$$R = 1 - \frac{(E_a/E_{a,0})}{(\ln A/\ln A_0)} \tag{7}$$

where $E_{a,0}$ and A_0 correspond to the kinetic parameters for the reference case. A negative sign of R indicates a lower reactivity than that of the reference case. In Table 4, two relative reactivity values are reported: R_i and R_j. The first one was calculated with respect to the most reactive char for the same biomass feedstock, whereas R_j was calculated using the most reactive char evaluated in the present study (CS_350_0.1_150) as the reference case.

The values of R_j reported in Table 4 were in acceptable agreement with the values of S listed in Table 3 (Spearman's rank correlation coefficient of 0.8404 with a p-value of 6.69×10^{-6}). To better reflect the level of association between R_j and S, Figure 7 shows, for each char, the normalized values of both indices. The reasonable level of similarity between the combustion performance index and relative reactivity suggests that S can be used as a convenient (and fast) rough indicator of the combustion reactivity of biomass-derived chars.

The CS-derived chars also exhibited the largest variability in the values of the apparent kinetic parameters. For the most reactive CS-derived chars, notably higher values for both E_a and A were found. For their part, the apparent kinetic parameters for the least reactive CS-derived chars were more similar in magnitude to those estimated for both VS- and WS-derived chars.

3.5. Multivariate Analysis. To further explore possible relationships that can be helpful to explain the different combustion patterns, partial least-squares (PLS) regression was performed using the "pls" package for the R environment.[41] PLS, which is a linear multivariate method for relating independent variables with responses, is often helpful when
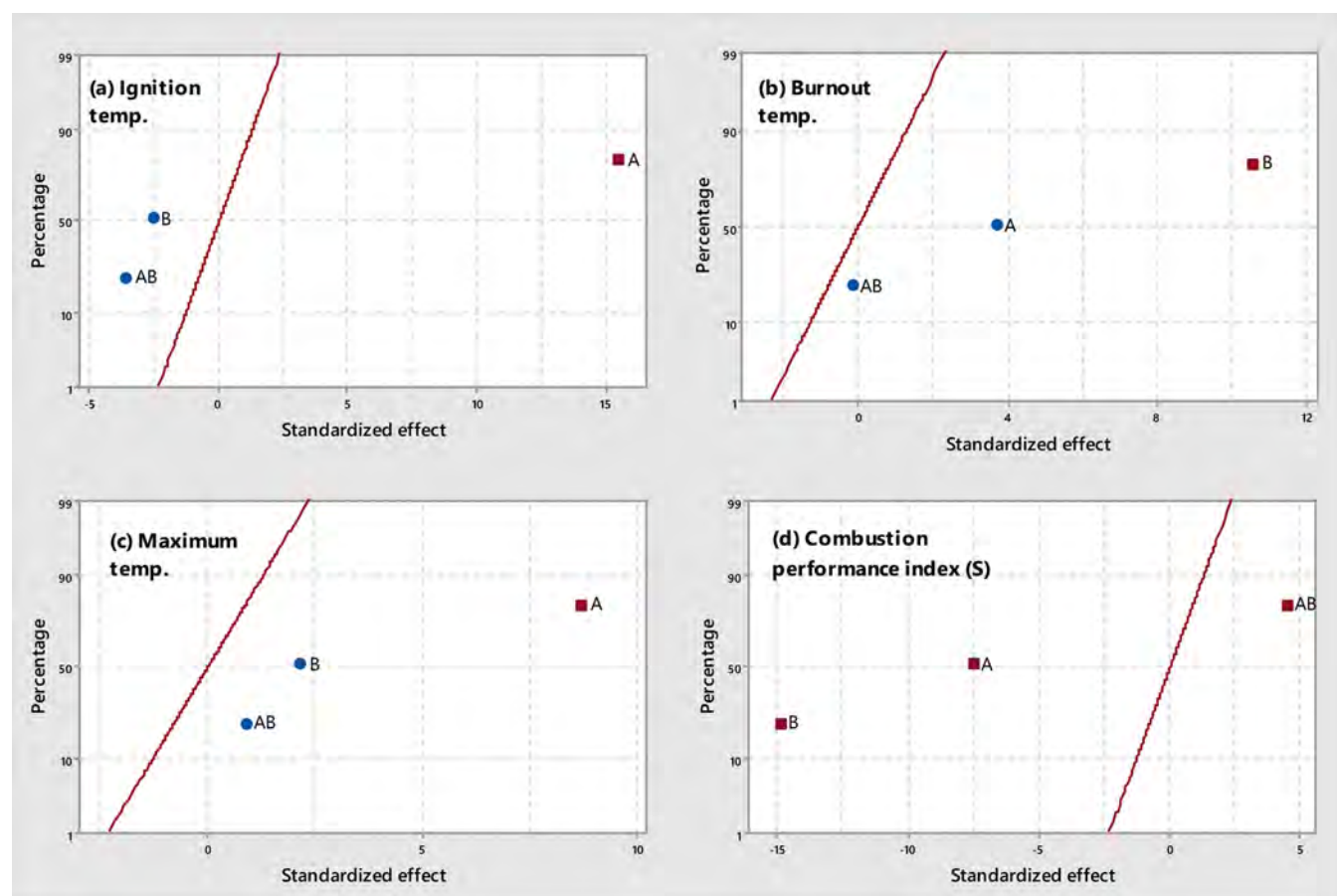
Figure 6. Normal plots of standardized effects ($\alpha = 0.05$) for CS-derived chars: (a) T_i, (b) T_b, (c) T_{max}, and (d) S (square, significant effect; circle, not significant effect; A, temperature; B, pressure).

Table 4. Estimated Apparent Kinetic Parameters from the CR Plot and Relative Reactivities

char	E_a (kJ mol^{-1})	A (min^{-1})	R^2	T_{avg} (°C)	R_i (−)	R_j (−)
VS_350_0.1_50	29.16	7.739	0.9930	534	−0.437	−1.17
VS_350_0.1_150	34.40	32.10	0.9970	458	0	−0.512
VS_350_0.5_50	36.67	29.22	0.9944	508	−0.0957	−0.657
VS_350_0.5_150	33.43	26.01	0.9958	463	−0.0345	−0.565
VS_425_0.3_100[a]	36.74	38.17	0.9968	481	−0.0172	−0.539
VS_500_0.1_50	36.74	30.23	0.9968	503	−0.0868	−0.644
VS_500_0.1_150	35.80	28.53	0.9965	492	−0.0773	−0.629
VS_500_0.5_50	34.29	21.27	0.9948	497	−0.131	−0.711
VS_500_0.5_150	35.82	28.51	0.9956	493	−0.0781	−0.631
WS_350_0.1_150	34.26	31.78	0.9970	455	0	−0.511
WS_350_0.5_150	34.34	27.24	0.9962	474	−0.0522	−0.585
WS_425_0.3_150[a]	34.97	24.40	0.9947	498	−0.112	−0.670
WS_500_0.1_150	41.84	58.88	0.9834	473	−0.0156	−0.566
WS_500_0.5_150	40.99	47.15	0.9830	480	−0.0545	−0.622
CS_350_0.1_150	51.97	2770	0.9942	367	0	0
CS_350_0.5_150	37.50	60.45	0.9966	447	−0.428	−0.428
CS_425_0.3_150[a]	60.77	7114	0.9969	406	−0.0422	−0.0422
CS_500_0.1_150	65.72	11 223	0.9953	433	−0.0713	−0.0713
CS_500_0.5_150	40.41	62.76	0.9966	493	−0.526	−0.526

[a] Center point (reported values were calculated from the average data of the three replicates).

numerous highly correlated predictor variables are present.[42] The approach is based on defining a relatively few latent variables (i.e., components) as linear combinations of the original independent variables that can then predict the responses. The influence of a given independent variable on a given response can be assessed using the variable importance in projection (VIP) scores, which reflects the relative importance of each independent variable on the response.[43]

The dependent variables (X) selected for PLS were the hemicelluloses, cellulose, lignin, potassium, and calcium
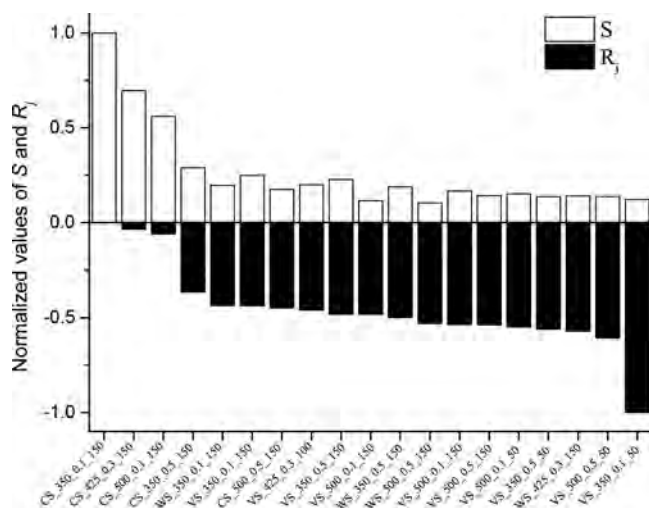
Figure 7. Comparison between the normalized values of S and R_j.

contents (in wt %) in the biomass feedstock (Hemicel, Cel, Lignin, K-bio, and Ca-bio); the fixed-carbon content (x_{FC}, in mass fraction in daf basis), the atomic O/C and H/C ratios, the specific surface area (S_{BET}, in m^2 g^{-1}) and HHV values (in kJ kg^{-1}) measured for chars (and also listed in Table 2); and the pyrolysis operating conditions (peak temperature and absolute pressure; T and P). Residence time of the gas phase (τ) was not considered, because its effect was only assessed for VS-derived chars. The combustion performance index (S) was selected as a response variable. Cross-validation using 10 random segments was conducted to choose the number of components that minimized the root-mean-square error of prediction (RMSEP).

Results from PLS regression with three components revealed that 35.7 and 27.7% of the total variance observed in S was explained by component 1 and component 2, respectively (see the Supporting Information for full results). From the PLS loading-weights plot shown in Figure 8, it can be seen that none of the independent variables were positively correlated with both the first and second components In addition, K-bio and, to a lesser extent, HHV and P were the strongest negative variables affecting S. The negative effect of potassium on the combustion performance index could mainly be explained by differences in the pyrolysis behavior. A relatively high content of K in the
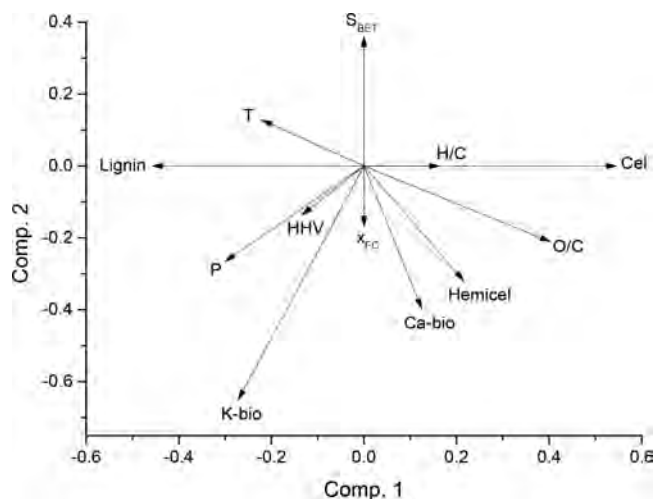

Figure 8. PLS loading-weights plot for dependent variables.

biomass feedstock could result in a greater extent of secondary reactions (both cracking and coking), leading to the formation of more stable chars. In fact, the pyrolysis of WS, which had the highest potassium content, led to chars with higher fixed-carbon contents compared to those produced from VS and CS at the same operating conditions (see Table 2) and despite the relatively low content of lignin in WS.

On the other hand, Ca-bio was positively correlated with the first component and negatively correlated with the second component. Given the percentages of variance explained by the first two components and the loading weights obtained for Ca-bio (0.125 and −0.397 for components 1 and 2, respectively), a globally negative effect of calcium on S can be deduced. However, this negative effect was much lower than that of potassium. It is generally agreed that calcium has a lower catalytic activity on the biomass pyrolysis than that of potassium, especially at temperatures below 400 °C.[44] Although the catalytic activity on the char oxidation process of potassium is greater than that of calcium—see, for instance, the study by Abián et al.[33]—the low intrinsic reactivity of the more stable chars produced from K-rich biomass sources could act as a bottleneck and hinder the catalytic activity of inherent potassium.

Figure 9 displays the VIP-scores plot for PLS model. It is widely accepted that variables having a VIP score higher than 1
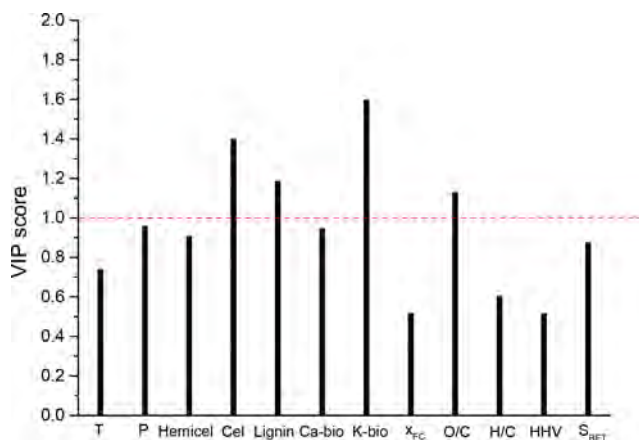

Figure 9. Variable importance projection (VIP) scores from PLS regression.

can be considered as the most influential ones.[45] Thus, and as can be seen in Figure 9, the most important dependent variables were—in addition to K-bio—Cel, Lignin, and O/C.

The negative effect of Lignin on the combustion performance of chars was confirmed (i.e., Lignin was negatively correlated with the first component). From Figure 8, it can also be seen that Cel was highly (and positively) correlated with the first component. The positive effect of Cel on the combustion performance index seems to be in disagreement with the results by Pang et al.,[15] who reported a decrease in combustion reactivity for chars produced from some cellulose-rich biomass sources. Nevertheless, Ma et al.[46] observed that biomass sources having relatively low cellulose to lignin content ratios exhibited poorer combustion performances. In accordance with the argument made by Yan et al.,[17] a relatively low content of lignin could result in a lower insulation of cellulose, which could then easily decompose and lead to chars with enhanced ignition characteristics. In any case, trying to predict both the pyrolysis

behavior and combustion patterns as a function of the initial contents of cellulose and lignin is extremely difficult, since the encapsulated vapor–solid interactions between biomass constituents are extremely complex. These interactions could result in significant differences in porosity development, morphology, chemical structure, and availability of oxygen-containing functional groups between synthetic component mixtures (of hemicelluloses, cellulose, and lignin) and real biomass samples, as has recently observed by Hu et al.[47]

With regard to the importance accounted for O/C, which globally favored the combustion performance (see Figure 8), it is widely believed that higher oxygen contents in char can be related to a greater availability of active sites and, therefore, a higher reactivity.[14] As previously discussed in Section 3.2, an increased pyrolysis temperature resulted in a significant decrease in the atomic O/C ratio of resulting chars for all biomass sources. In the case of CS (the feedstock with the highest oxygen content), the substantial improvement of the O/C ratio for chars produced at 0.5 MPa and 500 °C (with respect to those produced at 0.1 MPa and 500 °C) did not translate to a better combustion performance. This finding suggests that the positive effect of O/C on S could be restricted to chars having less stable forms of carbon (i.e., chars produced at the lowest levels of both T and P).

4. CONCLUSIONS

The combustion patterns of chars were more influenced by the type of feedstock than by the pyrolysis operating conditions (for the parameters and their ranges studied here). Among the three biomass sources, corn stover appeared to be the most interesting one in order to produce highly reactive chars. Furthermore, less reactive CS-derived chars (which can be preferred for certain applications) can also be produced by increasing either the pressure or the peak temperature during the pyrolysis process. PLS regression can serve as a useful tool to evaluate the effect and importance of each explanatory variable on the combustion reactivity of biomass chars. For the feedstocks and pyrolysis process parameters assessed here, PLS regression revealed that the most important factors affecting char reactivity were the contents of K (negative effect) and cellulose (positive effect) in the raw biomass. Further studies for a wider range of biomass sources appear to be necessary to confirm the preliminary results reported here as well as confirm the usefulness of this multivariate statistical tool.

■ ASSOCIATED CONTENT

ⓈI Supporting Information

The Supporting Information is available free of charge at https://pubs.acs.org/doi/10.1021/acs.energyfuels.0c04180.

> Tables S1–S3 (summary statistics for the regression models based on the data given in Table 2); Figure S1 (schematic diagram of the experimental pyrolysis setup), Figure S2 (an example of estimation of T_i and T_b); Tables S4–S6 (summary statistics for the regression models based on the data given in Table 3); Table S7 (expressions for kinetic models); Figure S3 (CR plots for the VS_500_0.5_150 char); full results from PLS regression approach (PDF)

■ AUTHOR INFORMATION

Corresponding Author

Joan J. Manyà − *Aragón Institute of Engineering Research (I3A), Thermochemical Processes Group, University of Zaragoza, Escuela Politécnica Superior, 22071 Huesca, Spain;* ⓞ orcid.org/0000-0002-0118-3254; Email: joanjoma@ unizar.es

Authors

Darío Alvira − *Aragón Institute of Engineering Research (I3A), Thermochemical Processes Group, University of Zaragoza, Escuela Politécnica Superior, 22071 Huesca, Spain*

María Videgain − *University of Zaragoza, Escuela Politécnica Superior, 22071 Huesca, Spain*

Gozde Duman − *Faculty of Science, Department of Chemistry, Ege University, 35100 Izmir, Turkey;* ⓞ orcid.org/0000-0002-9427-8235

Jale Yanik − *Faculty of Science, Department of Chemistry, Ege University, 35100 Izmir, Turkey;* ⓞ orcid.org/0000-0001-9575-9973

Complete contact information is available at:
https://pubs.acs.org/10.1021/acs.energyfuels.0c04180

Author Contributions

The manuscript was written through the contributions of all authors. All authors have given approval to the final version of the manuscript.

Notes

The authors declare no competing financial interest.

■ ACKNOWLEDGMENTS

■ REFERENCES

(1) Yan, W.; Perez, S.; Sheng, K. Upgrading Fuel Quality of Moso Bamboo via Low Temperature Thermochemical Treatments: Dry Torrefaction and Hydrothermal Carbonization. *Fuel* **2017**, *196*, 473−480.

(2) Ronsse, F.; van Hecke, S.; Dickinson, D.; Prins, W. Production and Characterization of Slow Pyrolysis Biochar: Influence of Feedstock Type and Pyrolysis Conditions. *GCB Bioenergy* **2013**, *5*, 104−115.

(3) Manyà, J. J.; Azuara, M.; Manso, J. A. Biochar Production through Slow Pyrolysis of Different Biomass Materials: Seeking the Best Operating Conditions. *Biomass Bioenergy* **2018**, *117*, 115−123.

(4) Suliman, W.; Harsh, J. B.; Abu-Lail, N. I.; Fortuna, A. M.; Dallmeyer, I.; Garcia-Perez, M. Influence of Feedstock Source and Pyrolysis Temperature on Biochar Bulk and Surface Properties. *Biomass Bioenergy* **2016**, *84*, 37−48.

(5) Lee, Y.; Park, J.; Ryu, C.; Gang, K. S.; Yang, W.; Park, Y.-K.; Jung, J.; Hyun, S. Comparison of Biochar Properties from Biomass Residues Produced by Slow Pyrolysis at 500 °C. *Bioresour. Technol.* **2013**, *148*, 196−201.

(6) Tag, A. T.; Duman, G.; Ucar, S.; Yanik, J. Effects of Feedstock Type and Pyrolysis Temperature on Potential Applications of Biochar. *J. Anal. Appl. Pyrolysis* **2016**, *120*, 200−206.

(7) Lu, J. J.; Chen, W. H. Investigation on the Ignition and Burnout Temperatures of Bamboo and Sugarcane Bagasse by Thermogravimetric Analysis. *Appl. Energy* **2015**, *160*, 49−57.

(8) Jiang, T. L.; Chen, W. S.; Tsai, M. J.; Chiu, H. H. A Numerical Investigation of Multiple Flame Configurations in Convective Droplet Gasification. *Combust. Flame* **1995**, *103*, 221−238.

(9) Mundike, J.; Collard, F. X.; Görgens, J. F. Co-Combustion Characteristics of Coal with Invasive Alien Plant Chars Prepared by Torrefaction or Slow Pyrolysis. *Fuel* **2018**, *225*, 62−70.

(10) Wang, Y.; Qiu, L.; Zhu, M.; Sun, G.; Zhang, T.; Kang, K. Comparative Evaluation of Hydrothermal Carbonization and Low Temperature Pyrolysis of Eucommia Ulmoides Oliver for the Production of Solid Biofuel. *Sci. Rep.* **2019**, *9*, 5535.

(11) Barbanera, M.; Cotana, F.; Di Matteo, U. Co-Combustion Performance and Kinetic Study of Solid Digestate with Gasification Biochar. *Renewable Energy* **2018**, *121*, 597−605.

(12) Peta, S.; du Toit, C.; Naidoo, R.; Schmitz, W.; Jestin, L. Investigations of Operation Problems at a 200 MW e PF Boiler. *Chem. Process Eng.* **2015**, *36*, 305−320.

(13) Guizani, C.; Jeguirim, M.; Valin, S.; Limousy, L.; Salvador, S. Biomass Chars: The Effects of Pyrolysis Conditions on Their Morphology, Structure, Chemical Properties and Reactivity. *Energies* **2017**, *10*, 796.

(14) Morin, M.; Pécate, S.; Hémati, M.; Kara, Y. Pyrolysis of Biomass in a Batch Fluidized Bed Reactor: Effect of the Pyrolysis Conditions and the Nature of the Biomass on the Physicochemical Properties and the Reactivity of Char. *J. Anal. Appl. Pyrolysis* **2016**, *122*, 511−523.

(15) Pang, C. H.; Lester, E.; Wu, T. Influence of Lignocellulose and Plant Cell Walls on Biomass Char Morphology and Combustion Reactivity. *Biomass Bioenergy* **2018**, *119*, 480−491.

(16) Recari, J.; Berrueco, C.; Abelló, S.; Montané, D.; Farriol, X. Effect of Temperature and Pressure on Characteristics and Reactivity of Biomass-Derived Chars. *Bioresour. Technol.* **2014**, *170*, 204−210.

(17) Yan, Y.; Meng, Y.; Tang, L.; Kostas, E. T.; Lester, E.; Wu, T.; Pang, C. H. Ignition and Kinetic Studies: The Influence of Lignin on Biomass Combustion. *Energy Fuels* **2019**, *33*, 6463−6472.

(18) Searle, S. Y.; Malins, C. J. Waste and Residue Availability for Advanced Biofuel Production in EU Member States. *Biomass Bioenergy* **2016**, *89*, 2−10.

(19) Wang, L.; Skreiberg, O.; Gronli, M.; Specht, G. P.; Antal, M. J. Is Elevated Pressure Required to Achieve a High Fixed-Carbon Yield of Charcoal from Biomass? Part 2: The Importance of Particle Size. *Energy Fuels* **2013**, *27*, 2146−2156.

(20) Van Soest, P. J.; Robertson, J. B.; Lewis, B. A. Methods for Dietary Fiber, Neutral Detergent Fiber, and Nonstarch Polysaccharides in Relation to Animal Nutrition. *J. Dairy Sci.* **1991**, *74*, 3583−3597.

(21) Rodriguez Correa, C.; Hehr, T.; Voglhuber-Slavinsky, A.; Rauscher, Y.; Kruse, A. Pyrolysis vs. Hydrothermal Carbonization: Understanding the Effect of Biomass Structural Components and Inorganic Compounds on the Char Properties. *J. Anal. Appl. Pyrolysis* **2019**, *140*, 137−147.

(22) Manyà, J. J.; Alvira, D.; Azuara, M.; Bernin, D.; Hedin, N. Effects of Pressure and the Addition of a Rejected Material from Municipal Waste Composting on the Pyrolysis of Two-Phase Olive Mill Waste. *Energy Fuels* **2016**, *30*, 8055−8064.

(23) Greco, G.; Videgain, M.; Di Stasi, C.; González, B.; Manyà, J. J. Evolution of the Mass-Loss Rate during Atmospheric and Pressurized Slow Pyrolysis of Wheat Straw in a Bench-Scale Reactor. *J. Anal. Appl. Pyrolysis* **2018**, *136*, 18−26.

(24) Kim, K. C.; Yoon, T. U.; Bae, Y. S. Applicability of Using CO2 Adsorption Isotherms to Determine BET Surface Areas of Microporous Materials. *Microporous Mesoporous Mater.* **2016**, *224*, 294−301.

(25) Pickard, S.; Daood, S. S.; Pourkashanian, M.; Nimmo, W. Robust Extension of the Coats-Redfern Technique: Reviewing Rapid and Realiable Reactivity Analysis of Complex Fuels Decomposing in Inert and Oxidizing Thermogravimetric Analysis Atmospheres. *Energy Fuels* **2013**, *27*, 2818−2826.

(26) Chong, Y. Y.; Thangalazhy-Gopakumar, S.; Gan, S.; Ng, H. K.; Lee, L. Y.; Adhikari, S. Kinetics and Mechanisms for Copyrolysis of

Palm Empty Fruit Bunch Fiber (EFBF) with Palm Oil Mill Effluent (POME) Sludge. *Energy Fuels* **2017**, *31*, 8217−8227.

(27) Fedunik-Hofman, L.; Bayon, A.; Donne, S. W. Kinetics of Solid-Gas Reactions and Their Application to Carbonate Looping Systems. *Energies* **2019**, *12*, 2981.

(28) Antal, M. J.; Allen, S. G.; Dai, X.; Shimizu, B.; Tam, M. S.; Grønli, M. Attainment of the Theoretical Yield of Carbon from Biomass. *Ind. Eng. Chem. Res.* **2000**, *39*, 4024−4031.

(29) Collard, F. X.; Blin, J. A Review on Pyrolysis of Biomass Constituents: Mechanisms and Composition of the Products Obtained from the Conversion of Cellulose, Hemicelluloses and Lignin. *Renewable Sustainable Energy Rev.* **2014**, *38*, 594−608.

(30) Nowakowski, D. J.; Jones, J. M.; Brydson, R. M. D. D.; Ross, A. B. Potassium Catalysis in the Pyrolysis Behaviour of Short Rotation Willow Coppice. *Fuel* **2007**, *86*, 2389−2402.

(31) Zhou, L.; Jia, Y.; Nguyen, T. H.; Adesina, A. A.; Liu, Z. Hydropyrolysis Characteristics and Kinetics of Potassium-Impregnated Pine Wood. *Fuel Process. Technol.* **2013**, *116*, 149−157.

(32) Haddad, K.; Jeguirim, M.; Jellali, S.; Guizani, C.; Delmotte, L.; Bennici, S.; Limousy, L. Combined NMR Structural Characterization and Thermogravimetric Analyses for the Assessment of the AAEM Effect during Lignocellulosic Biomass Pyrolysis. *Energy* **2017**, *134*, 10−23.

(33) Abián, M.; Alzueta, M. U.; Carvalho, A.; Rabaçal, M.; Costa, M. Role of Potassium and Calcium on the Combustion Characteristics of Biomass Obtained from Thermogravimetric Experiments. *Energy Fuels* **2017**, *31*, 12238−12246.

(34) Safar, M.; Lin, B. J.; Chen, W. H.; Langauer, D.; Chang, J. S.; Raclavska, H.; Pétrissans, A.; Rousset, P.; Pétrissans, M. Catalytic Effects of Potassium on Biomass Pyrolysis, Combustion and Torrefaction. *Appl. Energy* **2019**, *235*, 346−355.

(35) Azuara, M.; Sáiz, E.; Manso, J. A.; García-Ramos, F. J.; Manyà, J. J. Study on the Effects of Using a Carbon Dioxide Atmosphere on the Properties of Vine Shoots-Derived Biochar. *J. Anal. Appl. Pyrolysis* **2017**, *124*, 719−725.

(36) Wafiq, A.; Reichel, D.; Hanafy, M. Pressure Influence on Pyrolysis Product Properties of Raw and Torrefied Miscanthus: Role of Particle Structure. *Fuel* **2016**, *179*, 156−167.

(37) Qin, L.; Wu, Y.; Hou, Z.; Jiang, E. Influence of Biomass Components, Temperature and Pressure on the Pyrolysis Behavior and Biochar Properties of Pine Nut Shells. *Bioresour. Technol.* **2020**, *313*, 123682.

(38) Di Blasi, C. Combustion and Gasification Rates of Lignocellulosic Chars. *Prog. Energy Combust. Sci.* **2009**, *35*, 121−140.

(39) Al-Qayim, K.; Nimmo, W.; Hughes, K.; Pourkashanian, M. Kinetic Parameters of the Intrinsic Reactivity of Woody Biomass and Coal Chars via Thermogravimetric Analysis. *Fuel* **2017**, *210*, 811−825.

(40) Han, Y. N.; Liao, J. J.; Bai, Z. Q.; Bai, J.; Li, X.; Li, W. Correlation between the Combustion Behavior of Brown Coal Char and Its Aromaticity and Pore Structure. *Energy Fuels* **2016**, *30*, 3419−3427.

(41) Mevik, B.-H.; Wehrens, R.; Liland, K. H.; Hiemstra, P. *pls: Partial Least Squares and Principal Component Regression*, R package version 2.7−3. Available from: https://CRAN.R-project.org/package=pls.

(42) Wold, S.; Sjöström, M.; Eriksson, L. PLS-Regression: A Basic Tool of Chemometrics. *Chemom. Intell. Lab. Syst.* **2001**, *58*, 109−130.

(43) Kuuliala, L.; Abatih, E.; Ioannidis, A. G.; Vanderroost, M.; De Meulenaer, B.; Ragaert, P.; Devlieghere, F. Multivariate Statistical Analysis for the Identification of Potential Seafood Spoilage Indicators. *Food Control* **2018**, *84*, 49−60.

(44) Zhang, L.; Zhang, B.; Yang, Z.; Yan, Y. Pyrolysis Behavior of Biomass with Different Ca-Based Additives. *RSC Adv.* **2014**, *4*, 39145−39155.

(45) Mehmood, T.; Liland, K. H.; Snipen, L.; Sæbø, S. A Review of Variable Selection Methods in Partial Least Squares Regression. *Chemom. Intell. Lab. Syst.* **2012**, *118*, 62−69.

(46) Ma, Y.; Guan, Y.; Zhang, K.; Xu, G.; Yang, Y.; Stevenson, P. Dependency of the Combustion Behavior of Energy Grass and Three Other Types of Biomass upon Lignocellulosic Composition. *Environ. Prog. Sustainable Energy* **2018**, *37*, 815−823.

(47) Hu, J.; Jiang, B.; Liu, J.; Sun, Y.; Jiang, X. Influence of Interactions between Biomass Components on Physicochemical Characteristics of Char. *J. Anal. Appl. Pyrolysis* **2019**, *144*, 104704.

Supporting Information

Assessing the importance of pyrolysis process conditions and feedstock type on the combustion performance of agricultural residues-derived chars

Joan J. Manyà[,†], Darío Alvira[†], María Videgain[†], Gozde Duman[‡], and Jale Yanik[‡]*

[†] Aragón Institute of Engineering Research (I3A), Thermochemical Processes Group, University of Zaragoza, Escuela Politécnica Superior, crta. Cuarte s/n, 22071 Huesca, Spain

[‡] Faculty of Science, Department of Chemistry, Ege University, 35100 Bornova, Izmir, Turkey
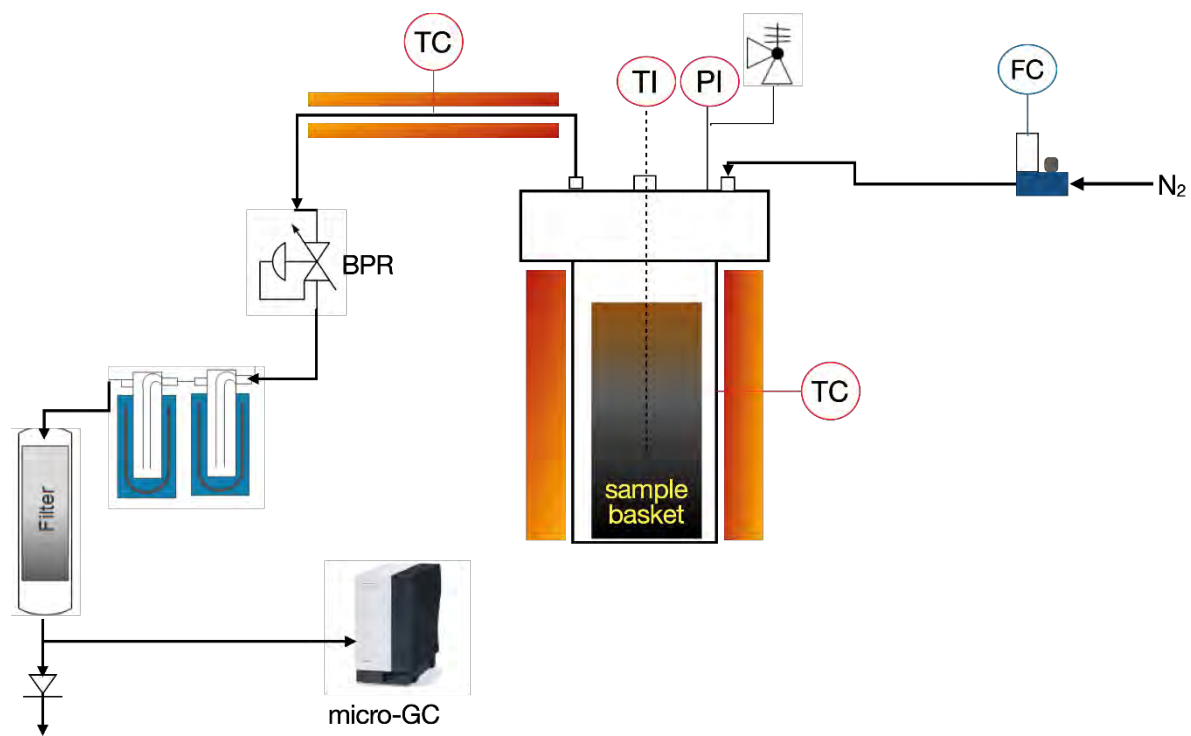
Figure S1. Schematic diagram of the experimental pyrolysis setup used in the present study.

Table S1. Summary statistics for the regression models based on the data given in Table 2 for VS-derived chars (values in brackets correspond to the p-values resulting from t-tests; significant terms are marked in bold)

$Term^a$	Response variables							
	y_{char}	x_{FC}	H:C ratio	O:C ratio	Fuel ratio	HHV	S_{BET}	V_{ultra}
β_0	0.365	0.534	0.728	0.065	1.343	26.37	170	0.049
β_1 (T)	**–0.046**	**0.085**	**–0.344**	**–0.040**	**0.464**	**1.076**	**42.1**	**0.020**
	(0.031)	**(0.003)**	**(0.000)**	**(0.015)**	**(0.002)**	**(0.001)**	**(0.000)**	**(0.001)**
β_2 (P)	–0.009	–0.015	0.009	0.005	–0.030	0.026	–1.42	0.000
	(0.526)	(0.186)	(0.318)	(0.562)	(0.538)	(0.734)	(0.605)	(0.986)
β_3 (τ)	0.010	–0.006	0.000	–0.002	–0.036	0.026	0.33	0.001
	(0.476)	(0.575)	(0.988)	(0.793)	(0.470)	(0.734)	(0.903)	(0.768)
β_{12} (T·P)	0.010	0.006	–0.016	0.001	0.047	0.151	5.08	0.004
	(0.486)	(0.547)	(0.125)	(0.867)	(0.364)	(0.122)	(0.132)	(0.073)
β_{13} (T·τ)	0.014	0.002	**0.027**	0.013	–0.012	0.101	–2.17	–0.002
	(0.320)	(0.811)	**(0.039)**	(0.204)	(0.801)	(0.247)	(0.444)	(0.259)
β_{23} (P·τ)	0.006	0.001	0.013	0.000	–0.020	–0.149	0.83	0.000
	(0.639)	(0.931)	(0.178)	(0.989)	(0.681)	(0.126)	(0.760)	(0.889)
$\beta_{curvature}$	–0.027	0.006	**–0.069**	–0.010	–0.067	–0.311	4.38	–0.002
	(0.397)	(0.780)	**(0.028)**	(0.608)	(0.545)	(0.147)	(0.491)	(0.629)
Adjusted R^2	0.603	0.906	0.984	0.719	0.920	0.960	0.970	0.952

---

^{a} The structure of the regression model (using normalized values for factors in the range from –1 to 1) for a given response variable was the following:

$$\hat{y} = \beta_0 + \beta_1 T + \beta_2 P + \beta_3 \tau + \beta_{12} T{\cdot}P + \beta_{13} T{\cdot}\tau + \beta_{23} P{\cdot}\tau + \beta_{curvature} CenterPt$$

where $\beta_0, \beta_i, \beta_{ij}$ are the intercept, linear, and 2-way interaction coefficients, respectively. $\beta_{curvature}$ is the coefficient for the center point (CenterPt) term.

Table S2. Summary statistics for the regression models based on the data given in Table 2 for WS-derived chars (values in brackets correspond to the p-values resulting from t-tests; significant terms are marked in bold)

Term	Response variables							
	y_{char}	x_{FC}	H:C ratio	O:C ratio	Fuel ratio	HHV	S_{BET}	V_{ultra}
β_0	0.300	0.718	0.617	0.149	3.321	27.40	128	0.028
β_1 (T)	**−0.037**	**0.080**	**−0.144**	**−0.045**	**1.344**	0.500	**24.2**	**0.010**
	(0.007)	**(0.003)**	**(0.021)**	**(0.017)**	**(0.002)**	(0.063)	**(0.020)**	**(0.017)**
β_2 (P)	−0.001	0.016	0.002	0.018	**0.309**	0.050	−0.23	0.001
	(0.883)	(0.066)	(0.916)	(0.092)	**(0.040)**	(0.742)	(0.954)	(0.729)
β_{12} (T·P)	−0.010	0.001	−0.003	−0.014	0.170	−0.150	8.23	0.004
	(0.883)	(0.921)	(0.899)	(0.148)	(0.118)	(0.374)	(0.141)	(0.070)
$\beta_{curvature}$	−0.018	0.025	−0.023	0.006	0.032	−0.400	4.23	0.003
	(0.062)	(0.069)	(0.546)	(0.602)	(0.772)	(0.186)	(0.508)	(0.278)
Adjusted R^2	0.964	0.983	0.880	0.920	0.987	0.723	0.895	0.919

Table S3. Summary statistics for the regression models based on the data given in Table 2 for CS-derived chars (values in brackets correspond to the p-values resulting from t-tests; significant terms are marked in bold)

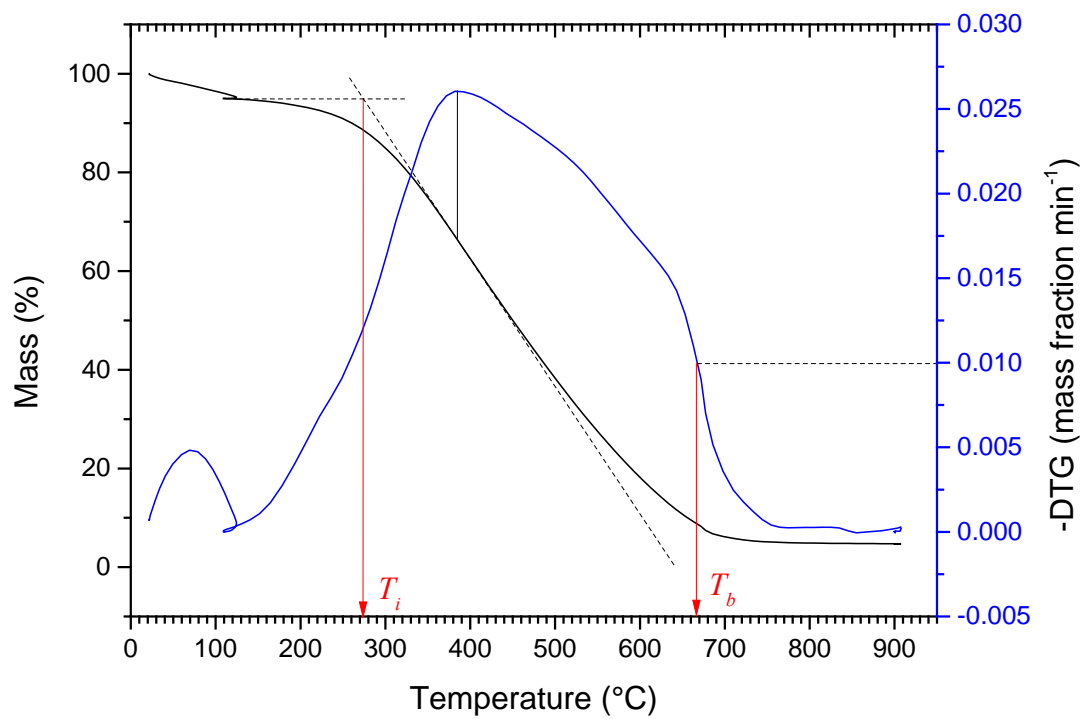| Term	Response variables							
	y_{char}	x_{FC}	H:C ratio	O:C ratio	Fuel ratio	HHV	S_{BET}	V_{ultra}
β_0	0.336	0.651	0.651	0.164	2.275	27.18	173	0.047
β_1 (T)	**−0.050**	**0.096**	**−0.150**	**−0.053**	**0.962**	**0.515**	**40.0**	**0.018**
	(0.010)	**(0.001)**	**(0.009)**	**(0.006)**	**(0.000)**	**(0.029)**	**(0.003)**	**(0.002)**
β_2 (P)	0.002	−0.004	−0.004	0.012	**−0.105**	**0.475**	4.00	0.000
	(0.756)	(0.205)	(0.788)	(0.103)	**(0.022)**	**(0.042)**	(0.208)	(1.000)
β_{12} (T·P)	0.013	−0.082	0.031	**0.018**	**−0.112**	**−0.525**	−6.00	−0.002
	(0.115)	(0.069)	(0.169)	**(0.047)**	**(0.017)**	**(0.034)**	(0.111)	(0.102)
$\beta_{curvature}$	−0.002	0.014	0.004	**−0.032**	−0.087	0.125	**−15.0**	−0.003
	(0.0838)	(0.055)	(0.875)	**(0.037)**	(0.067)	(0.499)	**(0.046)**	(0.151)
Adjusted R^2	0.946	0.997	0.946	0.973	0.998	0.930	0.984	0.986

Figure S2. An example of estimation of T_i and T_b (VS_350_0.5_150 char). Black solid line: TG curve; blue solid line: DTG curve.

Table S4. Summary statistics for the regression models based on the data given in Table 3 for VS-derived chars (values in brackets correspond to the p-values resulting from t-tests; significant terms are marked in bold)

Term	Response variables			
	T_i	T_b	T_{max}	$S \cdot 10^{-7}$
β_0	298.5	707.4	445.0	0.749
β_1 (T)	9.41 (0.060)	0.34 (0.961)	**40.9 (0.004)**	**–0.102 (0.027)**
β_2 (P)	–1.09 (0.754)	–4.16 (0.560)	–1.31 (0.810)	–0.051 (0.138)
β_3 (τ)	–7.59 (0.097)	–19.7 (0.054)	–8.06 (0.205)	**0.112 (0.021)**
β_{12} (T·P)	–3.34 (0.371)	10.3 (0.203)	–2.06 (0.707)	–0.042 (0.195)
β_{13} (T·τ)	6.16 (0.149)	**24.3 (0.031)**	13.7 (0.071)	**–0.138 (0.012)**
β_{23} (P·τ)	0.66 (0.850)	14.8 (0.102)	4.44 (0.440)	–0101 (0.138)
$\beta_{curvature}$	–2.25 (0.850)	–31.7 (0.102)	–15.5 (0.265)	**0.189 (0.045)**
Adjusted R^2	0.583	0.752	0.879	0.877

Table S5. Summary statistics for the regression models based on the data given in Table 3 for WS-derived chars (values in brackets correspond to the p-values resulting from t-tests; significant terms are marked in bold)

Term	Response variables			
	T_i	T_b	T_{max}	$S \cdot 10^{-7}$
β_0	298.0	708.0	422.2	0.688
β_1 (T)	**18.5 (0.017)**	36.0 (0.055)	**24.2 (0.008)**	**–0.190 (0.018)**
β_2 (P)	2.50 (0.417)	9.00 (0.414)	0.75 (0.764)	–0.022 (0.478)
β_{12} (T·P)	–2.00 (0.503)	–3.00 (0.766)	–0.25 (0.919)	–0.005 (0.876)
$\beta_{curvature}$	–1.33 (0.757)	–0.30 (0.982)	–8.25 (0.131)	–0.034 (0.470)
Adjusted R^2	0.900	0.698	0.955	0.898

Table S6. Summary statistics for the regression models based on the data given in Table 3 for CS-derived chars (values in brackets correspond to the p-values resulting from t-tests; significant terms are marked in bold)

Term	Response variables			
	T_i	T_b	T_{max}	$S \cdot 10^{-7}$
β_0	301.8	591.0	424.2	2.311
β_1 (T)	**22.2** **(0.004)**	27.0 (0.067)	**37.8** **(0.013)**	**−0.632** **(0.017)**
β_2 (P)	−3.75 (0.122)	**77.5** **(0.009)**	9.25 (0.168)	**−1.252** **(0.004)**
β_{12} (T·P)	−5.25 (0.068)	−1.50 (0.857)	3.75 (0.481)	**0.371** **(0.047)**
$\beta_{curvature}$	8.92 (0.056)	**−187.0** **(0.004)**	**84.4** **(0.006)**	**0.861** **(0.021)**
Adjusted R^2	0.978	0.985	0.975	0.983

Table S7. Expressions of functions $f(\alpha)$ and $g(\alpha)$ and their corresponding mechanism[1]

| Code	Name	$f(\alpha)$	$g(\alpha)$	Mechanism
F1	first order	$1-\alpha$	$-\ln(1-\alpha)$	
F2	second order	$(1-\alpha)^2$	$(1-\alpha)^{-1}-1$	
F3	third order	$\dfrac{1}{2}(1-\alpha)^3$	$(1-\alpha)^{-2}-1$	chemical reaction
F1/3	one-third order	$\dfrac{3}{2}(1-\alpha)^{1/3}$	$1-(1-\alpha)^{2/3}$	
F3/4	three-quarters order	$4(1-\alpha)^{3/4}$	$1-(1-\alpha)^{1/4}$	
F3/2	one and a half order	$2(1-\alpha)^{3/2}$	$(1-\alpha)^{-1/2}-1$	
D1	parabola law	$1/(2\alpha)$	α^2	1-D diffussion
D2	Valensi equation	$\left[-\ln(1-\alpha)\right]^{-1}$	$\alpha+(1-\alpha)\ln(1-\alpha)$	2-D diffussion
D3	Jander equation	$\dfrac{3}{2}(1-\alpha)^{2/3}\left[1-(1-\alpha)^{1/3}\right]^{-1}$	$\left[1-(1-\alpha)^{1/3}\right]^2$	3-D diffussion, spherical
D4	Ginstling−Brounstein equation	$\dfrac{3}{2}\left[(1-\alpha)^{-1/3}-1\right]^{-1}$	$1-\dfrac{2}{3}\alpha-(1-\alpha)^{2/3}$	3-D diffussion, cylindrical
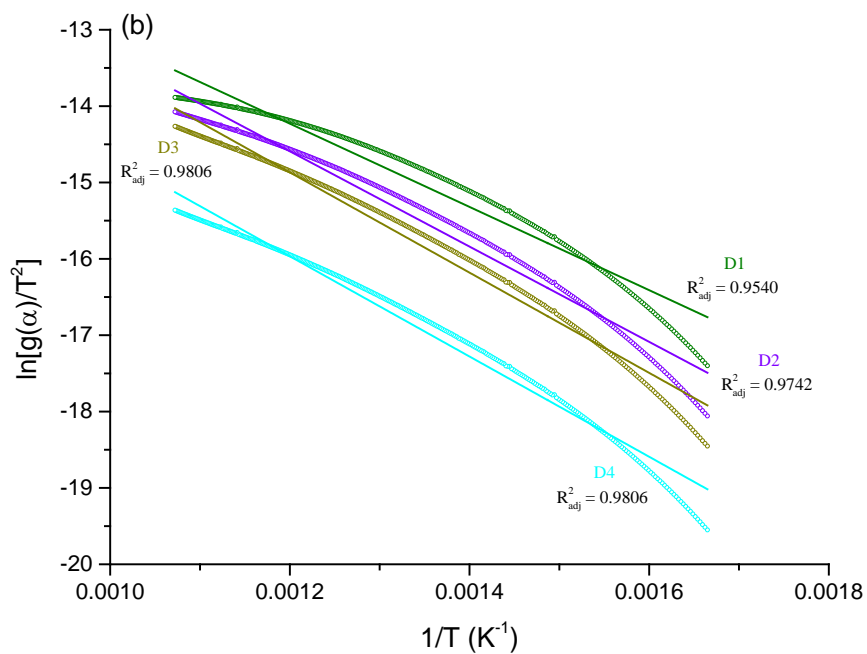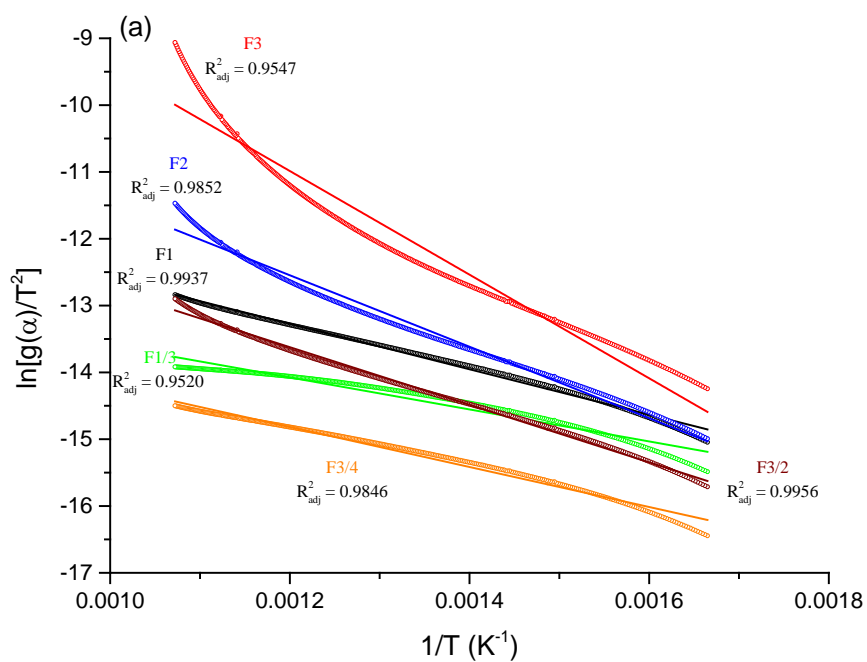
Figure S3. CR plots for the VS_500_0.5_150 char adopting different expressions of *g(α)*: (a) those corresponding to some chemical reactions mechanisms, and (b) those corresponding to some diffusion-based mechanisms.

Results from PLS regression approach (response: S)

a) Cross validation (number of components)
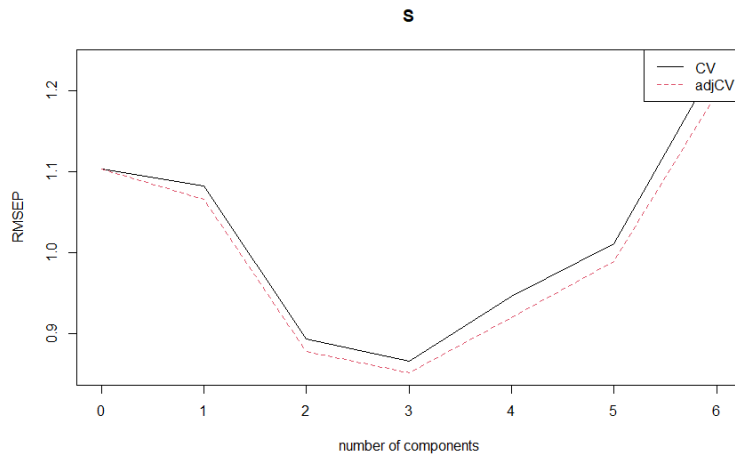
CV is the cross-validation estimate, and $adjCV$ is the bias-corrected cross-validation estimate. RMSEP is the root mean square error of prediction for the response ($S \cdot 10^7$ in wt.%^{2} min^{-2} °C^{-3}).

b) Regression coefficients

T	–0.10229
P	–0.31871
Hemicel	0.01966
Cel	0.39977
Lignin	–0.29230
Ca-bio	–0.07526
K-bio	–0.45752
x_{FC}	–0.08698
O/C	0.19583
H/C	0.10221
HHV	–0.14983
S_{BET}	0.08056

c) Scores

X variable	Comp. 1	Comp. 2	Comp. 3
VS_350_0.1_50	–0.0084	1.3688	–2.3386
VS_350_0.1_150	–0.3888	1.2350	–2.1015
VS_350_0.5_50	–0.6190	0.2496	–3.3498
VS_350_0.5_150	–0.7072	0.4294	–3.1863
VS_425_0.3_100	–1.4508	0.4745	–0.7962
VS_500_0.1_50	–1.9051	0.8189	1.1659
VS_500_0.1_150	–1.8710	0.7370	1.1518
VS_500_0.5_50	–2.6619	–0.2776	0.8508
VS_500_0.5_150	–2.6250	–0.2203	0.7216
WS_350_0.1_150	1.7279	–1.1763	–1.1110
WS_350_0.5_150	1.4861	–2.3811	–1.9305
WS_425_0.3_150	0.8776	–1.9094	0.0274
WS_500_0.1_150	0.3038	–1.8636	1.5758
WS_500_0.5_150	–0.3030	–2.7549	1.2325
CS_350_0.1_150	3.1297	2.0209	–0.1756
CS_350_0.5_150	2.0217	0.5770	–0.0340
CS_425_0.3_150[f]	1.4832	0.8944	1.5685
CS_500_0.1_150	0.8425	1.3329	3.8614
CS_500_0.5_150	0.6676	0.4447	2.8678

d) Loadings and loading-weihgts

Loadings

Char	Comp. 1	Comp. 2	Comp. 3
T	–0.316	–0.127	0.417
P	–0.102	–0.261	0.000
Hemicel	0.454	–0.422	0.170
Cel	0.513	–0.114	0.251
Lignin	–0.510	0.214	–0.233
Ca-bio	0.421	–0.481	0.143
K-bio	0.213	–0.646	0.000
x_{FC}	0.000	–0.397	0.406
O/C	0.560	–0.108	–0.126
H/C	0.187	0.250	–0.446
HHV	0.000	–0.294	0.420
S_{BET}	–0.365	0.190	0.369

Loading-weights

Char	Comp. 1	Comp. 2	Comp. 3
T	−0.221	0.128	0.448
P	−0.300	−0.266	0.000
Hemicel	0.216	−0.320	0.178
Cel	0.546	0.000	0.277
Lignin	−0.458	0.000	−0.254
Ca-bio	0.125	−0.397	0.147
K-bio	−0.272	−0.651	0.000
x_{FC}	0.000	−0.168	0.403
O/C	0.403	−0.211	−0.180
H/C	0.164	0.000	−0.494
HHV	−0.134	−0.136	0.277
S_{BET}	0.000	0.360	0.299

e) Variable importance in projection (VIP)
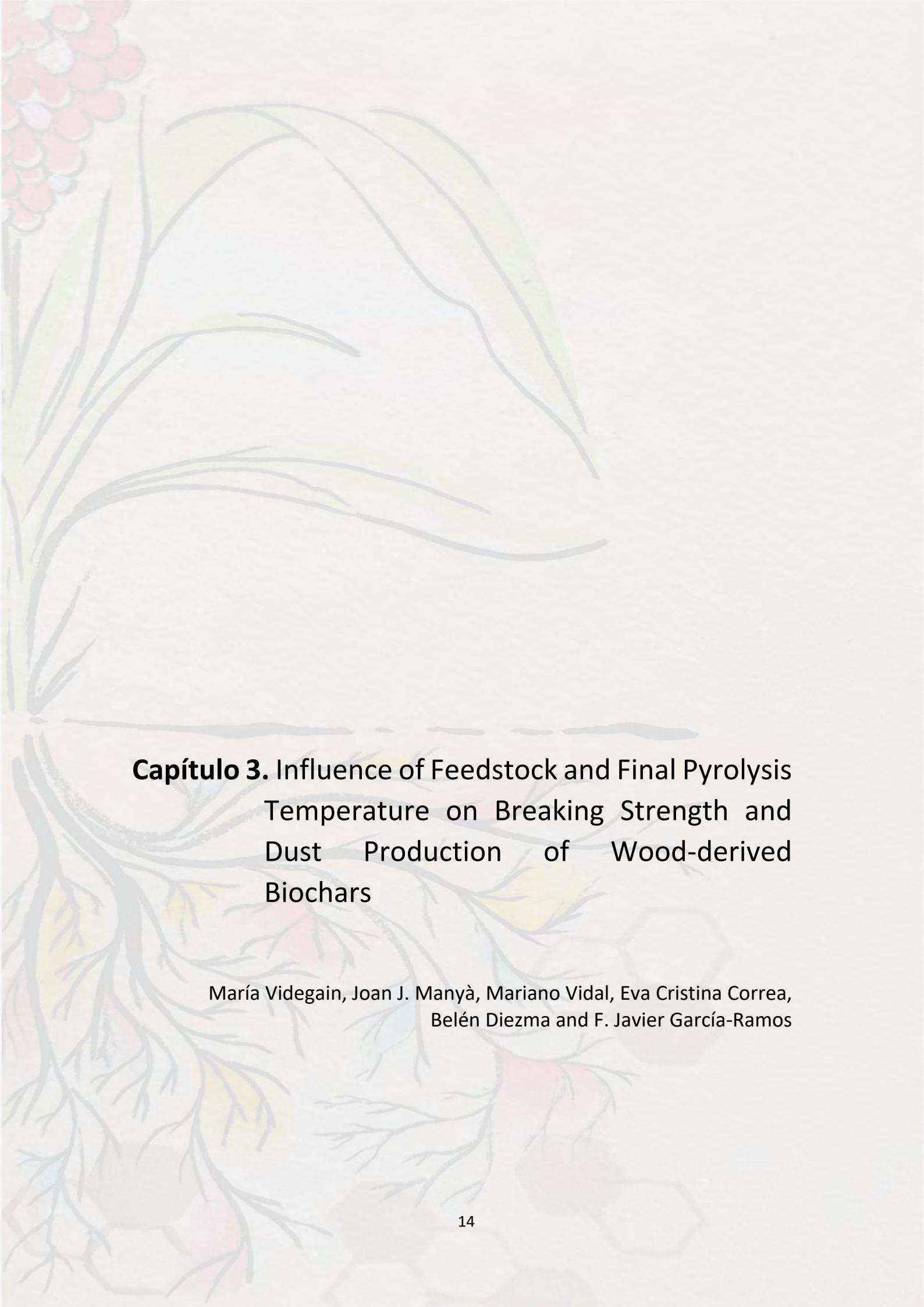
The VIP scores were defined as Mehmood et al.[2]:

$$VIP_j = \left(\frac{p \sum_{a=1}^{A} \left[SS_a \left(w_{aj} / \|w_a\|^2 \right) \right]}{\sum_{a=1}^{A} SS_a} \right)^{1/2} \tag{S1}$$

The basis behind this score is to assess the importance of each variable *j* being reflected by *w* (loading weigths) from each component *a*. SS_a is the sum of squares explained by the *a*th component, whereas *p* is the number of components finally selected (3 in our case). The VIP scores are shown in Figure 9.

References

(1)   Chong, Y. Y.; Thangalazhy-Gopakumar, S.; Gan, S.; Ng, H. K.; Lee, L. Y.; Adhikari, S. Kinetics and Mechanisms for Copyrolysis of Palm Empty Fruit Bunch Fiber (EFBF) with Palm Oil Mill Effluent (POME) Sludge. *Energy Fuels* **2017**, *31* (8), 8217–8227.

(2)   Mehmood, T.; Liland, K. H.; Snipen, L.; Sæbø, S. A Review of Variable Selection Methods in Partial Least Squares Regression. *Chemom. Intell. Lab. Syst.* **2012**, *118*, 62–69.

Capítulo 3. Influence of Feedstock and Final Pyrolysis Temperature on Breaking Strength and Dust Production of Wood-derived Biochars

María Videgain, Joan J. Manyà, Mariano Vidal, Eva Cristina Correa, Belén Diezma and F. Javier García-Ramos

Article

Influence of Feedstock and Final Pyrolysis Temperature on Breaking Strength and Dust Production of Wood-Derived Biochars

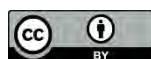**María Videgain** [1,*], **Joan J. Manyà** [2], **Mariano Vidal** [3], **Eva Cristina Correa** [4], **Belén Diezma** [4]
and **Francisco Javier García-Ramos** [1]

[1] Instituto Agroalimentario de Aragón—IA2 (CITA-Universidad de Zaragoza), EPS, Universidad de Zaragoza, Carretera de Cuarte s/n, E-22071 Huesca, Spain; fjavier@unizar.es

[2] Thermochemical Processes Group, Aragón Institute of Engineering Research (I3A), EPS, University of Zaragoza, Carretera de Cuarte s/n, E-22071 Huesca, Spain; joanjoma@unizar.es

[3] Departamento de Ingeniería Mecánica, EPS, University of Zaragoza, Carretera de Cuarte s/n, E-22071 Huesca, Spain; vidalcor@unizar.es

[4] Laboratorio de Propiedades Físicas y Técnicas Avanzadas en Agroalimentación, ETSIAAB, Universidad Politécnica de Madrid, Avda. Puerta de Hierro 2, E-28040 Madrid, Spain; evacristina.correa@upm.es (E.C.C.); belen.diezma@upm.es (B.D.)

* Correspondence: mvidegain@unizar.es; Tel.: +34-974292656

Abstract: The susceptibility to fragmentation of biochar is an important property to consider in field applications. Physical and mechanical properties of wood-derived biochars from vine shoots and holm oak were studied to evaluate the effect of biomass feedstock, final pyrolysis temperature and application conditions. Vine shoots and holm oak pruning residues were selected for biochar production. Slow pyrolysis experiments were conducted at two different final temperatures (400 and 600 °C). Physical and chemical characteristics of biomass and biochars were determined. Impact strength was evaluated through the measurement of the gravitational potential energy per unit area (J mm^{-2}) necessary for the breakage of biochar fragments. Shear strength (N mm^{-2}) and a combination of shear/compression strengths (N) were analyzed using a Universal Texture Analyzer. A particular mechanical treatment was carried out on biochar samples to simulate the processing bodies of a commercial manure spreader, under two gravimetric moisture contents. Holm oak-derived biochar was more resistant than vine shoot-derived biochar to the applied forces. Vine shoots-derived biochar did not show a significantly different mechanical behavior between temperatures. Holm Oak-derived biochar produced at the higher final pyrolysis temperature showed higher resistance to be broken into smaller pieces. Moistening resulted in an adequate practice to improve mechanical spreading.

Keywords: physical characterization; mechanical processing; vineyard pruning; holm oak pruning; particulate matter; biochar moistening

1. Introduction

Wood-derived biochar refers to the carbonaceous solid material resulting from the pyrolysis of wood at relatively low temperatures (<700 °C) in an oxygen-limited atmosphere [1]. Biochar has been widely studied in the last few years, owing to the wide range of agricultural benefits related to its application as an organic amendment (e.g., improvement of soil fertility, contribution to a carbon-negative process [2–5]). Based on the extensive available literature, it can be stated that the benefits of applying biochar on soil ecosystem services are site-specific [6], and they are influenced by the type of biomass used as feedstock [7,8]. Furthermore, the pyrolysis experimental conditions (i.e., final pyrolysis

temperature, pressure, heating time and residence time of the gas phase) govern the properties of resulting biochar [9–11]. The application rate [12] and particle size [13,14] also significantly affect the potential benefits of biochar use as a soil amendment. Ultimately, biochar is a general term that encompasses products of quite different nature and properties; the inclusion of details about its properties in research publications seems to be essential both to establish the most appropriate use and to gain deeper knowledge on this topic [15,16].

Some organizations have developed characterization standards (European Biochar Foundation-EBC [17] and International Biochar Initiative-IBI [1]), whose guidelines describe analytical methods for physical and chemical properties, storage instructions, and application conditions that ensure the quality of potential commercial biochars. In addition to other research works [18–20], these guidelines emphasize about the application conditions and the need to properly prescreening and characterizing the biochar batches after the pretreatments needed for their proper application (i.e., grinding, granulation, moistening, etc.) [21]. There are still technical and practical barriers both for safe handling and large-scale application of biochar [20]. The mechanical stresses resulting from biochar application to soil can favor its release into the atmosphere, specifically contributing to airborne particulate matter <10 μm in diameter (PM_{10}), which are liable to remain in the air and enter the respiratory tract of humans [22,23]. Anthropogenic Black Carbon aerosols (BCa) have a significant radiative forcing potential and a clear climate warming effect [24]. Fine particles of biochar can also promote the transport of adsorbed contaminants in water by percolation and runoff [25]. In addition, biochar dust is susceptible to ignition when stored in enclosed spaces [20]. Hence, moistening the biochar prior to its soil application is a recommended practice in order to reduce particulate matter emissions [1]. A recommended moisture content is not specified in EBC or IBI guidelines. Silva et al. [26] measured the threshold friction velocities of a range of biochar particles at different moisture contents, and they determined an optimum gravimetric moisture content above 15%. However, biochar resistance to be broken into smaller pieces is governed by mechanical properties of biochar, which so far have not been properly assessed [16].

On the one hand, both penetration resistance and aggregate stability of the soil once biochar is applied are some of the measured parameters [27,28] when the objective is to determine the mechanical properties of the amended soil. On the other hand, the mechanical behavior of biochar has been assessed for specific applications such as land-fill biocovers and in-ground filtration systems [29–31], addition of charcoal to construction materials or biocomposites [32], fuel pellets production [33–35], and heating blast furnaces to industrial iron production [36–39]. The characterization methodologies adopted for the aforementioned applications are based on standards for soils, geoengineering, plastics, and other specific materials. To the best of our knowledge, there are no standardized methods for determining strength properties of biochar related to its soil application, an issue whose standardization would be extremely complex due to the wide range of biomass feedstocks and pyrolysis process conditions, with consequent biochar of very diversified structures and textures.

Several studies showed clear correlations between the properties of the parent material used as biochar feedstock and the mechanical behavior of biochar [40–43]. Furthermore, relying on previous studies, pyrolysis operating conditions play a significant role in the final product behavior, with a general trend of increasing the material resistance with final pyrolysis temperature [37,41,42,44]. Kumar et al. [37] determined—for chars produced from acacia and eucalyptus species—a decrease in crushing and impact strengths with increasing carbonization temperature up to 600 °C, followed by an increase above this temperature. Das et al. [41], via nanoindentation, concluded that a combination of high final pyrolysis temperature (≥500 °C) and relatively long residence time (~60 min) led to an increase in the values of hardness and elastic modulus of seven residues-derived biochars. Nevertheless, the opposite effect was also reported [45] with loss of dynamic hardness with increasing pyrolysis temperature.

The present study aims to assess the influence of feedstock and final pyrolysis temperature on both the particle size distribution of wood-derived biochar and its mechanical behavior through the measurement of shear strength and a combination of forces (shear/compression). A Universal Texture Analyzer was used to test these properties on biochar fragments. The effect of experimental conditions (biomass feedstock and pyrolysis temperature) on biochar particle size distribution was also evaluated by a mechanical process simulating biochar spreading at the soil surface.

2. Materials and Methods

2.1. Biomass Origin and Characterization

Pruning remains from thinning in a scrub area (Clean Cellulosic Biomass [1]) of holm oaks (HO) (*Quercus ilex* L.), and vine shoots pruning residues from the province of Huesca (Spain), were used as biochar feedstocks. The agronomic characteristics of vineyards are detailed in a previous publication [46]. Both pruning remains corresponded to branches of one year of age.

Biomass was selected by diameter (between 5.0 and 10.0 mm) and chopped up using a domestic shredder (ZI-GHAS2800, ZIPPER Maschinen GmbH, Schlüblberg, Austria) into pieces of 20–50 mm in length. These particle sizes were used in order to following a cutting practice that could be carried out under field conditions in a reasonable way. In addition, these particle sizes could enhance the carbonization efficiency of the pyrolysis process [47].

Proximate analyses were performed by following the ASTM standards [48]as it is detailed in a previous publication [46]. X-ray fluorescence (XRF) spectroscopy was used to determine the inorganic elements of biomass, by means of a Niton XL3t GOLD++ portable analyzer (Thermo Fisher Scientific, Waltham, MA, USA). TestAll™ Geo mode was used, with a 120 s acquisition time, and at least three measurements per analysis were conducted.

Van Soest method was adopted to determine the biomass constituents (lignin, cellulose, hemicellulose and extractives) [49]. The complete description of this procedure is available in previous publications [47,50].

EBC methodology [1] was followed to measuring bulk density of three composite samples of biomass and biochar, determining the mass that could be packed into a 20 mL stainless-steel cylinder with minimal compression.

Water holding capacity (WHC) of biochar samples was determined by gravimetry through pressure plates (Richards chambers, −33 kPa–1500 kPa).

2.2. Production of Biochar and Characterization

Slow pyrolysis runs were performed under atmospheric pressure and at two different final pyrolysis temperatures (400 and 600 °C). The average heating rate was 5 °C min⁻¹. A total of 20 experiments were conducted (5 repetitions for each type of feedstock and final pyrolysis temperature). The pyrolysis device and experimental conditions details are reported in previous publications [46,51]. Proximate, elemental and XRF analyses were carried out following the aforementioned methodology. The specific surface area (S_{BET}) was determined using a gas sorption analyzer through the measurements of CO_2 adsorption isotherms at 0 °C. The detailed procedure for S_{BET} determination and pore volume (volume total–V_{total} and ultramicropore–V_{ultra}) is available in a previous publication [47].

The raw biochars were sieved to different sizes to establish the particle size distribution. The amount of biochar retained on each sieve was weighed on a precision balance. Dry sieving was used to separate large fragments (≥2 mm), while wet sieving was applied for the fine fraction (<2 mm, but ≥0.001); the finest particles (<0.010 mm) were retained on filter papers through an in-line filter holder (Sartorius, Goettingen, Germany) connected to a vacuum pump. The fraction of particles <0.010 mm was calculated as the difference between the fraction measured in 2 mm sieve and the sum of the retained fractions values

measured by wet sieving (0.01–2.00 mm). Both the sieves used for the wet sieving and the filter papers were dried prior to the sample retention and subsequently dried in an oven at 70 °C until constant weight. The work was carried out inside an airless extraction hood. The difference between the initial weight of the samples and the sum of the different size fractions was negligible.

Morphological characterization was carried out for three samples (i.e., three different pyrolysis runs) of each type of biochar (or treatment). 10% in weight of the coarse fraction (>2 mm length) was sampled fragment (resulting in 368 and 172 fragments for VS and HO-derived biochars, respectively) and the following measures were performed: length and diameter (digital caliper Twin-Cal IP40, TESA, Renens, Switzerland), mass (precision balance cp224s-Oce, Sartorius, Goettingen, Germany), volume (by displacement of water in a graduate tube [43]), and bulk density of each individual fragment as a quotient between the two latter parameters. The shape coefficient was calculated as the quotient between the measured diameter of each fragment and the equivalent diameter (diameter of a cylinder with equivalent volume).

2.3. Mechanical Behavior

2.3.1. Impact Strength and Texturometer Measurements

The height (within a range from 1 to 3 m) necessary for the breakage of each fragment of biochar onto a metal surface was measured. The mass and the rupture area were determined to calculate the potential breakage energy ($E_p = mgh$) per unit area (J mm^{-2}). A total of 125 fragments of each sample was tested in this experiment.

In a second step, a Universal Texture Analyzer was used to evaluate the rheological behavior of biochar through different measurements. Shear strength (N mm^{-2}) was calculated as the maximum force per unit area that could be applied to a biochar fragment before crushing. It was determined for 30 fragments of each treatment using a texture analyzer TA-XT2 (Stable Micro Systems Ltd., Godalming, UK), a universal machine controlled by specific software. Each fragment of biochar was introduced horizontally in a methacrylate support with a separation of 0.75 cm between the fixed extremes. A central piece is vertically displaced by the load cell exerting the shear stress perpendicular to the fibers of each biochar fragment. The load cell of the texturometer descended at a speed of 3 mm s^{-1}. The unit area on which the force was exerted was calculated as twice the cross-sectional area of the fragment. The same texturometer, with a Kramer shear cell coupled, was used to determine the resistance to a combination of compression and shear strengths (N) exerted parallel to the fibers. This process was undertaken using 5 g of each sample by triplicate. The mass of fine particles (<2 mm) generated as a result of this test was measured. The maximum applied force (N), both for shear strength and Kramer shear cell measurements, was fixed in 25 kg.

2.3.2. Mechanical Simulation of Biochar Spreading and Moistening

A mechanical process was combined with two moisture contents to achieve a factorial design:

- Factor 1: biomass pyrolysis feedstock (VS: vine shoots—HO: Holm oak).
- Factor 2: final pyrolysis temperature (400–600 °C).
- Factor 3: mechanical process (Control: without mechanical processing—P: mechanically processed with the raw moisture content—P15: mechanically processed with 15 wt.% moisture content).

Three replicates were carried out for the 12 resulting samples.

The mechanical processing was carried out using an automatic mechanical agitation system, in which the movement in a manure spreader was reproduced. The constructive scheme is detailed in Figure 1. This process was performed for three biochar samples (i.e., 150 g from each sample) and treatments. The main velocity of the mechanical agitation process was 50 rpm. After processing, particle size distribution was measured following

the same methodology as described in Section 2.2. The 15 wt.% moisture content was attained following the same methodology as described by Silva et al. [26].
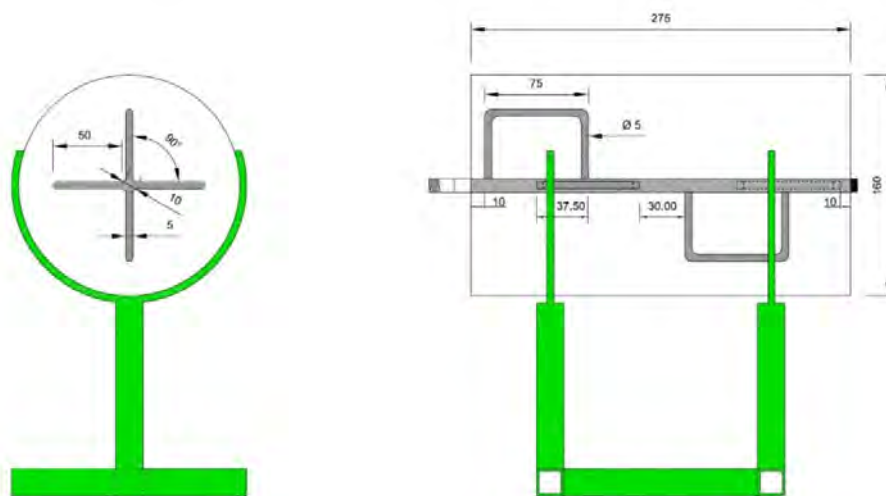

Figure 1. Automatic mechanical agitation system developed to simulate the mechanical spreading. Units: mm.

2.4. Statistical Analysis of Results

IBM SPSS Statistics v.26 (IBM Corp., Armonk, NY, USA) software package was used to perform the statistical analysis of data. Two-way ANOVA was conducted (at a significance level of 0.05) to detect significant differences in the response variables (both physical characterization and texturometer measurements) between the two biochar feedstocks and the two final pyrolysis temperatures, respectively. Three-way ANOVA was conducted to verify the effect of factors (biomass, temperature and mechanical process) and their interactions on the particle size distribution. The comparison between treatment means was performed using the Tukey's method at a significance level of 0.05. The data of particle size distribution (%) were transformed into arcsine for statistical analysis.

3. Results and Discussion

3.1. Biomass and Biochar Characterization

Table 1 details the results from proximate, ultimate, biomass constituents, surface area and porosity, bulk density and product yield fractions determined for both biomass and biochar samples.

Table 1. Results from proximate, ultimate, biomass constituents, porosity properties and product yield determined for the feedstocks and/or obtained biochars.

Proximate (wt.% from Triplicate)	VS	HO		VS400	VS600	HO400	HO600
Ash (dry basis)	2.75 ± 0.34	3.55 ± 1.08		6.49 ± 0.14	10.34 ± 0.81	8.28 ± 0.17	11.54 ± 0.49
Moisture	10.47 ± 0.11	7.48 ± 0.07		0.57 ± 0.22	0.72 ± 0.34	0.38 ± 0.01	0.88 ± 0.12
Volatile matter (dry basis)	81.46 ± 2.35	77.86 ± 2.83		22.17 ± 0.01	2.47 ± 0.71	25.22 ± 0.06	7.38 ± 0.21
Fixed Carbon (dry basis)	15.79 ± 1.13	18.59 ± 1.99		71.34 ± 6.45	87.20 ± 1.32	66.50 ± 3.61	81.07 ± 2.52
Elemental (wt.% in daf [1] basis from triplicate) [2]							
C	42.29 ± 0.49	46..2 ± 0.54		71.50 ± 0.48	82.89 ± 0.33	63.76 ± 0.32	72.74 ± 0.01
H	5.24 ± 0.06	8.16 ± 0.07		4.46 ± 0.19	1.95 ± 0.08	3.86 ± 0.05	2.30 ± 0.07
N	13.52 ± 0.35	9.21 ± 0.16		1.58 ± 0.10	1.52 ± 0.01	0.93 ± 0.01	0.74 ± 0.04
O	38.96 ± 0.45	36.43 ± 0.22		22.42 ± 0.77	13.63 ± 0.31	31.67 ± 0.27	24.20 ± 0.11
Elemental inorganic matter (wt.% from triplicate) [3]							
Ca	1.13 ± 0.40	2.64 ± 0.40		2.61 ± 0.32	3.02 ± 0.39	4.30 ± 0.12	7.50 ± 0.62
Si	0.47 ± 0.03	0.69 ± 0.32		0.31 ± 0.05	0.24 ± 0.01	0.61 ± 0.01	0.41 ± 0.06
K	0.38 ± 0.15	0.19 ± 0.01		1.48 ± 0.18	4.29 ± 0.52	0.63 ± 0.02	0.95 ± 0.04
S	0.21 ± 0.06	0.17 ± 0.02		0.13 ± 0.03	0.40 ± 0.03	0.15 ± 0.02	0.12 ± 0.01
Al	0.09 ± 0.01	0.15 ± 0.12		0.03 ± 0.00	0.16 ± 0.01	0.19 ± 0.01	0.06 ± 0.00
Mg	0.11 ± 0.00	0.12 ± 0.01		0.31 ± 0.01	0.45 ± 0.02	0.58 ± 0.04	0.41 ± 0.02
P	0.21 ± 0.02	0.07 ± 0.01		0.27 ± 0.02	1.01 ± 0.07	0.26 ± 0.02	0.15 ± 0.02
Fe	0.03 ± 0.01	0.05 ± 0.03		0.02 ± 0.00	0.03 ± 0.01	0.13 ± 0.01	0.10 ± 0.02
Lignocellulosic constituents and extractives (wt.% from triplicate)			**Surface area and pore volume**				
Lignin + silica	20.16 ± 0.49	23.60 ± 0.54	S_{BET} (m^2 g^{-1})	105.80	227.50	122.30	232.79
Cellulose	34.18 ± 1.95	36.90 ± 0.50	V_{total} (cm^3 g^{-1})	0.0370	0.0819	0.0430	0.0930
Carbohydrate + protein	33.02 ± 0.18	29.03 ± 1.12	V_{ultra} (cm^3 g^{-1})	0.0361	0.0816	0.0428	0.0858
Hemicellulose + acid soluble ash	8.10 ± 1.63	7.25 ± 1.44	**Product yield (-) (n = 5)**				
Extractives	4.54 ± 0.05	3.22 ± 0.09	γ_{char}	0.38 ± 0.02	0.29 ± 0.01	0.41 ± 0.03	0.30 ± 0.01
Bulk density (g cm^{-3} from triplicate)	0.35 ± 0.05	0.86 ± 0.08		0.25 ± 0.06	0.23 ± 0.04	0.55 ± 0.12	0.51 ± 0.08
Water Holding capacity (wt.% from triplicate)				14.16 ± 1.25	18.35 ± 1.36	4.56 ± 0.79	13.66 ± 1.11

[1] Dry-ash-free. [2] Oxygen is calculated by difference. [3] Only listed components with a composition higher than 0.01%. VS: Vine Shoots; HO: Holm Oak; 400/600: final pyrolysis temperature of biochar-°C. Values are presented as mean ± standard deviation. Regarding the raw biomasses, results from proximate, elemental and inorganic matter are consistent with previous publications [10,46,52], with slight differences between both types of biomass. The ash content was higher in HO than VS, probably related to the presence of leaves in HO pruning residues. It should be highlighted the relatively large amount of calcium measured, especially for HO biomass.

Lignin (+silica) content was higher in HO biomass (20.16 and 23.60 wt.% for VS and HO, respectively), according to the different nature of these feedstocks. However, these contents were relatively low in absolute terms. This can be explained by the type of pruning residues selected in the present study, since they come from shoots/branches of one year of age with lower level of lignification than other more developed parts of these plants. It must be pointed out that lignin is the constituent, which mostly contributes to the char yield [53].

Regarding the results from biochar samples, as expected, the higher the final pyrolysis temperature, the larger the fixed carbon content. The nitrogen, oxygen and hydrogen fractions decreased with an increased temperature. Again, calcium was the predominant inorganic element, showing larger concentrations than the previously determined for raw biomass as a consequence of the loss of organic matter during the process. The concentration of inorganic compounds can significantly affect the pyrolysis process. The cracking and polymerization reactions of tar vapors, and the primary devolatilization reactions are influenced by alkali elements (particularly K). In addition to this, the degradation of hemicelluloses could be partly inhibited by the presence of Ca [47].

From the results of bulk density, measured in composite samples through the stainless-steel cylinder method, HO showed higher bulk density than VS (0.86 and 0.35 g cm^{-3} respectively). This difference was maintained in bulk density determinations for biochar samples, although with slightly higher values from biochars produced at lower final pyrolysis temperatures.

Both pore volume and S_{bet} increased with final pyrolysis temperature. Higher porous structures are developed due to the removal of Oxygen and hydrogen during the devolatilization process. The same trend was observed in WHC values. VS-derived biochar showed higher general values for WHC than HO biochar. It was consistent with bulk density results, despite the S_{bet} and pore volume values of VS biochar being slightly lower than HO biochar. An in-depth study of the pore structure and the correlation for both types of biochar could help to understand these results. HO400 showed a particularly low WHC value (4.56 wt.% versus a mean value of 15 wt.% in the other samples). This may be related to the low fixed carbon content (and high volatile matter content and density) determined for this biochar.

Results from physical characterization of the biochar fragments are shown in Table 2.

Table 2. Influence of feedstock and final pyrolysis temperature on physical properties of the produced biochars.

Parameter	VS400	VS600	HO400	HO600
M (g)	0.32 ± 0.15 c	0.29 ± 0.13 c	0.92 ± 0.17 b	0.97 ± 0.29 a
L (mm)	43.08 ± 9.55 ab	41.38 ± 8.81 b	45.17 ± 6.52 a	45.67 ± 7.83 a
V (cm^3)	0.99 ± 0.34 c	0.80 ± 0.31 d	1.65 ± 0.41 b	1.84 ± 0.52 a
Ø (mm)	4.58 ± 1.02 b	4.50 ± 1.00 b	7.37 ± 1.18 a	7.28 ± 0.95 a
Shape coefficient (-)	0.86 ± 0.16 c	0.93 ± 0.17 b	0.96 ± 0.11 a	0.98 ± 0.14 a
Bulk density (g cm^{-3})	0.33 ± 0.11 d	0.38 ± 0.16 c	0.56 ± 0.05 b	0.53 ± 0.09 a

Different letters within a row denote statistically significant differences ($p < 0.05$) between the biochar samples (Tukey´s test). Values are presented as mean ± standard deviation. VS: Vine Shoots; HO: Holm Oak; 400/600: final pyrolysis temperature of biochar-°C.

Feedstock was found to be the main effect influencing all the physical properties of biochars ($p < 0.0001$). Mass was also significantly affected by pyrolysis temperature ($p < 0.0001$). In addition, all the variables were significantly affected by the interaction of the two factors. Biochar from VS featured fragments with lower values of mass (0.32 and 0.29 g for VS400 and VS600, respectively) and average values of approx. 42.2 mm in length. HO fragments showed higher values of mass (0.92 and 0.97 for HO400 and HO600, respectively) and an average value of approx. 45.4 mm in length. The volume of VS600 was significantly lower than that of VS400, while the behavior for HO biochar was the opposite. The measured diameters did not show significant differences as a function of pyrolysis temperature (for a given feedstock) and, therefore, the shape coefficients were relatively high and homogeneous.

Bulk density is one of the most important properties to consider for field application, both due to the importance of knowing the units of elements that are applied into the soil, and the need to regulate the machinery for its application. The results obtained from bulk density through the two different methodologies adopted for composite samples and

fragments varied considerably for the VS-derived biochar. This could be related to an underestimation of the volume measured under the immersion method. Different methodologies developed to measure skeletal density through helium pycnometry combined with the determination of envelope density by displacement of a dry granular suspension [54] could be more suitable for this purpose. In addition, an in-depth study on the hydrophobicity of both types of biochar analyzed could help to understand the different behavior showed for VS and HO biochar, since the values of HO biochar were close between the two methods.

Physical characterization confirmed the different type of product to be handled in field applications, due to both the nature of feedstock and final pyrolysis temperature. These biochar characteristics allow one to select the type of machinery for its appropriate application.

3.2. Strength Measurements

From the results obtained in impact tests, a contingency table was built (see Table 3). From the table, it can be seen that none of the HO biochar fragments broke due to the impact at a maximum drop height of 3 m. Regarding VS biochar, no significant differences were detected between pyrolysis temperatures for the percentage of fragments that suffered breakage.

Table 3. Impact test results.

Sample	Break	No Break	χ^2	Breaking Ep (J mm^{-2})	p-Value
VS400	70.4%	29.6%	0.143	0.20 ± 0.09	0.648
VS600	77.1%	22.9%		0.22 ± 0.11	
HO400	0%	100%			
HO600	0%	100%			

VS: Vine Shoots; HO: Holm Oak; 400/600: final pyrolysis temperature of biochar-°C.

The number of pieces (mean value + SD) in which each fragment broke into was 2.10 ± 0.04 and 2.20 ± 0.03 for VS400 and VS600, respectively. Difference was not statistically significant.

Regarding the effect of final pyrolysis temperature on the breaking gravitational potential energy per unit area required to break the VS biochar samples, the mechanical behavior between VS400 and VS600 were statistically similar (see Table3) with an average value of 0.21 ± 0.16 J mm^{-2}.

Figure 2 shows the results obtained for shear strength (N mm^{-2}) and Kramer cell force (N) as a function of both biomass feedstock and final pyrolysis temperature. Results from two-way ANOVA revealed a clear effect of biomass type ($p < 0.0001$) on the shear strength, with significantly higher values of shear strength for HO-derived biochars. No significant differences were detected between temperatures for this experiment (average values of 0.65 N mm^{-2} for VS, and 1.03 N mm^{-2} for HO).
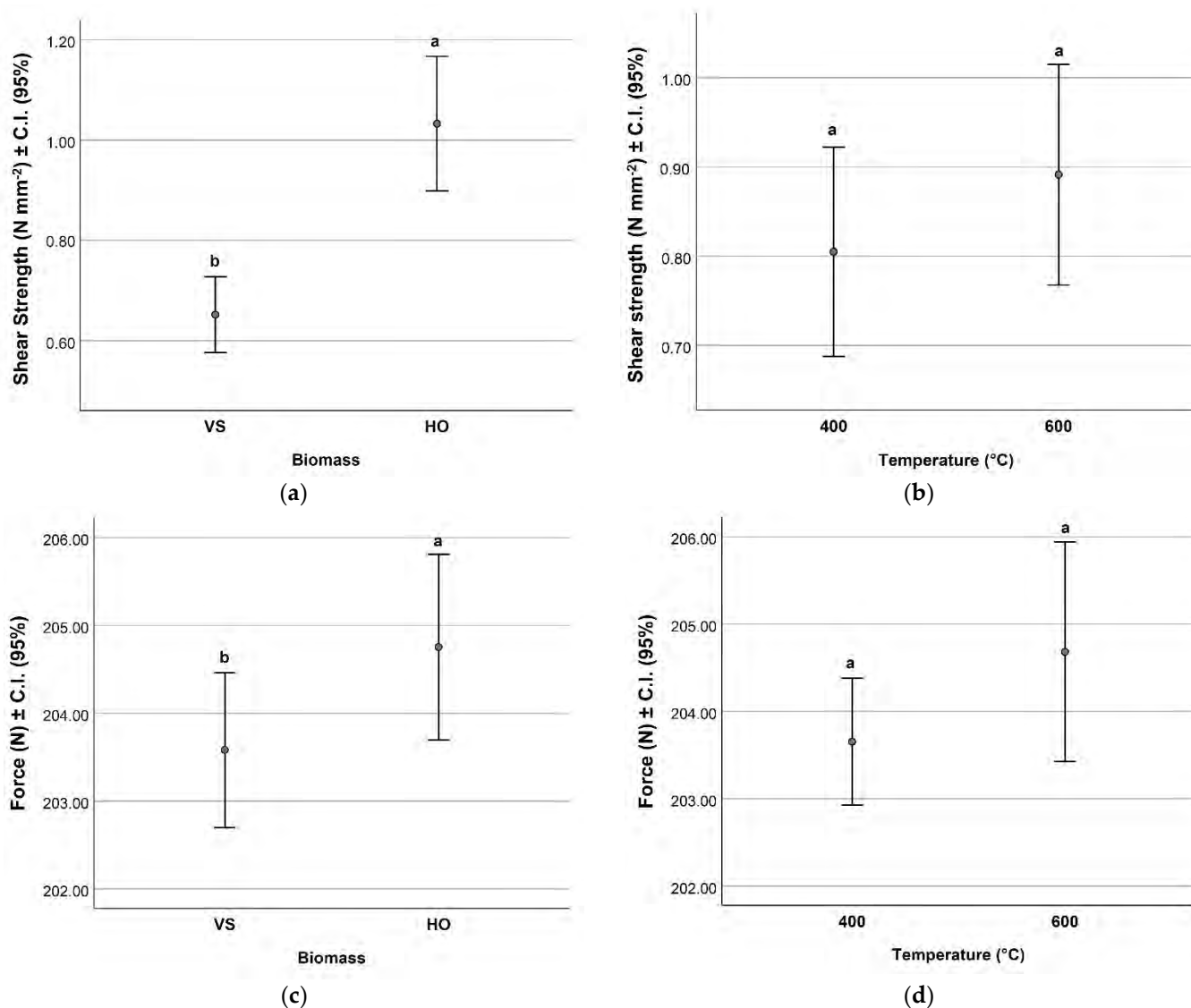
Figure 2. Effect of final pyrolysis temperature on: (**a**) shear strength as a function of biomass and- (**b**) final pyrolysis temperature. (**c**) The breaking force supported into the Kramer shear cell as a function of biomass and- (**d**) final pyrolysis temperature. VS: Vine Shoots; HO: Holm Oak; 400/600: final pyrolysis temperature-°C; different letters within a graph show statistically significant differences ($p < 0.05$).

Significant differences ($p = 0.031$) were detected between biochars produced from different biomass sources during the load tests conducted using the shear Kramer cell (see Figure 2c). HO-derived biochar supported higher levels of force (N) than VS-derived biochars. Selecting by feedstock, ANOVA revealed no significant differences between temperatures for this experiment (average values of 203.65 ± 0.69 and 204.68 ± 1.19 N for 400 and 600 °C, respectively). A significant effect was observed in this experiment for HO400, in which a significantly ($p = 0.001$) higher content of fine particles was collected after each experiment (average values of 0.027 ± 0.001 g for HO400 and 0.009 ± 0.002 g for HO600, respectively). This difference was not found between feedstocks and VS pyrolysis temperatures which presented an average value of 0.017 ± 0.01 g. Chrzazvez et al. [55] studied the fragmentation of different charcoal samples from tree species. They reported the higher level of fragmentation under compression forces for *Quercus* charcoal linked to the presence of a significant porous zone and a specific fragmentation mode of this species, which differs from others by the presence of multiseriate rays, related to the formation of fragile zones after combustion.

As mentioned above, the lignocellulosic composition of the biomass used as feedstock is of special interest in this study, since biochar usually keeps the morphological features of its feedstock after thermochemical conversion [41,56]. Wood pyrolysis commonly leads to a higher proportion of lignin than herbaceous biomasses, which usually have a higher cellulose content [41,57,58]. The lignocellulosic constituents degrade at different temperatures during the pyrolysis process (hemicellulose–complete starting at 330 °C; cellulose–greatest proportion degradation at 427 °C; lignin–complete degradation after 607 °C) [41,57–60]. The contents of lignin in the raw biomasses (see Table 1) were slightly higher for HO than for VS. This could explain the higher resistance of HO-derived biochars to impact strength. Nevertheless, the analyzed feedstocks have different bulk densities, which could also play a key role in determining the impact resistance and shear strength of HO-derived. This is in line with the results reported by Kumar et al. [37] and de Abreu Neto et al. [43], who observed a positive correlation between hardness and apparent density of wood chars. However, Dias Júnior et al. [38], in view on their breaking strength measurements for several charcoals produced at different pyrolysis temperatures, suggested that the apparent density of charcoal by itself was not a suitable indicator of its mechanical resistance.

With regard to the influence of temperature on mechanical strength, previous studies [37,42] reported a clear decrease in compressive/crushing/impact strength with increasing carbonization temperature up to 500–600 °C. However, the results reported herein suggest that an increment in the final pyrolysis temperature from 400 °C to 600 °C led to a better mechanical behavior of biochar under specific forces. This finding seems to be consistent with the observations reported by Xie et al. [44], who observed a gradual increase in hardness with the pyrolysis temperature (in the range of 300–700 °C) for corn stalk pellets-derived biochars. Zickler et al. [56] also observed a continuous increase in the elastic modulus and hardness above 400 °C (via nanoindentation). Dias Júnior et al. [38] showed the same correlation in wood-derived charcoals. According to Das et al. [41], biochar made at temperature of around 450 °C presents a disintegrated micro-structure, exhibiting a defective structure of pyrolytic tars that lends to lower hardness. During the pyrolysis process, fragmentation and depolymerization occur, resulting in chemical degradation products that may have a certain effect on the final mechanical properties of the biochar [41]. This could be one of the reasons to explain the results from our study, in which lower average values of resistance were observed for VS400 (impact strength) and HO400 (shear strength), which exhibited higher contents of volatile matter (and, consequently, lower fixed-carbon contents) in comparison to VS600 and HO600 biochars (with more aromatic carbon structures). However, the above-explained effect of temperature was not statistically significant. The fact that the two types of biochar showed different behaviors under static and dynamic forces leads to the conclusion that feedstock nature plays an important role in determining the mechanical properties of resulting biochars.

### 3.3. Particle Size Distribution and Mechanical Processing

Table 4 details the *p*-value results from a three-way ANOVA performed to assess the influence of factors (i.e., biomass type, final pyrolysis temperature, and mechanical process) on the particle size distribution of biochar samples.

Table 4. Influence of biomass type, final pyrolysis temperature and process on the particle size distribution (mm).

| Factor	≥20	2–20	0.250–2	0.125–0.250	0.090–0.125	0.010–0.090	<0.010
Biomass (B)		0.008	<0.0001	<0.0001			
Temperature (T)	<0.0001	<0.0001	<0.0001	<0.0001	0.033	0.003	
Process (P)	<0.0001	<0.0001	<0.0001	0.012		0.007	
B × T	<0.0001	<0.0001	0.001	<0.0001			
B × P	<0.0001	<0.0001	0.004	0.007		<0.0001	
T × P	<0.0001	<0.0001	0.001		0.009	0.043	
B × T × P	<0.0001	<0.0001	0.021				

The type of biomass did not have a significant effect on either the fraction of larger particles (≥20 mm) nor the finest fractions (< 0.010–0.125 mm). Both the main effects and interactions were more significant for the coarser fractions (0.125–>20 mm). The fraction 0.090–0.125 mm was only significantly affected by temperature (as a main factor) as well as the interaction between temperature and process type. The fraction 0.010–90 mm was the finest fraction significantly affected by temperature and process type, and also by the interactions between biomass–process and temperature–process. In addition, the finest fraction (<0.010 mm) was not significantly affected.

Figure 3a,b illustrate the particle size distributions of the samples. Results from one-way ANOVA regarding the effect of process application are shown in order to facilitate the interpretation for the different fractions selecting by biomass. In Figure 3, fraction < 0.010–0.250 mm is clustered. In Figures 3c and 3d, the disaggregation of this fraction is specifically shown for each type of processed biochar.
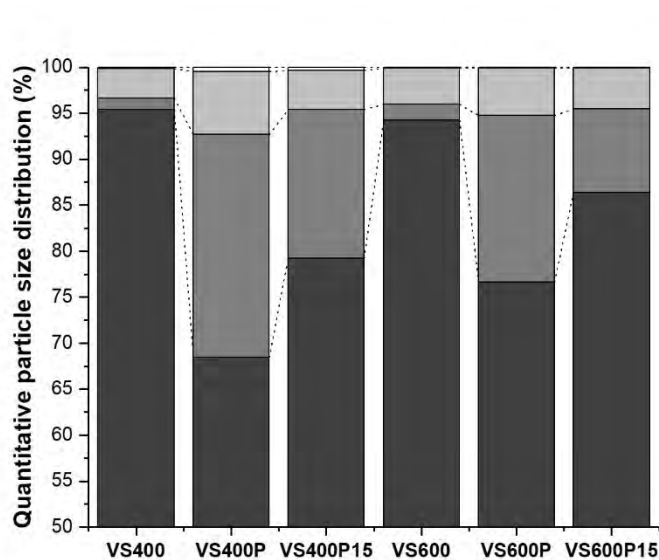
Fraction (mm)	VS400	VS400P	VS400P15	VS600	VS600P	VS600P15
< 0.250	ab	a	ab	b	b	b
2—0.250	b	a	ab	b	ab	ab
20—2	d	a	b	d	b	c
> 20	a	d	c	a	c	b

(a)
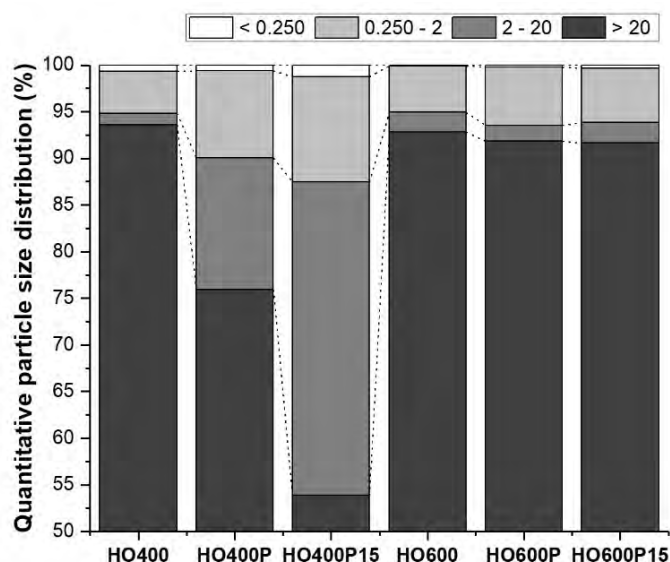
Fraction (mm)	HO400	HO400P	HO400P15	HO600	HO600P	HO600P15
< 0.250	bc	c	a	e	d	d
2—0.250	b	a	a	b	b	b
20—2	c	b	a	c	c	c
> 20	a	b	c	a	a	a

(b)

Fraction (mm)	VS400	VS400P	VS400P15	VS600	VS600P	VS600P15
0.250—0.125	ab	a	a	bc	bc	c
0.125—0.090	c	ab	a	c	c	bc
0.090—0.010	b	a	b	b	b	b
< 0.010	a	a	a	a	a	a

Fraction (mm)	HO400	HO400P	HO400P15	HO600	HO600P	HO600P15
0.250—0.125	b	bc	a	bc	c	bc
0.125—0.090	a	a	a	a	a	a
0.090—0.010	b	b	a	b	b	ab
< 0.010	a	a	a	a	a	a

(**c**)   (**d**)
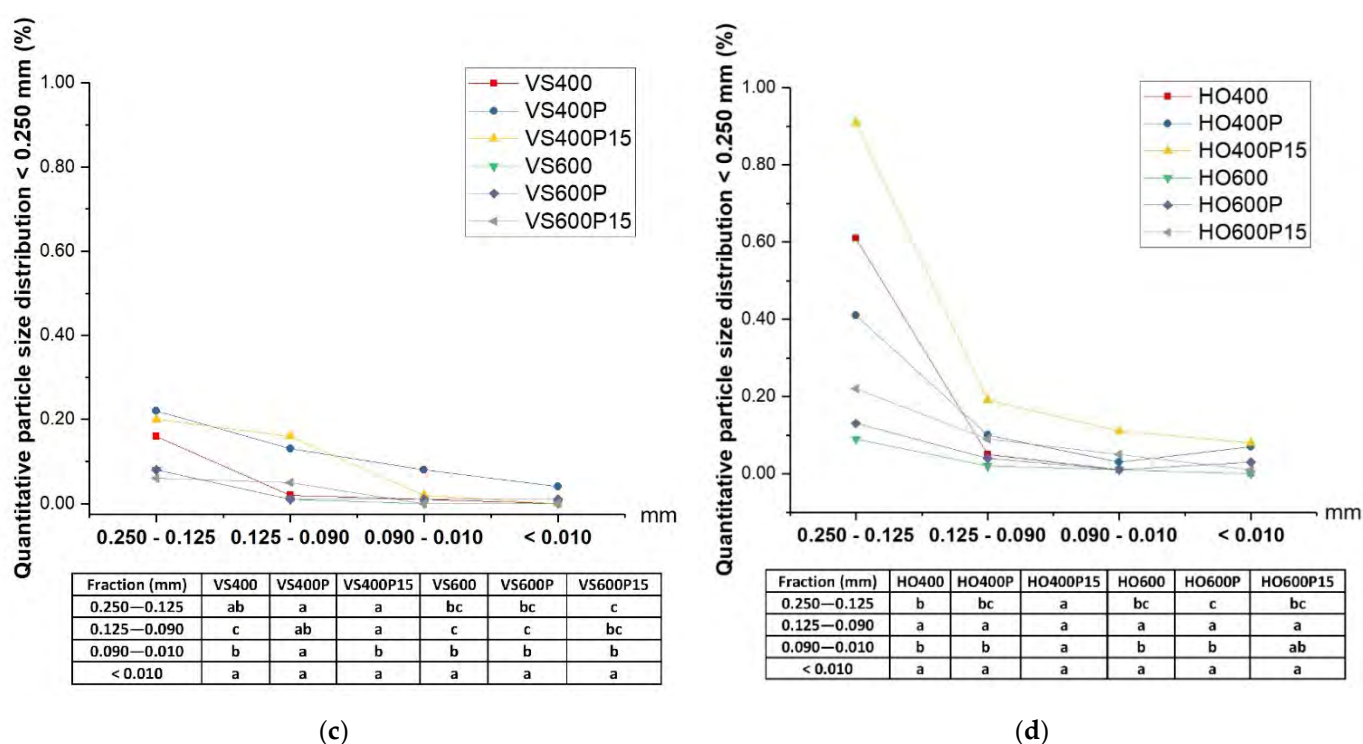
Figure 3. Quantitative particle size distribution (%): (**a**) VS- and (**b**) HO-derived biochar, both lower and larger size classes (mm) were considered; (**c**) VS- and (**d**) HO-derived biochar, the former smallest class (<0.250) was broken down into further classes. (VS/HO: Vine shoots/Holm Oak; 400/600: final pyrolysis temperature-°C; P: processed into the mechanical agitation system; P15: 15 wt.% moisture content; different letters within a row show significant differences at $p < 0.05$–Tukey´s test).

The initial average values for the percentage of fragments between 2 and 20 mm were 1.24% and 1.18% for VS and HO, respectively. Biochar produced at 400 °C significantly increased this percentage after the mechanical processing for both feedstocks (24.18% for VS400 and 14.18% for HO400). Moistening significantly reduced this percentage in VS400 (16.20%). However, regarding HO400, the larger percentage of this fraction was measured under wet conditions (33.61%). In the processing of VS-derived biochar produced at 600 °C, it was observed a significant reduction of this fraction (2–20 mm) under wet conditions (55% with respect to the dry processing). In addition, a significant increase in the percentage of particles between 0.250–2 mm was observed for HO400 after the mechanical processing, regardless of the moisture content.

With respect to the clustered fraction (<0.250 mm), VS biochar did not show significant differences on its cumulative percentage. HO400P15, HO600P, and HO600P15 showed significant increases in this fraction, with particularities that are shown in Figures 3c and 3d.

The analysis of the particle size distribution below 0.250 mm is especially relevant, since fine particles can be dissolved into the atmosphere and lead to mass losses during the application process. In general, the particle size fraction below 0.250 mm was small, ranging from 0.09% (VS600) to 1.29% (HO400P15), in mass basis. As can be deduced from Figure 3c,d, HO biochars exhibited a more homogeneous behavior compared with VS biochars (the slightly significant differences are reported in the graphs with the purpose to provide useful information for future characterizations of VS and HO-derived biochars). In any case, the fine particle fractions reported herein are much lower than the percentage of mass losses (30%) measured by Blue Leaf Inc. during the application in field trials of a fine grained biochar produced by fast pyrolysis [18].

Moistening had a significant effect on particle size distribution, leading to a reduced fragmentation of coarse fractions in VS biochar; this could be attributed to an increase in

compressive strength through the increased bonding and bridging between biochar particles in the presence of moisture as a result of enhanced Van der Waals forces, as it was previously reported by Bazargan et al. [34]. Silva et al. [26] reported that 15 wt.% water content increased resistance to erodibility of larger particles due to weight gain by water absorption. For HO600 biochar, which appeared as the most homogeneous biochar, no significant variations were found between non-processed samples and processed under the two moisture contents. Conversely, HO400 showed again the lower resistance to mechanical stress, in line with the previous results reported for shear strength. For this biochar, moistening had the opposite effect to that expected, leading to an increase in fragmentation and thus in the fractions of fine particles. This finding could be ascribed to the heterogeneous structure of HO400 (in comparison with the more aromatic structure of HO600), as it has been aforementioned. On the other hand, the observed lower WHC of HO400 (4.56%) could also be related to its structure. In fact, this biochar did not retain the 15 wt.% of moisture applied before processing, suggesting that the disaggregation of fragments during mechanical processing was promoted by the high amount of free water in the mechanical agitation system.

Regarding PM_{10} fraction, the main percentages were higher for HO biochars than for VS biochars (with a maximum value of 0.08% for HO400P15). However, there was no statistically significant difference with respect to all the factors examined.

Biochar particle size is a key parameter that can affect the biological and physicochemical properties of the soil, which seem to be improved when relatively fine particles of biochar are used [13,14]. However, in order to determine the most appropriate biochar particle size it should also be considered aspects related to production, handling, and application systems, as well as ignition hazards and dust production issues. In this sense, the relatively large particle sizes tested in the preent study was previously studied, and several benefits derived from its application were reported [46,61]. Considering the results obtained, the potential benefits of moistening biochar prior to the application depend on the final purpose and the type of biochar. Dust production and percolation of fine particulate matter should not be controlled at the application time focusing on a moisture content, since fragmentation is regulated by structural properties of biochar.

4. Conclusions

Results reported herein revealed that vine shoots and holm oak pruning residues can be considered as interesting biomass sources, whose management is suitable for the production of biochar. The physicochemical properties of resulting biochars were appropriate for agricultural purposes.

The mechanical behavior of these two types of biochar varied a lot depending on the application of static or dynamic forces: HO biochar exhibited higher impact strength than VS biochar, whose value could not be determined from a maximum height of 3 m. Final pyrolysis temperature did not significantly affect the impact strength resistance for VS. HO biochar showed higher resistance to shear strength and compression/shear combination forces than VS biochar. Final pyrolysis temperature did not significantly influence the resistance to static forces. Significant effects of biomass type, final pyrolysis temperature and mechanical process were observed on the particle size distribution and its fragmentation under systematic mechanical solicitations. Moistening practice could reduce the fragmentation in some types of biochar if WHC of biochar and mechanical properties are considered.

Author Contributions: Conceptualization, F.J.G.-R. and J.J.M.; methodology, F.J.G.-R., J.J.M., M.V.-M., B.D., E.C.C. and M.V.; software, M.V.-M.; validation, F.J.G.-R., J.J.M., M.V., B.D. and E.C.C.; formal analysis, J.J.M., F.J.G.-R., M.V.-M., B.D., E.C.C. and M.V.; investigation, J.J.M., F.J.G.-R., M.V., B.D., E.C.C. and M.V.-M.; resources, J.J.M., F.J.G.-R. and M.V.-M.; data curation, J.J.M., F.J.G.-R. and M.V.-M.; writing—original draft preparation, M.V.-M.; writing—review and editing, F.J.G.-R., J.J.M., M.V., B.D. and E.C.C.; visualization, M.V.-M.; supervision, F.J.G.-R., J.J.M., B.D. and E.C.C.;

References

1. International Biochar Initiative Standardized Product Definition and Product Testing Guidelines for Biochar That Is Used in Soil. *Int. Biochar Initiat.* **2015**, *23*.
2. Guo, M.; He, Z.; Uchimiya, S.M. Introduction to Biochar as an Agricultural and Environmental Amendment. In *Agricultural and Environmental Applications of Biochar: Advances and Barriers*; Guo, M., He, Z., Uchimiya, S.M., Eds.; Soil Science Society of America, Inc.: Madison, WI, USA, 2016; pp. 1–14.
3. Paz-Ferreiro, J.; Méndez, A.; Tarquis, A.M.; Cerdà, A.; Gascó, G. Preface: Environmental benefits of biochar. *Solid Earth* **2014**, *5*, 1301–1303, doi:10.1002/ldr.971.
4. Ayaz, M.; Feizienė, D.; Tilvikienė, V.; Akhtar, K.; Stulpinaitė, U.; Iqbal, R. Biochar role in the sustainability of agriculture and environment. *Sustainability* **2021**, *13*, 1330, doi:10.3390/su13031330.
5. Khawkomol, S.; Neamchan, R.; Thongsamer, T.; Vinitnantharat, S.; Panpradit, B.; Sohsalam, P.; Werner, D.; Mrozik, W. Potential of biochar derived from agricultural residues for sustainable management. *Sustainability* **2021**, *13*, doi:10.3390/su13158147.
6. Blanco-Canqui, H. Does biochar improve all soil ecosystem services? *GCB Bioenergy* **2021**, *13*, 291–304, doi:10.1111/gcbb.12783.
7. Hussain, R.; Garg, A.; Ravi, K. Soil-biochar-plant interaction: Differences from the perspective of engineered and agricultural soils. *Bull. Eng. Geol. Environ.* **2020**, *79*, 4461–4481, doi:10.1007/s10064-020-01846-3.
8. Yan, T.; Xue, J.; Zhou, Z.; Wu, Y. The trends in research on the effects of biochar on soil. *Sustainability* **2020**, *12*, 7810, doi:10.3390/SU12187810.
9. Manyà, J.J.; Ortigosa, M.A.; Laguarta, S.; Manso, J.A. Experimental study on the effect of pyrolysis pressure, peak temperature, and particle size on the potential stability of vine shoots-derived biochar. *Fuel* **2014**, *133*, 163–172, doi:10.1016/j.fuel.2014.05.019.
10. Manyà, J.J.; Azuara, M.; Manso, J.A. Biochar production through slow pyrolysis of different biomass materials: Seeking the best operating conditions. *Biomass Bioenergy* **2018**, *117*, 115–123, doi:10.1016/j.biombioe.2018.07.019.
11. Ahmad, J.; Vakalis, S.; Patuzzi, F.; Baratieri, M. Effect of process conditions on the surface properties of biomass chars produced by means of pyrolysis and CO2 gasification. *Energy Environ.* **2020**, doi:10.1177/0958305X20948237.
12. Gale, N.V.; Thomas, S.C. Dose-dependence of growth and ecophysiological responses of plants to biochar. *Sci. Total Environ.* **2019**, *658*, 1344–1354, doi:10.1016/j.scitotenv.2018.12.239.
13. De Jesus Duarte, S.; Glaser, B.; Cerri, C.E.P. Effect of biochar particle size on physical, hydrological and chemical properties of loamy and sandy tropical soils. *Agronomy* **2019**, *9*, 165, doi:10.3390/agronomy9040165.
14. Liang, C.; Gascó, G.; Fu, S.; Méndez, A.; Paz-Ferreiro, J. Biochar from pruning residues as a soil amendment: Effects of pyrolysis temperature and particle size. *Soil Tillage Res.* **2016**, *164*, 3–10, doi:10.1016/j.still.2015.10.002.
15. Manyà, J.J. Pyrolysis for biochar purposes: A review to establish current knowledge gaps and research needs. *Environ. Sci. Technol.* **2012**, *46*, 7939–7954, doi:10.1021/es301029g.
16. Baveye, P.C. The Characterization of Pyrolysed Biomass Added to Soils Needs to Encompass Its Physical And Mechanical Properties. *Soil Sci. Soc. Am. J.* **2014**, *78*, 2112–2113, doi:10.2136/sssaj2014.09.0354l.
17. Schmidt, H. European Biochar Certificate (EBC)-guidelines version 6.1. *Biochar* **2015**, doi:10.13140/RG.2.1.4658.7043.
18. Major, J. Julie Major, PhD Extension Director International Biochar Initiative. In *Guidelines on Practical Aspects of Biochar Application to Field Soil in Various Soil Management Systems*; 2010; doi:10.1016/B978-0-12-385538-1.00003-2.
19. Liu, X.; Zhang, A.; Ji, C.; Joseph, S.; Bian, R.; Li, L.; Pan, G.; Paz-Ferreiro, J. Biochar's effect on crop productivity and the dependence on experimental conditions-a meta-analysis of literature data. *Plant Soil* **2013**, *373*, 583–594, doi:10.1007/s11104-013-1806-x.
20. Das, S.K.; Ghosh, G.K.; Avasthe, R. Application of biochar in agriculture and environment, and its safety issues. *Biomass Convers. Biorefinery* **2020**, doi:10.1007/s13399-020-01013-4.

21. Sadasivam, B.Y.; Reddy, K.R. Engineering properties of waste wood-derived biochars and biochar-amended soils. *Int. J. Geotech. Eng.* **2015**, *9*, 521–535, doi:10.1179/1939787915Y.0000000004.

22. Gelardi, D.L.; Li, C.; Parikh, S.J. An emerging environmental concern: Biochar-induced dust emissions and their potentially toxic properties. *Sci. Total Environ.* **2019**, *678*, 813–820, doi:10.1016/j.scitotenv.2019.05.007.

23. Li, C.; Bair, D.A.; Parikh, S.J. Estimating potential dust emissions from biochar amended soils under simulated tillage. *Sci. Total Environ.* **2018**, *625*, 1093–1101, doi:10.1016/j.scitotenv.2017.12.249.

24. Maienza, A.; Genesio, L.; Acciai, M.; Miglietta, F.; Pusceddu, E.; Vaccari, F.P. Impact of biochar formulation on the release of particulate matter and on short-term agronomic performance. *Sustainability* **2017**, *9*, 1131, doi:10.3390/su9071131.

25. Wang, D.; Zhang, W.; Hao, X.; Zhou, D. Transport of biochar particles in saturated granular media: Effects of pyrolysis temperature and particle size. *Environ. Sci. Technol.* **2013**, *47*, 821–828, doi:10.1021/es303794d.

26. Silva, F.C.; Borrego, C.; Keizer, J.J.; Amorim, J.H.; Verheijen, F.G.A. Effects of moisture content on wind erosion thresholds of biochar. *Atmos. Environ.* **2015**, *123*, 121–128, doi:10.1016/j.atmosenv.2015.10.070.

27. Busscher, W.J.; Novak, J.M.; Evans, D.E.; Watts, D.W.; Niandou, M.A.S.; Ahmedna, M. Influence of pecan biochar on physical properties of a Norfolk loamy sand. *Soil Sci.* **2010**, *175*, 10–14, doi:10.1097/SS.0b013e3181cb7f46.

28. Gümüş, İ.; Negiş, H.; Şeker, C. Influence of Biochar Applications on Modulus of Rupture and Aggregate Stability of the Soil Possessing Crusting Problems. *Toprak Su Derg.* **2019**, doi:10.21657/topraksu.538580.

29. Wani, I.; Ramola, S.; Garg, A.; Kushvaha, V. Critical review of biochar applications in geoengineering infrastructure: Moving beyond agricultural and environmental perspectives. *Biomass Convers. Biorefinery* **2021**, doi:10.1007/s13399-021-01346-8.

30. Xu, K.; Yang, B.; Wang, J.; Wu, M.Z. Improvement of mechanical properties of clay in landfill lines with biochar additive. *Arab. J. Geosci.* **2020**, *13*, 1–12, doi:10.1007/s12517-020-05622-1.

31. Yargicoglu, E.N.; Sadasivam, B.Y.; Reddy, K.R.; Spokas, K. Physical and chemical characterization of waste wood derived biochars. *Waste Manag.* **2015**, *36*, 256–268, doi:10.1016/j.wasman.2014.10.029.

32. Akinyemi, B.A.; Adesina, A. Recent advancements in the use of biochar for cementitious applications: A review. *J. Build. Eng.* **2020**, *32*, 101705, doi:10.1016/j.jobe.2020.101705.

33. Azargohar, R.; Nanda, S.; Kang, K.; Bond, T.; Karunakaran, C.; Dalai, A.K.; Kozinski, J.A. Effects of bio-additives on the physicochemical properties and mechanical behavior of canola hull fuel pellets. *Renew. Energy* **2019**, *132*, 296–307, doi:10.1016/j.renene.2018.08.003.

34. Bazargan, A.; Rough, S.L.; McKay, G. Compaction of palm kernel shell biochars for application as solid fuel. *Biomass Bioenergy* **2014**, *70*, 489–497, doi:10.1016/j.biombioe.2014.08.015.

35. Hu, Q.; Shao, J.; Yang, H.; Yao, D.; Wang, X.; Chen, H. Effects of binders on the properties of bio-char pellets. *Appl. Energy* **2015**, *157*, 508–516, doi:10.1016/j.apenergy.2015.05.019.

36. Assis, M.R.; Brancheriau, L.; Guibal, D.; Napoli, A.; Trugilho, P.F. Assis_2020_SpecificMethods.pdf. *BioResources* **2020**, *15*, 7660–7670.

37. Kumar, M.; Verma, B.B.; Gupta, R.C. Mechanical properties of acacia and eucalyptus wood chars. *Energy Sources* **1999**, *21*, 675–685, doi:10.1080/00908319950014425.

38. Dias Junior, A.F.; Esteves, R.P.; da Silva, Á.M.; Sousa Júnior, A.D.; Oliveira, M.P.; Brito, J.O.; Napoli, A.; Braga, B.M. Investigating the pyrolysis temperature to define the use of charcoal. *Eur. J. Wood Wood Prod.* **2020**, *78*, 193–204, doi:10.1007/s00107-019-01489-6.

39. de Abreu Neto, R.; Ramalho, F.M.G.; Costa, L.R.; Hein, P.R.G. Estimating hardness and density of wood and charcoal by near-infrared spectroscopy. *Wood Sci. Technol.* **2021**, *55*, 215–230, doi:10.1007/s00226-020-01232-y.

40. Winsley, P. Biochar and bioenergy production for climate change mitigation. *Sci. Technol.* **2007**, *64*, 5–10.

41. Das, O.; Sarmah, A.K.; Bhattacharyya, D. Structure-mechanics property relationship of waste derived biochars. *Sci. Total Environ.* **2015**, *538*, 611–620, doi:10.1016/j.scitotenv.2015.08.073.

42. Assis, M.R.; Brancheriau, L.; Napoli, A.; Trugilho, P.F. Factors affecting the mechanics of carbonized wood: Literature review. *Wood Sci. Technol.* **2016**, *50*, 519–536, doi:10.1007/s00226-016-0812-6.

43. de Abreu Neto, R.; De Assis, A.A.; Ballarin, A.W.; Hein, P.R.G. Dynamic Hardness of Charcoal Varies According to the Final Temperature of Carbonization. *Energy Fuels* **2018**, *32*, 9659–9665, doi:10.1021/acs.energyfuels.8b02394.

44. Xie, R.; Zhu, Y.; Zhang, H.; Zhang, P.; Han, L. Effects and mechanism of pyrolysis temperature on physicochemical properties of corn stalk pellet biochar based on combined characterization approach of microcomputed tomography and chemical analysis. *Bioresour. Technol.* **2021**, *329*, 124907, doi:10.1016/j.biortech.2021.124907.

45. de Abreu Neto, R.; de Assis, A.A.; Ballarin, A.W.; Hein, P.R.G. Effect of final temperature on charcoal stiffness and its correlation with wood density and hardness. *SN Appl. Sci.* **2020**, *2*, 1–9, doi:10.1007/s42452-020-2822-0.

46. Videgain-Marco, M.; Marco-Montori, P.; Martí-Dalmau, C.; Jaizme-Vega, M.D.C.; Manyà-Cervelló, J.J.; García-Ramos, F.J. Effects of Biochar Application in a Sorghum Crop under Greenhouse Conditions: Growth Parameters and Physicochemical Fertility. *Agronomy* **2020**, *10*, 104, doi:10.3390/agronomy10010104.

47. Manyà, J.J.; Alvira, D.; Videgain, M.; Duman, G.; Yanik, J. Assessing the Importance of Pyrolysis Process Conditions and Feedstock Type on the Combustion Performance of Agricultural- Residue-Derived Chars. *Energy Fuels* **2021**, doi:10.1021/acs.energyfuels.0c04180.

48. American Standard of Testing Material: Standard Test Method for Chemical Analysis of Wood Charcoal ASTM D 1762-84 2001.

49. Van Soest, P.J.; Robertson, J.B.; Lewis, B.A. Methods for Dietary Fiber, Neutral Detergent Fiber, and Nonstarch Polysaccharides in Relation to Animal Nutrition. *J. Dairy Sci.* **1991**, *74*, 3583–3597, doi:10.3168/jds.S0022-0302(91)78551-2.

50. Greco, G.; Di Stasi, C.; Rego, F.; González, B.; Manyà, J.J. Effects of slow-pyrolysis conditions on the products yields and properties and on exergy efficiency: A comprehensive assessment for wheat straw. *Appl. Energy* **2020**, *279*, doi:10.1016/j.apenergy.2020.115842.

51. Greco, G.; Videgain, M.; Di Stasi, C.; González, B.; Manyà, J.J. Evolution of the mass-loss rate during atmospheric and pressurized slow pyrolysis of wheat straw in a bench-scale reactor. *J. Anal. Appl. Pyrolysis* **2018**, *136*, 18–26, doi:10.1016/j.jaap.2018.11.007.

52. López-Cano, I.; Cayuela, M.L.; Mondini, C.; Takaya, C.A.; Ross, A.B.; Sánchez-Monedero, M.A. Suitability of different agricultural and urban organic wastes as feedstocks for the production of Biochar-Part 1: Physicochemical characterisation. *Sustainability* **2018**, *10*, 2265, doi:10.3390/su10072265.

53. Collard, F.X.; Blin, J. A review on pyrolysis of biomass constituents: Mechanisms and composition of the products obtained from the conversion of cellulose, hemicelluloses and lignin. *Renew. Sustain. Energy Rev.* **2014**, *38*, 594–608, doi:10.1016/j.rser.2014.06.013.

54. Brewer, C.E.; Chuang, V.J.; Masiello, C.A.; Gonnermann, H.; Gao, X.; Dugan, B.; Driver, L.E.; Panzacchi, P.; Zygourakis, K.; Davies, C.A. New approaches to measuring biochar density and porosity. *Biomass Bioenergy* **2014**, *66*, 176–185, doi:10.1016/j.biombioe.2014.03.059.

55. Chrzazvez, J.; Théry-Parisot, I.; Fiorucci, G.; Terral, J.F.; Thibaut, B. Impact of post-depositional processes on charcoal fragmentation and archaeobotanical implications: Experimental approach combining charcoal analysis and biomechanics. *J. Archaeol. Sci.* **2014**, *44*, 30–42, doi:10.1016/j.jas.2014.01.006.

56. Zickler, G.A.; Schöberl, T.; Paris, O. Mechanical properties of pyrolysed wood: A nanoindentation study. *Philos. Mag.* **2006**, *86*, 1373–1386, doi:10.1080/14786430500431390.

57. Askeland, M.; Clarke, B.; Paz-Ferreiro, J. Comparative characterization of biochars produced at three selected pyrolysis temperatures from common woody and herbaceous waste streams. *PeerJ* **2019**, *7*, 1–20, doi:10.7717/peerj.6784.

58. Azargohar, R.; Jacobson, K.L.; Powell, E.E.; Dalai, A.K. Evaluation of properties of fast pyrolysis products obtained, from Canadian waste biomass. *J. Anal. Appl. Pyrolysis* **2013**, *104*, 330–340, doi:10.1016/j.jaap.2013.06.016.

59. Yeo, J.Y.; Chin, B.L.F.; Tan, J.K.; Loh, Y.S. Comparative studies on the pyrolysis of cellulose, hemicellulose, and lignin based on combined kinetics. *J. Energy Inst.* **2019**, *92*, 27–37, doi:10.1016/j.joei.2017.12.003.

60. Buss, W.; Mašek, O.; Graham, M.; Wüst, D. Inherent organic compounds in biochar-Their content, composition and potential toxic effects. *J. Environ. Manag.* **2015**, *156*, 150–157, doi:10.1016/j.jenvman.2015.03.035.

61. Videgain-Marco, M.; Marco-Montori, P.; Martí-Dalmau, C.; Jaizme-Vega, M.C.; Manyà-Cervelló, J.J.; García-Ramos, F.J. The Effects of Biochar on Indigenous Arbuscular Mycorrhizae Fungi from Agroenvironments. *Plants* **2021**, *10*, 950, https://doi.org/10.3390/plants10050950.

Capítulo 4. Effects of Biochar Application in a Sorghum Crop under Greenhouse Conditions: Growth Parameters and Physicochemical Fertility

María Videgain-Marco, Pedro Marco-Montori, Clara Martí-Dalmau, María del Carmen Jaizme-Vega, Joan Josep Manyà Cervelló and Francisco Javier García Ramos

Effects of Biochar Application in a Sorghum Crop under Greenhouse Conditions: Growth Parameters and Physicochemical Fertility

María Videgain-Marco [1,*], **Pedro Marco-Montori** [2], **Clara Martí-Dalmau** [1],
María del Carmen Jaizme-Vega [3], **Joan Josep Manyà-Cervelló** [4] and
Francisco Javier García-Ramos [1]

1   Departamento de Ciencias Agrarias y del Medio Natural, EPS, Universidad de Zaragoza, Carretera de Cuarte s/n, E-22071 Huesca, Spain; cmarti@unizar.es (C.M.-D.); fjavier@unizar.es (F.J.G.-R.)
2   Instituto Agroalimentario de Aragón—IA2 (CITA-Universidad de Zaragoza), Unidad de Recursos Forestales, Centro de Investigación y Tecnología Agroalimentaria del Gobierno de Aragón (CITA), Avenida Montañana 930, E-50059 Zaragoza, Spain; pmarcomo@cita-aragon.es
3   Departamento de Protección Vegetal, Instituto Canario de Investigaciones Agrarias (ICIA), Carretera de El Boquerón s/n, Valle Guerra, La Laguna, E-38270 Tenerife, Spain; mcjaizme@icia.es
4   Aragón Institute of Engineering Research (I3A), Biochar Research Lab, EPS, University of Zaragoza, Carretera de Cuarte s/n, E-22071 Huesca, Spain; joanjoma@unizar.es
*   Correspondence: mvidegain@unizar.es; Tel.: +34-974292656

Abstract: Application of biochar from vine shoots (*Vitis vinifera* L.) as an organic amendment in the soil is an alternative agricultural management of interest. The behavior of this type of amendment in the soil requires more information to adjust the pyrolysis conditions in order to obtain a high-quality biochar. The aim of this work is determining the influence of the application of this type of biochar on the soil-plant system. For this purpose, an agronomic test was performed in greenhouse pots. A randomized tri-factorial block design was adopted with the following factors: final pyrolysis temperature (400 and 600 °C), application rate (0 wt. % as a control, 1.5 and 3 wt. %) and texture of the growing media (sandy-loam and clay-loam origin). The selected crop was sorghum (*Sorghum bicolor* L. Moench), the development and production of which was evaluated during two complete growing cycles under greenhouse conditions. Application of biochar produced at 400 °C significantly increased plants roots dry weight in the sandy-loam growing substrate (52% compared to the control). Grain production was also significantly affected by biochar application, showing better results after addition of biochar produced at 400 °C. Water holding capacity and K, Ca, and Mg contents were enhanced by biochar addition, with evident effects of the application ratios for some of these variables. The effect on the pH of substrates in the sandy-loam texture was weak; however, a significant decrease was observed after the addition of biochar produced at 600 °C.

Keywords: carbon sequestration; organic amendment; pyrolysis; vineyard pruning; vine shoots

1. Introduction

One of the traditional ways to improve the energy efficiency of agricultural systems is to return to the soil part of the biomass produced by crops, which in many cases is removed from the field to be used for other purposes or even destroyed.

Returning crop waste into the soil, either without any processing or through organic amendments, represents a management strategy that, in addition to the improvement of energy efficiency for agroecosystems, may help to combat soil degradation phenomena. In Spain, almost 74% of the territory

is susceptible to desertification due to climatic reasons and human activity, among which agricultural management methods acquire relevant importance [1].

An alternative to returning biomass into the soil is the integration of biochar as an organic amendment in the crop production process. The term biochar can be defined as a carbonaceous material obtained from biomass by thermal decomposition at low or no oxygen concentration, through a thermochemical process known as pyrolysis [2]. There is also a scientific consensus that its specific application to soil is expected to sustainably sequester carbon and improve the soil functions [3,4].

A growing number of previous studies have emerged describing diverse aspects of biochar regarding its production, characterization, and application [5–9]. However, there is a broad spectrum of results when analyzing the biochar application effects on soil physical, chemical, and biological fertility. The degree of knowledge about the effect of biochar on the soil–plant–microorganisms system is very recent and the results already published are contradictory and dependent on the specificity of the experiment conducted [5,10–14].

Final properties of biochar (porosity, ash content, total fixed carbon content, available nutrients, etc.) depend on the pyrolysis operating conditions (e.g., temperature and pressure conditions, and residence time of the gas phase within the reactor), which also play a key role on the process performance [15–18]. Besides these conditions, it is necessary to consider the nature of selected feedstock (in terms of composition, moisture and granulometry) [18,19], which could also affect the pyrolysis process itself and the final behavior of resulting biochar in the soil. The differences in the physicochemical properties of biochars obtained from different precursors at different operating conditions can allow researchers to produce tailored products for specific purposes. In general, a higher lignin content is responsible for the development of a macroporous structure, whereas a relatively higher cellulose content yields a microporous one [20]. The final pore size distribution determines its hydraulic properties, the improvement of which has widely been reported in earlier studies for wood-derived biochar [21–23].

Biochar application as a soil amendment is motivated by its capacity to enhance crop yields and alter the soil physical and chemical properties, such as soil water holding capacity (WHC), pH, cation exchange capacity (CEC), nutrient retention, and organic carbon [22,24,25]. Nevertheless, this influence is strongly dependent on biochar final temperature production, particle size, soil texture and mineralogy [26,27]. In fact, the largest effects has been observed for acidic and sandy texture soils [28,29]. In addition, the biochar application rate (into the soil) is also an important factor, which can influence both the crop response and modification of soil parameters. In this regard, dose–response relationships have been reported as linear [30,31] and not linear [26,32–34], thus suggesting that many research efforts are needed to better clarify the influence of the biochar application rate.

Due to the high volume of vine shoots offered every year from vineyard winter pruning [35] as well as problems related to plant diseases derived from a direct application of theses residues into the soil [36], conversion of vine shoots into biochar and its subsequent application to the field (towards an improvement of soil quality) appears to be a sustainable and very attractive alternative.

Since relatively little information is available regarding the application of this type of biochar as an organic amendment [37–39], our study aims at achieving a wide understanding on the influence of different factors (such as the final pyrolysis temperature, biochar application rate, and soil texture) on the crop response variables. Outcomes from this kind of assessment studies will help researchers and agricultural advisors to make decisions concerning the viability of using biochar as a soil amendment in agricultural lands. To this aim, sorghum (*Sorghum bicolor* L. Moench) was selected as a test crop. A bioassay was conducted in pots under controlled greenhouse conditions. This work collects the information about the effects of biochar application on the crop growth parameters and some physicochemical properties of the soils studied. Previous studies [40,41] have reported positive responses of these variables to biochar addition in sorghum crop. Previous experience on the study of operating conditions for vine shoots slow pyrolysis process (at low temperatures in the range of 300–700 °C) [18,40,42,43] and other studies in the same line of research [36,44,45], have allowed us to develop this work in a logical way, starting from a properly characterized biochar.

2. Materials and Methods

2.1. Biomass Feedstock Collection and Characterization

Vine shoots (*Vitis vinifera* L.) were used as biochar precursor. They were collected during winter pruning in a winery located in the D.O. Somontano, northeast of Aragón (Aragón, Spain). The grape variety was Cabernet Sauvignon with two different rootstocks and in maximum production stage (average Ravaz index of 6).

The collected feedstock was stored in cardboard boxes to allow drying before processing. Vine shoots were selected by diameter (between 8.5 and 15 mm) and they were then cut using a domestic chipper into smaller pieces of 4–7 cm in length.

For a representative biomass sample, proximate analyses were performed following standardized procedures published by the American Society for Testing and Materials (ASTM) [46] (D3173 for moisture, D3174 for ashes, and D3175 for volatile matter), which are commonly used for coal and charcoal characterization. The moisture content was calculated from the mass loss at 105 °C. From the mass loss obtained at 950 °C under an O_2-free atmosphere, the content of volatile matter was estimated. The final mass obtained after heating the remaining biochar up to 750 °C in air led to the ash content. Finally, the fixed-carbon content was calculated by difference. Elemental analysis was also conducted using an elemental micro CHNS analyzer from LECO (St. Joseph, MI, USA). Ash composition was analyzed according to ASTM D4326-04 through X-ray fluorescence (XRF) using an ADVANT'XP + XRF spectrometer from Thermo ARL (Ecublens, Switzerland).

The contents of the main constituents of the biomass feedstock (lignin + silica, cellulose, carbohydrate + protein, and hemicellulose + acid soluble ash) were determined according to the Van Soest method [47]. Organic extractives were previously extracted using a mixture of ethanol and toluene (1:2 v/v) as solvent.

2.2. Biochar Production, Characterization, and Processing

Pyrolysis experiments were conducted in a fixed-bed laboratory reactor. It consisted of a cylindrical and vertical reactor (140 mm ID; 465 mm long) made of Sandvik 253 MA ^{TM} stainless steel (Demede, Madrid, Spain) and heated by two electric resistances of 2.1 kW with proportional integral derivative (PID) temperature control. A basket of 4 L, made of AISI 316 stainless steel wire mesh, was used to put the biomass into the reactor. The temperature inside of the bed was measured using four thermocouples placed in a thermowell at different heights. More details about the configuration of the reactor are available in previous publications [18,48]. A total of 13 experiments were carried out at two different final pyrolysis temperatures at atmospheric pressure. Approximately 500 g of vine shoots were heated at an average heating rate of 5 °C min^{-1} to the final temperature (400 and 600 °C) with a soaking time of 60 min at this temperature. The mass flow rate at standard temperature and pressure (STP) conditions of the carrier gas (N_2) was adjusted to keep a constant real flow rate of N_2 within the reactor (at the corresponding final temperature) of 1.8 L min^{-1}, which corresponds to a carrier gas residence time of 180 s. The particle size adopted resulted appropriate to improve the carbonization efficiency (i.e., higher fixed-carbon content in the resulting biochar) during pyrolysis process because of the enhancement of secondary charring reactions at an intra-particle level [18,39].

Proximate and elemental analyses were performed for each biochar following the standards specified above. In addition, biochar samples were sent to an external certified soils laboratory in order to analyze the several crop nutrients of biochar using an organic amendment as reference.

Due to the highly microporous structure of biochar, specific surface area (S_{BET}) and pore volumes (V_{total} and V_{ultra} for total micropores and narrow micropores or ultra-micropores, respectively) were determined from the CO_2 adsorption isotherms at 0 °C (using an ASAP 2020 gas sorption analyzer from Micromeritics, Norcross, GA, USA) and assuming a Density Functional Theory (DFT) model for slit-pore geometry [43].

The obtained biochars were mechanically processed through an automatic agitation system, which was specifically designed to reproduce product movement in a regular fertilizer spreader. A detailed scheme of the agitation system is shown in Figure S1 (Supplementary Material). Approximately 150 g of biochar were introduced into the agitation system, which was powered by a combined drill (BL 18V LXT 115 Nm, Makita, Madrid, Spain) at the main speed of 50 rpm for approximately 2 min. The resulting biochar (keeping the same particle size distribution than that obtained after agitation) was used for the agronomic test.

2.3. Phytotoxicity Test

Biochars were evaluated for phytotoxicity according to the test proposed by Zucconi et al. [49] and applied in similar studies by other authors [50]. The test was conducted for five different species: watercress (*Lepidium sativum*, L.), barley (*Hordeum vulgare* L.), lettuce (*Lactuca sativa* L.), basil (*Ocimum basilicum* L.) and sorghum (*Sorghum bicolor* L.).

A total of 20 seeds of each species were distributed in three-replicated Petri dishes with 5 mL of biochar extract (1:10) poured over sterile filter paper. All Petri dishes were incubated at 25 °C in the dark. After 72 h, root length was measured and the germination index (GI) was calculated as described below:

$$GI = (G/G_0) \times (L/L_0) \tag{1}$$

where G and G_0 are the germination percentages (G—biochar extract; G_0—distilled water—control) and L and L_0 are the mean of the root lengths of the samples and the control, respectively.

2.4. Selection and Sampling of Bioassay Soils

Soil texture was one of the factors considered evaluating the influence of biochar on the crop response. Soils under organic management with two contrasting textures (Soil 1 Calcisol—sandy-loam; Soil 2 Cambisol—clay-loam) were selected. A 10-point sampling from the top 30 cm was performed with an auger to obtain a representative soil sample. Samples were air-dried in the laboratory and sieved through a 2 mm mesh. A physicochemical analysis was performed. The following parameters were analyzed: pH (potenciometry), electrical conductivity (electrometry), oxidable organic matter (espectrofotometry), N (N-NO_3—espectrofotometry), P (Olsen—espectrofotometry), K and Mg (ammonium acetate extract buffered at pH 7) and water holding capacity (WHC—gravimetry—difference in water content between field capacity and permanent wilting point through Richards chamber). Table S1 reports detailed properties for both soils.

2.5. Bioassay Experimental Design

An agronomic experiment growing sorghum crop (*Sorghum bicolor* L. Moench) in pots was conducted under controlled greenhouse conditions. Both soil types were mixed with sterilized fine gravel (60:40 v/v) to avoid soil compaction in the containers forming two final mixtures to receive biochar incorporation. A randomized factorial block design was adopted with the following factors as independent variables:

- Factor 1: growing media texture (S1—substrate 1—sandy-loam growing media; S2—substrate 2—clay-loam growing media).
- Factor 2: final pyrolysis temperature (B1—biochar 1—400 °C; B2—biochar 2—600 °C).
- Factor 3: biochar application rate (D0—control—without biochar; D1—1.5 wt. %; D2—3 wt. %).

Five replicates were established for the 10 treatments: S1D0, S1B1D1, S1B1D2, S1B2D1, S1B2D2, S2D0, S2B1D1, S2B1D2, S2B2D1, S2B2D2; therefore, a total of 50 pots were filled with the mixtures and planted.

2.6. Bioassay Establishment and Development

Greenhouse bioassay was installed in November 2017. Polyethylene trays with twelve fillers of 650 cm^3 volume capacity, 18 cm deep, and 64 cm^2 of the upper surface, were used for carrying out the bioassay. The pots were filled with the growing substrate mixture (soil + fine gravel), and the corresponding amount of biochar was homogeneously added to each one.

Chemically untreated sorghum seeds were pre-germinated and previously sterilized in tempered bleach solution (1 vol. %) for 30 min. Three pre-germinated seeds per tray filler were placed and carefully watered for two months until a thinning was performed (maintaining one plant per tray filler).

Temperature and relative humidity control at the greenhouse were controlled through a temperature/humidity sensor HOBO Pro v2 (Onset, Bourne, MA, USA), allowing us to adjust the intervals and irrigation rates during the crop cycle, considering crop evapotranspiration (30 mL of water/irrigation interval). Leached water was collected and weighed in separate trays in order to adjust water needs to 70–80% of field capacity. Throughout the first four months of crop development, plants were watered only with water. At the end of the fourth month, all the plants began to present nutrient deficiency symptoms; therefore, a Hewitt nutritive solution with minimum phosphorus concentration (P^-) [51] was added to water them for the rest of the experiment (composition 1 L: 0.4044 g NO_3K; 0.9446 g $NO_3Ca \cdot 4H_2O$; 0.3697 g $SO_4Mg \cdot 7H_2O$; 0.027 g PO_4H_2K; 0.0421 g Na EDTA-Fe; 0.00223 g $SO_4Mn \cdot 4H_2O$; 0.00309 g BO_3H_3; 0.000288 g $SO_4Zn \cdot 2H_2O$, and 0.00025 g $SO_4Cu \cdot 5H_2O$). Greenhouse conditions enabled cushioning outside temperatures—in any case, the temperature range reached inside along the year was broad (from 2.6 °C minimum winter temperatures to 37.0 °C maximum summer temperatures).

The duration of the trial was 13 months, during which the crop completed two production cycles. Since sorghum is a crop with re-sprouting capacity, once the first cycle was completed (210 days after sowing—D_{210}), sorghum plants were cut about 2 cm from the growing substrate surface and re-sprouted to complete a new crop cycle (390 days after sowing—D_{390}).

2.7. Plant Measurements and Substrate Analysis

After completing both production cycles, all the plants were cut and the following measures were taken:

- Biological yield (by drying in an oven until weight stabilization at 70 °C): dry grain weight (when presence), shoot dry weight, and roots dry weight were differentiated. Data related to the root dry weight were only measured in the second harvest, when the trial was completely finished.
- Plants size: height from stem base to insertion point of flag leaf; stem diameter and flag leaf length (when presence).

In addition to the above parameters, growing substrates and leaf analyses were done once the trial was finished. The following parameters were analyzed:

- Growing substrates: primary and selected secondary nutrients, soil organic matter (SOM), cation exchange capacity (CEC–volumetric titration), water holding capacity (WHC). Leaves: elemental N, total P and K.

2.8. Statistical Analysis of Results

Final data were statistically analyzed using the IBM SPSS Statistics v.22 (IBM Corp., Armonk, NY, USA) software package by three-way ANOVA, where the effects of factors and their interactions were studied. Two-way ANOVA was conducted as a function of texture substrate when significant differences were detected for this factor. One-way ANOVA was adopted to analyze biochar effects on seed germination. Means comparisons were combined with Tukey's test with a significance level of 0.05. Contingency tables were adopted to analyze grain production.

3. Results and Discussion

3.1. Biomass and Biochar Properties

Results from proximate and elemental analyses are summarized in Table 1. As expected, these results were primarily dependent on pyrolysis operating conditions. Results from physicochemical analyses of produced biochars are reported in Table 2, from which it can be concluded that nutrient contents of produced biochars were mainly affected by the biomass feedstock.

Table 1. Proximate and elemental analyses of biochar produced at two different temperatures (400 °C—B400 and 600 °C—B600).

Proximate			Elemental (wt. % in daf [1] Basis) [2]		
	B400	**B600**		**B400**	**B600**
Ash (wt. % in dry basis)	6.45 ± 0.14	10.02 ± 0.81	C	71.50 ± 0.48	82.89 ± 0.33
			H	4.46 ± 0.19	1.95 ± 0.08
Moisture (wt. %)	0.57 ± 0.22	3.05 ± 0.34	N	1.58 ± 0.10	1.52 ± 0.01
			O	22.42 ± 0.77	13.63 ± 0.31
Volatile matter (wt. % in dry basis)	22.03 ± 0.01	2.39 ± 0.71	Surface area and pore volume		
			S_{bet} (m^2 g^{-1})	105.8	227.5
Fixed carbon (wt. % in dry basis)	70.88 ± 6.45	84.54 ± 1.32	V_{total} (cm^3 g^{-1})	0.0370	0.0819
			V_{ultra} (cm^3 g^{-1})	0.0361	0.0816

[1] Dry-ash-free. [2] Oxygen is calculated by difference.

Table 2. Physicochemical analyses of biochar produced at two different temperatures (400 °C—B400 and 600 °C—B600).

Physicochemical Analyses (Organic Amendment Reference)									
Principal Nutrients	**Method**	**Unit**	**Result**		**Secondary Nutrients**	**Method**	**Unit**	**Result**	
			B400	**B600**				**B400**	**B600**
N total Kjeldahl	MT-FER-001	wt %	1.40	1.20	Ca total (CaO)	ICP-OES	wt %	2.90	3.80
P total (P$_2$O$_5$)	VISIB. ULTR.	wt %	2.08	2.45	Mg total (MgO)	ICP-OES	wt %	0.68	0.79
K total (K$_2$O)	ICP-OES	wt %	1.70	2.10	Na total (Na$_2$O)	ICP-OES	mg kg^{-1}	850.00	540.00
Microel.	**Method**	**Unit**	**Result**		**Phys-Chem**	**Method**	**Unit**	**Result**	
			B400	**B600**				**B400**	**B600**
Fe total	ICP-OES	mg kg^{-1}	280	210	SOM [1]	Calcin.	wt %	86.40	85.40
Co total	ICP-OES	mg kg^{-1}	43	38	Apparent density		g (cm^3)$^{-1}$	0.33	0.40
Mn total	ICP-OES	mg kg^{-1}	100	102	WHC [2]	Gravim.	v %	14.16	18.35
Zn total	ICP-OES	mg kg^{-1}	145	135	pH (1:2.5)	Potenc.		8.6	8.57

[1] Soil Organic Matter. [2] Water holding capacity.

B600 had a higher fixed carbon and ash compared to B400, which conversely had a higher amount of volatile matter. The hydrogen, nitrogen, and oxygen fractions decreased with increasing pyrolysis final temperature. Both specific surface area (S_{bet}) and pore volume increased with rising pyrolysis final temperature, as a result of the removal of H and O during the enhanced devolatilization process, which resulted in more developed pore structures. The total pore volume increased with pyrolysis peak temperature.

Physicochemical analyses were carried out in the same way as any other organic amendment, in order to quantify the levels of available nutrients. Principal and secondary nutrient levels showed no major differences between B400 and B600 that would justify different application rates for the same crop.

It was interesting to analyze total N content in biochars, also taking into account the ammonia fraction instead of just the organic N. However, the biochar´s resistance against digestion with acids should be considered when analytical methods, such as total N Kjeldhal, are applied [9]. This explains

the results reported in Table 2 for N-total Kjeldhal, which are slightly lower than those reported in Table 1 for C organ found in elemental analyses, with increasing pyrolysis final temperature. Both B400 and B600 WHC was shown higher WHC than the other biochars during pyrolysis. In addition, both B400 and B600 showed higher values while high through WHC which could not be affected significantly (see Table Supplementary Table (S1)).

Particle size distribution of biochar after mechanical biochar processing are listed in Table 3.

Table 3. Average particle size distribution after mechanical biochar processing with automatic remover for the two pyrolysis temperatures (400 °C—B400 and 600 °C—B600).

Fraction	B400 (wt. %)	B600 (wt. %)
<2 mm	7	4
2 mm < x < 20 mm	24	19
20 mm < x < 40 mm	43	55
≥40 mm	26	22

The obtained mass fraction for particle sizes below 2 mm was very low. In addition, 69–77% of the biochar applied in field trials like this biochar had particle sizes ranging from 20 mm up to more than 40 mm. Smaller particle sizes were obtained, while this parameter has to be evaluated in the different effect of this parameter is evaluated [50]. It is relevant, it is needed for biochar which to determine the most appropriate particle size to apply to biochar as a soil solid before pyrolysis is needed for non-energy-intense pretreatment and grinding from agro-industrial biomasses, excluding the production of powder-like particles, which are difficult to apply in soil or implement as sorbent in soil analysis, and biomass components of vine shoots are summarized in Table S2 and Table S3 report the proximate, ultimate, and elemental, and compositions of vine shoots are summarized in Tables S2 and the Table S2: mass yields from pyrolysis experiments. As expected, the biochar average yields from pyrolysis experiments could be observed while the pyrolysis final temperature increased (B400—$y_{char} = 0.38$ and B600—$y_{char} = 0.29$).

3.2. Phytotoxicity Test

The germination index (GI) is an integrative measure of compounds of low toxicity (affecting root growth) and high toxicity (affecting germination) [50]. Table 4 shows the main GI values and standard deviation for the selected species. One-way analysis of variance evaluating the effect of biochar temperature on GI for this species did not detect significant differences ($p > 0.05$) between treatments. However, in agreement with Zucconi et al. [49], GI values between 50%–80% represent moderate phytotoxicity. Those below 50% represent high phytotoxicity. Values above GI 80% for both watercress and lettuce. On the other hand, GI values above 80% reveal a slight phytotoxicity and GI values slightly higher in B400 than in B600 treatment. Values between 80%–100% denote a lack of phytotoxicity. Therefore, negative effects of biochar were found on watercress and sorghum germination through this type of phytotoxicity test. According to Busch et al. [53], high ash content in biochar can cause negative effects due to salinity. It could explain some of the effects in the smaller seeds (watercress, lettuce and basil), which showed greater sensitivity to the higher B600 extract than the larger seeds. Biochar could also affect seed germination through other ways like direct contact or volatile elements [54]. However, the evaluation of these alternative ways is out of the scope of the present paper.

Table 4. Germination index and standard deviation for different species and two pyrolysis temperatures of biochar (400 °C—B400 and 600 °C—B600).

Specie	B400	B600
Watercress	92 ± 6	71 ± 5
Barley	89 ± 8	95 ± 8
Lettuce	111 ± 12	75 ± 8
Basil	109 ± 7	99 ± 9
Sorghum	85 ± 7	98 ± 5

Table 4. Germination index and standard deviation for different species and two pyrolysis temperatures of biochar (400 °C—B400 and 600 °C—B600).

Specie	B400	B600
Watercress	92 ± 6	71 ± 5
Barley	89 ± 8	95 ± 8
Lettuce	111 ± 8	75 ± 8
Basil	102 ± 12	99 ± 9
Sorghum	85 ± 7	98 ± 5

From the results obtained from a phytotoxicity test, it can be concluded that a preliminary washing step of biochar with water is not absolutely required. In other words, for the pyrolysis operating conditions adopted in this study, the organic compounds available on biochar surface did not inhibit germination of selected seeds.

3.3. Crop Response

3.3.1. First Crop Development Cycle

Results of the three-way ANOVA concerning the effect of growing substrate type, pyrolysis final temperature, and application rate on the growth parameters did not show statistically significant differences for the first crop cycle ($p > 0.05$). All the plants produced grain and no differences were observed for the total biomass generated. It should be pointed out, however, that we were unable to measure the root dry weights at this stage, since plants were re-sprouted to complete a new cycle.

Differences in crop growth and yield were reported in other studies when biochar was applied in short-term experiments [32,38,44,45]. Other studies based on biochar application on sorghum crop showed clear effects on crop growth under short-term trials [44]; in addition, vine-shoots derived biochar had an influence when it was applied to growing different crops in many studies [38]. In this sense, we have to emphasize that the larger biochar particles used here, in conjunction with the calcareous-like growing substrates, could limit biochar effects on this first crop stage. Furthermore, and according to Igalavithana et al. [24], for soils with organic matter and plant-available nutrients, the potential capacity of biochar to supply nutrients could not be ruled out. In this sense, nutrient deficiency symptoms observed in our experiment forced us to water the plants with a nutritive solution, which provided easily available nutrients for plants and which could mask the possible effect of supplying nutrients by biochar addition.

The main values and standard deviation of principal productive parameters measured at the final of the first completed crop cycle (D_{210}) are summarized in Table S4.

3.3.2. Second Crop Development Cycle

The results of the three-way ANOVA of plant dry weight data at the end of the second crop development cycle are shown in Table 5. Soil texture was the main factor that significantly affected the studied variables. At the same time, a significant influence of the biochar temperature and application rate on root weight was also observed. An additional effect of the application rate on plants' total weight, shoot weight, and root weight was also detected (see Figure 1).

Table 5. Three-way ANOVA results of the effect of growing substrate texture, biochar temperature and application rate on biomass dry weight of sorghum crop in pots experiment.

Factor	df	W_T	W_S	W_G	W_R
Growing substrate texture (S)	1	***	***	ns	*
Biochar temperature (B)	1	ns	ns	ns	*
Application rate (D)	1	*	*	ns	*
S × B	1	ns	ns	ns	*
S × D	1	ns	ns	ns	ns
B × D	1	ns	ns	ns	ns
S × B × D	1	ns	ns	ns	ns

* $p \leq 0.05$: *** $p \leq 0.001$; and ns = not significantly different. W_T: total dry weight; W_S: shoot dry weight; W_G: grain dry weight; W_R: root dry weight.
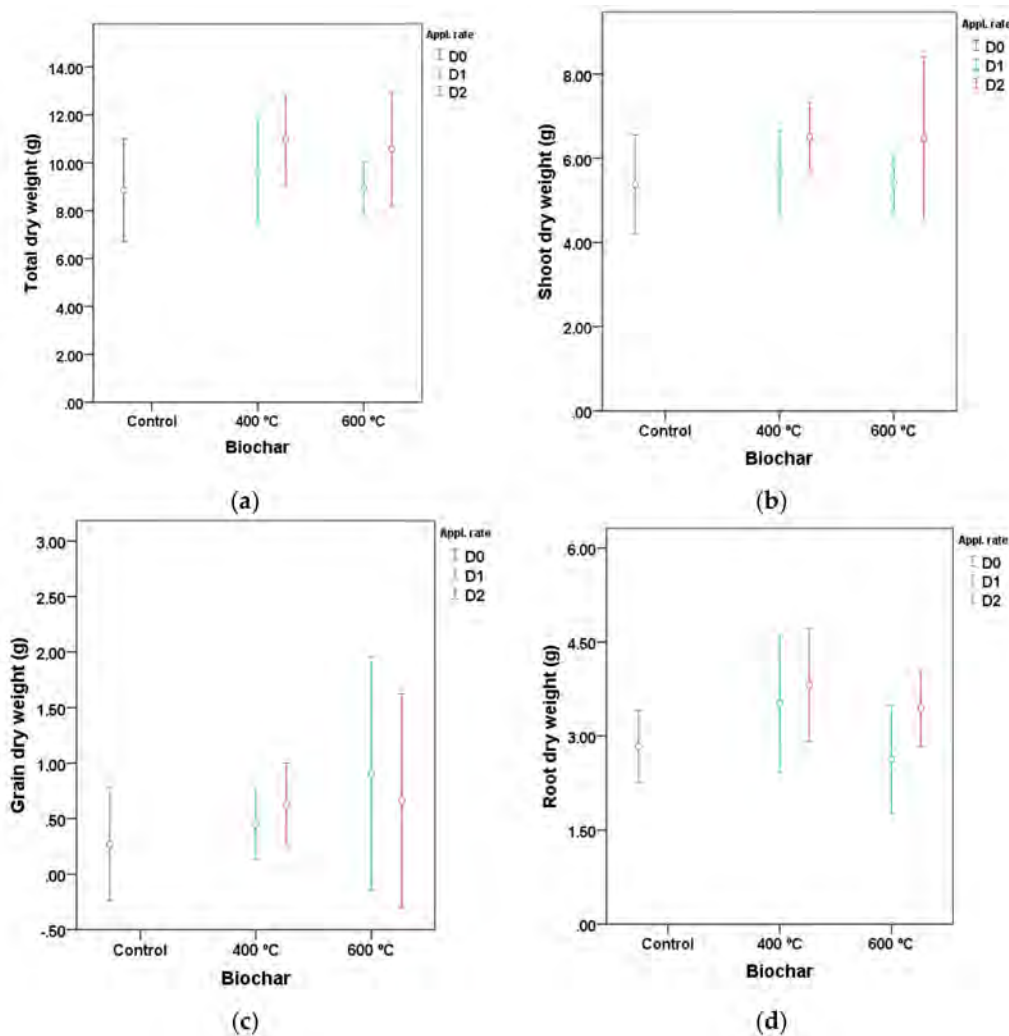
Figure 1. Main value and confidence interval at 95% of biomass dry weight on the second cycle of a sorghum crop under different application rates (0 wt. %—D0; 1.5 wt. %—D1; 3 wt. %—D2) of biochar at 400 °C and 600 °C. (**a**) total dry weight, (**b**) shoot dry weight, (**c**) grain dry weight, (**d**) root dry weight; average values between the sandy-loam growing substrate (S1) and the clay-loam growing substrate (S2).

The results of two-way ANOVA for different soil textures showed significant differences ($p < 0.05$) in root dry weight when sorghum – were growing in the sandy-loam substrate (S1) with the addition of the biochar produced at 400 °C (regardless of the application rate). These differences were found

between B400 and B600 treatments ($p < 0.0001$) and between B400 and Control treatments ($p = 0.002$). Root dry weight in B400 treatment increased by 52% compared to the Control treatment and by 57% compared to B600. This analysis did not show significant differences in the clay-loam growing substrate (S2). The main values of root dry weight in S1 are shown in Figure 2.
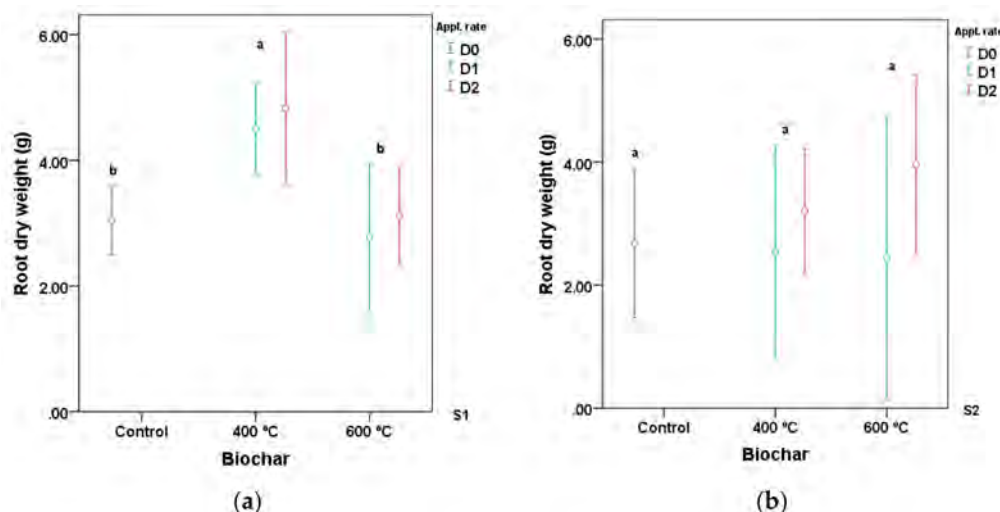

Figure 2. Main value and confidence interval at 95% of root dry weight on the second cycle of a sorghum crop under different application rates of biochar at 400 °C and 600 °C (**a**) total root dry weight in the growing substrate with the sandy-loam component—S1, (**b**) total root dry weight in clay-loam—S2. Different letters indicate significant differences ($p < 0.05$; Tukey's test).

Although no significant differences were found for grain dry weight, not all of the plants produced grain yield in this second harvest. Contingency tables showed a statistically significant relationship (Table 6) between the grain production and the three factors selected for this study. Based on these results, biochar produced at 400 °C could enhance crop productivity in sandy-loam soils.

Table 6. Summarized contingency tables for sorghum plants grain production (% plants) under different treatments (growing substrate S1: sandy-loam; growing substrate S2: clay-loam; B400—Biochar 400 °C; B600—biochar 600 °C; app. rate D1—1.5 wt. %; app. rate D2—3 wt. %).

Grain Production	Growing Substrate		Biochar			Application Rate	
	S1	S2	Control	B400	B600	D1	D2
Yes	86	57	22	88	65	76	25
No	14	43	78	12	35	24	75
χ^2	0.004		0.005			0.012	

In agreement with earlier results reported by Khaled and Schoenau [55] and Laghari et al. [44], the application of biochar produced at low temperature (B400) leads to higher biological yield compared to the control treatment and biochar produced at higher temperatures (B600) in a sandy-loam growing substrate. Olmo et al. [56], who worked with olive-tree pruning-derived biochar, found significant differences for biochar application in root morphology as a result of the effect on some nutrient availability and the subsequent fine root proliferation. Butnan et al. [26] reported that lower final temperatures of biochar (350 °C) showed higher benefits on crop development than the higher temperatures (800 °C) in two textured soils. Gale and Thomas [32] recently reported a high dose-dependence of biomass and physiological traits response. These works related crop yield enhancement to increased nutrient uptake. However, in the present study, there was no clear increase in nutrient uptake, as explained in the next section. According to these results, root morphology could be a parameter for assessing, since the study of root morphology would complement conclusions both

for physicochemical analyses and biological response in growing substrates. A not yet published study of root mycorrhization by arbuscular mycorrhizal fungi (AMF) in this experiment will complement the information reported in this study, in which AMF colonization was increased with B400 application. This parameter was highly correlated with root dry weight.

3.4. Growing Substrates Changes and Leaves' Nutrient Contents

A significant increase in WHC was observed by the addition of biochar ($p < 0.05$ between Control treatment and biochar amendment); the increase in WHC was observed for both studied substrates textures. There was also a significant influence of thepyrolysis final temperature on water retention, which increased by 3–6% with biochar temperature ($p \leq 0.05$ between B600 and B400; $p \leq 0.05$ between biochars and control treatment without biochar). Only in clay-loam substrate, WHC increased significantly ($p \leq 0.001$) with application rate. This behavior was also reported by Ali et al. [57] using biochar application rates of 25 and 50 Mg ha^{-1} of biochar. Figure 3 illustrates the behavior of each type of growing substrate. Numerous studies have demonstrated that biochar amendment improves WHC [3,57,58]; the present study reports a direct relationship between WHC and pyrolysis final temperature, which is directly correlated with WHC values already measured for individual biochar analyses (see Table 2). In agreement with Marshall et al. [39], who also reported a high hydrophobicity in vine shoots-derived biochar produced at 400 °C, it could be an important parameter to take into account, and not only the macroporous structure of biochar which could led to attribute higher WHC at lower pyrolysis peak temperatures. Accordingly, the dependence of this parameter on pyrolysis temperature is an aspect that could be of interest for agronomic contributions.
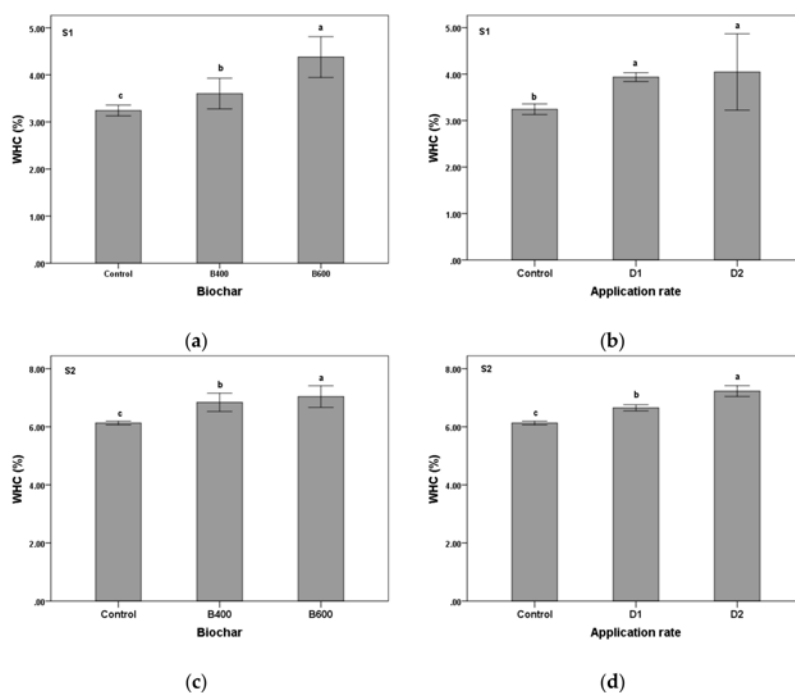

Figure 3. Main value and confidence interval at 95% of substrates water holding capacity (WHC) in two different texture of growing substrates, temperature of biochar applied (400 °C—B400 and 600 °C—B600) and application rate (D1: 1.5 wt. %; D2: 3 wt. %). (**a**) effect of final pyrolysis temperature of biochar applied on WHC in substrate with sandy-loam component—S1, (**b**) effect of biochar application rate on WHC in substrate with sandy-loam component—S1, (**c**) effect of final pyrolysis temperature of biochar applied on WHC in substrate with clay-loam component—S2, (**d**) effect of biochar application rate on WHC in substrate with clay-loam component—S2. Different letters indicate significant differences ($p < 0.05$; Tukey's test).

Differences in nutrient concentrations in growing media and leaves are deduced from Table 7. In the present experiment, biochar application had a significant influence (p < 0.05) on pH in the sandy-loam substrate, decreasing values over 0.1 points. The obtained results are in agreement with those by Liu and Zhang [59], who reported that biochar application decreased growing media pH in a sandy-loam texture. In their study, pH reduction was enhanced with an increasing biochar application rate and incubation time, related to the production of acidic materials from biochar oxidation.

Table 7. Nutrient concentrations in growing media and sorghum leaves, and water holding capacity (WHC) with different pyrolysis temperatures of biochar (400 °C—B400 and 600 °C—B600; S1: sandy-loam growing substrate; S2: clay-loam growing substrate).

Variable	S1			S2		
	Control	B400	B600	Control	B400	B600
pH	8.43 ± 0.14 a [2]	8.33 ± 0.15 ab	8.27 ± 0.06 b	ns [3]	ns	ns
K (mg kg^{-1})	297.0 ± 31.0 b	305 ± 8.9 b	358.5 ± 18.7 a	267.0 ± 51.0 c	369.8 ± 26.7 b	448.5 ± 61.6 a
Mg (mg kg^{-1})	ns	ns	ns	329.0 ± 3.0 b	371.2 ± 16.5 a	371.5 ± 21.9 a
Ca (mg kg^{-1})	4329.0 ± 253.0 a	3860.0 ± 142.5 b	4191.2 ± 253.3 a	6088.0 ± 123.0 b	6154.3 ± 173.2 a	5779.5 ± 281.7 b
K/Ca	0.068 ± 0.004 c	0.079 ± 0.003 b	0.086 ± 0.004 a	0.044 ± 0.009 c	0.060 ± 0.005 b	0.078 ± 0.014 a
K/Mg	1.338 ± 0.058 b	1.373 ± 0.036 b	1.519 ± 0.036 a	0.811 ± 0.150 c	0.996 ± 0.034 b	1.205 ± 0.124 a
K-leaf	ns	ns	ns	2.1 ± 0.2 b	2.4 ± 0.2 a	2.3 ± 0.2 a
WHC [1] (%)	3.24 ± 0.04 c	3.60 ± 0.32 b	4.37 ± 0.41 a	6.13 ± 0.03 c	6.84 ± 0.30 b	7.04 ± 0.35 a

[1] WHC: Water Holding Capacity. [2] For the same kind of growing substrate, means followed by different letter (within a row) are significantly different at $p < 0.05$ (Tukey's test). [3] ns = not significantly different at $p < 0.05$.

No differences were observed in total SOM or CEC between treatments (Tables S5 and S6). It could be explained by the large particle size of biochar adopted in this experiment. In this sense, when substrates' chemical analyses were carried out, particles of biochar were considered thick elements, and were separated from the analytical samples; the fine fraction able of interacting with clay and organic matter in the soil represented 4–7% of the total amount of biochar applied, which is a small addition to influence soil parameters.

Complete nutrient concentration data are given in Tables S5 and S6.

In contrast to other studies [14,43,46], the three-way ANOVA showed that the application of biochar did not significantly modify the cation exchange capacity, soil organic matter, total nitrogen concentration, and available phosphorus concentration. Significant differences ($p < 0.05$) were found for both types of textures in K and Ca concentrations. The content of available K was significantly related to the texture of the substrate ($p < 0.0001$). In addition, there was a positive interaction between texture growing media and application rate ($p = 0.006$), and between biochar and application rate ($p = 0.037$). Two-way ANOVA for a given texture showed that significant differences ($p < 0.05$) on K concentration in S1 are related to B600 addition but not to application rate. S2 showed significant differences ($p < 0.05$) for biochar addition and application rate in this texture. B600 application at 3 wt. % improved soil K content by 67% in comparison with control treatment (see Figure 4).
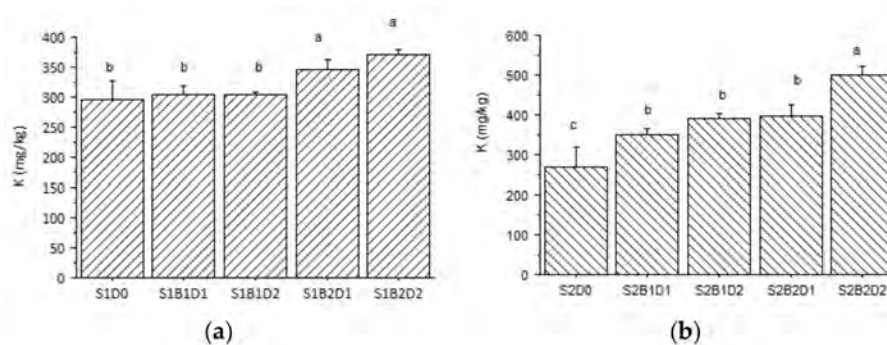
Figure 4. Main value and standard deviation of K concentration in two different growing media with a different application rate of biochar. (**a**) K concentration in the sandy-loam growing substrate—S1, (**b**) K concentration in the clay-loam substrate—S2; B1: biochar produced at 400 °C; B2: biochar produced at 600 °C; D1: 1.5 wt. %; D2: 3 wt. %). Different letters indicate significant differences ($p < 0.05$; Tukey's test).

K concentration in leaves also showed significant differences ($p < 0.005$) related to biochar application.

Positive interactions were found between the effect of texture growing media and biochar ($p < 0.0001$) and between texture and application rate ($p = 0.035$) on Ca concentrations. Analyzing each textural type individually, it was observed that significant differences ($p \leq 0.05$) in Ca concentration in S1 were related to B600 applied at the higher rate (3 wt. %). Different behavior was observed in S2, where significant differences ($p \leq 0.05$) in Ca concentration were observed for B400 application.

Biochar addition at higher doses had significant effects ($p < 0.0001$) on Mg concentration only in the clay-loam growing substrate, regardless of the pyrolysis final temperature ($p = 0.950$).

In both substrates, the K/Ca ratio used resulted in being extremely low because of the elevated Ca content, indicating the high difficulty of K absorption by plants. In general, this ratio ranges between 2–10, and the values obtained in this study vary from 0.044 to 0.089.

Significant differences were observed for this ratio between growing substrates ($p < 0.0001$), also between biochar temperatures ($p < 0.0001$) and between application rate ($p = 0.0002$). Biochar addition increases K/Ca for both textures of growing media in comparison with control treatment ($p < 0.05$), and K/Ca increases with application rate only in the clay-loam growing substrate ($p < 0.05$).

Another cation ratio related to soil and crop fertility is K/Mg. This ratio followed the same trend observed for the previous one. Three-way ANOVA showed significant differences derived from biochar application in both textures ($p < 0.0001$) except the application of B400 at lower doses in the sandy-loam substrate compared to control treatment, where no differences were detected. Otherwise, analyzing the effects in the clay-loam growing substrate treatments, an evident increment in K/Mg, was observed when both pyrolysis temperature and application rate were increased ($p = 0.0008$ between B2 and B1; $p = 0.025$ between S2 and S1).

According to earlier studies [54,59–61], biochar application has an evident influence on essential macronutrients' availability. Significant differences have been reported in this experiment for K, Ca, Mg, and their ratios. Incorporation of biochar as a soil amendment stimulates plant growth by increasing the availability of essential nutrients [22]. However, a nutritive solution was necessarily adopted in this experiment to maintain plants development and to supply nutrient deficiencies shown by the crop. Complementary field-scale experiments, where plants growth is not limited by pot dimensions and growing substrate mixture, are needed to confirm the results reported in this study.

4. Conclusions

Vine shoots represent an interesting resource for biochar production, due to their relative easily handling and slow pyrolysis processing, and the most important aspect, the appropriate physicochemical properties of resulting biochars. A moderate risk of phytotoxicity effects on seed

germination was determined (just one of the tested species exhibited low GI values for biochar produced at 600 °C). The effects of biochar application as an organic amendment, on these experimental conditions, were clearly dependent on the texture of the growing media analyzed. The highest effect on root development was found for the sandy-loam texture with biochar produced at 400 °C, regardless of the application rate. The physicochemical properties of substrates were more severely affected when the highest-temperature biochar was applied. However, further research should be required to optimize the particle size range and application rate of biochar, since an increasing trend in crop development was observed for both texture types when biochar was added at the highest addition rate.

Supplementary Materials: The following are available online at http://www.mdpi.com/2073-4395/10/1/104/s1, Figure S1: Scheme of the automatic remover used to process the biochar, Figure S2: Nutrients concentration, soil organic matter (MOT) and CEC (CICT) deviation of experimental treatments, under different temperatures of biochar and application rate, from control treatment in sandy-loam growing substrate, Figure S3: Nutrients concentration, soil organic matter (MOT) and CEC (CICT) deviation of experimental treatments, under different temperatures of biochar and application rate, from control treatment in clay-loam growing substrate, Table S1: Fertility analyses results of soils collected for the trial, Table S2: Proximate, elemental, X-Ray Fluorescence (XRF) analysis and biomass components of vine shoots, Table S3: Average value of pyrolysis product yield under two different temperature conditions, Table S4: Results from productive parameters at the final of the first completed sorghum cycle[1] under different biochar and application rates, Table S5: Nutrient concentrations both in sorghum leaves and growing media with different pyrolysis temperatures of biochar added, Table S6: Nutrient concentrations in sorghum leaves and growing substrate with different application rates of biochar.

References

1. Sanjuán, M.E.; del Barrio, G.; Ruiz, A.; Rojo, L.; Puigdefábregas, J.; Martínez, A. *Evaluación de la Desertificación en España: Mapa de la Condición de la Tierra 2000-2010*; Ministerio de Agricultura, Alimentación y Medio Ambiente: Madrid, Spain, 2010; p. 80.

2. Chica, A.; Artola, A.; Rosal, A.; Solé-Mauri, F.; Fernandez, F.; García, J.; Dios, M.; Díaz, M.; Ramón, G.; Font, X. De Residuo a Recurso, El camino hacia la Sostenibilidad. In *III. Recursos Orgánicos. Aspectos Agronómicos y Mediambientales. Cap. 8: Enmiendas Orgánicas y de Nueva Generación: Biochar y Otras Biomoléculas*; Red Española de Compostaje, Ed.; Mundi-Prensa: Madrid, Spain, 2015; p. 290.

3. Guo, M.; He, Z.; Uchimiya, S.M. Introduction to Biochar as an Agricultural and Environmental Amendment. In *Agricultural and Environmental Applications of Biochar: Advances and Barriers*; Guo, M., He, Z., Uchimiya, S.M., Eds.; Soil Science Society of America, Inc.: Madison, WI, USA, 2016; pp. 1–14.

4. Jeffery, S.; Verheijen, F.G.A.; Velde, M.; Van Der Bastos, A.C. Agriculture, Ecosystems and Environment A quantitative review of the effects of biochar application to soils on crop productivity using meta-analysis. *Agric. Ecosyst. Environ.* **2011**, *144*, 175–187. [CrossRef]

5. Paz-Ferreiro, J.; Méndez, A.; Gascó, G.; Guo, M.; He, Z.; Uchimiya, S.M. Application of Biochar for Soil Biological Improvement. In *Agricultural and Environmental Applications of Biochar: Advances and Barriers*; Guo, M., He, Z., Uchimiya, S.M., Eds.; Soil Science Society of America, Inc.: Madison, MA, USA, 2016; pp. 145–174.

6. Lal, R. Biochar and Soil Carbon Sequestration. In *Agricultural and Environmental Applications of Biochar: Advances and Barriers*; Guo, M., He, Z., Uchimiya, S.M., Eds.; Soil Science Society of America, Inc.: Madison, MA, USA, 2016; pp. 175–198.

7. Camps Arbestain, M.; Saggar, S.; Leifeld, J. Environmental benefits and risks of biochar application to soil. *Agric. Ecosyst. Environ.* **2014**, *191*, 1–167. [CrossRef]

8. Alburquerque, J.A.; Sánchez, M.E.; Mora, M.; Barrón, V. Slow pyrolysis of relevant biomasses in the Mediterranean basin. Part Char characterisation for carbon sequestration and agricultural uses. *J. Clean. Prod.* **2016**, *120*, 191–197. [CrossRef]

9. Steiner, C. Considerations in Biochar Characterization. In *Agricultural and Environmental Applications of Biochar: Advances and Barriers*; Guo, M., He, Z., Uchimiya, S.M., Eds.; Soil Science Society of America, Inc.: Madison, MA, USA, 2016; pp. 87–100.

10. Herath, H.M.S.K.; Camps-Arbestain, M.; Hedley, M. Effect of biochar on soil physical properties in two contrasting soils: An Alfisol and an Andisol. *Geoderma* **2013**, *209*, 188–197. [CrossRef]

11. Jeffery, S.; Meinders, M.B.J.; Stoof, C.R.; Bezemer, T.M.; van de Voorde, T.F.J.; Mommer, L.; van Groenigen, J.W. Biochar application does not improve the soil hydrological function of a sandy soil. *Geoderma* **2015**, *251*, 47–54. [CrossRef]

12. Xu, G.; Sun, J.N.; Shao, H.B.; Chang, S.X. Biochar had effects on phosphorus sorption and desorption in three soils with differing acidity. *Ecol. Eng.* **2014**, *62*, 54–60. [CrossRef]

13. Arif, M.; Ilyas, M.; Riaz, M.; Ali, K.; Shah, K.; Ul Haq, I.; Fahad, S. Biochar improves phosphorus use efficiency of organic-inorganic fertilizers, maize-wheat productivity and soil quality in a low fertility alkaline soil. *Field Crop. Res.* **2017**, *214*, 25–37. [CrossRef]

14. Gul, S.; Whalen, J.K.; Thomas, B.W.; Sachdeva, V.; Deng, H. Physico-chemical properties and microbial responses in biochar-amended soils: Mechanisms and future directions. *Agric. Ecosyst. Environ.* **2015**, *206*, 46–59. [CrossRef]

15. Méndez, A.; Terradillos, M.; Gascó, G. Physicochemical and agronomic properties of biochar from sewage sludge pyrolysed at different temperatures. *J. Anal. Appl. Pyrolysis* **2013**, *102*, 124–130. [CrossRef]

16. Enders, A.; Hanley, K.; Whitman, T.; Joseph, S.; Lehmann, J. Characterization of biochars to evaluate recalcitrance and agronomic performance. *Bioresour. Technol.* **2012**, *114*, 644–653. [CrossRef]

17. Manyà, J.J. Pyrolysis for biochar purposes: A review to establish current knowledge gaps and research needs. *Environ. Sci. Technol.* **2012**, *46*, 7939–7954. [CrossRef] [PubMed]

18. Manyà, J.J.; Azuara, M.; Manso, J.A. Biochar production through slow pyrolysis of different biomass materials: Seeking the best operating conditions. *Biomass Bioenergy* **2018**, *117*, 115–123. [CrossRef]

19. Zhao, B.; Connor, D.O.; Zhang, J.; Peng, T.; Shen, Z.; Tsang, D.C.W.; Hou, D. Effect of pyrolysis temperature, heating rate, and residence time on rapeseed stem derived biochar. *J. Clean. Prod.* **2018**, *174*, 977–987. [CrossRef]

20. Ioannidou, O.; Zabaniotou, A. Agricultural residues as precursors for activated carbon production-A review. *Renew. Sustain. Energy Rev.* **2007**, *11*, 1966–2005. [CrossRef]

21. Kavitha, B.; Reddy, P.V.L.; Kim, B.; Lee, S.S.; Pandey, S.K.; Kim, K.H. Benefits and limitations of biochar amendment in agricultural soils: A review. *J. Environ. Manag.* **2018**, *227*, 146–154. [CrossRef]

22. Al-Wabel, M.I.; Hussain, Q.; Usman, A.R.A.; Ahmad, M.; Abduljabbar, A.; Sallam, A.S.; Ok, Y.S. Impact of biochar properties on soil conditions and agricultural sustainability: A review. *Land Degrad. Dev.* **2018**, *29*, 2124–2161. [CrossRef]

23. Lei, O.; Zhang, R. Effects of biochars derived from different feedstocks and pyrolysis temperatures on soil physical and hydraulic properties. *J. Soils Sediments* **2013**, *13*, 1561–1572. [CrossRef]

24. Igalavithana, A.D.; Ok, Y.S.; Usman, A.R.A.; Al-wabel, M.I.; Oleszczuk, P.; Lee, S.S. The Effects of Biochar Amendment on Soil Fertility Could Biochar Be Used as a Fertilizer? In *Agricultural and Environmental Applications of Biochar: Advances and Barriers*; Guo, M., He, Z., Uchimiya, S.M., Eds.; Soil Science Society of America, Inc.: Madison, MA, USA, 2016; pp. 123–144.

25. Bohara, H.; Dodla, S.; Wang, J.J.; Darapuneni, M.; Acharya, B.S.; Magdi, S.; Pavuluri, K. Influence of poultry litter and biochar on soil water dynamics and nutrient leaching from a very fine sandy loam soil. *Soil Tillage Res.* **2019**, *189*, 44–51. [CrossRef]

26. Butnan, S.; Deenik, J.L.; Toomsan, B.; Antal, M.J.; Vityakon, P. Biochar characteristics and application rates affecting corn growth and properties of soils contrasting in texture and mineralogy. *Geoderma* **2015**, *237*, 105–116. [CrossRef]

27. Guo, M. Pyrogenic Carbon in Terra Preta Soils. In *Agricultural and Environmental Applications of Biochar: Advances and Barriers*; Guo, M., He, Z., Uchiyama, S.M., Eds.; Soil Science Society of America, Inc.: Madison, MA, USA, 2016; pp. 18–28.

28. Bi, Y.; Cai, S.; Wang, Y.; Xia, Y.; Zhao, X.; Wang, S.; Xing, G. Assessing the viability of soil successive straw biochar amendment based on a five-year column trial with six different soils: Views from crop production, carbon sequestration and net ecosystem economic benefits. *J. Environ. Manag.* **2019**, *245*, 173–186. [CrossRef]

29. Liu, X.; Zhang, A.; Ji, C.; Joseph, S.; Bian, R.; Li, L.; Pan, G.; Paz-Ferreiro, J. Biochar's effect on crop productivity and the dependence on experimental conditions—A meta-analysis of literature data. *Plant Soil* **2013**, *373*, 583–594. [CrossRef]

30. Tanure, M.M.C.; da Costa, L.M.; Huiz, H.A.; Fernandes, R.B.A.; Cecon, P.R.; Pereira Junior, J.D.; da Luz, J.M.R. Soil water retention, physiological characteristics, and growth of maize plants in response to biochar application to soil. *Soil Tillage Res.* **2019**, *192*, 164–173. [CrossRef]

31. Laird, D.A.; Fleming, P.; Davis, D.D.; Horton, R.; Wang, B.; Karlen, D.L. Impact of biochar amendments on the quality of a typical Midwestern agricultural soil. *Geoderma* **2010**, *158*, 443–449. [CrossRef]

32. Gale, N.V.; Thomas, S.C. Dose-dependence of growth and ecophysiological responses of plants to biochar. *Sci. Total Environ.* **2019**, *658*, 1344–1354. [CrossRef] [PubMed]

33. Sun, C.X.; Chen, X.; Cao, M.M.; Li, M.Q.; Zhang, Y.L. Growth and metabolic responses of maize roots to straw biochar application at different rates. *Plant Soil* **2017**, *416*, 487–502. [CrossRef]

34. Wrobel-Tobiszewska, A.; Boersma, M.; Sargison, J.; Adams, P.; Singh, B.; Franks, S.; Birch, C.J.; Close, D.C. Nutrient changes in potting mix and Eucalyptus nitens leaf tissue under macadamia biochar amendments. *J. For. Res.* **2018**, *29*, 383–393. [CrossRef]

35. Peralbo-Molina, Á.; Luque deCastro, M.D. Potential of residues from the Mediterranean agriculture and agrifood industry. *Trends Food Sci. Technol.* **2013**, *32*, 16–24. [CrossRef]

36. Duca, D.; Toscano, G.; Pizzi, A.; Rossini, G.; Fabrizi, S.; Lucesoli, G.; Servili, A.; Mancini, V.; Romanazzi, G.; Mengarelli, C. Evaluation of the characteristics of vineyard pruning residues for energy applications: Effect of different copper-based treatments. *J. Agric. Eng.* **2016**, *47*, 22–27. [CrossRef]

37. Ronga, D.; Francia, E.; Allesina, G.; Pedrazzi, S.; Zaccardelli, M.; Pane, C.; Tava, A.; Bignami, C. Valorization of Vineyard By-Products to Obtain Composted Digestate and Biochar Suitable for Nursery Grapevine (*Vitis vinifera* L.) Production. *Agronomy* **2019**, *9*, 420. [CrossRef]

38. Kloss, S.; Zehetner, F.; Wimmer, B.; Buecker, J.; Rempt, F.; Soja, G. Biochar application to temperate soils: Effects on soil fertility and crop growth under greenhouse conditions. *J. Plant Nutr. Soil Sci.* **2014**, *177*, 3–15. [CrossRef]

39. Marshall, J.; Muhlack, R.; Morton, B.J.; Dunnigan, L.; Chittleborough, D.; Kwong, C.W. Pyrolysis Temperature Effects on Biochar–Water Interactions and Application for Improved Water Holding Capacity in Vineyard Soils. *Soil Syst.* **2019**, *3*, 27. [CrossRef]

40. Manyà, J.J.; Ortigosa, M.A.; Laguarta, S.; Manso, J.A. Experimental study on the effect of pyrolysis pressure, peak temperature, and particle size on the potential stability of vine shoots-derived biochar. *Fuel* **2014**, *133*, 163–172. [CrossRef]

41. Rosas, J.G.; Gómez, N.; Cara, J.; Ubalde, J.; Sort, X.; Sánchez, M.E. Assessment of sustainable biochar production for carbon abatement from vineyard residues. *J. Anal. Appl. Pyrolysis* **2015**, *113*, 239–247. [CrossRef]

42. Azuara, M.; Sáiz, E.; Manso, J.A.; García-Ramos, F.J.; Manyà, J.J. Study on the effects of using a carbon dioxide atmosphere on the properties of vine shoots-derived biochar. *J. Anal. Appl. Pyrolysis* **2017**, *124*, 719–725. [CrossRef]

43. Manyà, J.J.; González, B.; Azuara, M.; Arner, G. Ultra-microporous adsorbents prepared from vine shoots-derived biochar with high CO_2 uptake and CO_2/N_2 selectivity. *Chem. Eng. J.* **2018**, *345*, 631–639. [CrossRef]

44. Laghari, M.; Mirjat, M.S.; Hu, Z.; Fazal, S.; Xiao, B.; Hu, M.; Chen, Z.; Guo, D. Effects of biochar application rate on sandy desert soil properties and sorghum growth. *Catena* **2015**, *135*, 313–320. [CrossRef]

45. Mohamed, W.; Hammam, A. Poultry manure-derived biochar as a soil amendment and fertilizer for sandy soils under arid conditions. *Egypt. J. Soil Sci.* **2019**, *59*, 1–14. [CrossRef]

46. ASTM International. *American Standard of Testing Material: Standard Test Method for Chemical Analysis of Wood Charcoal*; ASTM: West Conshohocken, PA, USA, 2001.

47. Van Soest, P.J.; Robertson, J.B.; Lewis, B.A. Methods for Dietary Fiber, Neutral Detergent Fiber, and Nonstarch Polysaccharides in Relation to Animal Nutrition. *J. Dairy Sci.* **1991**, *74*, 3583–3597. [CrossRef]

48. Greco, G.; Videgain, M.; Di Stasi, C.; González, B.; Manyà, J.J. Evolution of the mass-loss rate during atmospheric and pressurized slow pyrolysis of wheat straw in a bench-scale reactor. *J. Anal. Appl. Pyrolysis* **2018**, *136*, 18–26. [CrossRef]

49. Zucconi, F.; Pera, A.; Forte, M.; De Bertoldi, M. Evaluating toxicity of immatre compost. *Biocycle* **1981**, *22*, 54–57.

50. Liang, C.; Gascó, G.; Fu, S.; Méndez, A.; Paz-Ferreiro, J. Biochar from pruning residues as a soil amendment: Effects of pyrolysis temperature and particle size. *Soil Tillage Res.* **2016**, *164*, 3–10. [CrossRef]

51. Hewitt, E.J. *the Technical communication 22 (2nd revised edittion)*; Commonwealth Agricultural Bureaux, Farnham Royal: Bucks, UK, 1969; p. 547.

52. He, P.; Liu, Y.; Shao, L.; Zhang, H.; Lü, F. Particle size dependence of the physicochemical properties of biochar. *Chemosphere* **2018**, *212*, 385–392. [CrossRef] [PubMed]

53. Busch, D.; Kammann, C.; Grünhage, L.; Müller, C. Simple Biotoxicity Tests for Evaluation of Carbonaceous Soil Additives: Establishment and Reproducibility of Four Test Procedures. *J. Environ. Qual.* **2012**, *41*, 1023–1032. [CrossRef]

54. Buss, W.; Mašek, O. Mobile organic compounds in biochar—A potential source ofcontamination—Phytotoxic effects on cress seed (Lepidiumsativum) germination. *J. Environ. Manag.* **2014**, *137*, 111–119. [CrossRef]

55. Alotaibi, K.D.; Schoenau, J.J. Addition of biochar to a sandy desert soil: Effect on crop growth, water retention and selected properties. *Agronomy* **2019**, *9*, 327. [CrossRef]

56. Olmo, M.; Villar, R.; Salazar, P.; Alburquerque, J.A. Changes in soil nutrient availability explain biochar's impact on wheat root development. *Plant Soil* **2016**, *399*, 333–343. [CrossRef]

57. Ali, K.; Wang, X.; Riaz, M.; Islam, B.; Khan, Z.H.; Shah, F.; Munsif, F.; Ijaz Ul Haq, S. Biochar: An eco-friendly approach to improve wheat yield and associated soil properties on sustainable basis. *Pakistan J. Bot.* **2019**, *51*, 1255–1261. [CrossRef]

58. Sun, Y.; Gao, B.; Yao, Y.; Fang, J.; Zhang, M.; Zhou, Y.; Chen, H.; Yang, L. Effects of feedstock type, production method, and pyrolysis temperature on biochar and hydrochar properties. *Chem. Eng. J.* **2014**, *240*, 574–578. [CrossRef]

59. Liu, X.H.; Zhang, X.C. Effect of biochar on ph of alkaline soils in the Loess Plateau: Results from incubation experiments. *Int. J. Agric. Biol.* **2012**, *14*, 745–750.

60. Lehmann, J.; Da Silva, J.P.; Steiner, C.; Nehls, T.; Zech, W.; Glaser, B. Nutrient availability and leaching in an archaeological Anthrosol and a Ferralsol of the Central Amazon basin: Fertilizer, manure and charcoal amendments. *Plant Soil* **2003**, *249*, 343–357. [CrossRef]

61. Hailegnaw, N.S.; Mercl, F.; Pračke, K.; Száková, J.; Tlustoš, P. Mutual relationships of biochar and soil pH, CEC, and exchangeable base cations in a model laboratory experiment. *J. Soils Sediments* **2019**, *19*, 2405–2416. [CrossRef]
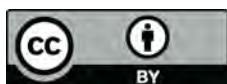
Effects of Biochar Application in a Sorghum Crop under Greenhouse Conditions: Growth Parameters and Physicochemical Fertility

María Videgain-Marco, Pedro Marco-Montori, Clara Martí-Dalmau, María del Carmen Jaizme-Vega, Joan Josep Manyà-Cervelló and Francisco Javier García-Ramos
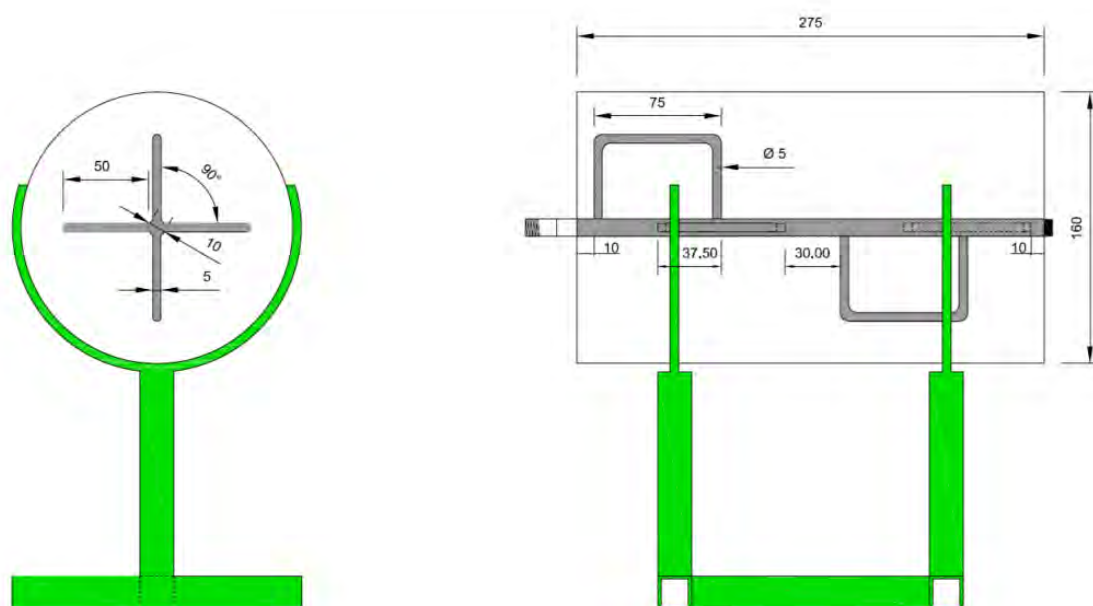
SUPPORTING INFORMATION

Figure S1. Scheme of the automatic remover used to process the biochar. Units: mm.

Table S1. Fertility analyses results of soils collected for the trial

Determination	Method	Unit	Soil 1	Soil 2
pH (1 : 2.5 water)	Potenciometry		8.0 ± 0.5	8.4 ± 0.5
Electrical conductivity (1 : 5)	Electrometry	dS m^{-1}	0.20 ± 0.03	0.20 ± 0.03
Oxidable organic matter	Espectrofotometry	wt. %	3.04 ± 0.38	1.70 ± 0.21
N (N-NO$_3$)	Espectrofotometry	mg kg^{-1}	59 ± 8	12 ± 2
P (Olsen)	Espectrofotometry	mg kg^{-1}	32 ± 3	29 ± 3
K	AAS	mg kg^{-1}	232 ± 39	88 ± 15
Mg	AAS	mg kg^{-1}	160 ± 33	252 ± 52
Water holding capacity	Gravimetry – Richards chamber	v %	5.41	10.22

Table S2. Proximate, elemental, X-Ray Fluorescence (XRF) analysis and biomass components of vine shoots

Proximate		Elemental (wt. % in daf[1] basis)[2]		Biomass components (wt. %)	
Ash (wt. % in dry basis)	2,46 ± 0,37	C	42,29 ± 0,49	Lignin + silica	20.16 ± 0.49
Moisture (wt. %)	10,47 ± 0,13	H	5,24 ± 0,06	Cellulose	34.18 ± 1.95
Volatile matter (wt. % in dry basis)	72,93 ± 1,64	N	13,52 ± 0,35	Carbohydrate + protein	33.02 ± 0.18
Fixed carbon (wt. % in dry basis)	14,14 ± 1,38	O	38,96 ± 0,45	Hemicellulose + acid soluble ash	8.10 ± 1.63
				Extractives	4.54 ± 0.05
Inorganic matter (wt. % of ash)					
CaO	58,30	PbO	0,26	MgO	6,66
K_2O	18,40	SnO_2	0,26	TiO_2	0,34
SiO_2	5,73	CuO	0,09	Cl	0,47
Fe_2O_3	3,51	MnO	0,53	SO_3	0,60
Al_2O_3	2,57	ZnO	0,33	P_2O_5	1,24

[1] Dry-ash-free.

[2] Oxigen is calculated by difference.

Table S3. Average value of pyrolysis product yield under two different temperature conditions (400 °C — B400 and 600 °C — B600)

Biochar	Number of experiments	Pyrolysis temperature (°C)	Total amount of feedstock (g)	Total amount of biochar (g)	Average product yield (y_{char})
B400	5	400	2.536,52	959,63	0,38
B600	8	600	4.083,69	1.206,74	0,29

Table S4. Results from productive parameters at the final of the first completed sorghum cycle[1] under different biochar and application rates (S1: substrate 1 sandy-loam; S2: substrate 2 clay-loam; B1: biochar 400 °C; B2: biochar 600 °C; D: biochar application rate, D0—0 wt. %, D1—1.5 wt. %, D2—3 wt. %)

Treatment	Plant length (cm)	Flag leaf length (cm)	Stem diameter (cm)	Dry aerial weight (g)	Grain dry weight (g)
S1D0	39.7 ±1.6	27.0 ± 5.0	0.9 ± 0.2	8.1 ± 1.2	1.9 ± 1.3
S1B1D1	37.4 ± 2.1	20.6 ± 3.6	0.9 ± 0.6	6.7 ± 0.7	1.8 ± 1.6
S1B1D2	40.1 ± 3.8	21.1 ± 3.2	1.0 ± 0.3	8.1 ± 0.7	1.5 ± 0.9
S1B2D1	37.8 ± 3.0	19.9 ± 5.6	0.8 ± 0.5	7.9 ± 0.6	1.7 ± 1.2
S1B2D2	39.5 ± 5.0	19.7 ± 3.3	1.0 ± 0.4	7.1 ± 2.4	1.9 ± 1.0
S2D0	35.2 ± 2.9	17.1 ± 3.5	1.0 ± 0.6	5.8 ± 0.5	1.6 ± 0.6
S2B1D1	32.8 ± 3.8	17.6 ± 2.6	0.9 ± 0.8	5.4 ± 0.9	1.3 ± 0.8
S2B1D2	34.3 ± 0.9	19.4 ± 2.6	1.0 ± 0.2	8.1 ± 0.7	1.5 ± 1.1
S2B2D1	36.2 ± 2.8	21.0 ± 4.3	1.0 ± 0.6	5.5 ± 0.8	1.7 ± 0.3
S2B2D2	34.8 ± 5.1	19.5 ± 5.2	1.0 ± 0.8	5.5 ± 1.7	1.5 ± 0.4

Table S5. Nutrient concentrations both in sorghum leaves and growing media with different pyrolysis temperatures of biochar added (400°C — B400 and 600 °C — B600; S1: sandy-loam growing substrate; S2: clay-loam growing substrate)

Variable	S1			S2		
	Control	B400	B600	Control	B400	B600
pH	8.43 ± 0.14**a**	8.33 ± 0.15**ab**	8.27 ± 0.06**c**	8.09 ± 0.03a	8.09 ± 0.06a	8.21 ± 0.11a
CEC (cmol kg^{-1})	5.4 ± 0.6a	6.0 ± 0.3a	5.8 ± 0.2a	9.4 ± 0.2a	9.3 ± 0.5a	7.9 ± 2.1a
N-nitric (mg kg^{-1})	63.5 ± 11.4a	56.8 ± 4.7a	69.4 ± 13.7a	77.2 ± 5.5a	82.05 ± 9.0a	69.6 ± 10.5a
P (mg kg^{-1})	3.8 ±0.7a	4.12 ± 0.4a	4.0 ± 0.5a	2.0 ± 0.2a	2.4 ± 0.4a	2.2 ± 0.3a
K (mg kg^{-1})	297.0 ± 31.0**b**	305 ± 8.9**b**	358.5 ± 18.7**a**	267.0 ± 51.0**c**	369.8 ± 26.7**b**	448.5 ± 61.6**a**
Mg (mg kg^{-1})	221.0 ± 15.0a	222.2 ± 5.6a	236.2 ± 15.0a	329.0 ± 3.0**b**	371.2 ± 16.5**a**	371.5 ± 21.9**a**
Ca (mg kg^{-1})	4329.0 ± 253.0**a**	3860.0 ± 142.5**b**	4191.2 ± 253.3**a**	6088.0 ± 123.0**b**	6154.3 ± 173.2**a**	5779.5 ± 281.7**b**
K/Ca	0.068 ± 0.004**c**	0.079 ± 0.003**b**	0.086 ± 0.004**a**	0.044 ± 0.009**c**	0.060 ± 0.005**b**	0.078 ± 0.014**a**
K/Mg	1.338 ± 0.058**b**	1.373 ± 0.036**b**	1.519 ± 0.036**a**	0.811 ± 0.150**c**	0.996 ± 0.036**b**	1.205 ± 0.124**a**
Na (mg kg^{-1})	30.0 ± 4.0**a**	27.5 ± 1.5**ab**	24.2 ± 2.3**b**	42.0 ± 7.0a	38.0 ± 3.0a	42.7 ± 14.2a
SOM (%)	2.1 ± 0.2a	2.1 ± 0.1a	2.0 ± 0.2a	1.4 ± 0.1a	1.4 ± 0.3a	1.3 ± 0.1a
P$_{total}$ (mg kg^{-1})	546.0 ± 10.0a	578.2 ± 89.1a	592.5 ± 64.1a	566.0 ± 21.0**b**	514.8 ± 14.4**a**	569.8 ± 24.1**b**
N-leaf	1.13 ± 0.1a	1.19 ± 0.1a	1.1 ± 0.2a	1.06 ± 0.2a	1.1 ± 0.1a	1.2 ± 0.2a
P-leaf	0.03 ± 0.01a	0.04 ± 0.01a	0.06 ± 0.01a	0.04 ± 0.01a	0.04 ± 0.01a	0.04 ± 0.01a
K-leaf	2.5 ± 0.5a	2.2 ± 0.6a	2.6 ± 0.3a	2.1 ± 0.2**b**	2.4 ± 0.2**a**	2.3 ± 0.2**a**

For the same kind of growing substrate, means followed by the same letter (within a row)are not significantly different at p ≤ 0.05 (Tukey´s test).

Table S6. Nutrient concentrations in sorghum leaves and growing substrate with different application rates of biochar (400°C — B400 and 600 °C — B600; D1: 1.5 wt. %; D2: 3 wt. %)

Variable	S1		S2	
	D1	D2	D1	D2
pH	8.36 ± 0.13a	8.25 ± 0.07a	8.13 ± 0.07a	8.17 ± 0.114a
CEC (cmol kg^{-1})	5.7 ± 0.3a	6.0 ± 0.2a	8.7 ± 1.8a	8.5 ± 1.7a
N-nitric (mg kg^{-1})	59.25 ± 13.8a	66.9 ± 8.8a	75.6 ± 15.5a	76.0 ± 6.7a
P (mg kg^{-1})	4.1 ± 0.3a	4.0 ± 0.5a	2.2 ± 0.3a	2.5 ± 0.3a
K (mg kg^{-1})	325.2 ± 26.0a	338.3 ± 36.9a	372.5 ± 33.6**b**	445.8 ± 62.1**a**
Mg (mg kg^{-1})	222.8 ± 13.3a	235.5 ± 10.1a	335.7 ± 9.1**b**	387.0 ± 8.8**a**
Ca (mg kg^{-1})	3990.7 ± 152.7a	4060.5 ± 352.2a	6099.8 ± 271.3a	5834.0 ± 278.7a
K/Ca	0.082 ± 0.006a	0.083 ± 0.003a	0.061 ± 0.008**b**	0.077 ± 1.153**a**
K/Mg	1.459 ± 0.076a	1.433 ± 0.096a	1.048 ± 0.096**a**	0.014 ± 0.165**a**
Na (mg kg^{-1})	25.0 ± 2.7a	26.7 ± 2.3a	43.7 ± 13.8a	37.0 ± 3.0a
SOM (%)	2.0 ± 0.2a	2.1 ± 0.1a	1.3 ± 0.2a	1.5 ± 0.1a
P$_{total}$ (mg kg^{-1})	610.7 ± 91.4a	560.0 ± 47.8a	533.5 ± 27.9a	551.2 ± 40.5a
N-leaf	1.1 ± 0.1a	1.1 ± 0.2a	1.1 ± 0.2a	1.1 ± 0.1a
P-leaf	0.03 ± 0.01a	0.04 ± 0.01a	0.04 ± 0.01a	0.04 ± 0.01a
K-leaf	2.7 ± 0.3a	2.7 ± 0.2a	2.3 ± 0.2a	2.3 ± 0.1a

Means within a row followed by the same letter are not significantly different por the same kind of growing substrate at p ≤ 0.05 (Tukey´s test).
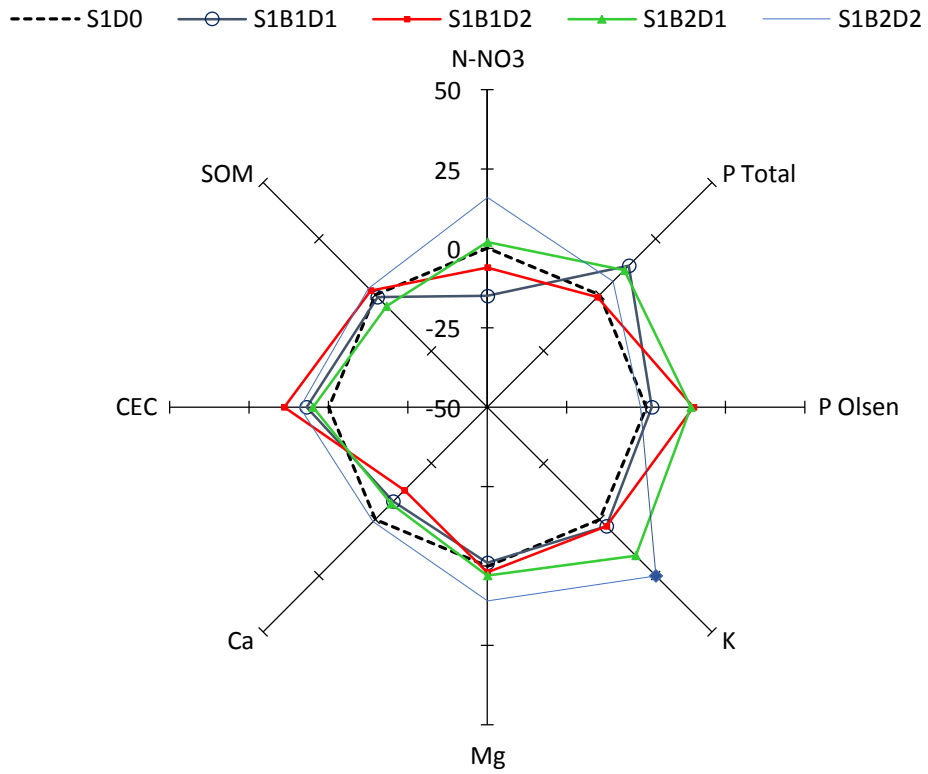
Figure S2. Nutrients concentration, SOM and CEC deviation of experimental treatments, under different temperatures of biochar (400°C — B400 and 600 °C — B600) and application rate (D1: 1.5 wt. %; D2: 3 wt. %), from control treatment (D0) in a sandy-loam growing substrate
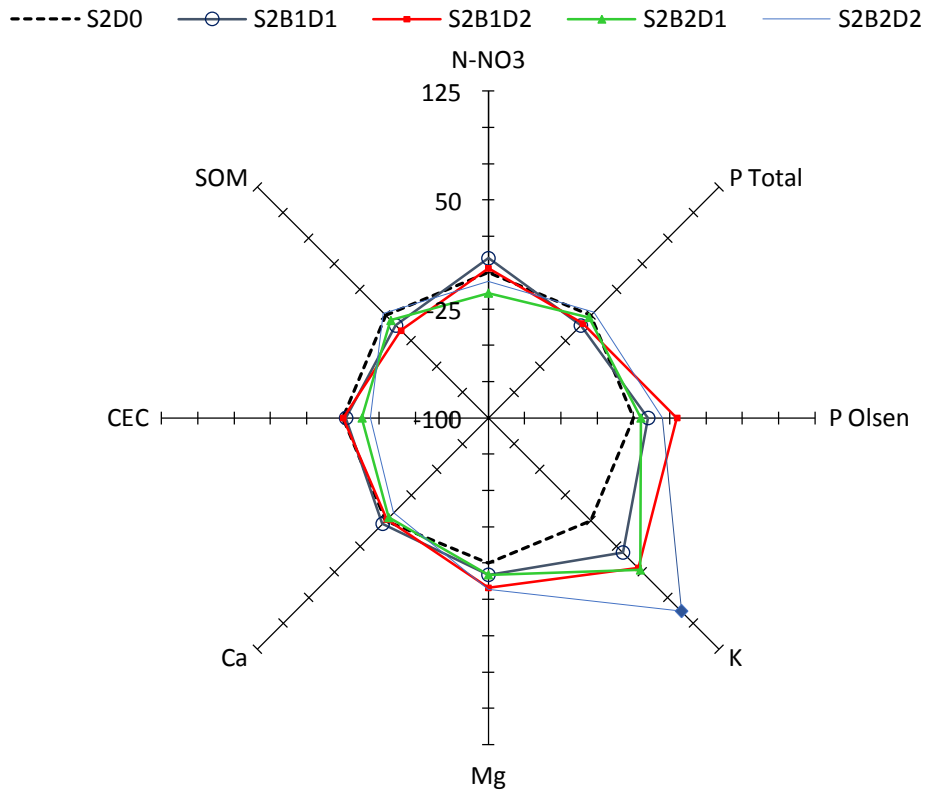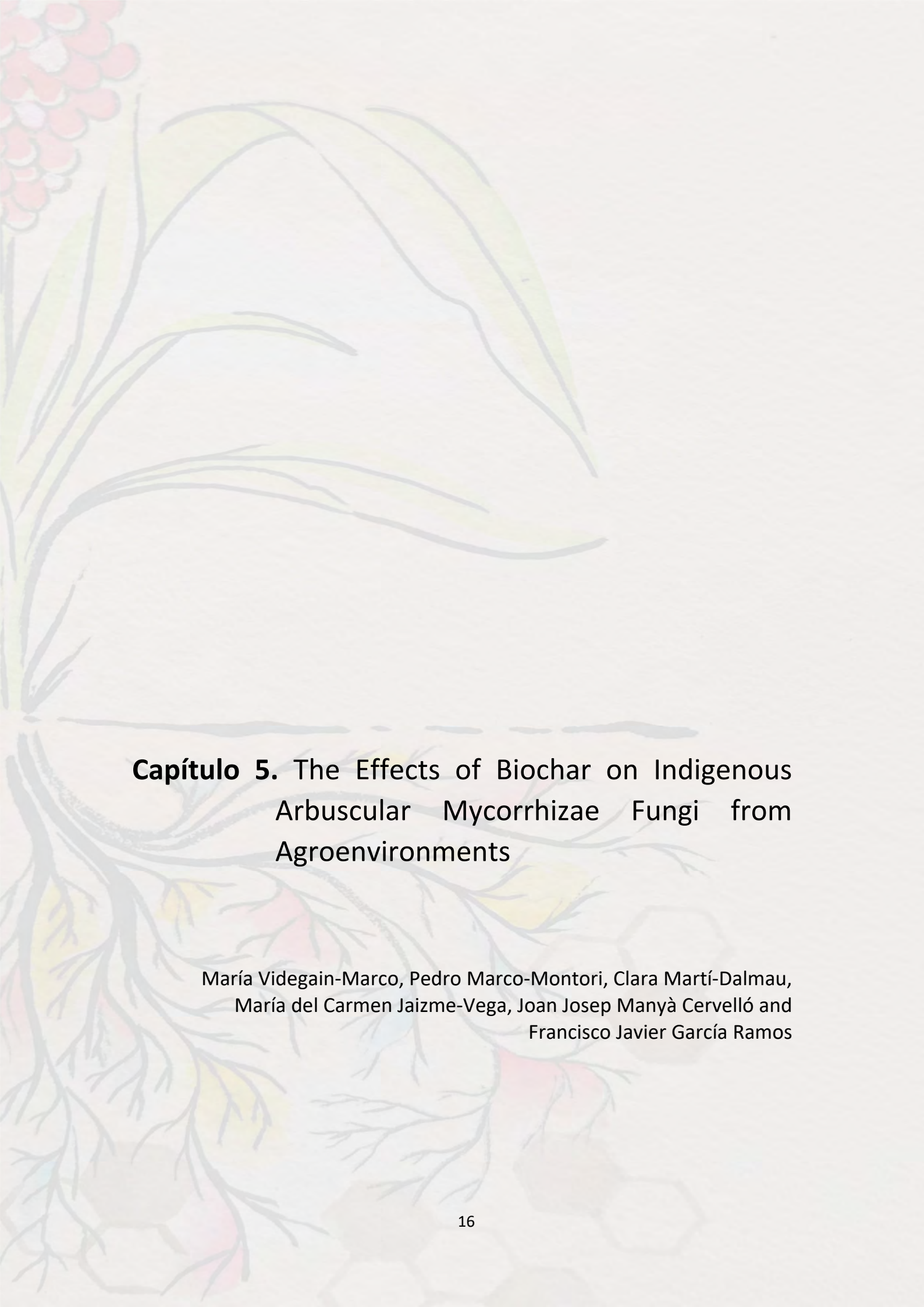
Figure S3. Nutrients concentration, SOM and CEC deviation of experimental treatments under different temperatures of biochar (400°C — B400 and 600 °C — B600) and application rate (D1: 1.5 wt. %; D2: 3 wt. %) from control treatment (D0) in a clay-loam growing substrate

Capítulo 5. The Effects of Biochar on Indigenous Arbuscular Mycorrhizae Fungi from Agroenvironments

María Videgain-Marco, Pedro Marco-Montori, Clara Martí-Dalmau, María del Carmen Jaizme-Vega, Joan Josep Manyà Cervelló and Francisco Javier García Ramos

The Effects of Biochar on Indigenous Arbuscular Mycorrhizae Fungi from Agroenvironments

María Videgain-Marco [1,*] , **Pedro Marco-Montori** [2] , **Clara Martí-Dalmau** [1] , **María del Carmen Jaizme-Vega** [3] , **Joan Josep Manyà-Cervelló** [4] and **Francisco Javier García-Ramos** [1,5]

1 Departamento de Ciencias Agrarias y del Medio Natural, EPS, Universidad de Zaragoza, Carretera de Cuarte s/n, E-22071 Huesca, Spain; cmarti@unizar.es (C.M.-D.); fjavier@unizar.es (F.J.G.-R.)
2 Centro de Investigación y Tecnología Agroalimentaria de Aragón (CITA), Instituto Agroalimentario de Aragón—IA2 (CITA-Universidad de Zaragoza), Unidad de Recursos Forestales, Avenida Montañana 930, E-50059 Zaragoza, Spain; pmarcomo@cita-aragon.es
3 Departamento de Protección Vegetal, Instituto Canario de Investigaciones Agrarias (ICIA), Carretera de El Boquerón s/n, Valle Guerra, La Laguna, E-38270 Tenerife, Spain; mcjaizme@icia.es
4 Thermochemical Processes Group, Aragón Institute of Engineering Research (I3A), EPS, University of Zaragoza, Carretera de Cuarte s/n, E-22071 Huesca, Spain; joanjoma@unizar.es
5 Instituto Agroalimentario de Aragón—IA2 (CITA-Universidad de Zaragoza), EPS, Universidad de Zaragoza, Carretera de Cuarte s/n, E-22071 Huesca, Spain
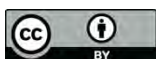* Correspondence: mvidegain@unizar.es; Tel.: +34-974292656

Abstract: The effects of biochar on soil–plant–microorganisms systems are currently being extensively investigated. Considering that arbuscular mycorrhizal fungi (AMF) play an essential role in nutrient dynamics, the present study aims at understanding vine shoot-derived biochar effects on AMF activity and the impact of their multiplication in soils on water-stress resistance of plants. Three agronomic tests were performed in greenhouse pots. The first experiment evaluated the effects of three factors: final pyrolysis temperature for biochar production (400 °C and 600 °C), application rate (0 weight-wt.-% as a control, 1.5 wt. %, and 3.0 wt. %) and texture of the growing media (sandy-loam and clay-loam origin) on AMF, microbial communities and phosphatase activity. In the second experiment, an indigenous consortium of AMF was multiplied through the solid substrate method and sorghum as a trap plant with biochar addition. This process was compared to a control treatment without biochar. Obtained inocula were tested in a third experiment with lettuce plants under different water irrigation conditions. Results from the first experiment showed a general increase in AMF activity with the addition of the biochar produced at 400 °C in the sandy-loam texture substrate. Results of the second experiment showed that the biochar addition increased AMF root colonization, the number of AMF spores and AMF infective potential. Results of the third experiment showed that biochar-derived AMF inoculum increased AMF root colonization, AMF spores, dry biomass and the SPAD index in a lettuce crop under low-water irrigation conditions.

Keywords: vine-shoots; sorghum; lettuce; drought stress; trap plant; waste management

1. Introduction

New crop varieties and biotechnologies are being investigated in dealing with drought-stress events in agriculture [1]. Concurrently, indigenous crop varieties and their adaptation mechanisms have been valued as agroecological strategies that contribute to improving drought resistance in rainfed areas. Improving the physical and biological fertility of the soil is becoming a mandatory practice to preserve its productive capacity, even though chemical fertilization remains the focus of intensive agricultural systems.

Currently, one of the most studied organic amendments to enrich soil fertility is biochar, a carbon-rich product obtained by thermal degradation of biomass under a limited supply of oxygen, at temperatures usually below 700 °C, which is produced to be added to the soil as a means of improving its quality and increasing carbon storage [2].

Previous studies have already reported that biochar is highly recalcitrant and able to improve some soil properties by influencing biochemical and biological processes [2–5]. Biochar amendment significantly enhances the nutrient availability and nutrient retention of a wide range of soils [6], in addition to the positive contribution to the improvement of other physical and biological soil properties [7–10] and to metal retention [11]. However, the capacity of this material to provide or enhance soil fertility extremely depends on the type of feedstock and pyrolysis conditions [12].

The effects of biochar (when it is used as a soil amendment) on the soil–plant–microorganisms system are currently being extensively investigated. Since microorganisms play an essential role in soil nutrient dynamics, they can be used as bioindicators due to their high sensitivity to small short-term habitat modifications. Furthermore, microorganisms have high resilience to degradation processes and biotic/abiotic stresses [13].

Droughts are a limiting factor in agricultural production. In addition, due to climate change, droughts are increasing in frequency and severity in some regions [14]. Alleviation of this abiotic stress through the enhancement of the arbuscular mycorrhizal fungi (AMF) presence in soils could be an interesting agroecological strategy, since AMF can shape the adaptative strategy of plants. The most important mechanisms by which symbiosis can alleviate drought stress in host plants are related to the direct uptake of water through the fungal hyphae, changes in soil water retention properties, better osmotic adjustment of AM plants, enhancement of plant gas exchange and water-use efficiency, and protection against oxidative damage generated by drought [15,16].

Research studies involving biochar and AMF processes show a wide spectrum of results, depending on experimental conditions, biochar composition and particle size [17]. The indigenous AMF consortia in soils are usually selected as bioindicators, since they are considered crucial components of soil fertility, either due to symbiotic relationships with plant roots or interactions with rhizosphere microorganisms [18]. Some earlier studies reported negative effects of biochar addition on AMF root colonization for both indigenous AMF consortia and introduced species. Warnock et al. [19] reported a decrease in the AMF abundance with wood-based biochar addition accompanied by changes in phosphorous availability. In line with this, several research studies reported negative or no significant effects [20,21] of biochar on AMF development. But there is a clear interaction between biochar, microorganisms, mineral nutrients available in the soil and water conditions. LeCroy et al. [22] showed that biochar reduced biomass production of sorghum plants in the presence of high levels of nitrogen fertilizer; they suggested that soil nitrogen controls the ability of char to influence the mycorrhizal symbiosis and the degree to which the fungi oxidize the char surface. Vanek and Lehmann [23] found that positive biochar-AMF interactive effects on bean phosphorus (P) uptake were fostered by sparingly soluble Fe-P; however, they were not observed when soluble P was combined with biochar. In this sense, Blackwell et al. [24] and Solaiman et al. [25] also correlated AMF increases to low nutrients availability in soil. Hammer et al. [26] observed AM fungal hyphae accessing microsites within biochar mediating plant P uptake from the biochar surface.

Considering the wide range of results reported in the literature, the possibility of using biochar as a component of the growing media in containerized plant production [27] and its utility as a potential carrier material for delivery inoculants [28], assessing the suitability of biochar as a component of the growing media on the multiplication process of an indigenous consortium of AMF is proposed herein. For this purpose, a first bioassay was conducted in pots under controlled greenhouse conditions. Sorghum (*Sorghum bicolor* L. Moench) was selected as a classic mycotrophic test crop to evaluate the effect of the addition of two types of vine shoot-derived biochar on the AMF activity and other biological indicators (i.e., phosphatase activity and microbial community variations). The experiment measured the influence of different factors (the final pyrolysis temperature at which the biochar was produced, application rate and growing media substrate texture). Based on the results of the abovementioned bioassay, it was hypothesized that biochar could be suitable as a component of the growing media on the multiplication process of indigenous AMF

Based on the results of the abovementioned bioassay, it was hypothesized that biochar could be suitable as a component of the growing medium for the production of indigenous AMF consortia in soils through the method of solid substrate and trap plants [29]. This approach was tested experimentally, and the final inoculum obtained was then evaluated in terms of water-stress resistance for lettuce (*Lactuca sativa*) plants, which were grown in the same soil under study.

2. Results

2.1. Biochar Properties

The complete characterization of the two types of biochar produced is detailed in a previous publication [30]. The results were primarily dependent on pyrolysis operating conditions. The biochar averaged mass yield (Y_{char}) notably decreased when the pyrolysis final temperature increased (biochar at 400 °C—Y_{char} = 0.38; biochar at 600 °C—Y_{char} = 0.29). The biochar produced at 600 °C (B600) had a higher fixed carbon content measured on a dry basis (84.54 wt.%) and ash (10.02 wt.%) compared to biochar produced at 400 °C (B400: 70.88 wt.% and 6.45 wt.%, respectively), which conversely had a higher amount of volatile matter (+19.64 wt.%). The specific surface area and pore volume increased with rising pyrolysis final temperature. Related to its water-holding capacity (WHC) increased with pyrolysis final temperature, from 14.16% in B400 up to 18.35% in B600. Primary and secondary elements showed no major differences between B400 and B600. Table S1 (Supplementary Materials) details the results from proximate, elemental, and physico-chemical analyses of the biochar produced.

2.2. Soils Characterization

Results from the AMF infective potential of soils and microbiological analyses are summarized in Table 1.

Table 1. AMF infective potential and microbiological composition of soils.

Determination [1]	Unit	S1 [2]	S2
AMF potential (MPN)	Number of infective mycorrhizal propagules 100 cm^{-3}	39.6 ± 9.3	30.9 ± 13.1
Number of AMF spores	Number of AMF spores 100 g soil^{-1}	420 ± 18	465 ± 23
Identified genera	% spores	20 *Gigaspora* spp. 3 *Scutellospora* spp. 77 *Glomus* spp.	6 *Acaulospora* spp. 94 *Glomus* spp.
Culturable microbial communities			
Mesophilic aerobic microorganisms	log cfu g^{-1}	6.59 ± 0.90	7.08 ± 0.67
Actinomycetes	log cfu g^{-1}	6.08 ± 0.45	6.45 ± 0.27
Pseudomonas genus	log cfu g^{-1}	5.74 ± 0.13	5.96 ± 0.34
Mycobiota	log cfu g^{-1}	4.75 ± 0.65	4.71 ± 0.43

[1] Results from five replicates of each sample of soil. Average values and standard deviation. [2] S1—soil 1: sandy-loam; S2—soil 2: clay-loam.

Student *t*-test did not show statistical differences between Soil 1 and Soil 2 for the biological characteristics analyzed.

The AMF infective potential showed mean values of 39.6 and 30.9 propagules in 100 cm^3 of soil for sandy-loam soil (S1) and clay-loam soil (S2), respectively. The mean number of AMF spores was 420 spores in S1 and 465 spores in S2. The morphological identification of the spores reveled that *Glomus* spp. was the main species identified in the

samples of both soils (77% in S1 and 94% in S2). This species is largely found in natural and cultivated ecosystems and stands out for its high efficiency on a large number of crops and its adaptation to a wide pH range [31]. In addition, it was detected, in lower percentages, the availability of other species such as *Gigaspora* spp. (20% in S1), *Scutelloespora* spp. (3% in S1) and *Acaullospora* spp. (6% in S2).

With respect to the culturable microbial communities, soils achieved an average initial total microbial count, mesophilic aerobic microorganisms (MAM), of 7.5 and 8.0 log cfu g^{-1}, for sandy-loam and clay-loam substrates, respectively. The predominant microbial group in both soils was actinomycetes (ACT) (6.1 and 6.5 log cfu g^{-1}, respectively for each substrate), followed by *Pseudomonas* genus (PS) (5.7 and 6.0 log cfu g^{-1}, for sandy-loam and clay-loam substrates, respectively). The mycobiota (molds and yeasts) was present at relatively lower numbers with average counts of 4.7 cfu g^{-1} for both substrates.

Results from physicochemical fertility of Soil 1 and Soil 2 are shown in Table S2 (Supplementary Material). The main differences between both samples were found in the content of oxidable organic matter (S1: 3.04 wt. %; S2: 1.70 wt. %), macroelements content (mg kg^{-1}: N-NO$_3$: S1—59, S2—12; P Olsen: S1—32, S2—29; K: S1—160, S2—252) and WHC (S1—5.41 v. %; S2—10.22 v. %).

2.3. Experiment 1: Effects of Soil Texture, Addition Rates and Final Pyrolysis Temperatures on AMF Performance, Microbial Communities' Variation and Phosphatase Activity

During crop development, a general increase in root AMF colonization was observed from 210 to 330 days after sowing (D_{210} and D_{330}); the average values of AMF root colonization decreased in the last period, which could be related to winter temperatures and the final development of the crop. The average values measured and standard deviation for this parameter and the number of AMF spores at the final of the experiment are summarized in Table 2.

No differences on root colonization were observed for the measurements performed during the first seven months of the experiment (from D_{120} to D_{210}) in either of the two types of growing media.

Significant differences in root colonization were observed in measurements made from D_{330}. For both sandy-loam and clay-loam substrates, the highest percentage of colonization was observed in the treatment with B400 addition (20.0% and 31.7% for S1 and S2 respectively), although there were no differences in comparison to Control treatment for the clay-loam substrate. This trend between the treatments was maintained up to the last measurement date (D_{390}) with lower average colonization values, as mentioned above. It should be noted that there was a marked decline of AMF root colonization in B600 treatments with lower doses in S1 (from 10% to 5%) and with high doses in S2 (from 18.3% to 6.7%) at the end of the experiment (D_{390}).

The number of AMF spores at the end of the experiment (D_{390}) had significantly different results between treatments (see Table 2). In particular, a clear influence of biochar addition in the sandy-loam substrate in comparison to Control treatment was observed. The highest value in this substrate was reported in B400 at high doses of biochar addition (1511 spores per 100 g of soil) with no significative differences with respect to B600 treatments (1380 and 1095 spores per 100 g of soil in D1 and D2 treatments, respectively). Concerning the clay-loam substrate, no differences were observed in the number of AMF spores between treatments with the exception of B600 at a high dose of biochar addition (5245 spores per 100 g of soil). Identified genera information is available in Table S3. No differences were observed between treatments for genera distribution at the end of the experiment.

Table 2. Effect of biochar addition on root AMF colonization and number of AMF spores (final pyrolysis temperature of biochar B400—400 °C and B600—600 °C; application rate D0—Control without biochar, D1—1.5 wt. %, D2—3 wt. %). Average values and standard deviation (in brackets).

Variable Measured		Sandy-Loam Substrate					Clay-Loam Substrate				
		B400			B600		D0	B400		B600	
		D0	D1	D2	D1	D2		D1	D2	D1	D2
Root AMF colonization %	D_{120}	10.0 a (1.0)	13.3 a (5.7)	12.5 a (1.0)	10.0 a (1.5)	10.0 a (1.5)	10.5 a (2.0)	13.3 a (6.7)	10.0 a (0.0)	11.6 a (4.0)	13.3 a (5.7)
	D_{210}	11.7 a (2.8)	18.3 a (5.7)	16.7 a (2.9)	11.7 a (2.8)	13.3 a (2.9)	21.7 a (5.7)	21.7 a (5.7)	13.3 a (28.9)	13.3 a (2.8)	15.0 a (0.0)
	D_{330}	8.3 b (2.9)	13.3 ab (2.9)	20.0 a (0.0)	10.0 b (5.0)	11.7 ab (2.9)	26.7 ab (2.9)	26.7 ab (7.3)	31.7 a (2.9)	26.7 ab (2.9)	18.3 b (2.9)
	D_{390}	5.7 bc (1.1)	13.3 ab (2.9)	18.3 a (2.9)	5.0 c (0.0)	10.0 bc (0.0)	25.0 a (0.0)	23.3 a (2.9)	31.6 a (2.9)	25.0 a (0.0)	6.7 b (5.8)
Number of AMF spores 100 g soil^{-1}	D_{390}	548 c (103)	830 bc (198)	1511 a (170)	1380 ab (275)	1095 ab (230)	1668 b (200)	2058 b (232)	1930 b (287)	1978 b (95)	5245 a (1399)

Means within a row followed by the same letter are not significantly different for the same kind of growing substrate at $p \leq 0.05$ (Tukey's test).

(1511 spores per 100 g of soil) with no significative differences with respect to B600 treatments (1380 and 1095 spores per 100 g of soil in D1 and D2 treatments, respectively). Concerning the clay-loam substrate, no differences were observed in the number of AMF spores between treatments with the exception of B600 at a high dose of biochar addition (5245 spores per 100 g of soil). Identified genera information is available in Table S3. No differences were observed between treatments for genera distribution at the end of the experiment.

MAM and PS were the microbial communities in which significant differences were observed after biochar addition. As shown in Figure 1, the overall average value of MAM increased slightly from the initial counts, and the biochar application significantly increased the average values in the sandy-loam substrate, from 7.5 cfu g^{-1} in Control treatment to 8.2 cfu g^{-1} after biochar addition. For this texture soil, PS counts showed the highest values when B400 was added. In S1, B400 and B600 show similar effects, B400 increased the average value in comparison to Control treatment for this texture soil. However, no differences were observed for these microbial communities under biochar addition in the clay-loam substrates.
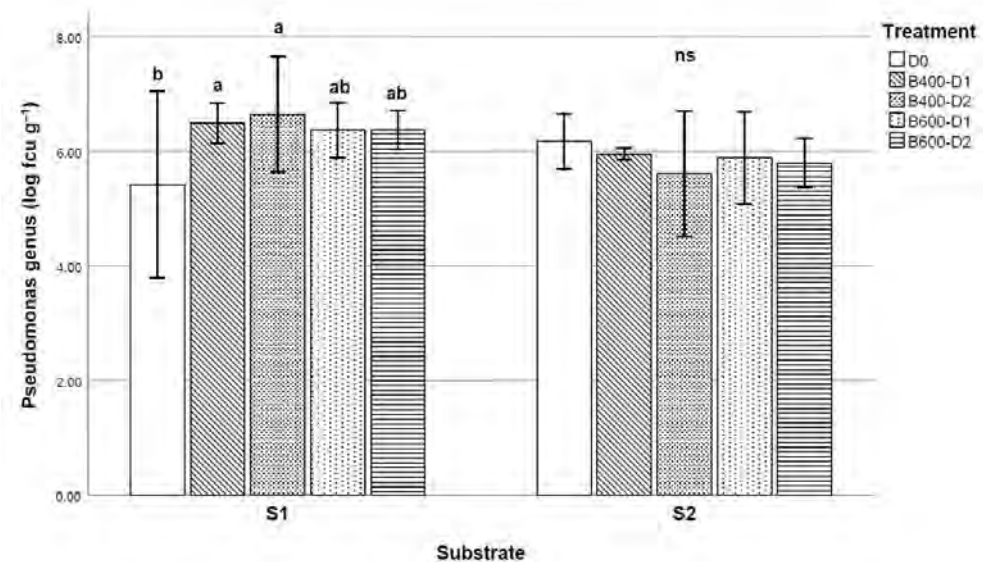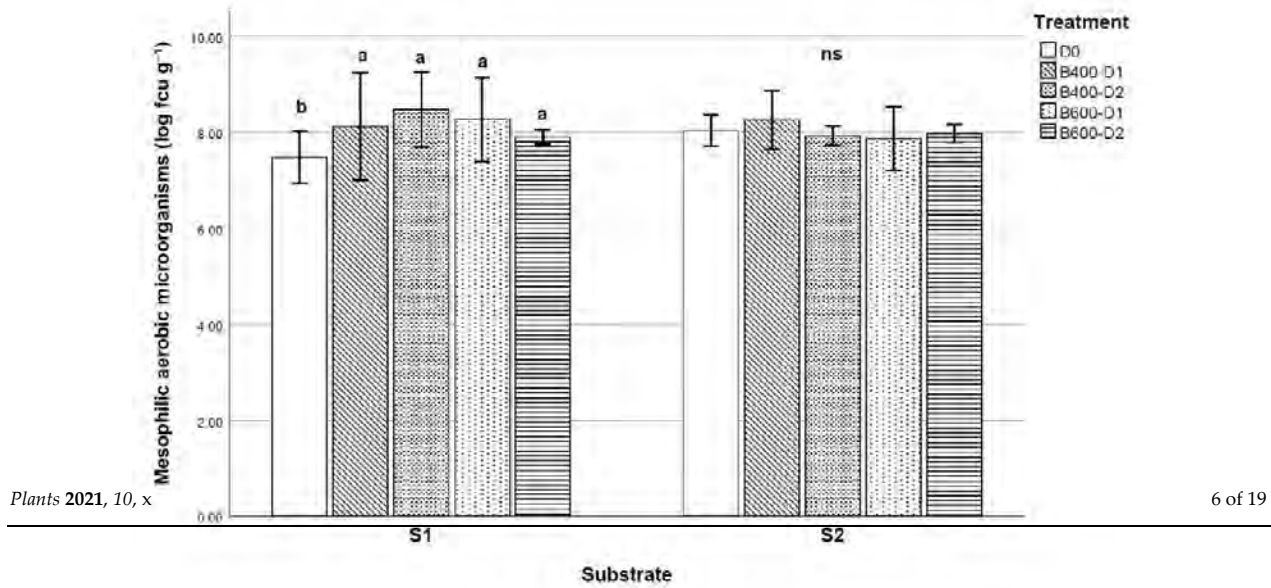
(b)

Figure 1. Effect of biochar application on (**a**) mesophilic aerobic microorganisms and (**b**) *Pseudomonas* genus. (Final pyrolysis temperature of biochar B400—400 °C and B600—600 °C; D0–Control without biochar, D1—1.5 wt. %, D2—3 wt. %; S1—sandy-loam substrate, S2—clay-loam substrate). Different letters show statistically significant differences at $p \leq 0.05$ (Tukey's test).

Complete counts of the mesophilic aerobic microorganisms, *Pseudomonas* genus, actinomycetes, and mycobiota (yeasts and molds) are detailed in Table S3. The statistical analysis of microbiological counts performed in substrates at the end of the experiment (D$_{390}$) did not show significant differences in actinomycetes and mycobiota populations. The final values were similar to those measured during the initial characterization.

For the specific results of our experiment, no differences in P content were found on

Complete counts of the mesophilic aerobic microorganisms, *Pseudomonas* genus, actinomycetes, and mycobiota (yeasts and molds) are detailed in Table S3. The statistical analysis of microbiological counts performed in substrates at the end of the experiment (D_{390}) did not show significant differences in actinomycetes and mycobiota populations. The final values were similar to those measured during the initial characterization.

For the specific results of our experiment, no differences in P content were found on substrates or plant tissue [30]; however, a positive correlation between AMF activity and *Pseudomonas* abundance was confirmed for the sandy-loam substrate (see Table S4).

Enzymatic activities have an important function in organic P mineralization and in P plant nutrition, especially in calcareous soils subjected to frequent retrogression processes of available P [32]. For all the substrates and biochar application rates assessed herein, the AcdP activity values (1.38 μmol h^{-1} in average) were lower than AlkP ones (2.98 μmol h^{-1} g^{-1} in average). This finding, however, was somewhat expected, since microbial population in soils can be sensitive to the growing pH media of both soils sampled for substrate preparation.

From the analysis of the phosphatase activity in relation to substrate granulometry, it was deduced that, for the sandy-loam substrate, both AcdP and AlkP values had similar behavior (see Figure 2), leading to significant activity increases with the addition of B600 in comparison with B400. Both AcdP and AlkP values did not show significant differences between B400 and Control treatment in the sandy-loam substrate (S1).

Nevertheless, for the clay-loam substrate (S2), AcdP only showed significant differences in B600 treatment; in contrast, the highest main value of AlkP in S2 was obtained for the Control treatment without biochar, which had results significantly differents from treatments with biochar. In this texture (S2), the lower dose of biochar addition was related to a decrease in AlkP activity, both with B400 and B600 addition. The complete results are detailed in Table S3.

Table 3 shows the results from the three-way ANOVA on the significant effects of the factors (i.e., growing substrate texture, biochar final temperature, and application rate) on root AMF colonization at different dates after sowing (D_{210}, D_{330} and D_{390}), number of AMF spores, phosphatase activity and microbial communities at the end of the second crop development cycle (D_{390}).

As can be seen from the results reported above, the growing-substrate medium was the most influential factor for the response variables assessed. Results obtained in S1 demonstrate that biochar addition had the greatest positive influence in fine texture, in terms of AMF root colonization, number of AMF spores and enzymatic activity. Biochar temperature also had an important effect, with a positive trend in AMF root colonization under B400 addition. Application rate had the lower effect considering it separately (only significant in enzymatic activities); however, significant effects were observed by the interactions with biochar on the studied variables.

Considering these results, B400 was selected as a component of the solid substrate used in Experiment 2 to multiply the AMF consortium present in the sandy-loam substrate (S1). The amount of biochar selected to prepare the multiplication substrate was 1.5 wt. %, since this concentration value could be relatively easily implemented in real field conditions.
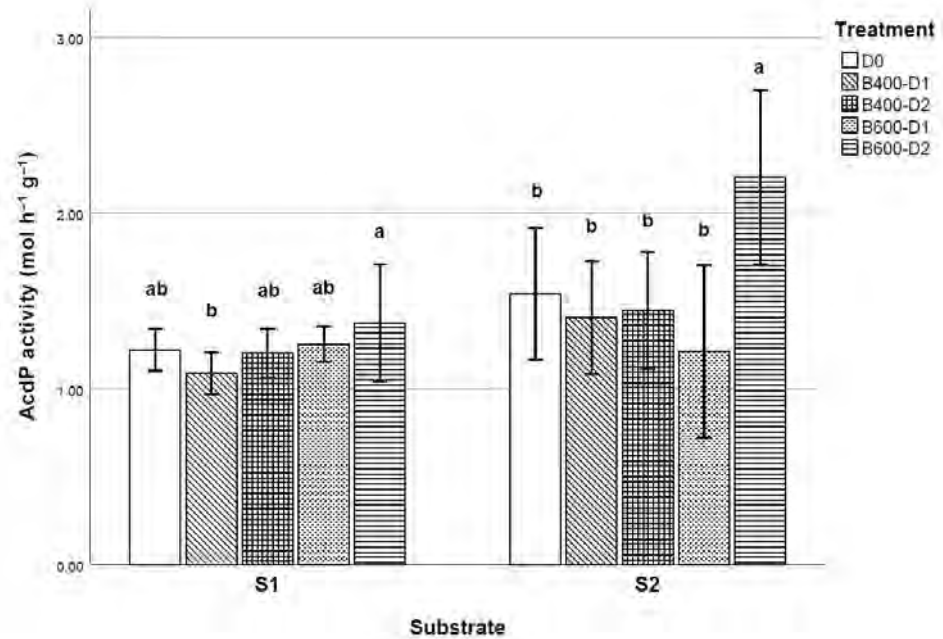
(a)
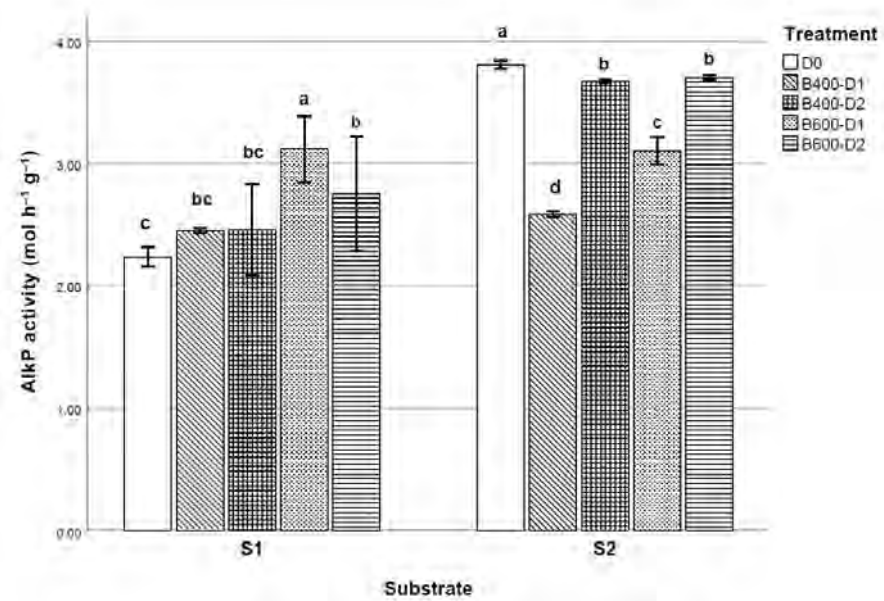
(b)

Figure 2. Effect of biochar application on (**a**) acid phosphatase activity and (**b**) alkaline phosphatase activity. (Final pyrolysis temperature of biochar B400—400 °C and B600—600 °C; D0–Control without biochar, D1—1.5 wt. %, D2—3 wt. %; S1—sandy-loam substrate, S2—clay-loam substrate). Different letters show statistically significant differences at $p \leq 0.05$ (Tukey's test).

Table 3. Three-way ANOVA results on the effects of growing substrate texture, biochar temperature and application rate on root AMF colonization, number of AMF spores, phosphatase activities and microbial communities.

Factor	Root AMF Colonization			AMF Spores	Phosphatase Activity		Microbial Communities	
	D_{210}	D_{330}	D_{390}		AcdP	AlkP	MAM	PS
Growing substrate texture (S)		<0.0001	<0.0001	<0.0001	<0.0001	<0.0001		0.040
Biochar temperature (B)		0.001	<0.0001		0.001	<0.0001		<0.0001
Application rate (D)					<0.0001	<0.0001		
S × B						0.006		0.012
S × D			0.002		0.006	<0.0001		
B × D	0.048	0.007	<0.0001	0.005	0.001			0.001
S × B × D			<0.0001	0.003	0.001		0.011	

$D_{210/330/390}$: days after sowing; AcdP: Acid phosphatase activity: AlkP: Alkaline phosphatase activity; MAM: mesophilic aerobic microorganisms; PS: *Pseudomonas* genus.

2.4. Experiment 2: Multiplication Process of AMF Consortium on Solid Substrate with Biochar

The results of AMF root colonization (%), number of AMF spores and infective AMF potential of substrates at the end of the experiment are summarized in Table 4.

Table 4. Effects of biochar addition on AMF measurements at the end of the multiplication process of an indigenous AMF consortium (T0: 0 wt. % biochar; T1: 1.5 wt. % biochar).

Treatment	AMF Root Colonization (%)	Number of AMF Spores 100 g Soil^{-1}	Infective Mycorrhizal Propagules 100 cm$^{3-1}$
T0	15.5 ± 2.1	514.6 ± 59.3	72.4 ± 32.0
T1	32.8 *** ± 5.2	866.9 *** ± 125.0	161.5 ** ± 80.3

Data are average of six replicates for AMF root colonization (basil + sorghum) and three replicates for the rest of the parameters ± SD. Statistically significant differences at ** $p \leq 0.01$; *** $p \leq 0.001$.

The results of this experiment followed the same trend as in Experiment 1, with significant increases ($p \leq 0.05$) in all measurements carried out in T1 with respect to T0. Biochar addition increased AMF root colonization by 211%, AMF spores by 168% and infective AMF potential by 223% with respect to the treatment without biochar.

It should be highlighted that there were a relatively large number of AMF spores, regardless of the procedure adopted for their quantification (i.e., counts of their isolation through wet sieving and the most probable number of mycorrhizal propagules).

2.5. Experiment 3: Effects of Inoculum Application on Water-Stress Resistance and Development of Lettuce Plants

As expected, results obtained in Experiment 3 showed a strong interaction between water-irrigation conditions and AMF application ($p \leq 0.05$) for all the parameters studied, with the exception of the SPAD index in D_{60}. This interaction allowed us to analyze the data among the different scenarios of water contributions.

The results of AMF root colonization (%), number of AMF spores, dry biomass and the SPAD index at the end of the experiment are shown in Table 5.

Table 5. Effects of AMF inoculum addition on AMF measurements, dry biomass and the SPAD index in lettuce crop (WID1: 70–80% container capacity, WID2: 10% container capacity; −AMF: without inoculum, +AMF: with AMF inoculum, +B+AMF: with AMF inoculum obtained from a solid substrate with biochar; ADB: aerial dry biomass at the end of the experiment, RDB: root dry biomass at the end of the experiment; $D_{30,50,62}$: days after sowing; *n*: number of living plants at the end of the experiment).

Factors		Root AMF Coloniz. (%) D_{62}	Number of AMF Spores	Dry Biomass		SPAD Index			*n*
Irrigation	Inoculum			ADB	RDB	D_{30}	D_{50}	D_{62}	
WID 1	−AMF	1.0 ± 3.0 c	2.0 ± 4.3 c	2.70 ± 0.35 ab	1.28 ± 0.20 b	27.4 ± 3.2	36.2 ± 2.1 a	37.2 ± 2.5 a	10
	+AMF	13.0 ± 3.5 b	51.8 ± 14.3 b	3.45 ± 0.50 ab	0.93 ± 0.23 b	27.5 ± 1.2	36.9 ± 2.0 a	37.24 ± 1.8 a	9
	+B+AMF	24.5 ± 7.2 a	144.1 ± 35.6 ab	3.71 ± 0.48 a	1.26 ± 0.21 b	29.0 ± 1.0	35.7 ± 2.3 a	35.9 ± 2.6 a	9
WID 2	−AMF	2.0 ± 4.2 b	1.9 ± 4.2 c		1.25 ± 0.45 b	28.5 ± 3.0	21.6 ± 4.2 c		0
	+AMF	19.0 ± 10.0 a	178.6 ± 17.9 a	2.49 ± 0.21 c	1.39 ± 0.39 b	27.6 ± 3.5	28.1 ± 3.8 b	16.5 ± 1.1 c	5
	+B+AMF	24.0 ± 6.0 a	201.3 ± 73.0 a	2.69 ± 0.25 bc	1.92 ± 0.60 a	27.1 ± 4.1	33.7 ± 1.4 a	17.2 ± 1.4 b	8

Data are average of 10 replicates ± SE with except for ADB and SPAD D_{62}, in which data is average of *n* ± SD. Different letters within a column denote statistically significant differences at $p \leq 0.05$ (Scheffe's test).

During the first month of crop development, in which all the plants received the same amount of water, no differences were observed in the SPAD index among the treatments.

At the beginning of the second month (D_{50}), in which the irrigation dose was reduced (i.e., half of the plants), the SPAD index showed differences between treatments only in those plants that received less water (WID2). Plants growing with AMF inoculum produced with biochar B400 (+B+AMF) showed a significantly higher SPAD index with respect to the plants inoculated with the inoculum produced in the conventional way (+AMF) under low-irrigation conditions. Furthermore, under this irrigation scenario, non-mycorrhized plants showed significantly lower values than mycorrhized plants.

During the period elapsed between D_{50} and D_{62}, plants without inoculum and under low-irrigation conditions died. Despite this, the root system of the plants was collected, dried, weighed and stained with trypan blue. AMF root colonization was measured because the roots maintained their consistence few days after plants died. These plants developed a total of five leaves, which is a lower value in comparison to the rest of the treatments (in which plants developed six to eight leaves).

At the end of the experiment, both the root AMF colonization and number of AMF spores showed similar trends among treatments. For highly irrigated treatments, AMF activity was significantly higher in the +B+AMF treatment. However, no differences between +AMF treatment and +B+AMF were observed under low-irrigation conditions. Regarding the non-inoculated plants, AMF activity was significantly lower in both irrigation conditions. The observed peaks in the AMF activity were probably caused by (i) some contamination coming from the other treatments or (ii) the regeneration of these microorganisms by the substrate itself.

Both the AMF root colonization and number of spores presented higher values in WID2 in comparison to WID1. This confirms the greater development of mycorrhizae under stress conditions as an adaptation strategy.

The aerial and root dry biomass values also showed significant differences between treatments: +B+AMF treatment reported the highest values for ADB under both water irrigation treatments. However, these differences between inoculated plants were only statistically significant under lower doses of water. Non-mycorrhized plants exhibited a significant decrease in ADB under well irrigation conditions with respect to AMF treatments.

The root dry biomass (RDB) values showed a clear trend under low-irrigation doses, where +B+AMF treatments led to better results. However, for highly irrigated scenarios, the Control treatment without AMF showed similar behavior to +B+AMF mycorrhized plants.

Finally, the leaves nutrient concentrations did not show any significant difference among treatments. Table S5 details the complete information of these results.

3. Discussion

Results for AMF root colonization and number of AMF spores in Experiment 1 confirm that biochar application had a significant influence on AMF activity. Slight differences were observed, depending on the texture of the selected substrates.

According to previous publications [22,24,25], the activity of AMF increased after biochar application. However, depending on the experimental conditions and especially on soil-nutrient availability, decreases in AMF root colonization have also been reported [18,21]. In this particular experiment, it was confirmed that biochar had a positive effect on AMF development in the sandy-loam texture (S1); nevertheless, the higher activity of mycorrhized roots or number of AMF spores did not result in any marked increase in the biological crop yield, as reported in a previous publication [30]. The obtained results in B600 treatment at high doses in the clay-loam substrate, as mentioned above, showed the minimum value of root colonization and the maximum value for the number of AMF spores, which leads to the conclusion that the sporulation strategy by the mycorrhiza prevailed in this treatment over root colonization. This statement could be related to a stress in the plant. Considering the results obtained

in a previous publication [30], in which the productive parameters of this experiment were analyzed, no decrease in aerial biomass production was observed for this treatment. However, a lower number of plants fructified under this treatment, meaning that plants did not complete their productive cycle before drying.

Warnock et al. [33], assuming the importance of this community of microorganisms in their studies, elucidated the possible mechanisms that could explain how biochar could alter the total abundance of mycorrhizal fungi in soils and plant roots. In addition to the presence of available phosphorus in the soil, these mechanisms are affected by several factors: (i) modifications in the activity of linked microorganisms, (ii) changes in signaling dynamics between plants and mycorrhizal fungi, and (iii) physical effects related to biochar porosity. Regarding these mechanisms, we relate the higher influence of biochar produced at 400 °C on AMF activity to the higher volatile content of the biochar with respect to biochar produced at 600 °C. Volatile compounds could alter signaling dynamics in the soil, combined with an increase in water-holding capacity of the affected substrate (sandy-loam origin) as it was reported in a previous publication [30]. The multiplication process developed in Experiment 2, where the substrate was composed of sandy-loam soil, as well as the results obtained from Experiment 3 sustain the preliminary results of Experiment 1, where increases in AMF activity in the presence of biochar were observed. It is important to emphasize the role played by the introduction of mycotrophic crops in order to optimize the development of indigenous AMF [15], as was seen when roots of basil and sorghum were combined in the multiplication containers. The average values of root colonization in Experiment 2 were lower than those expected according to the number of AMF spores measured. By comparing these results with those reported in a previous study (which was conducted for different solid substrates [34]), one can conclude that the observed increases in root colonization (caused by biochar addition) are in line with the outcomes reported for other substrates tested (i.e., vermiculite, perlite and volcanic residues).

The observed interactions between biochar and *Pseudomonas* genus represent a positive finding of this study. These PGPR bacteria appear to be "mycorrhizal helper bacteria" [29] and they were previously studied in order to investigate their relationships with plant nutrition on two fronts: alleviating the abiotic plant stresses [35] and enhancing the host plant defenses [36]. Ordóñez [37] observed a positive interaction between these genera, increasing P acquisition by plants. Other authors determined the synergistic use of biochar and PGPR for enhancing crop growth under water-deficit conditions [38]. Due to the reduced effects of biochar application on microbial communities observed in this study, further and longer-term studies are required. According to Yadav et al. [6], the aging of biochar could play an important role by increasing microbial biomass activity due to an easier access to carbon sources that are not available in the fresh biochar.

Regarding the enzymatic activity, the results reported here could be complemented by conducting an in-depth study on phosphorus availability in the soil and pH variations along the experiment. Several studies [39,40] have already observed inverse relationships between inorganic P availability and phosphatase activity, although this was dependent on initial bioavailable P. Soil pH also affects the activity of enzymes due to the pH sensitivity of amino acid functional groups (i.e., at different pH, the conformational preference and spatial structure of amino acids can change). In addition, pH can also affect enzyme activity by influencing the concentration of inhibitors or activators in the soil solution and the effective concentration of the substrate [41]. Nevertheless, previous publications reported increases in the phosphatase activity after the application of biochar produced at high temperatures ($\geq$500 °C) [42,43]. From the results reported above, a general trend for phosphatase behavior as a function of biochar application and application rates cannot be established. An apparent effect of B600 application was observed for the sandy-loam substrate in contrast to B400 addition and Control treatment. This influence of the high biochar temperature differs from other previous studies [44,45], in which phosphomonoesterase activity was increased to a greater extent when biochars produced at lower temperatures were applied.

The suitability of using this biochar as a component of growing media substrate in the multiplication process of AMF was demonstrated in Experiment 2. The search for alternatives to the use of *Sphagnum* peat as well as the facility to experimenting with biochar under controlled conditions results in a large number of pot-growth-based studies [27]. The physicochemical characteristics of this material have largely been related to some key processes in containerized plant production such as improvement of water retention [9,46–48] and utility as a potential carrier material for delivery of agrochemicals and inoculants [28]. In this sense, several factors influence the scalability of these processes, for which specific life-cycle analyses should be carried out in depth [49]. From the biotechnology perspective, a good microbial carrier should possess essential characteristics such as the capacity to deliver the suitable number of viable microbial cells at the right time [50], which has been reported in this study. Results from different studies show the potential of biochar to be used as an alternative inoculum carrier to peat and vermiculite. Hale et al. [51] tested biochar from different feedstocks and the influence of its characteristics on rhizobacteria survival. According to this study, Ghazi [52] reported a positive performance of biochar to support a *Rhizobia* inoculant in storage conditions. Various factors influence the scalability of these processes.

Biochar particle size deserves special attention in the present study, in which field conditions were simulated with a previous processing of biochar. Relatively large particle size was used for the pot experiments, with the exception of Experiment 3, in which solid substrate was grinded. One can expect a positive effect of reducing biochar particle size on all (or almost all) the parameters tested. Thus, biochar particle size appears to be an important factor that needs to be further investigated in order to explain the evolution of productive parameters as it has been studied in previous publications [53].

4. Materials and Methods

4.1. Biochar Production, Characterization and Processing

Vine shoots from winter pruning of vineyards (*Vitis vinifera* L.) were used as biochar precursor through slow pyrolysis at 400 °C (B400), and at 600 °C (B600) as the final pyrolysis temperatures. Vine shoots were cut using a domestic chipper into smaller pieces of 4–7 cm length. Pyrolysis experiments were carried out in a fixed-bed laboratory reactor. Information relative to the pyrolysis device, operating conditions and biomass/biochar characterization methodology are detailed in previous publications [30,54].

Both types of biochar were mechanically processed through an automatic agitation system [30] developed at laboratory scale to reproduce the movement in a commercial fertilizer spreader. Different particle sizes (wt. %) were obtained from this process: B400 (7% < 2 mm; 24% 2 mm < x < 20 mm; 43% 20 mm < x < 40 mm; 26% ≥ 40 mm); B600 (4% < 2 mm; 19% 2 mm < x < 20 mm; 55% 20 mm < x < 40 mm; 22% ≥ 40 mm).

4.2. Soils Characterization

Two different agricultural soils with contrasting textures (S1: Soil 1 Calcisol–sandy-loam; S2: Soil 2 Cambisol–clay-loam) were selected. Both soils were managed under agroecological techniques and were covered with spontaneous flora at the time of sampling. A 10-point sampling of the first 5–30 cm was performed to obtain a representative soil sample of the rhizosphere. Samples were air-dried in the laboratory and sieved through a 2 mm mesh. The methodology adopted for the physicochemical characterization of the soils is detailed in a previous publication [30].

A preliminary biological characterization was conducted and the following parameters were evaluated:

AMF infective potential. (a) The number of AMF infective propagules was quantified using the Most Probable Number (MPN) methodology [55,56], which was previously adopted by Sánchez de Prager et al. [57]. Serial dilutions of soils mixed with a sterilized substrate were established in tray fillers (60 cm^3/filler); a mycotrophic species (barley) was selected for this experiment. Chemically untreated barley seeds were pregerminated and

previously sterilized in tempered bleach solution (1 vol. %) for 30 min. One pregerminated seed per tray filler was cultivated for 6 weeks. After this period, plants' roots were separated from the substrate and washed with water, cleared with 2.5% KOH for 24 h, acidified with 0.01% HCl, stained following the methodology proposed by Phillips and Hayman with acidified glycerol (50% glycerol, 49.95% H_2O, 0.05% HCl) and 0.05% trypan blue [58], and cut in 1–2 cm pieces. Root colonization was quantified by the magnified intersect method proposed by McGonigle et al. [59]; (b) AMF spores were isolated from the soil samples following the procedure proposed by Gerdemann and Nicholson [60] and modified by Sieverding [56]. By the nature of the bioassay, the identification of the AMF was carried out morphologically at the genus level. A microscope at up to 400-fold magnification was used as described for glomeromycota classification by Oelh et al. [61] and Sanchez de Prager et al. [57].

Microbiological analyses. For that, 25 g were sampled of each soil. Samples were decimal diluted in 0.1% sterile distilled peptone water (Merck, Darmstadt, Germany) and homogenized using a laboratory blender Stomacher 400 Circulator (Seward Laboratory, London, England) for 2 min at 250 rpm. ISO standards were followed for each microbial group enumerated: Mesophilic aerobic microorganisms (4833–1:2014), *Pseudomonas* genus (13720:2011), and Mycobiota (21527:2008). Actinomycetes species were cultured on Starch Casein Agar (SCA) for 5–7 days at 30 °C according to Bawazir et al. [62].

4.3. Experimental Designs and Agronomic Tests Establishment

Three agronomic tests were carried out with different purposes:

Experiment 1 was carried out to optimize the biochar addition ratio and final pyrolysis temperature with AMF inoculum multiplication purposes. A pot-based experiment growing sorghum crop (*Sorghum bicolor* L. Moench) was conducted under controlled greenhouse conditions. Polyethylene trays with 12 conical fillers of 650 cm^3 volume capacity, 18 cm deep and 64 cm^2 of the upper surface were used for carrying out the bioassay. Three pregerminated seeds per tray filler were placed and carefully watered for 2 months until a thinning was performed (maintaining one plant per tray filler). Sorghum is a classic mycotrophic species widely used as a trap plant in studies and multiplication processes of AMF [63,64]. A randomized factorial block design was adopted with three factors as independent variables, as is detailed in Table 6. The duration of the trial was 13 months in which the crop completed two production cycles as is detailed in a previous publication [30].

Table 6. Experimental designs adopted to evaluate the effects of biochar addition as a component of the solid substrate in the multiplication process of AMF.

Experiment	Factors	Treatments	Replicates
1	1. Growing media texture	S1—substrate 1—sandy-loam growing media S2—substrate—2—clay-loam growing media	Five replicates/treatment: 50 experimental units
	2. Final pyrolysis temperature	B1—biochar 1—400 °C B2—biochar 2—600 °C	
	3. Biochar application rate	D0—Control—without biochar D1—1.5 wt. % D2—3 wt. %	
2	1. Biochar application rate	T0—Control—without biochar T1—1.5 wt. % B1	Three replicates/treatment: 6 experimental units
3	1. Inoculum composition	−AMF—Control—without inoculum +AMF—+ inoculum obtained from T0 +B+AMF—+ inoculum obtained from T1	Ten replicates/treatment: 60 experimental units
	2. Water irrigation dose	WID1—70–80% container capacity WID2—10% container capacity	

Experiment 2. Considering the results obtained in Experiment 1, B400 was evaluated as a component of solid substrate for the multiplication process of AMF consortium of

S1 (sandy-loam texture soil). The process was based on the growth of trap plants in solid substrate. A one-factor design was adopted with 2 levels for the biochar application rate. The distribution of treatments was randomized complete blocks, with 3 replicates for each one (see Table 6). The experimental unit was placed in an 8 L plastic container (40 × 20 × 16 cm) and was composed of 8 seedlings of sorghum (*Sorghum bicolor* L. Moench) as host/trap plants combined with 8 seedlings of basil (*Ocinum basilicum*), which was cut cyclically to avoid overdevelopment (all the seeds were previously sterilized and pregerminated as is described in Section 4.2.). These species were selected considering their high degree of mycorrhization and their adaptation to relatively high temperatures, since this experiment was carried out between the months of March and July (see Table S6 for more information about experimental conditions). At the end of the development cycle, the aerial part of the plants was cut and the solid substrate was processed, cutting the roots into small pieces (1–2 cm) and forming a homogeneous mixture of all components (roots, soil, fine gravel and peat, as is described in Table S6). Colonized roots and spores present in the substrate are the mycorrhizal propagules that constitute the new inoculum.

Experiment 3. The efficacy of the inoculants obtained in Experiment 2 was evaluated on a lettuce (*Lactuca sativa* var. Capitata) crop subjected to water-stress conditions. A randomized factorial block design was adopted with two factors as independent variables (see Table 6). The amount of each inoculum added was the equivalent to 50 AMF spores. One pregerminated lettuce seed was established per pot. Plastic pots with 704 cm^3 of volume capacity (8 × 8 × 11 cm) were selected for this agronomic test.

The duration of the test was 2 months. During the first 30 days, all the treatments received similar water irrigation inputs (WID1, see Table 6) through gravimetric measurements. From the second month, water irrigation for half of the plants was progressively stopped until 10% field capacity level for the rest of the experiment (62 days).

Detailed information on the sowing process, substrates composition, growing conditions and monitoring of environmental conditions at the greenhouse is available in Table S6 of supplementary material.

4.4. Substrate Analysis and Plant Measurements

For Experiment 1, a detailed report of productive parameters and physicochemical changes in the substrates is collected in a previous publication [30]. Regarding the biological parameters, the following measurements were carried out during the experiment and after the first harvest:

AMF root colonization: three measurements of AMF root colonization were done at different dates after sowing (120 days–D_{120}, 210 days–D_{210}, and 330 days–D_{330}) while the crop was established. A 3-point sampling was performed for each pot with a bipartite gouge auger (Eijkelkamp, Netherlands) 200 mm length and Ø13 mm. Plant roots were separated from substrates and washed with water before staining following the method described in Section 4.2. Direct estimation of AMF root colonization was carried out through microscopic examination following the "magnified intersection method" [58]. The final root system of each plant was processed through the same methodology after washing and drying at 70 °C to measure total root dry weight [30]; thus, final AMF root colonization was measured 390 days after sowing (D_{390}). The quantification of the number of AMF spores was carried out for each pot substrate at the end of the experiment (D_{390}) following the methodology detailed in Section 4.2. It is important to emphasize that no external mycorrhizal inoculum was added to the tested pots; only the indigenous mycorrhizal consortium of each soil was worked on.

Microbiological analyses: they were performed for each pot substrate at the end of the experiment (D_{390}) following the methodology detailed in Section 4.2.

Enzymatic activity: AcdP and AlkP were analyzed based on the colorimetric determination of the *p*-nitrophenol (PNP) released by the enzyme. The methodology followed was proposed by Tabatabai and Bremner [65], and it was adapted at pH 5.5 for AcdP and pH 11.0 for AlkP.

For Experiment 2: root colonization at the end of the experiment was measured in a representative number of both basil and sorghum roots. Once the aerial part of the plants was cut, and before grinding the solid substrate, a portion of the central part of the root system of all the plants in each experimental unit was sampled in order to obtain root-colonization information through the stain methodology described in Section 4.2. Three samples from the solid substrate of each experimental unit were reserved for wet sieving analyses and MPN methodology described in Section 4.2.

For Experiment 3: For AMF measurements, the methodologies described in Section 4.2 were conducted at the end of the experiment. Yield was measured by cutting the plants at the end of the experiment and drying in an oven until weight stabilization at 70 °C. Shoot and roots dry weight were differentiated. The analysis of elemental N (thermic conductivity), P (spectrometry) and K (spectrometry) in leaves was conducted once yields were measured. Leaf greenness was measured three times after sowing (D_{30}, D_{50}, D_{62}) in Experiment 3 as soil-plant analyses development (SPAD) readings (Chlorophyll Meter SPAD-502, Konica Minolta, Osaka, Japan).

4.5. Statistical Analysis of Results

Final data were statistically analyzed using the IBM SPSS Statistics v.26 software package. The T-Student test was conducted to analyze results from initial biological characterization and results of Experiment 2. Three-way ANOVA was conducted when the effects of factors and their interactions were studied. Two-way and one-way ANOVA were also conducted in selected cases (e.g., for different textures of growing substrate type and bifactorial experimental designs). Means comparisons were combined with Tukey´s and Scheffe´s test with a significance level of 0.05. In order to meet the criteria of statistical normality and homoscedasticity, data for the number of AMF spores and the number of infective propagules were transformed into natural logarithms, and the data of root colonization (%) were transformed into arcsine for statistical analysis.

5. Conclusions

The application of vine-shoots-derived biochar modifies the soil biological properties (i.e., AMF activity, microbial communities and enzymatic activity) to different extents depending on the factor being considered (texture substrate, biochar final pyrolysis temperature and application rate). The bioindicators selected in this study were affected by biochar application, despite the large particle size of the biochar used in this experiment. These indicators were more severely affected by the sandy-loam substrate compared to the clay-loam one. The suitability of using this biochar as a component of growing media substrate in the multiplication process of AMF was demonstrated. The combination of biochar and AMF could alleviate plant stress under drought conditions.

Considering the findings reported here, further specific field-scale experiments are required to understand better and assess the effects of vine-shoot-derived biochar application in soils. Results from these studies will also be useful to relate changes in the biological soil activity to physical properties (water-holding capacity, stability of soil aggregates, etc.) and productive parameters, which were slightly affected in this study.

Supplementary Materials: The following are available online at https://www.mdpi.com/article/10.3390/plants10050950/s1, Table S1: Proximate, elemental and physicochemical analyses of biochar produced at two different temperatures, Table S2: Results from physicochemical fertility analyses of soils collected for the agronomic test, Table S3: Average values and standard deviation (in brackets) of the effect of growing substrate texture, biochar temperature and application rate on the identified genera of AMF, culturing microbial communities and phosphatase activity in a pot sorghum crop experiment, Table S4: Pearson correlation and p-valor (in brackets) between AMF parameters and microbial communities in a sandy-loam substrate, Table S5: Effect of AMF inoculum addition on nutrient leaves of lettuce, Table S6: Additional information to Section 4.3. Experimental designs and agronomic tests establishment.

References

1. Hüseyin, B.; Hüdaverdi, G. Drought Stress Due To Climate Change. In Proceedings of the 8th Atmospheric Sciences Symposium (ATMOS 2017), Istanbul, Turkey, 1–4 November 2017.
2. Lehmann, J.; Joseph, S. Biochar for Environmental Management: An Introduction. In *Biochar for Environmental Management, Science and Technology*; Lehmann, J., Joseph, S., Eds.; Earthscan: London, UK, 2009; pp. 1–12.
3. Paz-Ferreiro, J.; Méndez, A.; Gascó, G.; Guo, M.; He, Z.; Uchimiya, S.M. Application of Biochar for Soil Biological Improvement. In *Agricultural and Environmental Applications of Biochar: Advances and Barriers*; Guo, M., He, Z., Uchimiya, S.M., Eds.; Soil Science Society of America, Inc.: Madison, MA, USA, 2016; pp. 145–174.
4. Arif, M.; Ilyas, M.; Riaz, M.; Ali, K.; Shah, K.; Ul Haq, I.; Fahad, S. Biochar improves phosphorus use efficiency of organic-inorganic fertilizers, maize-wheat productivity and soil quality in a low fertility alkaline soil. *Field Crop. Res.* **2017**, *214*, 25–37. [CrossRef]
5. Song, D.; Xi, X.; Zheng, Q.; Liang, G.; Zhou, W.; Wang, X. Soil nutrient and microbial activity responses to two years after maize straw biochar application in a calcareous soil. *Ecotoxicol. Environ. Saf.* **2019**, *180*, 348–356. [CrossRef]
6. Yadav, V.; Jain, S.; Mishra, P.; Khare, P.; Shukla, A.K.; Karak, T.; Singh, A.K. Amelioration in nutrient mineralization and microbial activities of sandy loam soil by short term field aged biochar. *Appl. Soil Ecol.* **2019**, *138*, 144–155. [CrossRef]
7. Igalavithana, A.D.; Ok, Y.S.; Usman, A.R.A.; Al-wabel, M.I.; Oleszczuk, P.; Lee, S.S. The Effects of Biochar Amendment on Soil Fertility Could Biochar Be Used as a Fertilizer. In *Agricultural and Environmental Applications of Biochar: Advances and Barriers*; Guo, M., He, Z., Uchimiya, S.M., Eds.; Soil Science Society of America, Inc.: Madison, MA, USA, 2016; pp. 123–144.
8. De Melo Carvalho, M.T.; De Holanda Nunes Maia, A.; Madari, B.E.; Bastiaans, L.; Van Oort, P.A.J.; Heinemann, A.B.; Da Silva, M.A.S.; Petter, F.A.; Marimon, B.H.; Meinke, H. Biochar increases plant-available water in a sandy loam soil under an aerobic rice crop system. *Solid Earth* **2014**, *5*, 939–952. [CrossRef]
9. Lei, O.; Zhang, R. Effects of biochars derived from different feedstocks and pyrolysis temperatures on soil physical and hydraulic properties. *J. Soils Sediments* **2013**, *13*, 1561–1572. [CrossRef]
10. Zhang, Q.; Song, Y.; Wu, Z.; Yan, X.; Gunina, A.; Kuzyakov, Y.; Xiong, Z. Effects of six-year biochar amendment on soil aggregation, crop growth, and nitrogen and phosphorus use efficiencies in a rice-wheat rotation. *J. Clean. Prod.* **2020**, *242*, 118435. [CrossRef]
11. Xing, D.; Magdouli, S.; Zhang, J.; Koubaa, A. Microbial remediation for the removal of inorganic contaminants from treated wood: Recent trends and challenges. *Chemosphere* **2020**, *258*, 127429. [CrossRef] [PubMed]
12. Chica, A.; Artola, A.; Rosal, A.; Solé-Mauri, F.; Fernandez, F.; García, J.; Dios, M.; Díaz, M.; Ramón, G.; Font, X. De Residuo a Recurso, El camino hacia la Sostenibilidad. In *III. Recursos Orgánicos. Aspectos Agronómicos y Mediambientales. España. Capítulo 8: Enmiendas Orgánicas y de Nueva Generación: Biochar y Otras Biomoléculas*; Red Española de Compostaje, Ed.; Mundi-Prensa: Madrid, Spain, 2015; p. 290.
13. Jaizme-Vega, M.C. Los microorganismos rizosféricos: Bioindicadores de sostenibilidad en suelos de tomate en las Islas Canarias. *AE. Revista Agroecológica de Divulgación* **2015**, *20*, 18–19.
14. Alizadeh, V.; Shokri, V.; Soltani, A.; Yousefi, M.A. Effects of Climate Change and Drought-Stress on Plant Physiology. *Int. J. Adv. Biol. Biomed. Res.* **2014**, *2*, 468–472.
15. Barea, J.M.; Palenzuela, J.; Cornejo, P.; Sánchez-Castro, I.; Navarro-Fernández, C.; Lopéz-García, A.; Estrada, B.; Azcón, R.; Ferrol, N.; Azcón-Aguilar, C. Ecological and functional roles of mycorrhizas in semi-arid ecosystems of Southeast Spain. *J. Arid Environ.* **2011**, *75*, 1292–1301. [CrossRef]

16. Ruíz-lozano, J.M.; Perálvarez, C.; Aroca, R. The application of a treated sugar beet waste residue to soil modifies the responses of mycorrhizal and non mycorrhizal lettuce plants to drought stress. *Plant Soil* **2011**, 153–166. [CrossRef]

17. Jaafar, N.M. Biochar as a Habitat for Arbuscular Mycorrhizal Fungi. In *Mycorrhizal Fungi: Use in Sustainable Agriculture and Land Restoration. Soil Biology*; Solaiman, Z., Abbott, L., Varma, A., Eds.; Springer: Berlin/Heidelberg, Germany, 2014; Volume 41. [CrossRef]

18. Jaizme-Vega, M.C. Microorganismos funcionales del suelo. Su papel en el manejo ecológico de los secanos. In *Agricultura Ecológica en Secano. Soluciones Sostenibles en Ambientes Mediterráneos*; Ministerio de Medio Ambiente y Medio Rural y Marino, Ed.; Mundi-Prensa: Madrid, Spain, 2011; pp. 417–439.

19. Warnock, D.D.; Mummey, D.L.; McBride, B.; Major, J.; Lehmann, J.; Rillig, M.C. Influences of non-herbaceous biochar on arbuscular mycorrhizal fungal abundances in roots and soils: Results from growth-chamber and field experiments. *Appl. Soil Ecol.* **2010**, *46*, 450–456. [CrossRef]

20. Amendola, C.; Montagnoli, A.; Terzaghi, M.; Trupiano, D.; Oliva, F.; Baronti, S.; Miglietta, F.; Chiatante, D.; Scippa, G.S. Short-term effects of biochar on grapevine fine root dynamics and arbuscular mycorrhizae production. *Agric. Ecosyst. Environ.* **2017**, *239*, 236–245. [CrossRef]

21. Cobb, A.B.; Wilson, G.W.T.; Goad, C.L.; Grusak, M.A. Influence of alternative soil amendments on mycorrhizal fungi and cowpea production. *Heliyon* **2018**, *4*, e00704. [CrossRef]

22. LeCroy, C.; Masiello, C.A.; Rudgers, J.A.; Hockaday, W.C.; Silberg, J.J. Nitrogen, biochar, and mycorrhizae: Alteration of the symbiosis and oxidation of the char surface. *Soil Biol. Biochem.* **2013**, *58*, 248–254. [CrossRef]

23. Vanek, S.J.; Lehmann, J. Phosphorus availability to beans via interactions between mycorrhizas and biochar. *Plant Soil* **2015**, *395*, 105–123. [CrossRef]

24. Ameloot, N.; Sleutel, S.; Das, K.C.; Kanagaratnam, J.; de Neve, S. Biochar amendment to soils with contrasting organic matter level: Effects on N mineralization and biological soil properties. *GCB Bioenergy* **2015**, *7*, 135–144. [CrossRef]

25. Solaiman, Z.M.; Abbott, L.K.; Murphy, D.V. Biochar phosphorus concentration dictates mycorrhizal colonisation, plant growth and soil phosphorus cycling. *Sci. Rep.* **2019**, *9*, 1–11. [CrossRef]

26. Hammer, E.C.; Balogh-Brunstad, Z.; Jakobsen, I.; Olsson, P.A.; Stipp, S.L.S.; Rillig, M.C. A mycorrhizal fungus grows on biochar and captures phosphorus from its surfaces. *Soil Biol. Biochem.* **2014**, *77*, 252–260. [CrossRef]

27. Medynska-Juraszek, A.; Cwielag-Piasecka, I. Biochar as a growing media component. In *Biochar as a Renewable-Based Material: With Applications in Agriculture, the Environment and Energy*; Manyà, J.J., Gascó, G., Eds.; World Scientific Publishing Europe Ltd.: London, UK, 2021; pp. 85–104.

28. Sashidhar, P.; Kochar, M.; Singh, B.; Gupta, M.; Cahill, D.; Adholeya, A.; Dubey, M. Biochar for delivery of agri-inputs: Current status and future perspectives. *Sci. Total Environ.* **2020**, *703*, 134892. [CrossRef]

29. Medina Peñafiel, A. Estudio de la Interacción Entre Inoculantes Microbianos y Residuos Agroindustriales Biotransformados Para su uso en Estrategias de Revegetación y Bioremediación. Ph.D. Thesis, Universidad de Granada, Granada, Spain, 2006.

30. Videgain-Marco, M.; Marco-Montori, P.; Martí-Dalmau, C.; Jaizme-Vega, M.D.C.; Manyà-Cervelló, J.J.; García-Ramos, F.J. Effects of Biochar Application in a Sorghum Crop under Greenhouse Conditions: Growth Parameters and Physicochemical Fertility. *Agronomy* **2020**, *10*, 104. [CrossRef]

31. Jaizme-vega, M.C.; Rodríguez-romero, A.S. Integración de microorganismos benéficos (Hongos micorrícicos y bacterias rizosféricas) en agrosistemas de las Islas Canarias. *Agroecología* **2008**, *3*, 33–40.

32. Qayyum, M.F.; Haider, G.; Iqbal, M.; Hameed, S.; Ahmad, N.; ur Rehman, M.Z.; Majeed, A.; Rizwan, M.; Ali, S. Effect of alkaline and chemically engineered biochar on soil properties and phosphorus bioavailability in maize. *Chemosphere* **2021**, *266*. [CrossRef] [PubMed]

33. Warnock, D.D.; Lehmann, J.; Kuyper, T.W.; Rillig, M.C. Mycorrhizal responses to biochar in soil—Concepts and mechanisms. *Plant Soil* **2007**, *300*, 9–20. [CrossRef]

34. González, A.J.H. *Posibilidades de la Producción de Inóculo de Micorrizas Vesiculo-Arbusculares Sobre Sustratos Canarios de Origen Volcánico*; Trabajo fin de carrera Universidad de La Laguna: Tenerife, Spain, 1993; p. 124.

35. Etesami, H.; Maheshwari, D.K. Use of plant growth promoting rhizobacteria (PGPRs) with multiple plant growth promoting traits in stress agriculture: Action mechanisms and future prospects. *Ecotoxicol. Environ. Saf.* **2018**, *156*, 225–246. [CrossRef] [PubMed]

36. Pérez-De-Luque, A.; Tille, S.; Johnson, I.; Pascual-Pardo, D.; Ton, J.; Cameron, D.D. The interactive effects of arbuscular mycorrhiza and plant growth-promoting rhizobacteria synergistically enhance host plant defences against pathogen. *Sci. Rep.* **2017**, *7*, 1–10. [CrossRef]

37. Ordoñez, Y. Interacción sinérgica entre hongos formadores de micorrizas arbusculares—Pseudomonas fluorescens y su relación en la nutrición vegetal de fósforo. In *Trabajo de Grado, Magíster en Ciencias*; Facultad de Ciencias, Maestría en microbiología; Universidad Nacional de Colombia: Bogotá, Colombia, 2009.

38. Nadeem, S.M.; Imran, M.; Naveed, M.; Khan, M.Y.; Ahmad, M.; Zahir, Z.A.; Crowley, D.E. Synergistic use of biochar, compost and plant growth-promoting rhizobacteria for enhancing cucumber growth under water deficit conditions. *J. Sci. Food Agric.* **2017**, *97*, 5139–5145. [CrossRef]

39. Olander, L.P.; Vitousek, P.M. Regulation of soil phosphatase and chitinase activity by N and P availability. *Biogeochemistry* **2000**, *49*, 175–190. [CrossRef]

40. Treseder, K.K.; Vitousek, P.M. Effects of soil nutrient availability on investment in acquisition of N and P in Hawaiian rain forests. *Ecology* **2001**, *82*, 946–954. [CrossRef]

41. Dick, W.A.; Cheng, L.; Wang, P. Soil acid and alkaline phosphatase activity as pH adjustment indicators. *Soil Biol. Biochem.* **2000**, *32*, 1915–1919. [CrossRef]

42. Paz-Ferreiro, J.; Gascó, G.; Gutiérrez, B.; Méndez, A. Soil biochemical activities and the geometric mean of enzyme activities after application of sewage sludge and sewage sludge biochar to soil. *Biol. Fertil. Soils* **2012**, *48*, 511–517. [CrossRef]

43. Masto, R.E.; Kumar, S.; Rout, T.K.; Sarkar, P.; George, J.; Ram, L.C. Biochar from water hyacinth (Eichornia crassipes) and its impact on soil biological activity. *Catena* **2013**, *111*, 64–71. [CrossRef]

44. Khadem, A.; Raiesi, F. Response of soil alkaline phosphatase to biochar amendments: Changes in kinetic and thermodynamic characteristics. *Geoderma* **2019**, *337*, 44–54. [CrossRef]

45. Jin, Y.; Liang, X.; He, M.; Liu, Y.; Tian, G.; Shi, J. Manure biochar influence upon soil properties, phosphorus distribution and phosphatase activities: A microcosm incubation study. *Chemosphere* **2016**, *142*, 128–135. [CrossRef]

46. Tanure, M.M.C.; da Costa, L.M.; Huiz, H.A.; Fernandes, R.B.A.; Cecon, P.R.; Pereira Junior, J.D.; da Luz, J.M.R. Soil water retention, physiological characteristics, and growth of maize plants in response to biochar application to soil. *Soil Tillage Res.* **2019**, *192*, 164–173. [CrossRef]

47. Paneque, M.; De la Rosa, J.M.; Franco-Navarro, J.D.; Colmenero-Flores, J.M.; Knicker, H. Effect of biochar amendment on morphology, productivity and water relations of sunflower plants under non-irrigation conditions. *Catena* **2016**, *147*, 280–287. [CrossRef]

48. Aller, D.; Rathke, S.; Laird, D.; Cruse, R.; Hatfield, J. Impacts of fresh and aged biochars on plant available water and water use efficiency. *Geoderma* **2017**, *307*, 114–121. [CrossRef]

49. Sara, M.; Rouissi, T.; Brar, S.K.; Blais, J.F. *Life Cycle Analysis of Potential Substrates of Sustainable Biorefinery*; Elsevier Incorporation: Amsterdam, The Netherlands, 2016; ISBN 9780128029800.

50. Bashan, Y.; de-Bashan, L.E.; Prabhu, S.R.; Hernandez, J.P. Advances in plant growth-promoting bacterial inoculant technology: Formulations and practical perspectives (1998–2013). *Plant Soil* **2014**, *378*, 1–33. [CrossRef]

51. Hale, L.; Luth, M.; Crowley, D. Biochar characteristics relate to its utility as an alternative soil inoculum carrier to peat and vermiculite. *Soil Biol. Biochem.* **2015**, *81*, 228–235. [CrossRef]

52. Ghazi, A. Potential for Biochar as an Alternate Carrier to Peat Moss for the Preparation of Rhizobia Bio Inoculum. *Microbiol. Res. J. Int.* **2017**, *18*, 1–9. [CrossRef]

53. Liang, C.; Gascó, G.; Fu, S.; Méndez, A.; Paz-Ferreiro, J. Biochar from pruning residues as a soil amendment: Effects of pyrolysis temperature and particle size. *Soil Tillage Res.* **2016**, *164*, 3–10. [CrossRef]

54. Greco, G.; Videgain, M.; Di Stasi, C.; González, B.; Manyà, J.J. Evolution of the mass-loss rate during atmospheric and pressurized slow pyrolysis of wheat straw in a bench-scale reactor. *J. Anal. Appl. Pyrolysis* **2018**, *136*, 18–26. [CrossRef]

55. Porter, W.M. The "most probable number" method for enumerating infective propagules of vesicular arbuscular mycorrhizal fungi in soil. *Aust. J. Soil Res.* **1979**, *17*, 515–519. [CrossRef]

56. Sieverding, E. *Vesicular-Arbuscular Mycorrhiza Management in Tropical Agrosystems*; GTZ, D., Ed.; TZ-Verlagsgesellschaft: Eschborn, Germany, 1991.

57. De Prager, S. *Metodologías Básicas Para el Trabajo con Micorriza Arbuscular y Hongos Formadores de Micorriza Arbuscular*; Universidad Nacional de Colombia, Ed.; Universidad Nacional de Colombia: Palmira, Colombia, 2016; p. 139. ISBN 9789588095608.

58. Phillips, N.C.; Hayman, D.S. Improved procedures for clearing roots and staining parasitic and vesicular-arbuscular mycorrhizal fungi for rapid assessment to infection. *Trans. Br. Mycol. Soc.* **1970**, *55*, 158–161. [CrossRef]

59. McGonigle, T.P.; Miller, M.H.; Evans, D.G.; Fairchild, G.L.; Swan, J.A. A new method which gives an objective measure of colonization of roots by vesicular—Arbuscular mycorrhizal fungi. *New Phytol.* **1990**, *115*, 495–501. [CrossRef]

60. Gerdemann, J.W.; Nicholson, T.H. Spores of mycorrhizal Endogone species extracted from soil by wet sieving and decanthing. *Trans. Br. Mycol. Soc.* **1963**, *46*, 235–244. [CrossRef]

61. Oehl, F.; Sieverding, E.; Palenzuela, J.; Ineichen, K.; Alves da Silva, G. Advances in Glomeromycota taxonomy and classification. *IMA Fungus* **2011**, *2*, 191–199. [CrossRef]

62. Bawazir, A.M.A.; Shivanna, G.B.; Shantaram, M. Impact of Different Media for Growth and Production of Different Soluble Pigments in Actinomycetes Isolated from Soils of Hadhramout, Yemen. *Eur. J. Biomed.* **2018**, *5*, 615–619.

63. Yao, Q.; Gao, J.L.; Zhu, H.H.; Long, L.K.; Xing, Q.X.; Chen, J.Z. Evaluation of the potential of trap plants to detect arbuscular mycorrhizal fungi using polymerase chain reaction-denaturing gradient gel electrophoresis analysis. *Soil Sci. Plant Nutr.* **2010**, *56*, 205–211. [CrossRef]

64. Jaizme-vega, M.C. *Las Micorrizas, Una Estrategia Agroecológica Para Optimizar la Calidad de los Cultivos*; Universidad de la Laguna, Instituto Canario de Investigaciones Agrarias, Phytoma España S.L., Eds.; Phytoma España S.L.: Valencia—San Cristóbal de la Laguna (Tenerife), Spain, 2019; p. 112. ISBN 978-84-946691-5-6.

65. Tabatabai, M.A.; Bremner, J.M. Use of p-nitrophenyl phosphate for assay of soil phosphatase activity. *Soil Biol. Biochem.* **1969**, *1*, 301–307. [CrossRef]

The Effects of Biochar on Indigenous Arbuscular Mycorrhizae Fungi from Agroenvironments

María Videgain-Marco, Pedro Marco-Montori, Clara Martí-Dalmau, M. Carmen Jaizme-Vega, Joan Josep Manyà-Cervelló and Francisco Javier García-Ramos

SUPPLEMENTARY MATERIAL

Table S1. Proximate, elemental and physicochemical analyses of biochar produced at two different temperatures (400°C — B400 and 600 °C — B600).

Proximate			Elemental (wt. % in daf[1] basis)[2]			
	B400	**B600**			**B400**	**B600**
Ash (wt. % in dry basis)	6.45 ± 0.14	10.02 ± 0.81	C		71.50 ± 0.48	82.89 ± 0.33
			H		4.46 ± 0.19	1.95 ± 0.08
Moisture (wt. %)	0.57 ± 0.22	3.05 ± 0.34	N		1.58 ± 0.10	1.52 ± 0.01
			O		22.42 ± 0.77	13.63 ± 0.31
Volatile matter (wt. % in dry basis)	22.03 ± 0.01	2.39 ± 0.71	Surface area and pore volume			
			S_{bet} (m^2 g^{-1})		105.8	227.5
Fixed carbon (wt. % in dry basis)	70.88 ± 6.45	84.54 ± 1.32	V_{total} (cm^3 g^{-1})		0.0370	0.0819
			V_{ultra} (cm^3 g^{-1})		0.0361	0.0816

Physicochemical analyses (organic amendment reference)

Principal nutrients	Method	Unit	Result B400	B600	Secondary nutrients	Method	Unit	Result B400	B600
N_{total} Kjeldahl	MT-FER-001	wt %	1.40	1.20	Ca_{total} (CaO)	ICP-OES	wt %	2.90	3.80
P_{total} (P_2O_5)	VISIB. ULTR.	wt %	2.08	2.45	Mg_{total} (MgO)	ICP-OES	wt %	0.68	0.79
K_{total} (K_2O)	ICP-OES	wt %	1.70	2.10	Na_{total} (Na_2O)	ICP-OES	mg kg^{-1}	850.00	540.00

Microel.	Method	Unit	Result B400	B600	Phys-Chem	Method	Unit	Result B400	B600
Fe_{total}	ICP-OES	mg kg^{-1}	280	210	SOM	Calcin.	wt %	86.40	85.40
Co_{total}	ICP-OES	mg kg^{-1}	43	38	Apparent density		g $(cm^3)^{-1}$	0.33	0.40
Mn_{total}	ICP-OES	mg kg^{-1}	100	102	Soil water retention	Gravim.	v %	14.16	18.35
Zn_{total}	ICP-OES	mg kg^{-1}	145	135	pH (1:2.5)	Potenc.		8.6	8.57

[1] Dry-ash-free.

[2] Oxygen is calculated by difference.

Table S2. Results from physicochemical fertility analyses of soils collected for the agronomic test (S1—soil 1: sandy-loam; S2—soil 2: clay-loam).

Determination	Method	Unit	S1	S2
pH (1 : 2.5 water)	Potenciometry		8.0 ± 0.5	8.4 ± 0.5
Electrical conductivity (1 : 5)	Electrometry	dS m^{-1}	0.2 ± 0.03	0.2 ± 0.03
Oxidable organic matter	Espectrofotometry	wt. %	3.04 ± 0.38	1.70 ± 0.21
N (N-NO$_3$)	Espectrofotometry	mg kg^{-1}	59 ± 8	12 ± 2
P (Olsen)	Espectrofotometry	mg kg^{-1}	32 ± 3	29 ±3
K	AAS	mg kg^{-1}	232 ± 39	88 ± 15
Mg	AAS	mg kg^{-1}	160 ± 33	252 ± 52
Water holding capacity	Gravimetry	v %	5.41	10.22

Table S3. Average values and standard deviation (in brackets) of the effect of growing substrate texture, biochar temperature and application rate on the identified genera of AMF, culturing microbial communities and phosphatase activity in a pot sorghum crop experiment

(B400 – Biochar 400 °C; B600 – biochar 600 °C; app. rate D1 – 1.5 wt. %; app. rate D2 – 3 wt. %; G: *Gigaspora* spp.; S: *Scutellospora* spp.; G: *Glomus* spp.; A: *Acaullospora* spp.).

Variable measured		Sandy-loam substrate					Clay-loam substrate				
		Control	**B400**		**B600**		**Control**	**B400**		**B600**	
			D1	**D2**	**D1**	**D2**		**D1**	**D2**	**D1**	**D2**
Identified genera of AMF %		16 G (5) 2 S (2) 82 G (3)	15 G (9) 6 S (4) 79 G (6)	15 G (7) 5 S (3) 80 G (12)	18 G (6) 6 S (4) 76 G (14)	16 G (5) 3 S (0) 81 G (11)	7 A (2) 93 G (3)	10 A (3) 90 G (9)	5 A (3) 95 G (8)	6 A (1) 94 G (6)	4 A (1) 96 G (4)
Microbial communities log cfu g^{-1}	MAM	7.49b (0.22)	8.12a (0.45)	8.48a (0.31)	8.27a (0.35)	7.90a (0.06)	8.04 (0.13)	8.26 (0.25)	7.93 (0.08)	7.87 (0.27)	7.98 (0.08)
	PS	5.42b (0.65)	6.49a (0.14)	6.65a (0.41)	6.37ab (0.19)	6.38ab (0.14)	6.17 (0.19)	5.95 (0.04)	5.61 (0.44)	5.88 (0.33)	5.79 (0.17)
	ACT	6.44 (0.08)	6.29 (0.36)	6.47 (0.31)	6.24 (0.13)	6.31 (0.25)	6.60 (0.06)	6.40 (0.18)	6.13 (0.35)	6.18 (0.09)	5.83 (0.66)
	M	4.94 (0.14)	5.06 (0.04)	5.10 (0.10)	4.83 (0.24)	4.88 (0.18)	4.92 (0.09)	4.94 (0.17)	5.09 (0.41)	4.53 (0.32)	4.89 (0.29)
	Y	3.45 (0.55)	3.25 (0.43)	3.74 (0.68)	3.90 (0.37)	3.59 (0.55)	3.95 (0.27)	4.26 (0.36)	3.94 (0.24)	3.74 (0.13)	3.70 (0.64)
Phosphatasa activity µmol h^{-1} g^{-1} dry wt.	AcP	1.22ab (0.05)	1.08b (0.05)	1.21ab (0.06)	1.25ab (0.06)	1.37a (0.13)	1.54b (0.15)	1.40b (0.13)	1.45b (0.13)	1.21b (0.20)	2.21a (0.29)
	AlkP	2.23c (0.12)	2.45bc (0.07)	3.42bc (0.15)	3.12a (0.11)	2.75b (0.19)	3.81a (0.01)	2.58d (0.01)	3.67b (0.01)	3.10c (0.04)	3.70b (0.01)

Means within a row followed by different letters are significantly different for the same kind of growing substrate at $p \leq 0.05$ (Tukey's test).

Table S4. Pearson correlation and p-valor (in brackets) between AMF parameters and microbial communities in a sandy-loam substrate (PS: *Pseudomonas* genus; MAM: Mesophilic aerobic microorganisms).

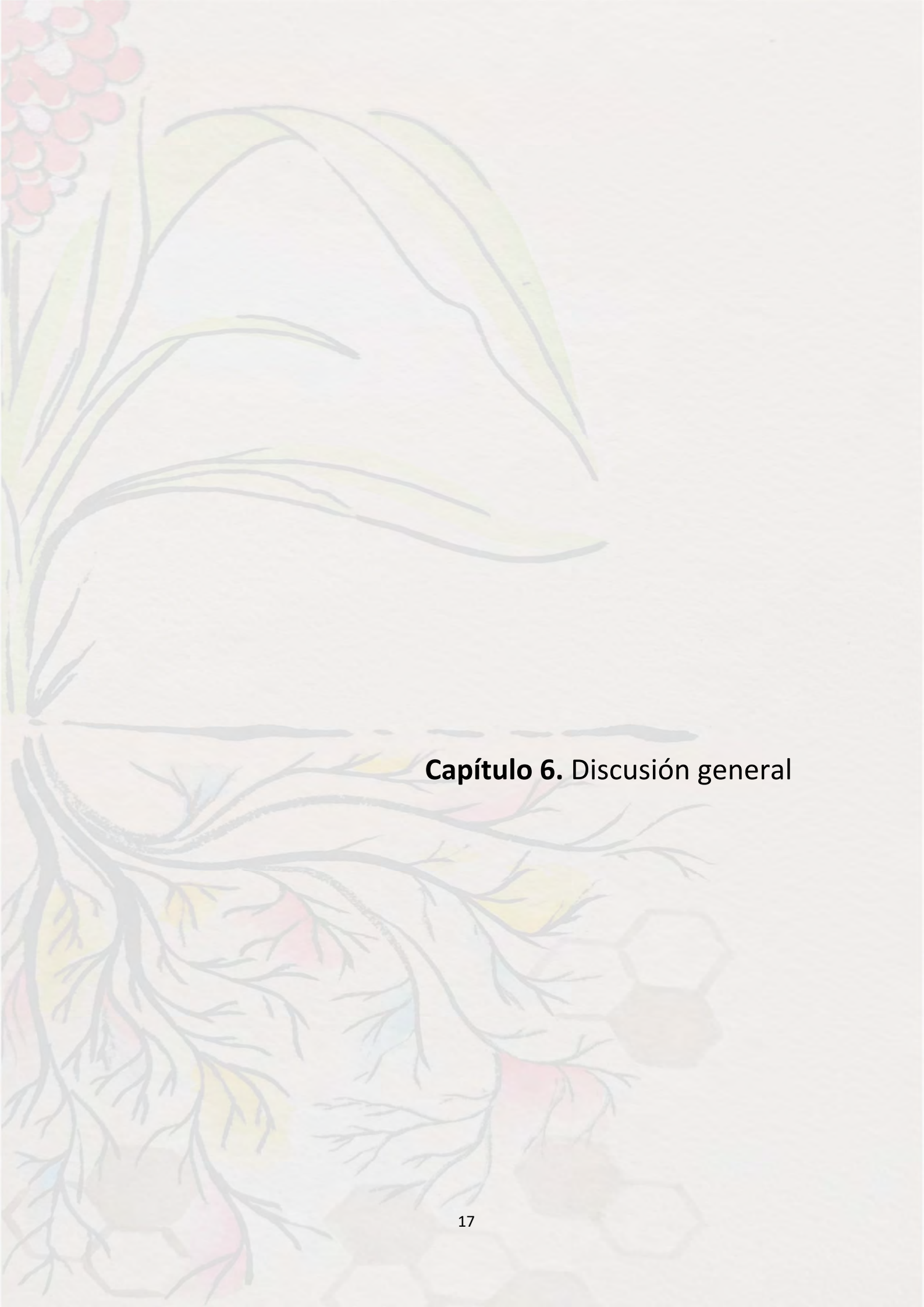|	Number of AMF spores	Root colonization D330	Root colonization D390	PS	MAM
Number of AMF spores	1				
Root colonization D$_{330}$	0,444 (0.097)	1			
Root colonization D$_{390}$	0,332 (0.226)	0.775** (0.001)	1		
PS	0,674** (0.006)	0.545* (0.035)	0.550* (0.034)	1	
MAM	0,731** (0.002)	0.568* (0.027)	0.539* (0.038)	0.697** (0.004)	1

* Statistically significant at p ≤ 0.05; *** Statistically significant at p ≤ 0.01.

Table S5. Effect of AMF inoculum addition on nutrient leaves of lettuce (400°C — B400 and 600 °C — B600; S1: sandy-loam growing substrate; S2: clay-loam growing substrate).

Nutrient	WID 1			WID 2		
	- AMF	+AMF	+B+AMF	- AMF	+AMF	+B+AMF
N-leaf	1.08 ± 0.05	1.10 ± 0.01	1.10 ± 0.03	-	1.11 ± 0.04	1.10 ± 0.03
P-leaf	0.04 ± 0.01	0.04 ± 0.01	0.04 ± 0.01	-	0.05 ± 0.01	0.04 ± 0.01
K-leaf	2.20 ± 0.15	2.21 ± 0.08	2.22 ± 0.09	-	2.18 ± 0.12	2.23 ± 0.06

Table S6. Additional information to section 4.3. Experimental designs and agronomic tests establishment.

Experiment	Additional information
1	- Hewitt nutritive solution with minimum phosphorus concentration (P⁻) was added to water the plants (composition 1 L: 0.4044 g NO3K; 0.9446 g NO3Ca·4H2O; 0.3697 g SO4Mg·7H2O; 0.027 g PO4H2K; 0.0421 g Na EDTA-Fe; 0.00223 g SO4Mn·4H2O; 0.00309 g BO3H3; 0.000288 g SO4Zn·2H2O, and 0.00025 g SO4Cu·5H2O). The last 15 days of the bioassay, the plants were not irrigated, with the aim of stressing the crop and favoring the production of AMF spores. - Sorghum crop completed two production cycles. Since sorghum is a crop with re-sprouting capacity, plants were cut about 2 cm from the growing substrate surface at 92 days after sowing. At that time, basil plants were allowed to grow until new sorghum leaves exceeded the height of basil. 156 days after sowing, plants were cut and substrates separated from the containers. Each substrate was processed cutting sorghum and basil roots in 1-2 cm pieces and remixing with the solid substrate itself; large biochar fragments (> 2 cm) still presents in the mixture were grinded up to sizes smaller than 5 mm. Solid substrates samples were stored in plastic jars for analysis and use in Experiment 3. - Both soil types were mixed with sterilized fine gravel (60:40 v/v) to avoid soil compaction in the containers forming two final mixtures in which biochar was homogeneously incorporated. The proportions of particle size obtained after the mechanical processing explained in section 4.1 were maintained. - Temperature and relative humidity were monitored with a sensor HOBO Pro v2 (Onset, Boune, MA, USA) installed at the plants level. It allowed to adjust the intervals and irrigation rates during the bioassay, considering crop evapotranspiration. Temperatures in this experiment ranged from 2.6 °C minimum winter temperatures to 37.0 °C maximum summer temperatures. Relative humidity ranged from 33.4% to 90.0%. Greenhouse was naturally lighted, with regular variations throughout the year from 9h light in winter months to 15 h light in summer months.
2	- The composition of solid substrates in treatments T0 and T1 was as follows: T1 (40% w/w soil S1; 40% w/w fine gravel; 20% w/w peat substrate: 25% white peat/ 55% black peat/ 17% coconut fiber/ 3% pearlite); T2 (40% w/w soil S1; 38.5% w/w fine gravel; 1.5% w/w B400; 20% peat substrate). - Fine gravel was washed with water and sterilized in autoclave for 20 min. In order to eliminate possible mycorrhizal propagules in peat substrate, it was autoclaved under flowing steam conditions during 1 h and three consecutive days. - Hewitt nutritive solution was added as described for Experiment 1 for all the irrigation events. - Temperature and relative humidity were monitored as described for Experiment 1. - Temperatures in this experiment ranged from 4.5 °C minimum spring temperatures to 42.0 °C maximum summer temperatures. Relative humidity ranged from 41.3% to 92.0%. Greenhouse was naturally lighted, with regular variations throughout the year from 11h light in March to 15 h light in July.
3	- Growing media composition was as follows: -AMF: 50% sterile soil S1 + 50% sterile fine gravel (to avoid compaction) + 1 ml filtered S1 solution to restitute microbial activity; +AMF: 50% soil S1 + 50% sterile fine gravel + AMF inoculum obtained from T0 in Experiment 2; +B+AMF: 50% soil S1 + 50% sterile fine gravel + AMF inoculum obtained from T1 in Experiment 2. - Hewitt nutritive solution was added as described for Experiment 1 but, in this experiment, it was added only in the irrigation events in which all the treatments were irrigated, and the same amount of nutrients was maintained for all the treatments. - Temperature and relative humidity were monitored as described for Experiment 1. - Temperatures in this experiment ranged from 16.0 °C minimum summer temperatures to 41.3 °C maximum summer temperatures. Relative humidity ranged from 59.7% to 92.0%. Greenhouse was naturally lighted, with regular variations throughout the year from 14h light at the beginning of the experiment to 13 h light at the end of the experiment.

Capítulo 6. Discusión general

Las líneas de trabajo desarrolladas y expuestas en este documento han reportado resultados de interés en relación a los objetivos inicialmente propuestos.

6.1. Objetivos 1 y 2 (idoneidad de las biomasas seleccionadas y análisis de las propiedades del biochar)

A lo largo del trabajo se testó la viabilidad de diferentes biomasas seleccionadas como precursoras de biochar y se compararon sus características fisicoquímicas en función de las condiciones experimentales de pirólisis. La selección inicial de biomasas de distinta morfología y composición (sarmiento de viña - VS, paja de trigo peletizada - WS, rastrojo de maíz - CS) permitió obtener biochars claramente diferentes y optar por la tipología de precursor y condiciones de pirólisis de mayor interés para los ensayos posteriores (Capítulo 2).

A través de la caracterización de las biomasas iniciales se observaron mayores niveles de carbono fijo en los residuos de sarmiento de viña en comparación con las otras biomasas. Este resultado se relacionó claramente con el mayor contenido de lignina obtenido en el análisis de los constituyentes principales (Antal et al., 2000; Collard et al., 2014).

El objetivo inicial de los experimentos fue el de estudiar el efecto de los tres principales factores que regulan el proceso de pirólisis (temperatura final, presión absoluta y tiempo de residencia de la fase vapor en el interior del reactor) sobre una selección de variables respuesta (rendimiento a producto, contenido de carbono fijo y cenizas, relación O:C y H:C, superficie específica y tamaño de ultramicroporo). En línea con publicaciones previas (Manyà et al., 2018; Azuara et al., 2017), la temperatura final de pirólisis resultó ser el factor que más afectó a todas las variables analizadas. El importante efecto observado sobre el rendimiento a producto, el contenido de carbono fijo y la porosidad del producto obtenido permitió seleccionar el biochar producido a partir de sarmiento de viña como el más apropiado para ensayos de aplicación en el suelo.

En la práctica, no fue posible realizar los experimentos con tiempos de residencia cortos (50 s) para WS y CS debido a la obstrucción producida en los conductos de salida del reactor, dando lugar a una sobrepresión excesiva. En este sentido, este fue un resultado inesperado interesante, a tener en cuenta en experimentos posteriores, con el objetivo de establecer condiciones de pirólisis razonables desde un punto de vista práctico.

En el caso del sarmiento de viña, los efectos significativos en las variables respuesta debido a las diferentes presiones y tiempos de residencia adoptados fueron marginales. El análisis de elementos inorgánicos en las cenizas de las biomasas reveló la significativa presencia de especies como K, Ca y Mg en todas las biomasas estudiadas, con diferencias entre ellas. La importancia de cuantificar estos elementos en la biomasa inicial radica en la gran actividad que presentan las especies metálicas alcalinas y alcalinotérreas durante el proceso de pirólisis. Dichas especies —especialmente el K— catalizan la descomposición térmica primaria (Abián et al., 2017; Safar et al., 2019) y, al mismo

tiempo, promueven las reacciones secundarias de los volátiles, dando lugar a mayores rendimientos de producto sólido (biochar) y gases permanentes.

El desarrollo de ensayos centrado en residuos de poda (Capítulo 3) permitió comparar las características iniciales del sarmiento de viña y los restos jóvenes de poda de encina, así como la variación de estas características tras la conversión a biochar bajo dos tipos de temperatura final de pirólisis. A través del análisis de los constituyentes principales de las biomasas se constató un contenido en lignina menor al esperado para este tipo de residuos, lo que se relacionó con la selección de restos de poda de partes jóvenes de las plantas, con un bajo grado de lignificación. Teniendo en cuenta que el contenido de lignina es el constituyente que contribuye en un mayor grado al rendimiento a producto en el proceso de producción de biochar (Collard y Blin, 2014), se observaron diferencias acordes a ello para los dos tipos de biomasa.

En línea con los primeros experimentos desarrollados en el Capítulo 2, en el estudio del Capítulo 3 se confirmó de nuevo la relación directa entre la temperatura final de pirólisis y el contenido de carbono fijo obtenido en los biochars. Las diferencias observadas en el análisis inicial de estas dos biomasas fueron mínimas, y las características de los biochars producidos fueron principalmente influenciadas por la temperatura final de pirólisis. En ambos tipos de biomasa y biochars producidos destacó la presencia de Ca, entre todos los elementos inorgánicos, que presenta cierta capacidad para inhibir parcialmente la degradación de la hemicelulosa (Haddad et al., 2017).

Desde un punto de vista agronómico, la cuantificación de los elementos inorgánicos en la biomasa inicial y su relación con los contenidos detectados en los biochars producidos, resulta de gran interés, puesto que se trata de elementos nutrientes para las plantas que incrementan el interés de la enmienda orgánica producida. En el Capítulo 4 se presentan los resultados del análisis fisicoquímico del biochar producido a partir de sarmiento de viña bajo dos temperaturas finales de pirólisis. Este análisis fisicoquímico se realizó con la metodología de referencia que se aplica a cualquier enmienda orgánica en un laboratorio agroalimentario. Los resultados obtenidos mostraron lo que, bajo una interpretación de analítica de enmienda orgánica ordinaria, supondrían mínimas diferencias entre biochars producidos a diferentes temperaturas finales de pirólisis.

La capacidad de retención de agua de los biochars obtenidos de residuos de poda, analizada por gravimetría a través del método de Placas Richards y cuyos resultados se han expuesto en los Capítulos 3 y 4, ofreció una información indispensable, tanto para los estudios posteriores de caracterización mecánica, como de aplicación de biochar al suelo. En general, la capacidad de retención de agua aumentó con la temperatura final de pirólisis y, por lo tanto, con la superficie específica y el volumen de poro, resultados acordes con descripciones previas (Teixeira et al., 2021). Valores particularmente bajos, como el detectado en el biochar producido a partir de restos de encina a 400 °C se relacionaron con valores altos de material volátil presente en las muestras y con la estructura desintegrada que presentó esta muestra, como se explica en el siguiente apartado.

Como continuación de los resultados de caracterización física expuestos en el Capítulo 3, los parámetros físicos medidos (masa, longitud, volumen, diámetro, coeficiente forma de los fragmentos y densidad aparente) resultaron influenciados significativamente por el tipo de biomasa de partida, aunque se observó una interacción con la temperatura final de pirólisis en todos los parámetros. En general, se obtuvieron mayores valores en los biochars producidos a partir de restos de encina. Entre los parámetros medidos, la densidad aparente es de especial interés en las aplicaciones al suelo, tanto por la información relacionada con las unidades fertilizantes aplicadas, como por la necesidad de calibrar adecuadamente la maquinaria utilizada para su aplicación. Los valores de densidad aparente tomados en fragmentos individuales de biochar procedente de residuos de poda difirieron de los obtenidos en muestras compuestas, especialmente en el caso del biochar procedente de sarmiento de viña, lo que se relacionó con una subestimación del volumen medido a través del método de desplazamiento de agua por inmersión de fragmentos. En este sentido, se considera recomendable ampliar la información y complementar las medidas de este estudio a través de otros métodos como la picnometría con helio combinada con la determinación de la densidad por desplazamiento de una suspensión granular (Brewer et al., 2014). Además, un estudio en profundidad sobre la posible hidrofobicidad de cada tipo de biochar ayudaría a validar en mayor medida los resultados obtenidos.

6.2. Objetivo 3 (comportamiento mecánico del biochar)

Respecto al comportamiento mecánico del biochar estudiado en el Capítulo 3, los biochars producidos a partir de restos de poda de encina resultaron significativamente más resistentes que los de sarmiento de viña, independientemente de la temperatura final de pirólisis adoptada. Estos resultados se relacionaron con el mayor contenido en lignina (aunque discreto) de los residuos de encina, así como con la mayor densidad aparente, lo que encaja con los resultados de otros autores que correlacionaron positivamente estos parámetros (Kumar et al., 1999; de Abreu Neto, 2018). Los resultados en algunos estudios previos (Zickler et al., 2006; Dias Junior et al., 2020; Xie et al., 2021) mostraron una correlación positiva entre la temperatura final de pirólisis y la resistencia a esfuerzos mecánicos de los chars producidos. Durante la aplicación de fuerzas estáticas sobre los fragmentos de biochar, en este trabajo se observó una tendencia en esta línea, con valores de resistencia medios que se incrementaron con el aumento de la temperatura. Sin embargo, las diferencias no resultaron estadísticamente significativas ($\alpha = 0,05$) en el rango de temperaturas seleccionado. Bajo la aplicación de fuerzas dinámicas (ensayos de impacto), el comportamiento de los fragmentos de biochar de sarmiento producidos bajo dos temperaturas de pirólisis distintas fue similar.

El texturómetro, utilizado normalmente para el análisis de propiedades físicas de alimentos, resultó una herramienta adecuada para evaluar la resistencia a esfuerzo cortante y a compresión de este tipo de biochar, teniendo en cuenta sus características físicas y el tamaño de fragmentos adoptado en este estudio. Otro tipo de herramientas serían necesarias para evaluar estas propiedades en biochars producidos en tamaño de

partícula fino, o procedentes de residuos herbáceos u otros materiales orgánicos que no presenten una morfología homogénea.

Los ensayos de simulación de procesado mecánico del biochar bajo distintas condiciones de humedad aportaron información interesante para planificar aportaciones al suelo en condiciones reales. Aportar humedad al biochar es una práctica recomendada para evitar la generación de polvo y la consecuente emisión de partículas finas a la atmósfera en el proceso de aplicación (International Biochar Initiative, 2015); no obstante, no hay recomendaciones específicas para cada tipo de biochar. Tanto la biomasa, como la temperatura, y el tipo de proceso realizado, tuvieron efectos significativos en la distribución de los tamaños de partícula. También, se observaron interacciones entre los distintos factores. En general, los valores de generación de partículas finas y pérdidas por emisión de polvo fueron muy inferiores a los reportados en estudios anteriores para biochars producidos en condiciones de pirólisis rápida (Major, 2010). El análisis estadístico de cada muestra por separado permitió observar comportamientos muy diferentes de cada tipo de biochar bajo distintas condiciones de humedad. El biochar procedente de residuos de poda de encina generó mayor cantidad de partículas finas, especialmente en el caso particular del biochar producido a menor temperatura (que previamente había mostrado los valores más altos de contenido en volátiles y menor capacidad de retención de agua). Esta muestra no pudo retener el contenido de humedad seleccionado (15%), probablemente debido su microestructura desintegrada (Das et al., 2015), lo que dio lugar a una desagregación de los fragmentos durante el procesado mecánico y una mayor generación de partícula fina que, aunque no se desprendió al ambiente, se recogió en el proceso de filtrado. En condiciones reales de aplicación, esto supondría una posible percolación de partículas finas, cuya repercusión ambiental podría resultar considerable.

6.3. Objetivo 4 (aplicación de biochar y desarrollo de un cultivo modelo)

En el Capítulo 4 se ha presentado el trabajo realizado para evaluar el efecto del biochar producido a partir de sarmientos de viña sobre el desarrollo de un cultivo de sorgo en condiciones de invernadero. De forma previa al desarrollo del bioensayo, se realizó un test de fitotoxicidad del biochar para la germinación de diferentes especies. Los resultados de este test variaron mucho en función de la especie seleccionada, mostrando valores de moderada fitotoxicidad únicamente en el caso del biochar producido a mayor temperatura (600 °C) para semillas de berro y de lechuga. El resto de muestras presentaron un efecto neutro o ligeramente fitoestimulante. Concretamente, sobre las semillas de sorgo, que se evaluaron con interés para el posterior establecimiento del bioensayo, el efecto fue neutro para ambas temperaturas de producción del biochar. En otros estudios realizados en el seno del grupo de investigación, enfocados al análisis de la presencia de compuestos policíclicos aromáticos en la superficie de biochars derivados de madera (Greco, 2021), quedó patente el efecto positivo del lavado con agua de las muestras de biochar sobre la germinación de algunas especies de semillas. Sin embargo, en las muestras estudiadas

en este trabajo no se consideró indispensable, teniendo en cuenta los resultados obtenidos.

En el ensayo con sorgo en condiciones de invernadero, se estudió el efecto de varios factores sobre la biomasa generada por el cultivo (diferenciada entre parte aérea, parte radicular y grano). En primer lugar, el tipo de suelo que conformó los sustratos de cultivo: se seleccionaron dos suelos con texturas muy diferenciadas; en segundo lugar, dos niveles de temperatura final de pirólisis del biochar; por último, dos dosis diferenciadas de aplicación, más un tratamiento control sin biochar. La capacidad de rebrote del sorgo permitió estudiar dos ciclos completos de desarrollo, no observándose diferencias significativas en el desarrollo de las plantas ni en su producción durante el primer ciclo. En otros estudios de corta duración bajo condiciones de invernadero, algunos autores habían detectado previamente efectos significativos derivados de la adición de biochar (Gale et al., 2019; Kloss et al., 2014; Laghari et al., 2015; Mohamed et al., 2019), pero en nuestro estudio fueron necesarios dos ciclos de cultivo para detectar diferencias significativas en alguna de las variables estudiadas. En el segundo ciclo de cultivo, se observó que la textura del suelo fue el factor que influyó en mayor medida sobre la biomasa total producida. Paralelamente, se detectaron efectos significativos derivados de la temperatura de producción de biochar y de la dosis de aplicación en la biomasa radicular generada, lo que no se pudo comprobar en el primer ciclo, ya que se dejaron intactas las raíces en los contenedores para su rebrote. El análisis separado de cada suelo permitió detectar un efecto positivo de la adición de biochar producido a 400 °C sobre la biomasa radicular generada por el cultivo en el suelo de textura franco-arenosa. Además, se constató un mayor número de plantas que produjeron grano bajo la aplicación de este tipo de biochar. Estos resultados están en línea con los reportados por otros autores (Alotaibi y Schoenau, 2019; Laghari et al., 2015; Olmo et al., 2016; Butnan et al., 2015), aunque no se observó la dependencia de la dosis observada en otros estudios (Gale and Thomas, 2019).

Para ambos tipos de sustrato, se observó un incremento significativo de la capacidad de retención de agua con la aplicación de biochar. Si bien dicho aumento ya había sido previamente descrito en numerosos estudios (Guo et al., 2016; Ali et al., 2019; Sun et al., 2014), en el presente trabajó se observó que la retención de agua aumentó con la temperatura final de pirólisis del biochar aplicado, lo que resultó acorde a los datos previos de retención de agua registrados en los análisis de las muestras individuales de biochar. La dosis de aplicación únicamente tuvo un efecto significativo en el sustrato de textura franco-arcillosa.

De acuerdo a estudios previos (Buss et al., 2014; Liu y Zhang, 2014; Lehmann et al., 2003; Hailegnaw et al., 2019; Al-Wabel et al., 2018), la aplicación de biochar tiene una fuerte influencia en la disponibilidad de nutrientes esenciales. En este trabajo se observaron incrementos significativos en el contenido de K, Ca, Mg en el sustrato, y sus relaciones, especialmente con la adición de biochar producido a 600 °C, en los dos tipos de sustratos estudiados. Sin embargo, la aplicación de biochar no fue suficiente para evitar los signos

de deficiencias nutricionales mostrados por las plantas, por lo que se tuvo que regar el ensayo con una solución nutritiva que pudo enmascarar algunos de estos resultados.

6.4. Objetivo 5 (efecto del biochar en la actividad biológica del suelo)

El primer experimento del trabajo presentado en el Capítulo 5 complementa los resultados descritos en el apartado anterior, evaluando el efecto de la adición de biochar sobre algunos indicadores de la actividad biológica del suelo (porcentaje de micorrización de las plantas a lo largo del ciclo de cultivo, contenido en esporas de micorrizas arbusculares de los sustratos, variaciones en las poblaciones de comunidades microbianas cultivables y actividad de la enzima fosfomonoesterasa).

Los resultados de estudios previos en los que se evalúa la influencia del biochar sobre la actividad de los hongos formadores de micorrizas son muy variados y dependientes de las condiciones experimentales, la composición del biochar y su tamaño de partícula (Jaafar, 2014; Warnock et al., 2010; Amendola et al., 2017; Cobb et al., 2018; LeCroy et al., 2013). En este trabajo se observó un efecto positivo de la adición de biochar procedente de sarmiento de viña a 400 °C sobre el grado de micorrización de las plantas de sorgo, y en las dos texturas de sustrato analizadas. Además, la adición de este tipo de biochar también incrementó el número de esporas en el sustrato de textura franco-arenosa. Estos resultados están en línea con los publicados por otros autores (LeCroy, 2013; Ameloot et al., 2015; Solaiman et al., 2019), que observaron un aumento de la actividad de las micorrizas arbusculares con la adición de biochar en sus ensayos. Los resultados obtenidos en estos análisis se relacionan positivamente con los obtenidos en las medidas de biomasa radicular descritos en el apartado anterior. Sin embargo, la alta actividad micorrícica y la generación de mayor biomasa radicular no se tradujo en un mayor rendimiento de las plantas testadas. Teniendo en cuenta los mecanismos de interacción biochar-micorrizas explicados en el trabajo de Warnock et al. (2010), los resultados positivos obtenidos por la aplicación de biochar producido a 400 °C probablemente se deban a los mayores contenidos en elementos volátiles de esta muestra, así como con el aumento de los valores de retención de agua en este sustrato.

En relación con el estudio de los microorganismos cultivables en ambos tipos de sustrato, se observó una interacción positiva entre la adición de biochar producido a 400 °C y la población de *Pseudomonas* genus, lo que representa un resultado muy positivo, teniendo en cuenta la interacción positiva entre este tipo de bacterias promotoras del crecimiento vegetal y las micorrizas arbusculares (Medina, 2006; Etesami, 2018; Pérez-De-Luque, 2017). La adición de biochar afectó en menor medida la actividad del resto de comunidades microbianas estudiadas. En este sentido, un estudio de mayor duración podría aportar resultados diferentes, de acuerdo a Yadav et al. (2019), el biochar de reciente producción no ofrece una fuente de recursos carbonosos de fácil acceso a los microorganismos, por lo que las variaciones observadas podrían ser mayores con el tiempo.

Con respecto a la actividad de la enzima fosfomonoesterasa, no se pudo establecer una tendencia general de comportamiento en función de la aplicación de biochar o la dosis de ésta. Se observó un efecto en el sustrato de textura franco-arenosa por la aplicación del biochar producido a alta temperatura final de pirólisis. Sin embargo, este resultado difiere de otros estudios previos, en los que se relacionaba inversamente la actividad de esta enzima con la temperatura de pirólisis (Khadem y Raiesi, 2019; Jin et al., 2016). Los resultados obtenidos en este trabajo podrían ser complementados con estudios que evaluaran en profundidad la relación entre la actividad de esta enzima con la disponibilidad de fósforo en el suelo y las variaciones de pH a lo largo del experimento.

En el experimento 2 de este trabajo se evaluó la idoneidad del biochar como componente del sustrato de cultivo en el proceso de multiplicación del consorcio de micorrizas arbusculares de uno de los suelos estudiados en el experimento anterior. Se obtuvieron de nuevo niveles de micorrización mayores en el tratamiento con biochar con respecto al de control, así como un mayor número de esporas y de propágulos micorrícicos, por lo que la aplicación de biochar tuvo un efecto muy positivo en este proceso. La utilidad del biochar como sustrato portador de inóculo había sido previamente demostrada (Sashidhar et al., 2020; Hale et al., 2015; Ghazi, 2017). Los estudios consultados normalmente trabajan con inóculos comerciales y no con consorcios nativos del suelo; por lo tanto, este puede ser un hallazgo novedoso del presente trabajo, aunque los resultados son específicos de las condiciones estudiadas.

Los beneficios de la aplicación del inóculo producido (con y sin biochar) fueron evaluados en un tercer experimento en el que se sometieron plantas de lechuga a diferentes condiciones de estrés hídrico. Se observó un efecto positivo de la aplicación de inóculo micorrícico sobre las plantas sometidas a estrés, y en especial del inóculo producido con biochar, lo que confirmó la importancia de la conservación del potencial micorrícico de los suelos como estrategia de lucha contra el estrés abiótico y el interés del uso de biochar como componente del sustrato de cultivo para la reproducción de este tipo de microorganismos.
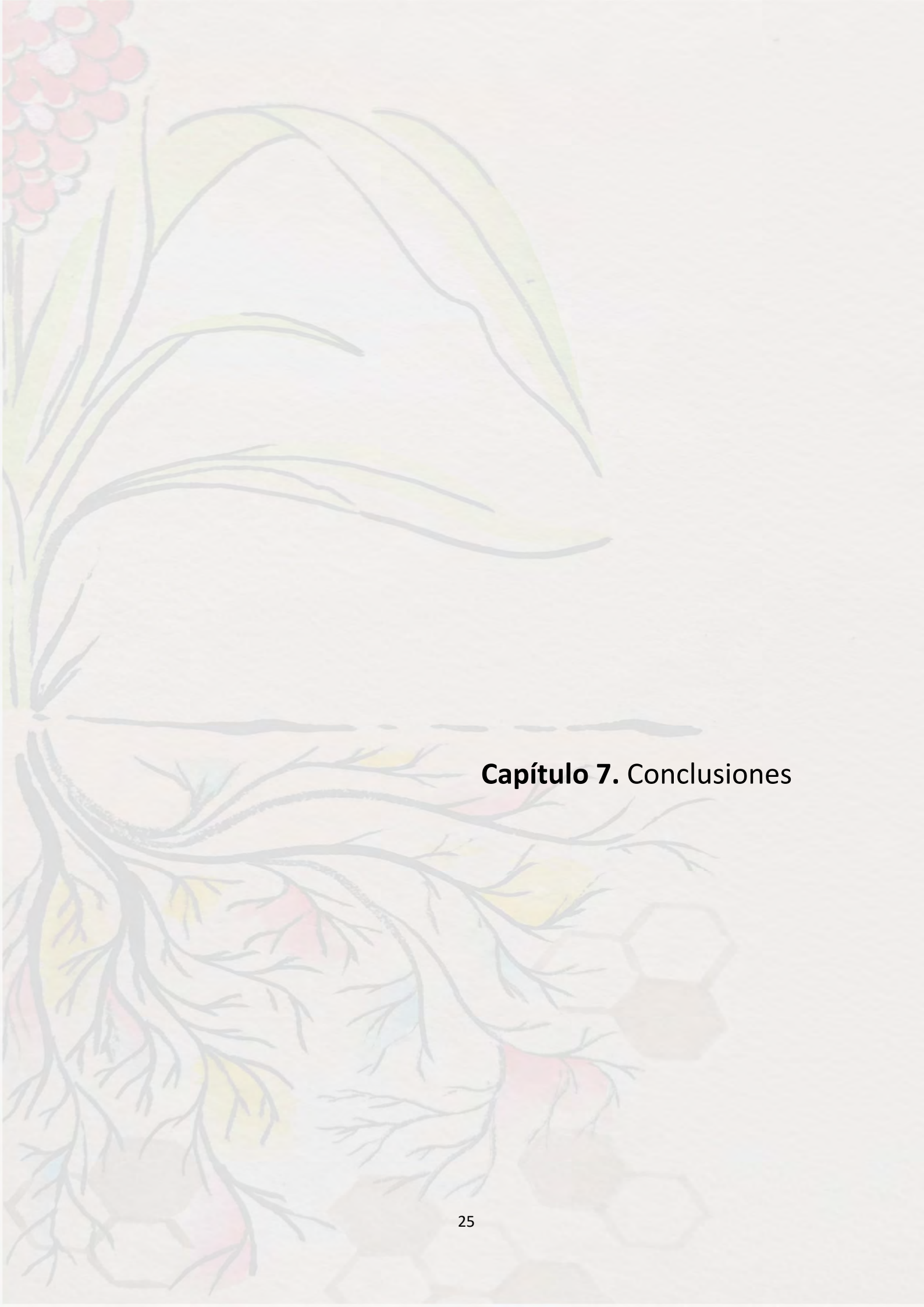
Capítulo 7. Conclusiones

Las conclusiones principales que pueden deducirse del presente trabajo son las siguientes:

1. Los residuos lignocelulósicos estudiados en este trabajo resultaron aptos para la producción de biochar a través de pirólisis lenta y presentaron características fisicoquímicas diferentes en función del tipo de biomasa y de las condiciones experimentales de pirólisis.

2. La temperatura final de pirólisis fue el parámetro que tuvo un mayor efecto sobre los rendimientos a producto de los biochars producidos y sobre las características fisicoquímicas evaluadas en los mismos.

3. El comportamiento mecánico de los biochars producidos a partir de restos de poda analizados en este estudio se vio influenciado en mayor medida por el tipo de biomasa seleccionada que por la temperatura final de pirólisis.

4. La humectación del biochar tuvo un efecto positivo en la prevención de formación de partículas finas, especialmente cuando el biochar presentó una estructura física estable y una relativamente elevada capacidad de retención de agua.

5. El biochar producido a partir de sarmientos de viña a una temperatura final de pirólisis de 400 °C tuvo un efecto positivo sobre la generación de biomasa radicular y el grado de micorrización de las raíces en plantas de sorgo desarrollado bajo condiciones de invernadero,

6. El biochar producido a partir de sarmientos de viña a una temperatura final de pirólisis de 400 °C tuvo un efecto positivo sobre el número de esporas de hongos formadores de micorrizas arbusculares y el número de unidades formadoras de colonias de *Pseudomonas* genus, analizados en el sustrato franco-arenoso de plantas de sorgo desarrolladas bajo condiciones de invernadero.

7. El biochar producido a partir de sarmientos de viña, independientemente de la temperatura final de pirólisis seleccionada, mejoró la capacidad de retención de agua de los sustratos estudiados y tuvo un efecto significativo sobre el nivel de algunos nutrientes en el suelo.

8. El biochar producido a partir de sarmientos de viña resultó un material adecuado como componente del sustrato de cultivo en el proceso de multiplicación de hongos formadores de micorrizas.

Bibliografía

Abián, M.; Alzueta, M. U.; Carvalho, A.; Rabaçal, M.; Costa, M. Role of Potassium and Calcium on the Combustion Characteristics of Biomass Obtained from Thermogravimetric Experiments. *Energy Fuels* 2017, 31, 12238–12246.

Albuquerque, J.A.; Sánchez, M.E.; Mora, M.; Barrón, V. Slow pyrolysis of relevant biomasses in the Mediterranean basin. Part 2. Char characterization for carbon sequestration and agricultural uses. *J. Clean Prod.* 2016, 120, 191–197.

Ali, K.; Wang, X.; Riaz, M.; Islam, B.; Khan, Z.H.; Shah, F.; Munsif, F.; Ijaz Ul Haq, S. Biochar: An eco-friendly approach to improve wheat yield and associated soil properties on sustainable basis. *Pakistan J. Bot.* 2019, 51, 1255–1261.

Alotaibi, K.D.; Schoenau, J.J. Addition of biochar to a sandy desert soil: Effect on crop growth, water retention and selected properties. *Agronomy* 2019, 9, 327.

Al-Wabel, M.I.; Hussain, Q.; Usman, A.R.A.; Ahmad, M.; Abduljabbar, A.; Sallam, A.S.; Ok, Y.S. Impact of biochar properties on soil conditions and agricultural sustainability: A review. *Land Degrad. Dev.* 2018, 29, 2124–2161.

Ameloot, N.; Sleutel, S.; Das, K.C.; Kanagaratnam, J.; de Neve, S. Biochar amendment to soils with contrasting organic matter level: Effects on N mineralization and biological soil properties. GCB *Bioenergy* 2015, 7, 135–144.

Amendola, C.; Montagnoli, A.; Terzaghi, M.; Trupiano, D.; Oliva, F.; Baronti, S.; Miglietta, F.; Chiatante, D.; Scippa, G.S. Short-term effects of biochar on grapevine fine root dynamics and arbuscular mycorrhizae production. *Agric. Ecosyst. Environ*. 2017, 239, 236–245.

Anca-Couce, A., Scharler, R. Modelling heat of reaction in biomass pyrolysis with detailed reaction schemes. *Fuel* 2017, 206, 572–579.

Antal, M. J.; Allen, S. G.; Dai, X.; Shimizu, B.; Tam, M. S.; Grønli, M. Attainment of the Theoretical Yield of Carbon from Biomass. Ind. *Eng. Chem. Res.* 2000, 39, 4024–4031.

Antal, M. J.; Gronli, M. 2003. The Art, Science, and Technology of Charcoal Production. *Ind. Eng. Chem. Res.* 42,8, 1619-1640.

Askeland, M.; Clarke, B.; Paz-Ferreiro, J. Comparative characterization of biochars produced at three selected pyrolysis temperatures from common woody and herbaceous waste streams. *PeerJ* 2019, 7, 1–20, doi:10.7717/peerj.6784.

Azuara, M.; Sáiz, E.; Manso, J. A.; García-Ramos, F. J.; Manyà, J. J. Study on the Effects of Using a Carbon Dioxide Atmosphere on the Properties of Vine Shoots-Derived Biochar. *J. Anal. Appl. Pyrolysis* 2017, 124, 719–725.

Baldock, J.; Smernik, R.J. 2002. Chemical composition and bioavalability of thermally altered Pinus resinosa (Red pine) wood. *Org. Geochem.* 33, 1093-1109.

Barea, J.M. Interacción de los factores que influyen en la calidad del suelo. Comunicación oral. 2017. Apuntes Máster Investigación y Avances en Microbiología. Universidad de Granada.

Blanco-Canqui, H. Does biochar improve all soil ecosystem services? *GCB Bioenergy* 2021, 13, 291–304, doi:10.1111/gcbb.12783.

Bohara, H.; Dodla, S.; Wang, J.J.; Darapuneni, M.; Acharya, B.S.; Magdi, S.; Pavuluri, K. Influence of poultry litter and biochar on soil water dynamics and nutrient leaching from a very fine sandy loam soil. *Soil Tillage Res.* 2019, 189, 44–51.

Brewer, C.E.; Chuang, V.J.; Masiello, C.A.; Gonnermann, H.; Gao, X.; Dugan, B.; Driver, L.E.; Panzacchi, P.; Zygourakis, K.; Davies, C.A. New approaches to measuring biochar density and porosity. *Biomass Bioenergy* 2014, 66, 176–185, doi:10.1016/j.biombioe.2014.03.059.

Buss,W.; Mašek, O. Mobile organic compounds in biochar—A potential source ofcontamination—Phytotoxic effects on cress seed (Lepidium sativum) germination. *J. Environ. Manag.* 2014, 137, 111–119.

Butnan, S.; Deenik, J.L.; Toomsan, B.; Antal, M.J.; Vityakon, P. Biochar characteristics and application rates affecting corn growth and properties of soils contrasting in texture and mineralogy. *Geoderma* 2015, 237, 105–116.

Buss W, Masek O, Graham M, Wüst D. Inherent organic compounds in biochar - their content, composition and potential toxic effects. *J. of Environ. Manage.* 2015, 156, 150-157 doi: 10.1016/j.jenvman.2015.03.035.

Camps Arbestain, M.; Saggar, S.; Leifeld, J. Environmental benefits and risks of biochar application to soil. *Agric. Ecosyst. Environ*. 2014, 191, 1–167.

Chan, K.Y.; Xu, Z. Biochar: nutrient properties and their enhancement. En Biochar for Environmental Management; Lehmann, J., Joseph, S., Eds.; Science and Technology. Earthscan, London, UK, pp. 67–84.

Cobb, A.B.; Wilson, G.W.T.; Goad, C.L.; Grusak, M.A. Influence of alternative soil amendments on mycorrhizal fungi and cowpea production. *Heliyon* 2018, 4, e00704.

Collard, F. X.; Blin, J. A Review on Pyrolysis of Biomass Constituents: Mechanisms and Composition of the Products Obtained from the Conversion of Cellulose, Hemicelluloses and Lignin. *Renewable Sustainable Energy Rev.* 2014, 38, 594–608.

Das, S.K.; Ghosh, G.K.; Avasthe, R. Application of biochar in agriculture and environment, and its safety issues. Biomass Convers. *Biorefinery* 2020, doi:10.1007/s13399-020-01013-4.

Day, D.; Evans, R.J.; Lee, J.W.; Reicosky, D. Economical CO_2, SOx, and NOx capture from fossil-fuel utilization with combined renewable hydrogen production and large-scale carbon sequestration. *Energy* 2015, 30, 2558–2579.

de Abreu Neto, R.; De Assis, A.A.; Ballarin, A.W.; Hein, P.R.G. Dynamic Hardness of Charcoal Varies According to the Final Temperature of Carbonization. *Energy Fuels* 2018, 32, 9659–9665, doi: 10.1021/acs.energyfuels.8b02394.

Dermibas, A. Effects of temperature and particle size on bio-char yield from pyrolisis of agricultural residues. *J. Anal. App. Pyrol.* 2004, 72: 243-48.

Dhyani, V.; Bhaskar, T. A comprehensive review on the pyrolysis of lignocellulosic biomass. *Ren. Energy* 2018, 129, 695–716.

Dias Junior, A.F.; Esteves, R.P.; da Silva, Á.M.; Sousa Júnior, A.D.; Oliveira, M.P.; Brito, J.O.; Napoli, A.; Braga, B.M. Investigating the pyrolysis temperature to define the use of charcoal. *Eur. J. Wood Wood Prod*. 2020, 78, 193–204, doi:10.1007/s00107-019-01489-6.

Elzobair, K.A.; Stromberger, M.; Ippolito, J.A.; Lentz, R.D. Contrasting effects of biochar versus manure on soil microbial communities and enzyme activities in an Aridisol. Chemosphere 2016, 52, 142–145, doi: 10.1016/j.chemosphere.2015.06.044.

Etesami, H.; Maheshwari, D.K. Use of plant growth promoting rhizobacteria (PGPRs) with multiple plant growth promoting traits in stress agriculture: Action mechanisms and future prospects. *Ecotoxicol. Environ. Saf.* 2018, 156, 225–246.

Di Blasi, C.; Signorelli, G.; Di Russo, C.; Rea, G.Product Distribution from Pyrolysis of Wood and Agricultural Residues. *Ind. Eng. Chem. Res*. 1999, 38, 6, 2216-2224.

Farooq M, Rehman A, Pisante M. Sustainable Agriculture and Food Security. En *Innovations in sustainable agriculture*. Springer, 2019; pp. 20–40, doi.org/10.1007/978-3-030-23169-9.

Gale, N.V.; Thomas, S.C. Dose-dependence of growth and ecophysiological responses of plants to biochar. *Sci. Total Environ*. 2019, 658, 1344–1354.

García, C.; Rosas, J.G.; Sánchez, M.E.; Pascual, J.A.; Hernández, M.T. De residuo a recurso: El camino hacia la sosteniblidad. Tomo III: Recursos orgánicos. Aspectos agronómicos y medioambientales. Cap.8: Enmiendas orgánicas de nueva generación: Biochar y otras biomoléculas. Mundi-Prensa, Madrid, 2014; p. 182.

Gelardi, D.L.; Li, C.; Parikh, S.J. An emerging environmental concern: Biochar-induced dust emissions and their potentially toxic properties. *Sci. Total Environ*. 2019, 678, 813–820, doi: 10.1016/j.scitotenv.2019.05.007.

Ghazi, A. Potential for Biochar as an Alternate Carrier to Peat Moss for the Preparation of Rhizobia Bio Inoculum. *Microbiol. Res. J. Int.* 2017, 18, 1–9.

Giuntoli, J.; Arvelakis, S.; Hartmut, S.; de Jong, W.; Verkooijen, A.H.M. Quantitative and Kinetic Thermogravimetric Fourier Transform Infrared (TG-FTIR) Study of Pyrolysis of Agricultural Residues: Influence of Different Pretreatments. *Energy Fuels* 2009 23, 5695–5706.

Godoy, M.G.; Gutarra, M.L.E., Maciel, F.M., Félix, S.P., Bevilaqua, J.V., Machado, O.L.T., Freire, D.M.G. Use of a BioTecnología, 2009, 16, 241.

González, J. F.; Ramiro, A.; González-García, C.M.; Gañán, J.; Encinar, J.M.; Sabio, E.; Rubiales, J. Pyrolysis of Almond Shells. Energy Applications of Fractions. *Ind. Eng. Chem. Res.* 2005, 44, 9, 3003-3012.

Greco, G.; Videgain, M.; Di Stasi, C.; Pires, E.; Manyà, J.J. Importance of pyrolysis temperature and pressure in the concentration of polycyclic aromatic hydrocarbons in wood waste-derived biochars. *J. Anal. Appl. Pyrolysis.* 2021, 159, 105337.

Guo, M. Pyrogenic Carbon in Terra Preta Soils. En Agricultural and Environmental Applications of Biochar: Advances and Barriers; Guo, M., He, Z., Uchimiya, S.M., Eds.; Soil Science Society of America, Inc.: Madison, MA, USA, 2016; pp. 18–28.

Guo, M.; He, Z.; Uchimiya, S.M. Introduction to Biochar as an Agricultural and Environmental Amendment. En Agricultural and Environmental Applications of Biochar: Advances and Barriers; Guo, M., He, Z., Uchimiya, S.M., Eds.; Soil Science Society of America, Inc.: Madison, WI, USA, 2016; pp. 1–14.

Haddad, K.; Jeguirim, M.; Jellali, S.; Guizani, C.; Delmotte, L.; Bennici, S.; Limousy, L. Combined NMR Structural Characterization and Thermogravimetric Analyses for the Assessment of the AAEM Effect during Lignocellulosic Biomass Pyrolysis. *Energy* 2017, 134, 10–23.

Hailegnaw, N.S.; Mercl, F.; Praˇcke, K.; Száková, J.; Tlustoš, P. Mutual relationships of biochar and soil pH, CEC, and exchangeable base cations in a model laboratory experiment. *J. Soils Sediments* 2019, 19, 2405–2416.

Hale, L.; Luth, M.; Crowley, D. Biochar characteristics relate to its utility as an alternative soil inoculum carrier to peat and vermiculite. *Soil Biol. Biochem*. 2015, 81, 228–235.

Hammer, E.C.; Balogh-Brunstad, Z.; Jakobsen, I.; Olsson, P.A.; Stipp, S.L.S.; Rillig, M.C. A mycorrhizal fungus grows on biochar and captures phosphorus from its surfaces. *Soil Biol. Biochem*. 2014, 77, 252–260.

Hu, S.; Jess, A.; Xu, M. 2007. Kinetic Study of Chinese Biomass Slow Pyrolysis: Comparison of Different Kinetic Models. *Fuel.* 86, 17–18, 2778-2788.

Igalavithana, A.D.; Ok, Y.S.; Usman, A.R.A.; Al-wabel, M.I.; Oleszczuk, P.; Lee, S.S. The E ects of Biochar Amendment on Soil Fertility Could Biochar Be Used as a Fertilizer? En Agricultural and Environmental Applications of Biochar: Advances and Barriers; Guo, M., He, Z., Uchimiya, S.M., Eds.; Soil Science Society of America, Inc.: Madison, MA, USA, 2016; pp. 123–144.

International Biochar Initiative Standardized Product Definition and Product Testing Guidelines for Biochar That Is Used in Soil. *Int. Biochar Initiat*. 2015, 23.

Imaz, M.J. y Virto, I. Indicadores de calidad del suelo. En Tecnología de Suelos: estudio de casos; Usón, A.; Boixadera, J.; Bosch, A.; Martín, A.E., Eds.; Prensas Universitarias de Zaragoza y Ediciones de la Universidad de Lleida. Colección de textos docentes 2010; pp. 141–155.

Jaafar, N.M. Biochar as a Habitat for Arbuscular Mycorrhizal Fungi. En Mycorrhizal Fungi: Use in Sustainable Agriculture and Land Restoration. Soil Biology; Solaiman, Z., Abbott, L., Varma, A., Eds.; Springer: Berlin/Heidelberg, Germany, 2014; Volumen 41.

Jaizme-Vega, M.C. Microorganismos funcionales del suelo. Su papel en el manejo ecológico de los secanos. En Agricultura Ecológica en Secano. Soluciones Sostenibles en Ambientes Mediterráneos; Ministerio de Medio Ambiente y Medio Rural y Marino, Meco, R.; Lacasta, C.; Moreno, M.M., Eds.; Mundi-Prensa, Madrid, Spain, 2011; pp. 417–439.

Jaizme-vega, M.C. Las Micorrizas, Una Estrategia Agroecológica Para Optimizar la Calidad de los Cultivos; Universidad de la Laguna, Instituto Canario de Investigaciones Agrarias, Phytoma España S.L., Eds.; Phytoma España S.L.: Valencia—San Cristóbal de la Laguna (Tenerife), Spain, 2019; p. 112. ISBN 978-84-946691-5-6.

Khadem, A.; Raiesi, F. Response of soil alkaline phosphatase to biochar amendments: Changes in kinetic and thermodynamic characteristics. Geoderma 2019, 337, 44–54.

Jin, Y.; Liang, X.; He, M.; Liu, Y.; Tian, G.; Shi, J. Manure biochar influence upon soil properties, phosphorus distribution and phosphatase activities: A microcosm incubation study. *Chemosphere* 2016, 142, 128–135.

Kloss, S.; Zehetner, F.; Wimmer, B.; Buecker, J.; Rempt, F.; Soja, G. Biochar application to temperate soils: Effects on soil fertility and crop growth under greenhouse conditions. *J. Plant Nutr. Soil Sci.* 2014, 177, 3–15.

Kumar, M.; Verma, B.B.; Gupta, R.C. Mechanical properties of acacia and eucalyptus wood chars. *Energy Sources* 1999, 21, 675–685, doi:10.1080/00908319950014425.

Laghari, M.; Mirjat, M.S.; Hu, Z.; Fazal, S.; Xiao, B.; Hu, M.; Chen, Z.; Guo, D. E ects of biochar application rate on sandy desert soil properties and sorghum growth. *Catena* 2015, 135, 313–320.

LeCroy, C.; Masiello, C.A.; Rudgers, J.A.; Hockaday, W.C.; Silberg, J.J. Nitrogen, biochar, and mycorrhizae: Alteration of the symbiosis and oxidation of the char surface. *Soil Biol. Biochem*. 2013, 58, 248–254.

Lehmann, J.; Gaunt, J.; Rondon, M. Bio-char sequestration in terrestrial ecosystems: a review. *Mitig. Adapt. Strateg. Glob. Chang*., 2006, 11, 403-427.

Lehmann, J.; Joseph, S. Biochar for Environmental Management. *London-Sterling: Earthscan*, 2009.

Lehmann, J.; Da Silva, J.P.; Steiner, C.; Nehls, T.; Zech, W.; Glaser, B. Nutrient availability and leaching in an archaeological Anthrosol and a Ferralsol of the Central Amazon basin: Fertilizer, manure and charcoal amendments. *Plant Soil* 2003, 249, 343–357.

Lehmann, J.; Rilling, M.C.; Thies, J.; Masiello, C.A.; Hockaday, W.C.; Crowley, D. Biochar effects on soil biota – a review. *Soil Biol. Biochem*., 2011, 43: 1812-36.

Li, C.; Bair, D.A.; Parikh, S.J. Estimating potential dust emissions from biochar amended soils under simulated tillage. *Sci. Total Environ*. 2018, 625, 1093–1101, doi: 10.1016/j.scitotenv.2017.12.249.

Liu, X.H.; Zhang, X.C. Effect of biochar on pH of alkaline soils in the Loess Plateau: Results from incubation experiments. *Int. J. Agric. Biol*. 2012, 14, 745–750.

Liu, X.; Zhang, A.; Ji, C.; Joseph, S.; Bian, R.; Li, L.; Pan, G.; Paz-Ferreiro, J. Biochar's effect on crop productivity and the dependence on experimental conditions-a meta-analysis of literature data. *Plant Soil* 2013, 373, 583–594, doi:10.1007/s11104-013-1806-x.

Maienza, A.; Genesio, L.; Acciai, M.; Miglietta, F.; Pusceddu, E.; Vaccari, F.P. Impact of biochar formulation on the release of particulate matter and on short-term agronomic performance. *Sustain.* 2017, 9, 1–10, doi:10.3390/su9071131.

Major, J. Julie Major, PhD Extension Director International Biochar Initiative www.biochar-international.org Guidelines on Practical Aspects of Biochar Application to Field Soil in Various Soil Management Systems. 2010, doi:10.1016/B978-0-12-385538-1.00003-2.

Manyà, J. J.; Velo, E.; Puigjaner, L. Kinetics of Biomass Pyrolysis: A Reformulated Three-Parallel-Reactions Model. *Ind. Eng. Chem. Res.* 2003, 42(3), 434-441.

Manyà, J.J. Pyrolysis for biochar purposes: A review to establish current knowledge gaps and research needs. *Environ. Sci. Technol.* 2012, 46, 7939–7954, doi:10.1021/es301029g.

Manyà, J.J.; Ortigosa, M.A.; Laguarta, S.; Manso, J.A. Experimental study on the effect of pyrolysis pressure, peak temperature, and particle size on the potential stability of vine shoots-derived biochar. *Fuel* 2014, 133, 163–172, doi: 10.1016/j.fuel.2014.05.019.

Manyà, J.J.; Azuara, M.; Manso, J.A. Biochar production through slow pyrolysis of different biomass materials: Seeking the best operating conditions. *Biomass and Bioenergy* 2018, 117, 115–123, doi: 10.1016/j.biombioe.2018.07.019.

Manyá, J.J.; Gascó G. Biochar as a sustainable resource to drive innovative green technologies. En Biochar as a renewable-based material with applications in agriculture, the environment and energy; Manyà, J.J., Gascó, Eds.; World Scientific Publishing Europe Ltd.: Toh Tuck Link, Singapore, 2021; pp. 1–33.

Meco, R.; Lacasta, C.; Moreno, M.M. 2011. Agricultura Ecológica en Secano: soluciones sostenibles en ambientes mediterráneos. Mundi-Prensa, Madrid; p. 495.

Medina Peñafiel, A. Estudio de la Interacción Entre Inoculantes Microbianos y Residuos Agroindustriales Biotransformados Para su uso en Estrategias de Revegetación y Bioremediación. Tesis Doctoral, Universidad de Granada, Granada, Spain, 2006.

Mohamed, W.; Hammam, A. Poultry manure-derived biochar as a soil amendment and fertilizer for sandy soils under arid conditions. *Egypt. J. Soil Sci.* 2019, 59, 1–14.

Monesma, E. Carbón vegetal. Temas de antropología aragonesa 1993, 4, 60–75.

Ogawa, M.; Okimori, Y.; Takahashi, F. Carbon sequestration by carbonization of biomass and forestation: Three case studies. *Mitig. Adaptat. Strateg. Global Change*, 2006, 11, 429-444.

Olmo, M.; Villar, R.; Salazar, P.; Alburquerque, J.A. Changes in soil nutrient availability explain biochar's impact on wheat root development. *Plant Soil* 2016, 399, 333–343.

Pérez-De-Luque, A.; Tille, S.; Johnson, I.; Pascual-Pardo, D.; Ton, J.; Cameron, D.D. The interactive effects of arbuscular mycorrhiza and plant growth-promoting rhizobacteria synergistically enhance host plant defences against pathogen. *Sci. Rep.* 2017, 7, 1–10.

Ronsse F.; Masek, O.; Manyà, J.J. Biochar production via pyrolysis. En Biochar as a renewable-based material with applications in agriculture, the environment and energy; Manyà, J.J., Gascó, Eds.; World Scientific Publishing Europe Ltd.: Toh Tuck Link, Singapore, 2021; pp. 35–60.

Rosas, J.G. Producción de biochar a partir de viñas agotadas mediante pirólisis en reactor a escala piloto y en reactor móvil energéticamente sostenible. Tesis Doctoral, Universidad de León, León, 2015.

Sadasivam, B.Y.; Reddy, K.R. Engineering properties of waste wood-derived biochars and biochar-amended soils. *Int. J. Geotech. Eng.* 2015, 9, 521–535, doi:10.1179/1939787915Y.0000000004.

Safar, M.; Lin, B. J.; Chen, W. H.; Langauer, D.; Chang, J. S.; Raclavska, H.; Pétrissans, A.; Rousset, P.; Pétrissans, M. Catalytic Effects of Potassium on Biomass Pyrolysis, Combustion and Torrefaction. *Appl. Energy* 2019, 235, 346–355.

Sashidhar, P.; Kochar, M.; Singh, B.; Gupta, M.; Cahill, D.; Adholeya, A.; Dubey, M. Biochar for delivery of agri-inputs: Current status and future perspectives. *Sci. Total Environ.* 2020, 703, 134892.

Schiefer J.; Lair G.J.; Blum W. Potential and limits of land and soil for sustainable intensification of European agriculture. *Agric Ecosyst Environ* 2016, 230, 283–293.

Shahzad B.; Tanveer M.; Che Z.; Rehman A.; Cheema S.A.; Sharma A.; Song H.; Rehman S.; Zhaorong D. Role of 24-epibrassinolide (EBL) in mediating heavy metal and pesticide
induced oxidative stress in plants: a review. *Ecotoxicol Environ Saf* 2018, 147, 935–944.

Shukla, M.K.; Lal, R.; Ebinger, M. Determining soil quality indicators by factor analysis. *Soil Tillage Res* 2006, 87 2, 194-204.

Sohi, S.P.; Krull, E.; López-Capel, E.; Bol, R. A review of biochar and its use and function in soil. *Adv Agron* 2010, 105, 47-82.

Solaiman, Z.M.; Abbott, L.K.; Murphy, D.V. Biochar phosphorus concentration dictates mycorrhizal colonisation, plant growth and soil phosphorus cycling. *Sci. Rep.* 2019, 9, 1–11.

Steiner, C.; Glaser, B.; Teixeira, W.G.; Lehmann, J.; Blum, W.E.H.; Zech, W. Nitrogen retention and plant uptake on a highly weathered central Amazonian ferrasol amended with compost and charcoal. *J. Plan Nutr. Soil Sci.* 2008, 171, 893-899.

Steiner, C. Considerations in biochar characterization. En Agricultural and Environmental Applications of Biochar: Advances and Barriers; Guo, M., He, Z., Uchimiya, S.M., Eds.; Soil Science Society of America, Inc.: Madison, WI, USA, 2016; pp. 87–100.

Stenseng, M.; Jensen, A.; Dam-Johansen, K. Investigation of Biomass Pyrolysis by Thermogravimetric Analysis and Differential Scanning Calorimetry. *J. Anal. Appl. Pyrolysis* 2001, 58-59, 765-780.

Sun, Y.; Gao, B.; Yao, Y.; Fang, J.; Zhang, M.; Zhou, Y.; Chen, H.; Yang, L. E ects of feedstock type, production method, and pyrolysis temperature on biochar and hydrochar properties. *Chem. Eng. J.* 2014, 240, 574–578.

Teixeira, W. G.; Verheijen, F.; de Oliveira Marques, D. Water holding capacity of biochar and biochar-amended soils. En Biochar as a renewable-based material with applications in agriculture, the environment and energy; Manyà, J.J., Gascó, Eds.; World Scientific Publishing Europe Ltd.: Toh Tuck Link, Singapore, 2021; pp. 61–83.

Tejada, M.; Gómez, I.; Hernández, M.T.; García, C. Utilization of vermicomposts in soil restoration: effects on soil biological properties. *Soil Sci. Am. J.* 2010, 74, 525-532.

Turpin N.; Ten Berge H.; Grignani C.; Guzmán G.; Vanderlinden K.; Steinmann H.H.; Siebielec G.; Spiegel A.; Perret E.; Ruysschaert G.; Laguna A.; Giráldez J.V.; Werner M.; Raschke I.; Zavattaro L.; Costamagna C.; Schlatter N.; Berthold H.; Sandàn T.; Baumgarten A. An assessment of policies affecting sustainable soil management in Europe and selected member states. *Land Use Policy* 2017, 66, 241–249.

Van de Velden, M.; Baeyens, J.; Brems, A.; Janssens, B.; Dewil, R. Fundamentals, kinetics and endothermicity of the biomass pyrolysis reaction. *Renewable Energy* 2010, 232-242.

Wang, D.; Zhang, W.; Hao, X.; Zhou, D. Transport of biochar particles in saturated granular media: Effects of pyrolysis temperature and particle size. *Environ. Sci. Technol.* 2013, 47, 821–828, doi:10.1021/es303794d.

Warnock, D.D.; Mummey, D.L.; McBride, B.; Major, J.; Lehmann, J.; Rillig, M.C. Influences of non-herbaceous biochar on arbuscular mycorrhizal fungal abundances in roots and soils: Results from growth-chamber and field experiments. *Appl. Soil Ecol.* 2010, 46, 450–456.

Xie, R.; Zhu, Y.; Zhang, H.; Zhang, P.; Han, L. Effects and mechanism of pyrolysis temperature on physicochemical properties of corn stalk pellet biochar based on combined characterization approach of microcomputed tomography and chemical analysis. *Bioresour. Technol.* 2021, 329, 124907, doi: 10.1016/j.biortech.2021.124907.

Yadav, V.; Jain, S.; Mishra, P.; Khare, P.; Shukla, A.K.; Karak, T.; Singh, A.K. Amelioration in nutrient mineralization and microbial activities of sandy loam soil by short term field aged biochar. *Appl. Soil Ecol.* 2019, 138, 144–155.

Yeo J.Y.; Chin B.L.F.; Tan J.K.; Loh Y.S. Comparative studies on the pyrolysis of cellulose, hemicellulose, and lignin based on combined kinetics. *Journal of the Energy Institute* 2017 92, 27–37.

Zickler, G.A.; Schöberl, T.; Paris, O. Mechanical properties of pyrolysed wood: A nanoindentation study. *Philos. Mag.* 2006, 86, 1373–1386, doi:10.1080/14786430500431390.